

**A multi-site methodology for understanding dependencies in
flood risk exposure in the UK**

Linda Speight

Submitted in partial fulfilment for examination for the degree of Doctor of Philosophy

School of Civil Engineering and Geosciences

NEWCASTLE UNIVERSITY

September 2013

Abstract

Recent large scale flood events in the UK and the continued threat of a major North Sea surge have motivated a re-appraisal of how flood risk is modelled. A new generation of flood risk models are starting to consider the spatial and temporal dependencies in flood events. This is important for a wide range of risk based decision making, with one of its most significant applications being the understanding of insurance exposure.

The aim of this thesis is to increase understanding of flood risk exposure in the UK and identify areas where existing modelling capabilities and data limitations contribute to large uncertainties in the estimation of risk. Illustrating a successful collaboration between academia and the insurance industry, a case study of one company's exposure from static caravans is used to develop a methodology for flood risk assessment at multiple sites nested within a national framework. This novel nested approach allows for greater detail to be included at sites of interest resulting in increased understanding of the risk driving processes while retaining the large scale dependence structure. This is demonstrated at high risk locations on the Lincolnshire and North Wales coastline and inland on the Rivers Severn and Thames. The proposed methodology takes a flexible component based approach and has potential adaptations to different receptors and end users.

A systems based model is used which explicitly considers all key components of risk. Extreme fluvial and coastal events are modelled statistically using the conditional dependence model of Heffernan and Tawn (2004). Coastal flood defences are essential for the protection of static caravan sites however their inclusion in existing risk models contributes significant uncertainties. The quality of data available on flood defence heights is reviewed and a methodology to incorporate spatial variations is proposed. The failure of flood defences is modelled using fragility curves and inundation modelling is used to route water on the floodplain. Finally the damage to the static caravans is modelled using depth-damage curves with reference to the impact of limited observed data on flood damage for caravans.

One of the biggest challenges of considering dependencies across multiple scales within a systems model is matching the data requirements across each component. To address this problem this thesis investigates the relationship between skew surge and wave height to estimate the total inshore water level, and develops a UK specific method to transform daily mean flow to peak flow. The modular structure of the proposed methodology means different component models can be used to suit the available data; here the integration of both 1D and 2D floodplain inundation models is demonstrated.

Acknowledgements

This PhD research project has been supported financially by an EPSRC studentship and CASE allowance from Catlin.

I would like to thank my supervisors, Professor Chris Kilsby and Professor Jim Hall for their help, ideas and encouragement over the course of this research. Paul Kershaw and his catastrophe modelling team at Catlin have provided useful data for the case study and motivation for this thesis, and I am grateful to them for the opportunity to spend time at their London offices and gain an insight into the insurance industry.

Various people have provided data and advice during the course of this research. Flow data was supplied by NRFA and the Environment Agency helpfully provided existing models, LiDAR data and most usefully the detailed flood defence data for the East Coast used in Chapter 8. Qihua Liang provided a copy of his 2D inundation model which was used for the coastal inundation modelling. Caroline Keef of JBA Consulting provided valuable expertise and extracts of code to help with fitting the conditional dependence model in the initial stages of this research.

Finally thanks to my friends and family who have supported me over the past four years. There are too many people to mention individually but special thanks must go to Steve Barton for his tireless proof reading and editing skills and for agreeing to marry a student!

List of Abbreviations

AAL	Average Annual Loss
ABI	Association of British Insurers
AEP	Annual Exceedance Probability
AREA	Catchment drainage area
BFIHOST	Base Flow Index derived from HOST soil classification
BODC	British Oceanic Data Centre
Cat Models	Catastrophe Models
CEH	Centre for Ecology and Hydrology
CTFRA	Conwy Tidal Flood Risk Assessment
DEFRA	Department for Environment, Food and Rural Affairs
DEM	Digital Elevation Model
DMF	Daily Mean Flow
DPLBAR	Mean of distances between each node on IHDTM grid and the catchment outlet
EA	Environment Agency
EFO	Extreme Flood Outline
EVT	Extreme Value Theory
FARL	Index of flood attenuation attributable to reservoirs and lakes
FEH	Flood Estimation Handbook
FPEXT	Floodplain extent
GEV	Generalised Extreme Value Distribution
GL	Generalised Logistic Method
GPD	Generalised Pareto Distribution
IHAM	Inundation Hazard Assessment Model
JRPM	Joint Return Period Method
MCM	Multi Coloured Manual
NFCDD	National Flood and Coastal Defence Database
NRFA	National Rivers Flow Archive
PCD	Physical Catchment Descriptor
POT	Peaks Over Threshold
PROPWET	Proportion of time when Soil Moisture Deficit was equal to, or below, 6mm
QMED	Median annual maximum flood
RASP	Risk Assessment for Strategic Pathways
ReFH	Revitalised Flood Hydrograph
RJPM	Revised Joint Probability Model
RMS	Risk Management Solutions
RMSE	Root mean squared error
SAAR	Standard average annual rainfall
SPRC	Source-Pathway-Receptor-Consequence Model
SRJPM	Spatial Revised Joint Probability Model
TIV	Total Insured Value
URBEXT	Extent of urban landcover

Table of Content

1	Introduction	1
1.1	Flood risk in the UK.....	1
1.2	Modelling flood risk.....	2
1.3	Flood insurance in the UK	4
1.4	Identification of research needs.....	5
1.5	Aims and objectives.....	7
1.6	Thesis outline.....	8
2	Flood risk modelling and analysis	9
2.1	Introduction.....	9
2.2	Defining risk.....	9
2.3	Who models flood risk?.....	11
2.4	How is flood risk modelled?	13
2.5	Informing risk based decision making.....	31
3	Case study	33
3.1	Introduction.....	33
3.2	The caravan portfolio	34
3.3	Pricing risk to caravans.....	35
3.4	Past claims data	45
3.5	Sites at risk.....	49
3.6	Summary of Catlin’s caravan exposure	60
4	A methodological framework for multi-site risk analysis	61
4.1	Modelling approach	61
4.2	Outline of the risk model.....	66
4.3	Data sources	71
4.4	Consideration of uncertainty.....	73
4.5	Informing decision making	74
4.6	Summary of methodological framework	75
5	Multi-variate spatial extremes.....	77
5.1	Defining “extreme”	77
5.2	Extreme events in the UK.....	78
5.3	Modelling extreme events	90
5.4	Selection of suitable statistical method to provide a robust ‘Sources’ component for the system model	122
6	A Multisite conditional dependence model for the selected risk clusters	125
6.1	Introduction.....	125

6.2	Establishing a gauged network for selected risk clusters	125
6.3	Development of a multisite conditional dependence model for the gauged network	139
6.4	Spatial and temporal dependences in simulated extreme events	166
6.5	Chapter conclusions	175
7	Statistical and physical modelling of water level	177
7.1	Extreme events at the receptors	177
7.2	Fluvial water levels	178
7.3	Coastal water levels	193
7.4	Floodplain inundation modelling	218
7.5	Water level and floodplain inundation in the system model	220
8	Spatial and temporal flood defence reliability	221
8.1	Importance of flood defences to flood risk	221
8.2	Flood defence types and failure models	222
8.3	Methods of modelling of flood defence failure	227
8.4	Development of methodology for variable flood defence crest height	236
8.5	Simulation of flood defence reliability state	252
8.6	Example application	255
8.7	Using defence reliability in the system model	258
9	Calculating damage, loss and risk	260
9.1	Calculation of damage	260
9.2	Calculation of risk	277
9.3	Informing decision making	278
9.4	Contribution of uncertainty to the risk estimate from the system model components	280
10	Conclusions	291
10.1	Meeting the research aims and objectives	291
10.2	Recommendations	298
10.3	Concluding comments	299
11	References	301

Appendices

Appendix A. Summary of main EVT methods

Appendix B. Fitting the conditional dependence model

Appendix C. DMF to POT conversion methods

Appendix D. Coastal data and wave heights

Appendix E. Flood defence reliability

List of Figures

Figure 2.1 Example exceedance probability curve	11
Figure 2.2 Basic structure of Catastrophe Models.....	12
Figure 2.3 Conceptual Source-Pathway-Receptor-Consequence model.....	14
Figure 2.4 Overtopping fragility curves used in national flood risk assessment	21
Figure 3.1 Accommodation type in the Compass Caravan account	34
Figure 3.2 Compass Caravan Account site locations	35
Figure 3.3 Compass Caravan Account Total Insured Value by postcode sector.....	35
Figure 3.4 Histograms of insured values for each accommodation type in the Compass Caravan Account	37
Figure 3.5 Results of previous Catlin analysis of the effect of changing construction and occupation class on flood losses.....	40
Figure 3.6 Results of previous Catlin analysis of the effect of changing vulnerability modifiers on flood loss.....	41
Figure 3.7 New sensitivity analysis of the effect of construction class on fluvial flood losses...	42
Figure 3.8 New sensitivity analysis of the effect of construction class on wind and storm surge losses.....	42
Figure 3.9 Discrepancies between caravan site postcode points and site outlines: Ingoldmells	44
Figure 3.10 Discrepancies between caravan site postcode points and site outlines: Stourport-on-Severn	44
Figure 3.11 Proportion of claims between 2006 and 2009 occurring on the same day as flood events.....	48
Figure 3.12 Selected risk clusters.....	50
Figure 3.13 Total insured value of at risk sites: Lincolnshire coast.....	52
Figure 3.14 Lincolnshire site elevation	53
Figure 3.15 Spatial extent of multiple caravan parks at Ingoldmells.....	53
Figure 3.16 Total insured value of at risk sites: North Wales coast.....	54
Figure 3.17 Caravan site at Abergyll	55
Figure 3.18 Continuous location of multiple sites along the North Wales Coast	55
Figure 3.19 Total insured value of at risk sites: River Severn near Stourport-on-Severn.....	57
Figure 3.20 Caravan sites on the Thames at Hurley	58
Figure 3.21 Total insured value of at risk sites: River Thames.....	59
Figure 4.1 Components of system model as considered in this thesis.....	61
Figure 4.2 Nested framework structure of systems components	64
Figure 4.3 Illustration of how spatial dependence is maintained through the nested model ...	65
Figure 4.4 Overview of the risk assessment methodology.....	66
Figure 5.1 Number and type of extreme rainfall events by month as identified by Collier et al (2002).....	79
Figure 5.2 Rainfall totals by type of extreme event as identified by Collier et al (2002).....	79
Figure 5.3 Map of areas affected by the summer 2007 floods.....	81
Figure 5.4 Components of still sea level	82
Figure 5.5 Calculating skew surge.....	84
Figure 5.6 The Chester to Holyhead railway and flooded caravan site at Towyn during the 1990 event	85
Figure 5.7 Spatial dependence in rainfall for a 55 year event over a radius of 30km	87

Figure 5.8 Spatial dependence in river flows for a 50 year event over a radius of 30km	87
Figure 5.9 Dependencies between river flow and sea surge for different time lags on the East Coast	88
Figure 5.10 Summary of past research on spatial dependencies of UK extreme events	90
Figure 5.11 Example mean residual life plot for Kingston upon Thames flow data	94
Figure 5.12 Scatter plot of Kingston on Thames daily flows by year	94
Figure 5.13 Peak sea levels at Southend 1997 - 2000	96
Figure 5.14 De-clustered peak sea levels at Southend 1997 - 2000	97
Figure 5.15 Location of raingauges in the Thames catchment	100
Figure 5.16 Thames rain gauges distance correlation coefficients	101
Figure 5.17 Thames rain gauges distance correlation coefficients for extreme events	101
Figure 5.18 Location of sample rain and flow gauges around the Severn risk cluster	104
Figure 5.19 Dependence measure $\chi(u)$ as $u \rightarrow 1$	107
Figure 5.20 Dependence measure $\chi(u)$ as $u \rightarrow 1$	107
Figure 5.21 Diagram of modelled spatial dependencies in the conditional dependence model	111
Figure 5.22 Relationship of conditional dependence measure $\Pr(X_{t+\tau} > u \mid X_t > u)$ with BFIHOST	113
Figure 5.23 Modelling temporal dependence in the conditional dependence model	115
Figure 5.24 Temporal inconsistencies in moving window de-clustering method	118
Figure 6.1 Gauging station locations: East Coast	129
Figure 6.2 Gauging station locations: North Wales	131
Figure 6.3 Gauging station locations: River Severn	133
Figure 6.4 Relationship between gauges 54006 and 54063 for POT events before and after the installation of the flood alleviation scheme in 2003	135
Figure 6.5 Gauging station locations: River Thames	137
Figure 6.6 Period of record for core gauges	139
Figure 6.7 Daily maximum skew surge at selected gauges	140
Figure 6.8 Pairwise plots of observed DMF and skew surge data for all core gauges	142
Figure 6.9 Identification of suitable de-clustering interval by comparing $\Pr(X_{t+\tau} > u \mid X_t > u)$ with BFIHOST for a range of r values	143
Figure 6.10 Comparison of number of events retained by runs and moving window de-clustering methods	144
Figure 6.11 Conditional dependence measure $\Pr(X_{t+\tau} > u \mid X_t > u)$ at costal gauges for a range of time lags	146
Figure 6.12 Identification of a suitable coastal de-clustering interval by comparing $\Pr(X_{t+\tau} > u \mid X_t > u)$ at different time lags with a range of r values	146
Figure 6.13 Evidence of independence of Z and X in the conditional dependence model	149
Figure 6.14 Diagram of the infilling process	153
Figure 6.15 Example of infilled coastal event peaks and time series	154
Figure 6.16 Temporal extreme dependence between gauge pairs ($p=Q99$)	157
Figure 6.17 Temporal extreme dependence between gauge pairs ($p=Q95$)	158
Figure 6.18 Comparison of simulated and observed peaks for 66001 and all core gauges	159
Figure 6.19 Comparison of simulated and observed peaks for CRO and all core gauges	160
Figure 6.20 Example DMF and skew surge simulated time series compared to observed	162
Figure 6.21 Comparison of simulated event peaks using infilled and non-infilled data	165
Figure 6.22 Spatial conditional dependency maps: probability of $y > u \mid x > Q99$	168

Figure 6.23 Spatial conditional dependency maps: expected proportion of gauges in $Y > u \mid X > Q99$	169
Figure 6.24 Spatial conditional dependency maps: expected proportion of gauges in $Y > Q99 \mid X > Q99$ by gauge type	170
Figure 6.25 Spatial conditional dependency maps: expected number of clusters with gauges $> Q95 \mid X > Q99$	172
Figure 6.26 Spatial conditional dependency maps: expected number of clusters with gauges $> Q99 \mid X > Q99$	173
Figure 7.1 Effect of hydrograph shape on POT:DMF ratio.....	178
Figure 7.2 Relationship between DMF and POT for UK gauges.....	178
Figure 7.3 Goodness of fit of DMF: flood peak multiple regression model compared to other methods	182
Figure 7.4 Illustration of the equipercntile technique to simulate time series at ungauged site	185
Figure 7.5 Number of gauges for which each tested ungauged site interpolation method provided the best fit with observed DMF.....	188
Figure 7.6 ReFH design hydrograph: 54001.....	190
Figure 7.7 ReFH design hydrograph: 66001.....	190
Figure 7.8 Summary of physically based fluvial event simulation method	193
Figure 7.9 Fifteen largest surges at Immingham: 1960 - 2010	195
Figure 7.10 Normalised AMAX surges at Immingham: 1960 - 2010.....	195
Figure 7.11 Immingham surge shape cluster dendrogram using Ward's clusters.....	197
Figure 7.12 Averaged surge shapes produced using Ward's clusters with different numbers of cluster groups at Immingham	197
Figure 7.13 Comparison of time-integrated duration surge shape with Wards algorithm surge shape at Cromer.....	199
Figure 7.14 Evidence of independence of skew surge and tide height at Immingham.....	201
Figure 7.15 Fifteed highest surge events with associated wave component at Dowsing.....	203
Figure 7.16 Joint probability of water level and wave height at Dowsing as calculated by Hawkes <i>et al</i> (2002)	205
Figure 7.17 Joint observed probabilities of wave height and water level at Dowsing	205
Figure 7.18 Temporal dependency of wave height with water level at Dowsing	206
Figure 7.19 Temporal dependency of wave height with skew surge at Dowsing	206
Figure 7.20 Joint probability of skew surge and wave height at Dowsing.....	207
Figure 7.21 Joint probability of skew surge and wave height at Liverpool.....	207
Figure 7.22 Simulated wave heights using pairwise relationship with skew surge at Dowsing.....	208
Figure 7.23 Relationship between wave height and wave period at Dowsing from Hawkes <i>et al</i> (2002)	209
Figure 7.24 Relationship between wave height and wave period at Dowsing from observed data	209
Figure 7.25 Wave rose showing wave height and direction at Dowsing	210
Figure 7.26 Wave rose showing wave height and direction at Liverpool Bay.....	210
Figure 7.27 Lincolnshire coastal bathymetry.....	213
Figure 7.28 North Wales coastal bathymetry	213
Figure 7.29 Summary of coastal simulation method	214
Figure 7.30 Graphical definition of maximum wave runoff	215
Figure 8.1 Failure modes for flood defence walls and embankments.....	223

Figure 8.2 Failure mode for dunes.....	224
Figure 8.3 Key features of the breaching process over time.....	225
Figure 8.4 Summary of consideration of defence reliability.....	235
Figure 8.5 Fit of long section mean crest height to surveyed crest elevation.....	239
Figure 8.6 Type of variation between long section mean crest height and surveyed crest elevation	240
Figure 8.7 Direction of variation between long section mean crest height and surveyed crest elevation	240
Figure 8.8 Magnitude of variation between long section mean crest height and surveyed crest elevation	241
Figure 8.9 Representativeness of long section mean crest height compared to surveyed crest elevation from different data sources	242
Figure 8.10 Fit of long section mean crest height to DTM crest height	243
Figure 8.11 Type of variation between long section mean crest height and DTM crest height.....	243
Figure 8.12 Direction of variation between long section mean crest height and DTM crest height	243
Figure 8.13 Magnitude of variation between long section mean crest height and DTM crest height	244
Figure 8.14 Plausible variation in long section crest height simulation	245
Figure 8.15 Fit of normal distribution for variation magnitude compared to observed proportional error between long section mean crest height and surveyed crest elevation....	248
Figure 8.16 Example simulations of plausible variations in crests heights for different defence types.....	249
Figure 8.17 500 plausible simulations of varying crest height for the Lincolnshire coast compared to the long section mean.....	250
Figure 8.18 Example observed variation in crest height from the Environment Agency survey data for different defence types.....	251
Figure 8.19 North Wales coastal model domain showing coastal defence sections and caravan site locations	256
Figure 8.20 Three example simulations of plausible variations in long section crest height for North Wales defences.....	257
Figure 8.21 Identification of defence breach locations for a North Wales example overtopping scenario using simulated water level and defence crest height.....	258
Figure 9.1 Variation in residential flood damages in Germany	261
Figure 9.2 Photographs of damage caused by the June 2012 floods at Riverside Caravan Park Llandre	263
Figure 9.3 MCM depth-damage curves for caravans.....	265
Figure 9.4 MCM depth-damage component curves for static caravans	265
Figure 9.5 Proposed depth-damage curve for static caravans	267
Figure 9.6 Proposed depth-damage component curves for static caravans	267
Figure 9.7 Still water level components used for location assumption testing.....	269
Figure 9.8 Simulated flood depths for a breach in North Wales defence section 4E.....	271
Figure 9.9 Simulated Flood depths for a breach in North Wales defence section 4H.....	271
Figure 9.10 Difference in damage calculated using point and distributed caravan unit locations compared to the total area flooded	272
Figure 9.11 Testing of the sensitivity of simulated flood damage to floor height by varying the shape of the depth-damage curve.....	274

Figure 9.12 Testing of the sensitivity of simulated flood damage to material vulnerability by varying the shape of the depth-damage curve.....	275
Figure 9.13 Testing of the sensitivity of flood damages to the point of total write off by varying the shape of the depth-damage curve	276
Figure 9.14 Variation of damage conditional on breach size	277
Figure 9.15 Assessment of uncertainty of systems model component.....	281

List of Tables

Table 2.1 Existing work of multivariate extremes in the UK.....	17
Table 2.2 Available catastrophe models for the UK	23
Table 2.3 Summary of RMS UK Inland Flood model	26
Table 2.4 Summary of RMS UK Storm-Surge model	28
Table 2.5 Summary of RMS European Windstorm model	28
Table 3.1 Data provided to Catlin about each insurance policy	36
Table 3.2 Summary of insured values of individual site structures in the Compass Private Clients and Compass Direct Schemes	36
Table 3.3 Cost to buy new of different types of caravan site accommodation.....	38
Table 3.4 Comparison of Catlin assumed number of units on caravan sites with aerial photography for given sample site locations.....	38
Table 3.5 Information recorded for each claim in the caravan account	45
Table 3.6 Description of main flood events in the claims period 2006:2009	47
Table 3.7 Exposure risk summary: Lincolnshire coast	52
Table 3.8 Exposure risk summary: North Wales coast.....	54
Table 3.9 Exposure risk summary: River Severn near Stourport-on-Severn	57
Table 3.10 Exposure risk summary: River Thames	59
Table 4.1 Data requirements for a system based model.....	72
Table 5.1 Parameter stability assessment for a GPD model fitted to DMF at Kingston on Thames for multiple thresholds.....	94
Table 5.2 Rain gauges near the Severn risk cluster	104
Table 5.3 Flow gauges near the Severn risk cluster	104
Table 5.4 Rain and flow gauge threshold for the χ dependence measure	105
Table 5.5 Dependence measure χ for all pairs of gauges around the Severn risk cluster	106
Table 5.6 Dependence measure χ for all pairs of gauges near the Severn risk cluster	107
Table 6.1 Details of available East Coast fluvial gauges.....	128
Table 6.2 Details of available East Coast coastal gauges	128
Table 6.3 Details of available North Wales fluvial gauges	130
Table 6.4 Details of available North Wales coastal gauges	130
Table 6.5 Details of available River Severn fluvial gauges	132
Table 6.6 Ratio of DMF peaks between 54006 and 54063 before and after the installation of the flood alleviation scheme in 2003.....	134
Table 6.7 Details of available River Thames fluvial gauges.....	135
Table 6.8 Selected gauges for use in conditional dependence model	138
Table 6.9 Number of retained extreme events after de-clustering skew surge data for a range of r values.....	147
Table 6.10 Fitted GPD parameters for selected network	147
Table 6.11 Confidence intervals for the GPD model fit at a 1.3 AEP event	148
Table 6.12 Number of days when core gauges have missing data 1979 - 2010.....	150
Table 6.13 Percentage of relative event maxima over 5 day lag at each site from a sample of 24000	161
Table 6.14 RMSE of peak events simulated from conditional dependence model using infilled and observed data	165
Table 7.1 Definition of FEH Physical Catchment Descriptors	177

Table 7.2 Goodness of fit of published DMF to peak flow conversion methods for UK data ..	180
Table 7.3 Goodness of fit of optimised DMF to peak flow conversion methods for UK data ..	181
Table 7.4 Goodness of fit of DMF to flood peak multiple regression model.....	182
Table 7.5 Available data for hydraulic river modelling	191
Table 7.6 Three representative surge shapes calculated used Ward's clusters for core coastal sites and their occurrence probabilities	198
Table 7.7 Conditional probability of wave direction at Dowsing.....	210
Table 7.8 Conditional probability of wave direction at Liverpool Bay.....	210
Table 7.9 Summary of offshore coastal water level simulation	211
Table 7.10 Example <i>a</i> and <i>b</i> coefficients for Owen's equation.....	216
Table 7.11 Example <i>r</i> coefficients for Owen's equation	216
Table 7.12 Summary of coastal modelling assumptions.....	217
Table 7.13 Available data for coastal inundation modelling	219
Table 7.14 2D Coastal inundation model input files.....	219
Table 8.1 Summary of Environment Agency flood defences survey data by defence type for the Lincolnshire coast.....	237
Table 8.2 Source of long section mean crest height by defence type for the Lincolnshire coast	237
Table 8.3 Classification of fit of long section mean crest height compared to survey data.....	238
Table 8.4 Classification of type of variation between long section mean crest height and survey data	238
Table 8.5 Probability of type of variation between long section mean crest height and survey data as calculated from the Lincolnshire defence survey data by defence type	245
Table 8.6 Distribution parameters characterising the degree of crest height variation	246
Table 8.7 Probability of low or height points within the defence section crest.....	246
Table 8.8 Distribution parameters characterising the shape of high or low points within the defence section crest.....	247
Table 8.9 Distribution parameters characterising the magnitude of variation from the long section mean crest height.....	247
Table 8.10 Distribution parameters of 1000 plausible simulations of magnitude of crest height variation compared to the long section mean.....	250
Table 8.11 Defence failure probabilities from overtopping	253
Table 8.12 Defence failure probabilities from wave run-up.....	253
Table 8.13 CTFRA assumed breach dimensions for North Wales defence sections.....	254
Table 8.14 Simulated breach dimensions for a North Wales example overtopping scenario .	258
Table 9.1 Damage and loss values for a breach in each North Wales defence section showing the difference between assumed point and distributed location of caravan units	270
Table 9.2 Percentage variation in damage and loss values for different assumed unit values	273
Table 9.3 Range of dimensions used to investigate sensitivity of flood damage to breach size	276
Table 9.4 Assessment of uncertainty in individual model components and contribution to overall uncertainty in system risk calculation.....	282

1 Introduction

1.1 Flood risk in the UK

The cost of extreme weather events globally has doubled each decade since the 1970s (Association of British Insurers 2005a). In the UK floods present the most significant risk and are expected to have an increasing impact in the future as the climate change (Defra and HM Government 2012; cite Rowland 2012). The Environment Agency estimate that one in six homes are currently at risk of flooding in England and Wales, with 2.8 million properties in areas at risk of flooding from rivers or the sea (Environment Agency 2009a). Notable flood events in the UK over the past century include the North Sea floods of 1953 and widespread inland flood events in 1998, 2000 and 2007. The Summer 2007 floods were the most costly flood in the world in 2007 (Pitt 2008). They resulted in the most costly insured weather event in the UK to date, with 165,000 insurance claims and £3 billion in pay outs (Association of British Insurers 2007), the equivalent of four years of normal claims (Pitt 2008). In societal terms the summer 2007 floods caused the largest loss of essential services since World War II (Pitt 2008).

The type of flood event that affects the UK is varied. In general the UK has a temperate climate with wet winters and dry summers. Heavy winter rainfall is expected to coincide with frontal systems from the Atlantic (Barrow and Hulme 1997) leading to frontal driven floods such as in Easter 2000. Summer floods are caused by intense local storms which lead to flash flooding such as in Boscastle in 2004 (Met Office 2011a). However the past five years has seen an increase in summer flooding for example in June and July 2007 and most recently in June 2012. These summer events have occurred following extended periods of wet weather followed by heavy storm events, possibly caused by a shifting of the jet stream from northern Scotland to the south east of England (Pitt 2008). Coastal events usually occur in the winter, driven by deep Atlantic low pressure systems causing storm surges which are a particular concern along the North Sea coastline (Haslett 2000; Pugh 2004).

The impact of extreme weather varies based on the local topography, geology, the presence of flood defences, the location of vulnerable assets and the ability of people to respond to flood warnings. Being able to correctly understand and model flood risk is of importance to a wide variety of people from property developers wanting to build on potential floodplains to the emergency services who provide the first response during a flood event. In the UK the Environment Agency (EA, in England and Wales) and the Scottish Environment Protection Agency (SEPA, in Scotland) are responsible for the management of most main watercourses in

the UK and for providing a flood warning service, as such many of the developments in flood risk modelling have been led by these bodies. The insurance industry also has a vital role to play in enabling people to continue living and working in areas of flood risk (Crichton 2003) and a vested interest in accurate modelling. Being able to understand the drivers of flood risk allows effective management of floods by both individuals and organisations, and enables prediction of how the risk might change in the future in response to climate and societal change.

1.2 Modelling flood risk

Models of flood risk take various forms depending on their purpose. Some focus more on the statistical distributions of extreme events (for example Keef, Lamb *et al.* 2009a), others on the hazard rather than a full consideration of risk (for example the Environment Agency flood maps 2009b). Increasingly it is becoming important to explicitly consider the uncertainty in flood risk models to enable informed flood risk management decision making (Beven *et al.* 2011). This presents additional challenges in communicating the uncertainty to end users in an accessible manner (Pappenberger and Beven 2006).

A fully integrated flood risk model requires consideration of sources of risk, pathways, receptors and consequences of flooding. Examples of these systems based models have been developed in the UK as part of the Risk Assessment for Strategic Pathways (RASP) project (Hall *et al.* 2003), in Europe by researchers at the University of Postdam (Apel *et al.* 2006), and by Catastrophe (Cat) modelling companies for insurance pricing, for example Risk Management Solutions (RMS) inland (RMS 2010) and coastal (Wood *et al.* 2005) models for the UK.

1.2.1 Sources

Flood risk in the UK is driven by extreme weather in the form of heavy rainfall or storm surges. Statistically an event is considered extreme if it exceeds some pre-specified threshold or is the largest in a specified set of observations. Extreme value theory is a special type of statistical modelling for events that meet these criteria. It addresses the difficulties of modelling events for which there are limited observations and where extrapolation beyond the observed data is required (Coles 2001). There is a long history of statistical analysis of extreme flood events in the UK, much of which was consolidated in the Flood Studies Report (NERC 1975) and updated in the Flood Estimation Handbook (CEH 1999).

In the case of flood risk, consideration of multivariate extremes is often required for events which cover large areas or are caused by multiple sources for example a combined fluvial and coastal event. Multivariate extremes present additional difficulties as they require identifying

which observations belong to the same underlying event across multiple sites. The area over which the event is classified also affects the extremeness, as the most extreme events tend to be very localised. Keef *et al* (2010) estimate the return period of the Summer 2007 floods for the week of the 19th July 2007 across the UK as 1 in 28 years, whereas flows at some individual gauges were estimated with return periods of over 1 in 150 years (Environment Agency 2008). Previous studies which have investigated the multivariate dependencies between extreme events in the UK include Svensson and Jones (2002; 2004) who used dependence measures to investigate the relationship between extreme sea surge, river flow and precipitation around the British coastline, Dixon and Tawn (1994; 1995; 1997) who conducted extensive research into spatial dependencies of extreme sea conditions around the UK, and Hawkes *et al* (2002) who developed a joint density statistical approach incorporating dependencies between wave height and period. The newest advance is the Heffernan and Tawn model (2004), a flexible multivariate model that allows relationships between variables to change as events gets more extreme and can be used when extreme values of all variables are unlikely to occur together. It is this model which has provided the basis for much of the recent work in the area of spatial dependencies of flood risk across the UK including the Environment Agency study “Spatial Coherence of Flood Risk” (SC060088/SR Keef *et al.* 2009a).

1.2.2 Pathways

Pathways refer to the obstacles between the meteorological sources and the receptors of flooding. They include the catchments, river system and flood defences water must pass through before any damage can occur.

In most cases high value receptors are protected by flood defences. The Environment Agency maintains 24,000 miles of defences in England and Wales (Environment Agency 2012).

Insurance cover for properties located within the floodplain is dependent on continued investment in flood defence infrastructure (Association of British Insurers 2008). While flood defences are essential to many communities their failure can be catastrophic as seen during the North Sea floods of 1953 and New Orleans in 2005.

Construction of flood defences has been somewhat piecemeal with defence heights gradually being increased as flood risk increases (Muir-Wood *et al.* 2005). Coupled with this is the problem that information on flood defence structure and condition is limited (Hall *et al.* 2003). In spite of these difficulties work by the FLOODsite project (for example Allsop *et al.* 2007 and Morris *et al.* 2009a), has made significant improvements in understanding flood defence failure mechanisms. The challenge remaining is to incorporate this detailed site level analysis into large scale models of flood risk. At present this is largely achieved through simplified

scenario based modelling (for example Hall et al. 2003) or by using simplistic empirical rules to enable breaches to be considered within a large risk sample (see Muir-Wood and Bateman 2005). In spite of continued research in the area, consideration of breaching remains a critical source of uncertainty in flood risk modelling (Muir-Wood and Bateman 2005).

1.2.3 Receptors and consequences

There is no risk from flooding if there are no receptors to suffer damage. In most flood risk applications receptors are considered to be property (Merz *et al.* 2010), however increasingly the impact on the economy, the environment, communities, and individuals is being considered (Messner *et al.* 2007). The standard means of assessing the impact on receptors is through the use of depth damage curves (for example see Penning-Rowell *et al.* 2005), whereby damage is specified as a function of flood depth. Damage curves provide a quick and efficient means of assessing damage however they make large assumptions about the construction of structures, and are based on limited observed data and expert judgement. As such damage curves can contribute a major source of uncertainty to flood risk models (Merz *et al.* 2010).

1.3 Flood insurance in the UK

Insurance is the process by which individuals can transfer risk from themselves onto an insurance company. The provision of insurance for natural catastrophes is invaluable to society as it helps communities recover from a flood event and enables property owners to secure a mortgage (Crichton 2003). Due to a historic agreement between Government and the insurance sector established around 1960 (Humber 2004), and the island geography of the country (Muir-Wood 1999), property owners in the UK are in a unique position compared to other countries as flood insurance is available to almost all properties as part of their standard household or business insurance. The agreement has continually changed over time, its current form, known as the Statement of Principles, states that the Association of British Insurers (ABI) will provide insurance cover to properties in areas where flood risk (including areas benefiting from defences) is less than 1 in 75 years provided that the Government maintains investment in flood defence infrastructure (Association of British Insurers 2005b). Following the summer 2007 floods, the ABI is reviewing the Statement of Principles but is committed to ensuring that flood cover remains as widely available as possible (Pitt 2008). To do this they require continued improvements in flood risk modelling.

The cost of flood insurance premiums is calculated based on estimation of the annual premiums needed to cover losses over time, termed the average annual loss (AAL) (Grossi and TeHennepe 2008), combined with a factor accounting for how much surplus insurance

companies require to be comfortable covering the risk (the Risk Load), and an allowance for their expenses and profit margins (Expense Load) as shown in Equation 1.1 (Grossi and Kunreuther 2005).

$$\text{Insurance premium} = AAL + \text{Risk Load} + \text{Expense Load} \quad 1.1$$

The AAL is the sum of expected losses for a set of natural disasters events each with an annual probability of occurrence, p_i , and an associated loss, L_i (Equation 1.2). Events are assumed to be independent however multiple events can occur each year.

$$AAL = \sum_i p_i L_i \quad 1.2$$

The calculation of AAL is subject to uncertainty in both the probability and loss terms. The insurance industry bases estimation of these terms on process based Catastrophe (Cat) models. A Cat model generally comprises of four modules (Sanders *et al.* 2002);

1. A stochastic module used to randomly generate catastrophic events
2. A hazard module used to determine effects based on local conditions
3. A vulnerability module used to calculate damages
4. A financial module which quantifies the financial loss

The first three of these modules correspond to the source-pathway-receptor terms outlined in Section 1.2. The financial module converts the damage to losses to the insurance company, for example by including the impact of policy excesses. One limitation of Cat models is that they are complex process based models which use a mixture of numerical and statistical methods making it difficult for the end user to fully understand the underlying processes.

1.4 Identification of research needs

Over the past decade the importance of taking a risk based approach to flood management has been realised and new methodologies have been developed covering different national and international contexts (e.g. Hall *et al.* 2003; Apel *et al.* 2006). While the risk from individual sources and at specific locations is extensively modelled, there is a growing need for understanding of risks from multiple sources and across large geographical areas. As yet there is no integrated risk model that incorporates all contributing factors and the spatial and temporal dependencies between them to enable integrated risk management strategies to be developed.

Recent large scale flood events in the UK and the continued threat of a major North Sea storm surge have motivated a reappraisal of how well flood risk is estimated by insurance companies. The new European Solvency II Framework (Directive 2009/138/EC European Parliament Council 2009) requires insurance companies to show evidence of understanding of the processes and potential uncertainties within their risk models. While the exact date of application is continually being revised (European Parliament Council 2012), from 2013 companies will be required to demonstrate greater understanding of, and transparency in, their risk pricing mechanisms. When considering extremes it is difficult to know which representation of risk is most accurate. Rather, the most suitable representation depends on the particular asset of interest, its geographical location and vulnerability, and the insurance company's appetite for risk. Therefore it is useful for an insurance company to increase its understanding of risk outside of the Cat modelling framework. This additional knowledge can then be compared with data produced by the Cat models and used to inform risk based decision making regarding the management of insurance policies.

An increasing openness from both Cat modelling companies and the insurance industry to work with academia has led to a new era of collaboration on flood risk modelling, for example through the Lighthill Risk Network (2011) from which this PhD initiated, and the Willis Research Network (2011). This sharing of expertise is beneficial to both parties as Cat models have long since been criticised for not being subject to peer review (Smith 2009) however the resources available to the insurance industry are far greater than those in academia and therefore collaboration provides unique opportunity to improve flood risk science.

Drawing together the need for continued advance in flood risk modelling to cover multiple sources and large geographical areas and the requirement for increased understanding of insurance risk pricing, this thesis develops a new methodology for considering multisite concurrent damage from fluvial and coastal flood events using a case study of risk to an insurance portfolio of static caravan located across the UK. The portfolio is underwritten by Catlin (Catlin Group Limited 2009) who have provided a CASE studentship and expertise on Cat modelling and insurance pricing for this project. Static caravans provide a useful example of the application of this methodology as they are generally located on large sites close to water, are distributed across the whole country and are particularly vulnerable to flood damage. A particular concern for Catlin is that their portfolio covers 80% of the static caravan stock in the UK, therefore if risk to the portfolio is not correctly modelled there is potential that following a major flood event Catlin may find that they were overexposed.

This thesis builds on the application of Heffernan and Tawn's (2004) multivariate conditional dependence model for the consideration of spatial and temporal dependencies in flood risk by Keef *et al* (Keef 2006; Keef *et al.* 2009a; Keef *et al.* 2009b; Keef *et al.* 2009c; Lamb *et al.* 2010) and shows how this robust but complex statistical model can be used in an applied case study and integrated into a full systems based approach. The methodology presented in this thesis was developed to address the issues facing Catlin's caravan portfolio, however due to its modular nature it can be adapted for use with a wide range of flood management decisions in the future, and is especially useful for spatially distributed risks.

1.5 Aims and objectives

The aim of this project is to develop a new method for multisite concurrent damage due to multiple weather related extremes based on spatial statistics and physical processes and to apply the method to assess the vulnerability of UK caravan sites. The research is unique as it will consider multivariate sources of risk rather than just fluvial or coastal flooding. It will be spatially distributed, looking at sites across the UK and it will take a whole system approach by investigating the influence of pathways on the system response.

By explicitly considering all major drivers in the risk system, the research aims to highlight potential weaknesses in the existing modelling of flood risk, with particular reference to Cat models and the pricing of insurance portfolios. Through working with Catlin it is hoped to be able to increase understanding of their caravan portfolio, the risks it is affected by and how the risk is modelled and priced. At a high level the project aims to start to make a contribution to the Solvency II requirements and help enable insurance companies to continue to provide the high level of cover currently available.

The project objectives are to;

1. Review the geographical disposition of fixed caravan sites in the UK and their approximate financial values and investigate trends in historic flood damage to these sites.
2. Establish a multivariate spatial extreme value statistical model for river flow, surge and waves at selected sites.
3. Develop a process-based method to connect these source terms with variables (e.g. flood depth) from which damage can be computed.
4. Consider the representation of flood defences and potential failure mechanisms in flood risk models and incorporate this into a systems based risk model.

5. Review the importance of each component in the systems risk model and discuss how the improved knowledge about each component and the links between them can help improve insurance pricing decisions and wider flood risk management

1.6 Thesis outline

This thesis brings together multiple specialities within the area of flood risk modelling and management. The thesis is structured in a way that clearly defines the contribution of each area but also demonstrates the importance of the interconnections between them. Following this introduction, Chapter 2 provides an overview of existing methods of flood risk modelling and analysis, discussing both insurance industry risk models and those used for wider flood risk management. This is followed by a summary of the specific way in which risk is modelled for the Catlin caravan portfolio in Chapter 3 and a review of historic events which have affected the portfolio. Chapter 4 then details the development of a new methodological framework for multi-site risk analysis. From this point the thesis largely follows the Source-Pathway-Receptor-Consequence (SPRC) structure outlined in Section 1.2. Chapter 5 reviews the spatial and temporal dependencies between extreme weather events in the UK and existing methodologies that have been used to model them. In Chapter 6 details the modelling of multivariate spatial extremes through a statistically based conditional dependence model. Chapters 7 and 8 cover the pathways term, discussing the conversion of simulated peak flow at gauges into water levels at the sites of interest, the incorporation of waves into the simulation of coastal flood events and the modelling of spatially variable flood defence reliability. Finally the assessment of damage is outlined in Chapter 9 followed by consideration of how to calculate multi-site risk and the embodied uncertainties in this calculation. Chapter 10 provides some final concluding remarks on the significance of the methodology developed in this thesis for improving understanding of dependencies in flood risk and identifies areas for further work.

2 Flood risk modelling and analysis

2.1 Introduction

Flood risk modelling is a complex science that includes multiple contributors with multiple priorities. As such a range of methods have been developed. This chapter will review the available statistical and systems based methods of analysis current in use by flood risk managers, the insurance industry and academic researchers. In doing so it will identify areas where the existing methods can offer useful tools to meet the aims and objectives set out in Section 1.5 and where there are limitations to the existing approaches that need to be addressed. This review is used to inform the development of a methodological framework for multi-site risk analysis as outlined in Chapter 4.

2.2 Defining risk

Much debate exists in the literature over how to define flood risk (For example see Sayers *et al.* 2003). Multiple definitions exist (some of which are listed by Kelman 2003), influenced by the social and cultural positioning of those making the definition and the purpose of the analysis. There is no universal definition of risk that is suitable for all (Sayers *et al.* 2002) however a common engineering definition is that risk equals the probability of an event multiplied by the consequence (Sayers *et al.* 2003). This is the definition that is used in this thesis. However it is acknowledged that a simplistic definition such as this is limited in its ability to represent risk in all situations since the way people respond to high probability low consequence events is different to their response to low probability high consequence events (Sayer *et al.* 2002). The insurance industry focusses on monetary risks which are devolved from societal weightings, however they are not immune from these issues. Although multiple high probability low consequence events could have the same impact as one low probability high consequence event, it is the low probability event that will cause a major shock to the industry and expose weaknesses in the risk management decision making of companies that are not fully prepared. High losses from low probability events also trigger re-insurance contracts. Re-insurance is the process by which insurance companies protect themselves from large losses by sharing the risk with other companies, often termed ‘insurance for insurers’(Swiss-Re 2002). Correctly setting the price point for re-insurance and the amount of cover required necessitates accurate modelling of high risk events.

The benefit of taking a risk based approach is that it deals with outcomes (Sayers *et al.* 2002) allowing decision makers to compare a wide range of options. Over the past 15 years risk based approaches have become commonplace in flood risk management and the methodologies behind them have become increasingly sophisticated. In spite of this there is

often still a lack of distinction between flood risk and flood hazard (Rougier, Sparks *et al.* In press). The Environment Agency Flood Risk Maps in the UK could more accurately be described as flood hazard maps since they consider only the return period of an event and the associated flood outline rather than an assessment of the consequences. De Moel *et al.* (2009) identify that this is the case for most flood risk national mapping programs in Europe; however this will have to change in the future as the EC Flood Directive requires vulnerability to be incorporated into risk analysis.

The units of risk depend on how the probability and consequence of an event are quantified. Probability may be expressed as a dimensionless percentage. This is usually given for a specific time frame, for example an annual exceedance probability (AEP). Probabilities may also be expressed as frequencies defining the number of expected occurrences of an event within a particular time period, for example a one in 100 year flood event (Sayers *et al.* 2003).

Consequence may be expressed in a variety of quantitative or qualitative forms depending on the consequence of interest for example number of deaths or degree of social interruption. Here the focus is on insured loss so the units of consequence are monetary.

Combining the probability and consequence terms gives the risk term. For financial analysis this usually takes the form of an Exceedance Probability (EP) Curve as shown in Figure 2.1, or it can be combined into a summary measure such as the AAL (Equation 1.2). An interesting mathematical aside is that the area under the EP curve is equal to the AAL.

The AAL is a useful comparative measure for insurance purposes as it specifies the minimum value at which the portfolio should be priced to ensure the company breaks even. Other insurance based risk metrics include the Value at Risk (VaR) and the Tail Value at Risk (TVaR) which can provide a useful means of assessing the sensitivity of the risk calculation to the extremes (Denuit *et al.* 2005; Society of Actuaries in Ireland 2011).

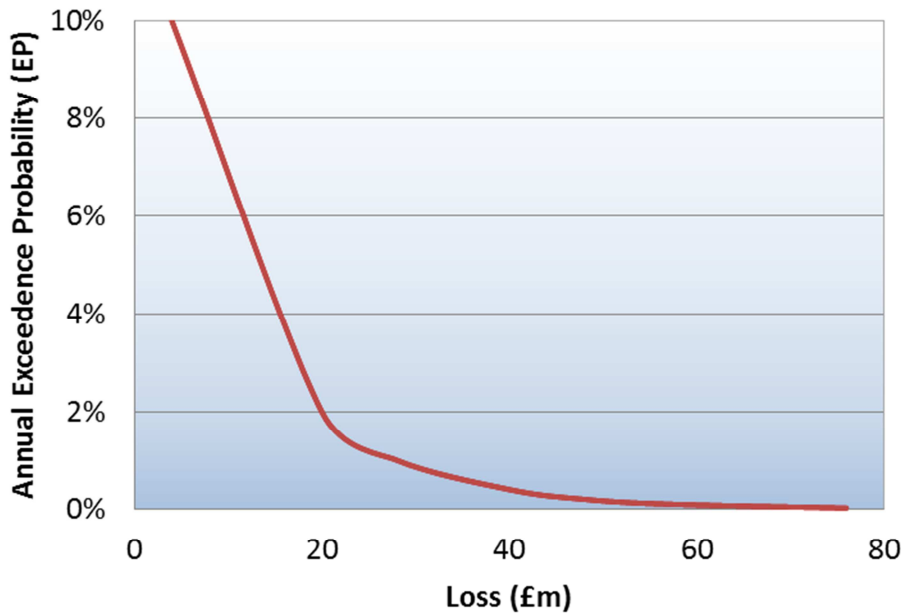


Figure 2.1 Example exceedance probability curve

2.3 Who models flood risk?

With one in six properties in the UK at risk of flooding from rivers or the sea (Environment Agency 2011a) consideration of flood risk forms an essential part of many decision making processes.

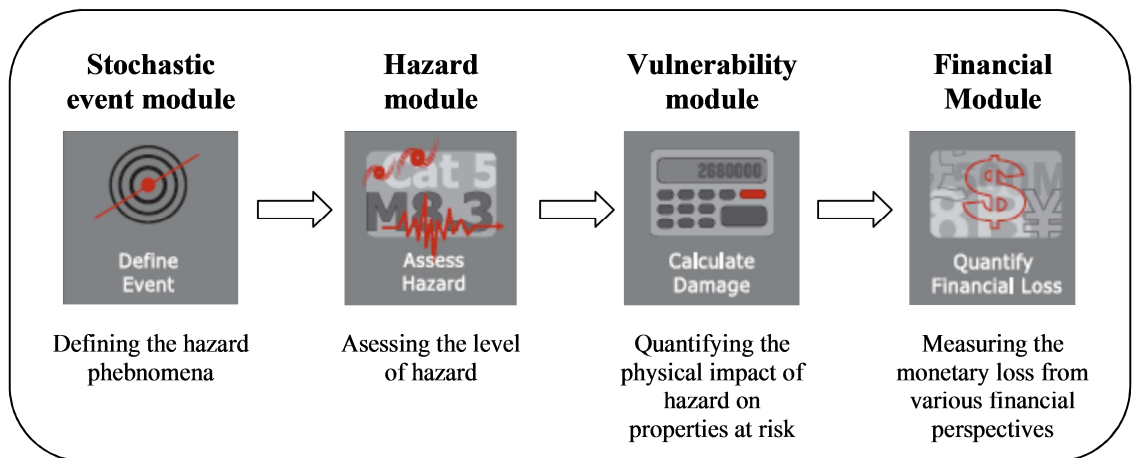
The Environment Agency is responsible for the management of most watercourses in the UK and for providing a flood warning service. As such a large proportion of the analysis of flood risk is carried out by, or for, the Environment Agency or DEFRA. This may take a number of forms, for example:

- Large scale, high level studies such as Catchment Flood Management Plans (CFMPs) and Shoreline Management Plans (SMPs),
- Detailed scientific studies such as the 'Spatial Coherences of Flood Risk' study (Keef et al. 2009a) discussed further in Chapter 5. The output from these detailed studies often informs the standard protocols for flood risk assessment for other purposes.
- Local applied studies for example to assess the need for, or design of, flood defence schemes in a specified area.
- High profile projects such as the National Flood Risk Assessment (NaFRA) scheme (Environment Agency, unknown date) which produces up to date flood maps of all main watercourses in the UK. The output of which is publically available (Environment Agency 2009b) and is used extensively for flood risk management in the form of

planning and flood warnings. The flood maps are also provided to the insurance industry.

Other organisations with a role in flood risk management include local councils and property developers who are required to produce Strategic Flood Risk Assessments (SFRAs) and follow the PPS25 (Communities and Local Government 2006) guidance on development in flood risk areas.

The insurance industry has a vested interest in understanding flood risk and uses Cat models to estimate the probability of flooding. These are large scale process driven models consisting of a stochastic event module which is then translated into risk through a hazard, damage and financial module as illustrated in Figure 2.2. Initially, in the UK, Cat models were developed for coastal storm events however the major floods of 1998 and 2000 promoted the development of inland flood models. As well as the high profile Cat models, the insurance industry also carries out independent studies into flood risk in an attempt to keep abreast of recent developments in the science, for example Lloyds produces its own flood map (Lloyds 2010) and the Willis Research Network provides a platform for exploring new areas of interest in the field. Cat models are discussed further in Section 2.4.3.



Modified from Grossi and TeHennepe (2008)

Figure 2.2 Basic structure of Catastrophe Models

Academic research has also played an important role in the development of flood risk model, either through collaborations with other stakeholders or in independent studies. The benefit of academic research is that it usually has more freedom to explore particular areas of interest without being constrained by applications or commercial deadlines. However there is often a significant time lag between the results of research projects being implemented in applied studies or assessment guidelines. This can be due to difficulties in communication between the

two groups and time and financial constraints on applied studies. One of the aims of the Environment Agency Science Program is to try to bridge this gap.

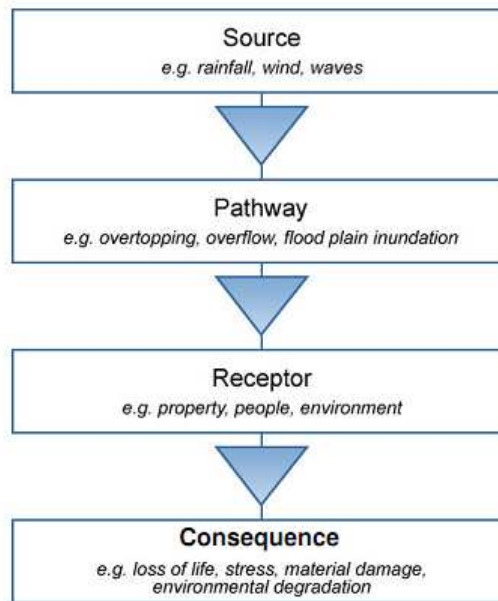
Flood risk is clearly not confined to the UK. Many of the key developments in the field originate in countries where particular issues are especially important, for example the Netherlands is particularly vulnerable to failures in its flood defence system and as such has been instrumental in developing methods of analysis for flood defence reliability such as the PC-RING software (Steenbergen *et al.* 2004). Similarly the long river systems such as the Rhine and Danube in mainland Europe have motivated cross border studies involving a strong consideration of spatial and temporal dependencies in flood risk (for example Apel *et al.* 2006).

2.4 How is flood risk modelled?

The methods used to assess risk depend on the scale of analysis and the resources available. Flood risk modelling requires consideration of both the probability of an event and its impact. As such a variety of different modelling methodologies are usually drawn upon. Setting up a flood risk model requires;

1. Establishing the required outputs - either event based such as the risk from a 1% AEP event, or reference quantities such as the AAL,
2. Choosing the scale of analysis - ranging from single site up to national or international assessment,
3. Identifying the main focus of analysis – either a full systems based model or focussing on particular elements such as the driving forces or defence reliability,
4. Selecting appropriate analysis methods for each component in the risk system based on the scale, focus and required output – methods may be statistical or physically based, scenario driven or fully probabilistic.

In most cases flood risk assessment methodologies can be broken down into a Source-Pathway-Receptor-Consequence framework (S-P-R-C), although this does not always form an explicit part of the methodology. As illustrated in Figure 2.3 the S-P-R-C framework considers all stages in the risk process identified in Chapter 1. If any one component of the S-P-R-C framework is missing there is no risk. For example a large event in a rural catchment may cause a flood however if there are no receptors in the floodplain there are no consequences and hence no risk.



(Source: Sayers, Gouldby *et al.* 2003)

Figure 2.3 Conceptual Source-Pathway-Receptor-Consequence model

Models that explicitly consider all stages of the S-P-R-C framework are known as systems based models. The first modelling framework to consider a full systems based approach was the UK RASP methodology (Hall *et al.* 2003), further details of which are given in Section 2.4.2. A similar approach was taken by Apel *et al.* (2006) working on the River Rhine in Germany. Insurance industry Cat models also have an underlying S-P-R-C framework and can be thought of a special case of systems based models. The development and construction of Cat modelled is discussed further in Section 2.4.3

A limitation of systems based models is that due to the multiplicity of factors involved it is difficult to assess the uncertainty in the model and in most cases it is not possible to go further than an uncertainty assessment for each component (Rougier *et al.* In press). The implications of this are discussed further in Section 9.4.

Systems based models are complex and computationally demanding, as such it is common for modellers to focus on the particular area of interest such as the source or flood outline without full consideration of all components. Models focussing on the source term usually take a statistical approach as discussed in Section 2.4.1 and may be coupled with simplistic inundation models to generate flood outlines for hazard focussed assessments.

The following sections discuss in further detail the types of model most relevant to this study, statistical models, systems based models and Cat models.

2.4.1 Statistical models

Statistical models largely only consider the event probability and not the risk, however by focussing on one aspect of the problem they can provide detailed analysis of the characteristics of extreme events. Often the output from statistical models is used as the basis of full risk based methods. A critical difficulty in the study of floods is the lack of data on very large events. A family of statistical methods known as Extreme Value Theory (EVT) provides a robust framework for overcoming this problem (readers with limited knowledge of EVT may find Coles 2001 a useful introduction to the subject). This section highlights some of the existing research and main resources covering the statistical modelling of extremes. Further details are provided in Chapter 5.

In the UK standard guidelines are available for estimating extreme fluvial events as part of the Flood Estimation Handbook (FEH) (CEH 1999). The main purpose of these guidelines is to enable users to create flood frequency curves from observed data to estimate design events such as the 1% AEP peak flow. Recently the Environment Agency has developed a set of guidelines (R&D SC060064) for coastal analysis which also enables users to establish a design event storm surge (McMillian *et al.* 2011a) and significant swell wave height (McMillian *et al.* 2011b) for any point on the UK coastline. These guidelines are less comprehensive than the FEH, but do represent the first application driven guidelines for extreme coastal events. A more comprehensive statistical assessment of extreme sea levels is provided by Dixon and Tawn (1997) although this does not include a wave component.

While single site statistical models for individual sources can be useful in enabling hazard maps to be drawn for given locations, they are of limited use for informing systems based models since there may be more than one driving event and many interacting processes within the system. In most cases there is some form of dependence structure exhibited in the variables of interest which can have spatial, temporal or multivariate components. This dependence structure requires specialised statistical modelling. There are a variety of existing studies that have investigated the importance of modelling the UK specific multivariate extremes of interest in this thesis. These are listed in Table 2.1 along with their findings which indicate the importance of including the dependence between extreme meteorological events in a risk analysis. More details of statistical models for multivariate spatial extremes are provided in Chapter 5.

An alternative to statistical modelling is continuous simulation. This is argued by Hawkes *et al.* (2008, p329) to provide the “simplest and most transparent approach to joint probability analysis” since the correlations between variables are implicitly included. Continuous

simulation has been investigated for flood risk modelling in the UK by CEH (Calver *et al.* 1999), however given the known difficulties in creating a useable model and the computational costs involved, it has not been considered further in this thesis.

The challenge of statistical modelling of flood risk is to use a statistical framework which is robust enough to preserve the extremal properties of the data and simple enough to be used in practical applications. Also fundamental to all applied statistical models is the problem of ensuring that reliable and long data records are available for the areas of interest (Hawkes *et al.* 2008). Often this is not the case and solutions have to be found to work with the available data sets.

The Environment Agency project 'Spatial Coherences of Flood Risk' (SC060088, Keef *et al.* 2009a) provides a good example of a framework for incorporating a multivariate spatial dependence model into practical flood risk applications, including consideration of the limitations of data availability (originally developed by Keef 2006). The scope for using the conditional dependence model for a variety of applications is discussed in a proof of concept report (Lamb *et al.* 2009) and by Lamb *et al.* (2010). At present this method has seen limited application beyond the original authors of the report, however there is clearly potential to extend the method for use in a full systems based model. Further details of the method and its potential extensions are discussed in Chapters 5 and 6.

Table 2.1 Existing work of multivariate extremes in the UK

Variables considered	Reference	Summary of method	Summary of results
River flow	Keef <i>et al.</i> (2009a); Keef <i>et al.</i> (2009c)	Uses the conditional dependence model of Heffenan and Tawn (2004) for daily mean flow (DMF). Estimates dependence statistics conditional on at least one gauge in the network being extreme.	<ul style="list-style-type: none"> • Lower spatial dependency in flows where catchment characteristics change rapidly over a small area and in areas with large water bodies in catchments or low permeability
River flow and rainfall	Keef (2006); Keef <i>et al.</i> (2009b)	Uses the conditional dependence model of Heffenan and Tawn (2004) for DMF and rainfall data. Estimates dependences statistics conditional on at least one gauge in the network being extreme.	<ul style="list-style-type: none"> • Events become more localised in space as they become more extreme. • Rainfall displayed weaker spatial dependence in upland areas and strongest dependence in the South-East • Flows displayed stronger spatial dependencies than rainfall
Coastal surge, river flow and rainfall	Svensson and Jones (2002); Svensson and Jones (2004)	Uses the threshold based χ measure (see Coles, Heffernan <i>et al.</i> 1999) for daily series of maximum surge, daily mean flow and daily precipitation accumulation	<ul style="list-style-type: none"> • Dependence between flow and surge stronger in winter than summer for the East and South West coast • Strongest dependence between flow and surge occurs in North East Scotland and hilly western areas, due to more rainfall and flashier catchments • Low dependence in South East where permeable catchments respond slowly to rainfall

Variables considered	Reference	Summary of method	Summary of results
Sea level and wave height	Hawkes <i>et al.</i> (2002)	Uses a joint density approach based on water level, wave height and wave period. Fits GPD to each variable and then fits dependence between pairs of variables to simulate a large sample from fitted distribution.	<ul style="list-style-type: none"> • The dependence between surge and wave height can be masked by the astronomical tidal component of sea level. • More extreme conditions show stronger dependencies than everyday conditions. • Modest correlation between waves and surge height. On the East coast strong northerly winds producer both large surges and swell. On the west coast the swell may be less correlated to local weather conditions.
Sea Level	Dixon and Tawn (1994); Dixon and Tawn (1997); Dixon <i>et al.</i> (1998)	Uses the Spatial Revised Joint Probability Model (SRJPM) to consider relationship between tide and surge then applied spatial model across whole coastline. Range of other models also investigated included r-largest, JPM and RJPM.	<ul style="list-style-type: none"> • Extreme sea level caused by high tide and moderate surge in all areas except Cromer to Dover where it is caused by high tide and extreme surge • In regions with complex bathymetry there is high spatial variability in sea level between locations due to changes in tide • Suggest ignoring tide surge interaction could lead to over estimation of extremes by 5%

2.4.2 Systems based models

System based models do not necessarily seek to develop new methods for analysis of all parts of the system but rather draw on existing methodologies to create frameworks for analysis of risk that explicitly consider all of the interacting processes. The driving source variables are modelled using the statistical approaches outlined above and the consequences are estimated using derived depth-damage curves (for example see Penning-Rowsell *et al.* 2005) which are discussed further in Chapter 9.

One area where system based models have contributed significantly to new component methodologies is in the consideration of flood defence failure. Although the traditional reliability analysis of flood defence has taken place in engineering projects such as FLOODsite (for example see Morris *et al.* 2009a; Morris *et al.* 2009b; Morris *et al.* 2009c) there was no consideration of how to include defence failure in flood risk analysis in the UK beyond a simplistic scenario based approach prior to the work of Hall *et al.* (2003) as part of the RASP project (DEFRA 2004). A probabilistic approach forming the basis of the PC-RING software (Steenbergen *et al.* 2004) had previously been developed in the Netherlands, however, as illustrated by Buijs *et al.* (2003; 2004) this approach was not directly transferable to the less heavily engineered defence systems found in the UK. The recent work of Apel and Vorogushyn *et al.* (Apel *et al.* 2006; Apel *et al.* 2009; Vorogushyn 2009; Vorogushyn *et al.* 2010) in Germany has built on the work from RASP and PC-RING and further enhanced the consideration of defence failure to incorporate varying spatial and temporal loading of the defences throughout the system. More details of flood defence failure methodologies are discussed in Chapter 8.

The modelling framework that is drawn on most in this project is that of RASP. The RASP approach is outlined below to illustrate the structure of a systems based model although contributions from the work of Apel and Vorogushyn *et al.* are discussed throughout the remainder of this thesis.

2.4.2.1 RASP

RASP is a set of methodologies developed to address the challenges of making risk based decisions at a range of scales given the restrictions of data availability and computational time. The strength of the methodology lies in its ability to incorporate analysis of defence overtopping and failure methods with limited data and without the need for multiple, time consuming hydraulic model runs. RASP incorporates a hierarchy of risk assessment methodologies (Hall *et al.* 2003) depending on the scale of application. The benefits of this approach mean that some form of risk assessment can be made even if the available data are

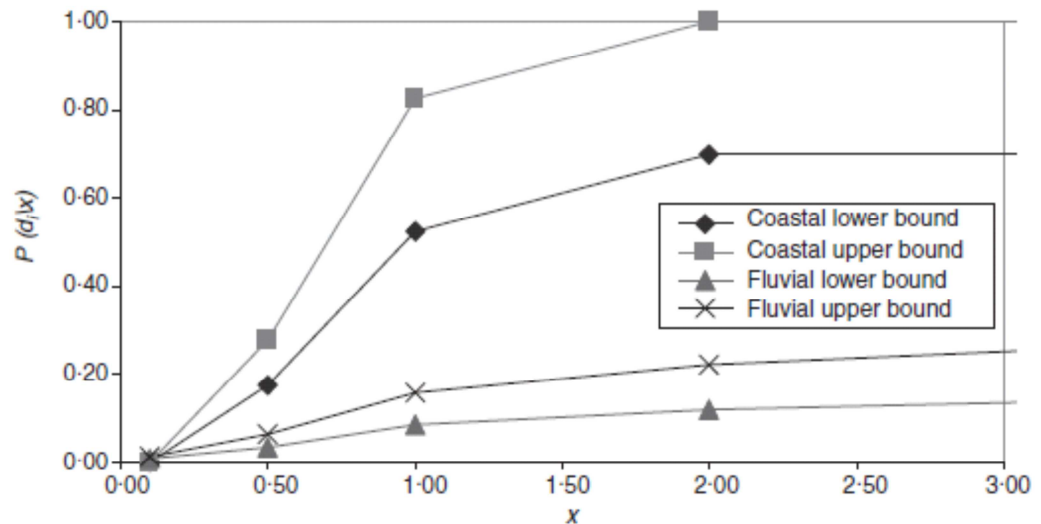
limited. This is particularly important given the limited data on flood defence properties in the UK.

The original ideas behind the RASP methodology were outlined in a paper by Hall *et al* in 2003 and extended to the more detailed regional level methods by Gouldby *et al* (2008). The methodology is now widely used in the UK including high profile applications as part of the Environment Agency National Flood Risk Assessment process (NaFRA) and in projects such as the Thames Estuary 2100 (TE2100) as well as local SFRA. Through collaboration with international organisations the ideas are also being applied outside the UK, for example in China as part of the 'China-UK Scenario Analysis Technology for River Basin Flood Risk Management in the Taihu Basin' project (Harvey *et al.* 2009). The existing RASP tools were recently improved to allow further exploration of future flood risks and management options, and new software developed to allow Monte Carlo based assessment of uncertainty when using the RASP methodology for NaFRA (HR Wallingford 2009a). The Environment Agency has accepted the methodology as the framework around which flood risk decision making in the UK should be based. A strong indicator of the significance of this is the inclusion of RASP methodologies in the new Multiple Decision Support Framework Software (MDSF2) which will provide a GUI for application of the RASP methodologies by all flood risk practitioners (HR Wallingford 2009b).

Within RASP, for each flood event, any given defence section (d_i) can either fail (D_i) or not fail (\bar{D}_i). The probability of failure is a combination of the probability of an extreme load (l) and the defence resistance to that load.

$$P(D_i) = \int_0^{\infty} p(l) P(D_i|l) dl \quad 2.1$$

A variety of failure mechanisms are considered by using fragility curves developed following reclassification of the Environment Agency National Flood and Coastal Defence Database (NFCDD) based on defence type, crest width, external protection, construction, and defence condition assessment, further details are provided by Hall *et al* (2003). The simplest failure mode to consider is breaching following overtopping. An example fragility curve for this scenario is shown in Figure 2.4. The loading variable is defined based on a factor (x) of the standard of protection (SOP) of each defence.



Source: Hall *et al.* (2003, p239)

Figure 2.4 Overtopping fragility curves used in national flood risk assessment

The amount of water on the floodplain is calculated from the rate of flow over or through the defence for an appropriate duration based on standard discharge equations as given in Hall *et al.* (2003). The main differences between the high and detailed methodologies occur in the floodplain inundation modelling. For the high level methodology water is distributed across pre-specified flood outlines based on valley type (Hall *et al.* 2003) however for the regional level methodology raster based flood routing is used (Gouldby *et al.* 2008). Given the development in computational power since 2003, arguably there is no longer a reason for this difference unless suitable Digital Elevation Model (DEM) data are not available.

The RASP methodology provided the first systematic approach to incorporate flood defence failure into risk models in the UK. It was therefore an important step forward in flood risk modelling however the defence failure methodology is based on three key assumptions (Hall *et al.* 2003);

1. Loading of all defences in the system is fully dependent, meaning all defences are subjected to the same load at the same time.
2. The strength of each defence section is assessed independently therefore although the load is the same, the probability of failure is unique for each defence section.
3. The resistance within each defence section is fully dependent meaning the whole section responds in the same way.

The first of these assumptions is arguably the hardest to sustain since it means that if a defence breaches upstream, the downstream defences continue to be subjected to the same load even though the stress of the downstream defences would be relieved by storage of water behind the upstream breached defence. Apel *et al* (2006; 2009) investigate the impact of spatially variable loading across a defence system and illustrate that for areas with significant floodplain storage behind the defence structure this assumption could lead to errors in the risk assessment. The third assumption is met by restricting the length of any individual defence section to 600m. The reasoning behind the value of 600m is largely based on the sampling frequency of observations on defence properties, however given the spatially varying nature of defences and the significance of random points of weakness (Institution of Civil Engineers 1953) this could lead to errors in the assessment of risk. The implications of these assumptions are discussed further in Chapter 8.

2.4.3 Catastrophe models

Cat models are a particular type of system based model used by the insurance industry to predict the probability and associated costs of extreme events. They provide a means of “event-specific stochastic modelling of highly correlated multi-location loss” (Muir-Wood 1999, p1). They are useful as the infrequent, highly severe and unpredictable nature of catastrophic events is such that catastrophe claims data are of limited use for setting policy rates (AIR Worldwide 2009). Cat models are usually developed by specialised modelling companies and then licenced for use by insurance companies. The results from the models are usually used to set policy prices although recent advances have seen the models being used for wider flood risk management (Shah 2008).

Cat modelling originated from the field of property fire insurance and from the practice of measuring natural hazards such as earthquake magnitude in the 1800s. Its current form, influenced by developments in measuring techniques and Geographical Information Systems (GIS), was born in the USA in the 1980s but did not become widely accepted until the destruction caused by Hurricane Andrew in 1992 highlighted the need for more sophisticated approach to catastrophe risk management (Grossi and Kunreuther 2005; Grossi and TeHennepe 2008).

Following their development in the USA, Cat models are now used across the developed world for a variety of natural hazard risks. In Europe the greatest risk is acknowledged to be windstorms which account for 80% of European Insured losses (RMS 2009) as such windstorm Cat models have been in used in the UK for over 20 years. There are also a number of models available for storm surge along the East coast of the UK motivated by fear of a repeat of the

1953 storm surge. Development of UK inland flood models is a relatively new aspect of Cat modelling. Arguably as following the relatively dry years of the early 1990s when Cat models were starting to develop, there was little political or economic incentive to develop a UK inland flood model. The widespread flood events of recent years have changed Cat modellers' perspectives. Risk Management Solutions (RMS) launched a UK Flood model following the 2000 events and AIR launched its inland flooding model in 2008 post the 2007 floods. EQECAT currently has a European inland flood model and is in the process of developing a UK model. A list of available Cat models for the UK is provided in Table 2.2.

As the prominence and capabilities of Cat models increases there is concern within the industry that insurers are relying too heavily on Cat models rather than their own judgement (Gray reported by Lloyd's 2006; Clarke reported by Gusman 2008). Clarke highlighted the need for the insurance industry to use Cat models as a tool rather than the absolute truth and to be aware of the limitations and assumptions contained within the models. This concern is reflected in the new Solvency II legislation which requires insurances companies to be able to justify any decisions and assumptions they make when pricing insurance (European Parliament Council 2009).

Table 2.2 Available catastrophe models for the UK

Company	Model Name	Risk
AIR	UK Flood	Coastal flooding
	Inland Flood Model	Inland flooding
	Extra Tropical Cyclone (ETC)	Wind
Benfield Grieg	UK GAPWind	Wind
	UK GAPFlood	Coastal flooding
EQECAT	Eurowind	Wind
	UK wind	Wind
	UK Flood	Coastal flooding
JBA Consulting	JCALF catastrophe modelling framework	Inland flooding
RMS	Europe Windstorm	Wind
	UK River Flood	Inland flooding
	East Coast UK Storm-Surge Flood Model	Coast flooding

Cat modelling companies, and the insurance companies who use the models, are in direct competition with each other. As such there is a lack of detailed information about Cat models available in the public domain. Some limited information is provided on the Cat modelling companies website although this is largely marketing material and unlikely to give an unbiased description. A review article by Sanders *et al* (2002) discusses a range of Cat models and draws some comparisons between different models, however this report is becoming increasingly

out of date as models are continually being updated in response to technology developments and demands for more detailed modelling. The RMS Storm Surge model is discussed in papers by Muir-Wood *et al* (Muir-Wood and Bateman 2005; Muir-Wood *et al.* 2005) with reference to flooding on the East coast of the UK. Beyond this online financial commentaries and publication of industry conference material can also provide a useful insight into progress made by, and issues facing the insurance and Cat modelling communities, although they are unlikely to provide any detailed information about the models themselves.

This lack of information has a threefold effect; firstly the insurance industry users need a better understanding of Cat models to use the results effectively. Secondly the general public is becoming more aware of climatic risks and as such are demanding more information on how these risks are modelled. Thirdly Cat models have traditionally been subjected to very little peer review, there is no benchmark to evaluate Cat models against and no one within the industry has taken responsibility for evaluating them. This means Cat models are being used without full knowledge of their ability (Pielke, reported by Green 2005).

Cat modelling companies are beginning to respond to this information gap with more information available online (for example RMS 2008) and AIR's new Inland Flood Model has been peer reviewed by experts from universities, HR Wallingford and CEH (AIR Worldwide 2008). The industry is realising that to enhance both its science and its credibility stronger links are required between insurers, Cat modellers, the regulator (Lloyd's) and academia. Research groups such as Wills Research Network and the Lighthill Risk Network are a means of achieving this, as is a strong presence at academic conferences, for example Guanasekera and Foote from Willis convened a session at EGU 2011 (NH9.1/EG8) at which work from this thesis was presented (Speight *et al.* 2011). An acceptance is starting to emerge amongst the Cat modelling companies that "today there are very significant differences between the various catastrophe models on the market, and it is in our interest that these differences be understood and evaluated by the users of modelling results" (AIR Worldwide 2009). The requirements of the new Solvency II legislation (European Parliament and the Council of the European Union 2009) also mean that insurance companies will have to show more scientific justification for their modelling and pricing decisions in the future which may promote more transparency within the industry. However much of the detailed information about the models is still only available to subscribed customers. The following review should be read in light of these constraints.

2.4.3.1 *Cat model structure*

The basic Cat model structure was illustrated in Figure 2.2. The following two sections outlines the main components, focussing on the RMS models as these form the basis of Catlin's modelling capabilities. Unless otherwise stated, the information used in this review is available from the RMS website (RMS 2009).

RMS UK River Flood

The RMS UK River Flood model provides high resolution modelling of risk on and off the floodplain including; major and minor rivers, temporary stream flow, surface water flows, ground water and drainage overflow in urban areas, and can capture correlations between different sources of flood risk. In total around one million kilometres of river and surface water flow routes are modelled on a 10m DEM grid. Since its first release in 2000 the model has been updated to include continuous simulation modelling for incorporating antecedent conditions, seasonality, and enhanced flood defence data from the Environment Agency database.

The weather input to RMS River Flood is based on a UK wide stochastic rainfall event set derived from the RMS time-stepping European precipitation model which simulates 100,000 years of frontal and convective extreme events over Western Europe. The spatial-temporal rainfall patterns have been verified against 45 years of reconstructed European rainfall. In total around 700 stochastic events are used in the River Flood model. Events are classified into four categories, Frontal, Mesoscale Convective Complexes (MCC), Thunderstorms and East Coast, with the areal extent of each event determined based on rainfall totals above 25mm. Rainstorms are assumed to be elliptical in shape with the greatest intensities in the centre of the ellipse. The storms can travel along predefined storm tracks with a stochastic velocity variable. Thunderstorms are assumed to be stationary (Smith 2009).

The model uses a continuous simulation approach to account for antecedent conditions and seasonality. Stochastic rainfall inputs can be specified as single or multiple events up to a duration of 168 hours (based on standard re-insurance event specification) allowing loss dependency between different locations on the same river to be incorporated (Sanders *et al.* 2002).

The statistical rainfall-runoff methods, as described by the FEH are used to convert rainfall into flow (Smith 2009). Different components of the system are modelled in different ways including a numerical model of major rivers and a hydrodynamic physical model of flooding on minor floodplains and surface water using separate models for each catchment. The model uses a variable resolution grid, up to 50m. Defences, and their potential of failure, are included

in the floodplain inundation model. Damage functions are calculated based on occupancy, height, age, and construction type. They include 12 risk modifiers to allow the client to change factors such as the presence of basements or particular vulnerability to water. If no building inputs are available then the model uses a database of typical building characteristics for the area. The damage function approach has been derived using a combination of theory and claims data from recent flood events (1998, 2000 and 2007). Results are produced at a postcode level.

The model can be used to produce return period flood maps, flood risk rating tools and probability loss models in RMS Risk Link. Analysis is possible at a range of scales including single sites referenced by latitude and longitude, street address, postcode units, postcode sectors and CRESTA zones (areas used as the basis for insurance portfolio analysis).

Table 2.3 Summary of RMS UK Inland Flood model

	Event Module	Hazard Module	Vulnerability Module
Description	<ul style="list-style-type: none"> • Uses a stochastic event set of 700 UK rainfall events • Rainfall is converted to flow using FEH Rainfall -Runoff methods 	<ul style="list-style-type: none"> • Allows modelling of on and off floodplain hazard including rivers, temporary streams, surface water, ground water and drainage overflow • Numerical model of major rivers • Hydrodynamic physical model of floodplain and surface water 	<ul style="list-style-type: none"> • Damage function based on: occupancy, height, age, and construction type • 12 risk modifiers available for client to change vulnerability • Results given at postcode level
Data sources	<ul style="list-style-type: none"> • RMS European precipitation model 	<ul style="list-style-type: none"> • 10m DEM • Environment Agency Flood Defence database 	<ul style="list-style-type: none"> • Theory and recent claims data from 1998, 2000 and 2007

RMS UK Storm-Surge

The RMS storm surge model covers the East Coast from Hornsea in the Humber Estuary to the Thames Estuary at Margate. A detailed description of the model is provided by Muir-Wood (1999), this is summarised below. An application of the model to investigate the impact of a repeat of the 1953 storm surge is described by Wood *et al* (2005). The model is based on stochastic storm surges with associated wind fields and different tidal states and includes a defence failure model. The wind fields are derived from the RMS European Windstorm model (summarised in Table 2.5) which is run in conjunction with the storm surge model. Floodwater

inundation is modelled using a time stepping approach which allows both the depth and duration to be accounted for. Tide data are used from 25 gauging stations along the East Coast.

The most intensive North Sea surges are caused by wind storms from three types of Extra Tropical Cyclones (ETCs) in the North Sea;

1. Northern North Sea – storms moving east across the north North Sea which cause northerly winds on the East Coast
2. South East tracking – storms moving to the South east of the eastern North Sea which cause high winds across the western North Sea and cause a storm surge along the East Coast towards the Netherlands. It was this type of weather system that caused the 1953 storm surge
3. Southern North Sea – storms moving slowly across the southern North Sea which become compressed by anticyclones over Norway and creates strong on-shore north-easterly winds.

Wind fields from historic events of these types were reconstructed and checked against surge forecasting models. Within the RMS European Windstorm model there are 586 stochastic windstorms that cause events of this type. As the surges are derived from the windstorm model it is possible to assess the correlations between windstorms and coastal surges using this model.

To account for the fact that storm surges may arrive at different points in the tide cycle and will have a different effect depending on the tidal state, the stochastic windstorm events are separated into groups of three potential outcomes dependant on the tide surge interaction. The more dominant the tide, the shorter the duration of high water during the event (Wood *et al.* 2005). Tide and surge are then combined at 69 reference points along the coast to define local water levels. The water levels were checked against Dixon and Tawn's (1994) statistical analysis of extreme water levels around the UK coastline (Wood *et al.* 2005). The model also takes account of the impact of extreme waves associated with the surges.

All of the East Coast is protected by either manmade sea defences or natural defences such as cliffs, sand dunes and pebble embankments. The sea defences have been modelled based on data from the Environment Agency's 1996 Sea Defence Survey. Each defence is assigned the water height of the nearest reference point. The probability of breaching or overtopping is then calculated based on defence fragility curves derived from the defence condition, length and duration of the event. The equations used to model breach failure are described by Wood *et al.* (2005). If breaching occurs the defence is assumed to erode rapidly to ground elevation.

Each stochastic event is divided into two breach scenarios, passive response (no breaching) or breaching response. Combined with the tidal interactions, this gives a maximum of six possible surge events per generating windstorm.

Flood water propagation inland is modelled based on the water flux, topography and ground roughness on a 50m grid. Vulnerability functions were developed based on RMS’s historic flood data based on property type, height and content. The impact of high velocity water, which can cause significant structural damage, was included in the damage functions through a multiplier effect for depths of over 1.5m and decreasing exponentially with distance from the source.

Table 2.4 Summary of RMS UK Storm-Surge model

	Event Module	Hazard Module	Vulnerability Module
Description	<ul style="list-style-type: none"> Combines characteristics of observed storm surge with stochastic wind fields likely to drive these events Combines surge and tide at 69 reference points along the coast to give total water level Adds an extreme wave component 	<ul style="list-style-type: none"> Consideration of defence breaching using fragility curves for defence condition, defence length and event duration Inland propagation calculated on 50m grid based on topography and ground roughness 	<ul style="list-style-type: none"> Damage function based on: occupancy, and construction type Includes multiplier function for high velocity flows
Data sources	<ul style="list-style-type: none"> 25 tide gauges RMS European Windstorm model 	<ul style="list-style-type: none"> EA Sea defence survey 	<ul style="list-style-type: none"> Observed flood losses database

Table 2.5 Summary of RMS European Windstorm model

	Event Module	Hazard Module	Vulnerability Module
Description	<ul style="list-style-type: none"> ETC large scale wind events and summer thunderstorm downdrafts Simulates storm tract with associated wind speeds for each event 	<ul style="list-style-type: none"> Model produces 3 second peak gusts and 10 minute mean wind speeds on a 1km grid. Wind speeds are adjusted for roughness up to 80km away 	<ul style="list-style-type: none"> Damage function based on: occupancy and construction Results given at postcode level
Data sources	<ul style="list-style-type: none"> European dataset of 2500 wind events Numerical models use to develop stochastic windstorm event set 	<ul style="list-style-type: none"> Roughness values from satellite data and aerial images 	<ul style="list-style-type: none"> Performance of different building types under laboratory and observed conditions

2.4.3.2 Data quality

The increasing sophistication of Cat models means that they are now more sensitive to high resolution data. Poor data quality accounted for up to 45% of the difference between modelled and actual loss following hurricane Katrina (Lavakare and Mawk 2008). Given the various different components involved in Cat models there are multiple data sources that can contribute to uncertainty including meteorological observations, resolution of spatial data such as DEMs and vulnerability data. Improving data quality has become a competitive advantage point between rival Cat modelling companies but at present there is no industry standard for data, although this is an issue that is currently being addressed by the industry (Lavakare and Mawk 2008).

2.4.3.3 Modelling assumptions

Cat models, like all other types of model, embody a number of assumptions and are forced to make a compromise between complexity, accuracy, available data, knowledge and computational costs. Cat models are heavily reliant on historic data to generate the stochastic event sets. Like all models, the data needs to be reliable and cover a long enough period to include the most extreme events in the record. Most Cat modelling companies have compiled their own event catalogues from a variety of sources to ensure that this assumption is met. The use of historic event data also relies on the premise that the past is a good approximation for the present and means that the models are of limited use to predict the impact of climate change as they do not appear to include any means of modifying the stochastic event set. This is not a major issue for insurance companies as they only need to price policies for the short term. Therefore so long as the Cat model is updated frequently with new observations the models are fit for purpose.

The generation of extreme events is the core element of Cat models and as such incorporates many assumptions. Cat models are all based on an event duration of seven days. This is motivated by re-insurance contracts which will pay out on losses sustained within a seven day period. This artificial constraint could result in correlated events being split into two insurance events by not fully considering the lag time, for example between a low pressure system causing coastal flooding and heavy rainfall and fluvial flooding. However given the nature of events in the UK, and the relatively short river length this is unlikely to be a major problem as previous research suggests these features will be contained within a two day window (Keef *et al.* 2009a). A linked concern is the effect of flood events like summer 2007 where two separate low pressure systems brought heavy rainfall to the UK within a four week window, the July

flooding therefore was partly dependant on the preceding event causing wet and waterlogged ground. These issues are discussed further in Chapters 5 and 6.

The stochastic event generators are assumed to simulate realistic event sets. Smith (2009) conducted a review of the stochastic rainfall module of RMS River Flood and concluded that it suffers from several limitations and assumptions, mainly due to the analysis of extreme events not adequately reflecting the variability in extreme rainfall and the variable storm generating mechanisms across the UK. However Smith concludes by saying that many of these limitations are not necessarily a deficiency of the model as more complex methods should only be used if the observed data supports them. Similar observations could be drawn for the windstorm and storm surge models, for example RMS have recently identified that the large scale correlations in wind gusts are not represented in their European Windstorm model (Bonazzi *et al.* 2011) and are therefore working on means to better represent this in future releases.

Awareness of the relationships between different sources of risk is starting to become apparent within the insurance industry (Collins 2008a; Collins 2008b). This is important as insurers need to be aware of risks that could affect their entire portfolio at the same time, however correlations between input sources are not explicitly represented in Cat models. The use of historic observed data to generate stochastic events implicitly represents the spatial correlations within events. However at present there is limited consideration of the links between fluvial and coastal flood events. The RMS Windstorm and Storm-Surge models can be linked together but the Inland Flood model must be run separately.

2.4.3.4 Variation between models

The degree of variation between different models depends on the phenomenon being modelled. Hurricanes are well understood so there is less difference between different companies' hurricane models than between different UK Flood models (Royal Meteorological Society 2010). The degree of variation also depends on the component or value being compared. For example the variation between the mean values may be different from the variation between the most extreme values (Royal Meteorological Society 2010).

The general structure of Cat models is very similar and from the high level descriptions available for review it is difficult to identify the major differences between them. An alternative method is to run the same portfolio through all available models and compare the results however the licensing fees prevent most companies from being able to do this. For the large companies and regulators who are able to (such as Willis and Lloyds), the terms of their license present the results from being made public.

Although the general structure is the same, differences are likely to occur within all of the four modules identified in Figure 2.2 due to the use of different data sets, different stochastic event generation, different flow propagation function, and assumptions around the defence fragility and the vulnerability calculations. Some qualitative remarks can be made, for example according to Jewson, the head of Cat modelling for RMS in the UK, one of the major differences between the models is in the vulnerability functions due to the lack of knowledge of how buildings may respond (Royal Meteorological Society 2010). Saunders *et al* (2002) make some more quantitative observations as part of their review, most interestingly for coastal models that EQECAT's probably maximum losses (PMLs) can be up to eight times higher than RMS' and RMS' assumptions regarding sea defence failure probabilities are more optimistic than EQECAT's.

The variation between models is due to epistemic and epistemological uncertainty. One model is not necessarily better than another but rather provides a different, but equally valid, representation of reality given current levels of data and scientific understanding (Royal Meteorological Society 2010). Communicating this to insurance companies is an on-going challenge for the regulators and modelling companies.

2.5 Informing risk based decision making

This chapter has identified a variety of flood risk assessment methodologies at various scales of analysis. To fully address all of the components of the flood risk system and the important interactions between them it is recognised that a systems based approach is required.

Cat models are an example of a specialised systems model for insurance pricing. Cat modelling companies have traditionally been criticised for the lack of information available about their models. The review of RMS' inland flood model and storm surge model provided in this chapter has illustrated that by combining information from a number of different sources it is possible to get a good overview of the main model components. In spite of this Cat models are essentially "plug and play" modelling systems and only the Cat modelling companies themselves are able to develop the models and have access to the internal knowledge about the processes and assumptions within the models. This limits the use of Cat models as a tool to help increase understanding of flood risk by end users. This situation could potentially be improved in the near future with the advent of Open Source Cat modelling which is a concept that appeals to a number of stakeholders in the area due to its potential to open up the Cat modelling business. One example is the OASIS project (OASIS 2012) supported by the Lighthill Risk Network which is developing, amongst other perils, a UK flood model. However there are

numerous political and logistical issues to be addressed before open source Cat modelling can become mainstream.

Despite the increasing partnerships between the insurance industry and academia the debate over the commercial sensitivity of Cat models is on-going and unlikely to be solved in this PhD. Instead the focus here is on developing a framework to help insurers better understand the type of questions they should be asking themselves when using Cat models. To do this the next chapter investigates how Catlin's portfolio is currently modelled using RMS' Cat models and then a systems based model is proposed in Chapter 4 which explicitly considers all of the important aspects of the flood risk process including sources, pathways, receptors and the links between them.

Rather than focusing on developing increasingly complex models, there is a need for the end users of Cat models to better understand the processes involved to meet future legislation and to improve their risk management. Systems based approaches are continually being developed and offer a coherent framework to achieve this aim. Research has been done on most individual components of systems model but there has been limited work on an end to end systems approach that incorporates all the relevant improvements in science and technology, and is focussed on the end user. Developing a framework that can be used by the insurance industry to aid understanding of Cat model output and inform insurance pricing would be a useful contribution to the area. Such a framework would also be beneficial for wider flood risk management.

Through this review of existing methods some essential modelling criteria emerge that would be beneficial for informed risk based decision making. Ideally the proposed model should be:

- Transparent – with well-defined methodology, assumptions, and input data quality
- Adaptable – to cope with varying data availability and potential natural and manmade changes in the future
- Flexible – for focussing on particular aspects of importance in any given system or area of interest
- Efficient - to run quickly enough to simulate a large sample set for risk based analysis while still providing a robust and realistic framework
- Simple – to enable end users to understand the system and potential uncertainties

3 Case study

3.1 Introduction

The methodology developed in this thesis is motivated by a case study exposure dataset of static caravan sites provided by Catlin (Catlin Group Limited 2009). Catlin is an international specialty property and casualty insurer. Established in 1984 it is a large and well recognised company, owning and operating the largest syndicate at Lloyds and writing \$4069m of premiums globally in 2010 (Catlin Group Limited 2010).

Catlin currently insures around 80% of the fixed caravan stock in the UK. This equates to a total insured value of over £4 billion. They have been providing cover for this portfolio since 2001. Catlin do not provide cover to the remaining 20% of static caravans in the UK due to restrictions on the insurance provision, including not providing insurance to caravans that have previously been flooded, are below threshold levels set by previous flood events or to caravans over five years old. Catlin believe it is these restrictions that prevented them suffering major losses during the autumn 2000 and summer 2007 floods in the UK when other caravan insurance providers had to pay out considerable claims.

Having run commercial models to assess the risk to their caravan stock, Catlin are concerned that the commercial models may be under estimating risk, particularly from flooding. This is a particular concern given the large proportion of caravan stock insured by Catlin and the potential over exposure risk from a large event affecting multiple sites. Catlin are therefore interested in gaining additional understanding of the weather related extremes affecting their stock which can then be used to help improve insurance pricing.

Catlin's caravan portfolio is separated into four sub profiles;

- **Compass Caravans** which covers static caravans, chalets, park homes and residential buildings,
- **Compass General** which covers general commercial structures on the sites for example the shop,
- **Compass Private Clients** for individual clients taking out insurance through the company, and
- **Compass Direct** which mainly covers park homes.

The largest sub portfolio is Compass Caravans, which incorporates 57% of the Total Insured Value (TIV) of the whole portfolio (JLT Re 2008a). For simplicity in data management, and to avoid the added complexities of dealing with commercial properties, this study has focussed

on the data associated with the Compass Caravan account only. The Compass Caravan portfolio is continuously changing in terms of both the stock insured and the way Catlin's exposure is modelled. This description of the portfolio is based on data and modelling information from March 2009. This section has been compiled using data from two reports on the Compass portfolio (JLT Re 2008a; JLT Re 2008b) and information from Catlin.

The aim of this chapter is to establish the current practice when modelling the portfolio and identify potential areas where further investigation would be beneficial. The first part of this chapter reviews the caravan portfolio and related risk exposure. This includes a discussion of how risk to the portfolio is currently priced, identification of the major limitations of this approach, and, analysis of the past claims data from the portfolio. The second half of the chapter concentrates on particular areas at risk and establishes a subset of the caravan sites that will be investigated in more detail through the remainder of the thesis.

3.2 The caravan portfolio

The TIV of stock in the Compass caravan account is over £2billion. This is predominantly from caravans as shown in Figure 3.1

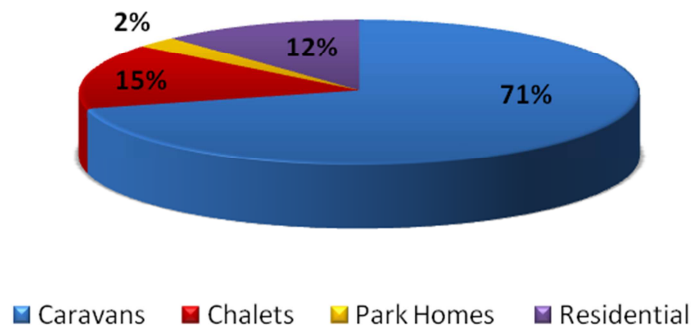


Figure 3.1 Accommodation type in the Compass Caravan account

The caravan stock is distributed around the UK as shown in Figure 3.2. Over a third of the sites are located within 1km of the coast with other notable concentrations in popular holiday hotspots such as the Yorkshire Dales and Lake District National Parks. The highest concentrations of insured values are in North Wales and along the Lincolnshire coastline as shown in Figure 3.3.

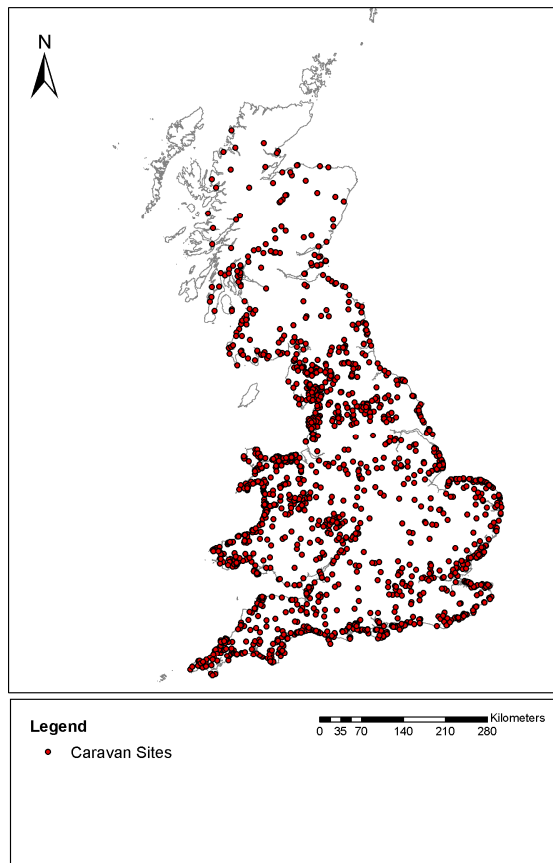


Figure 3.2 Compass Caravan Account site locations

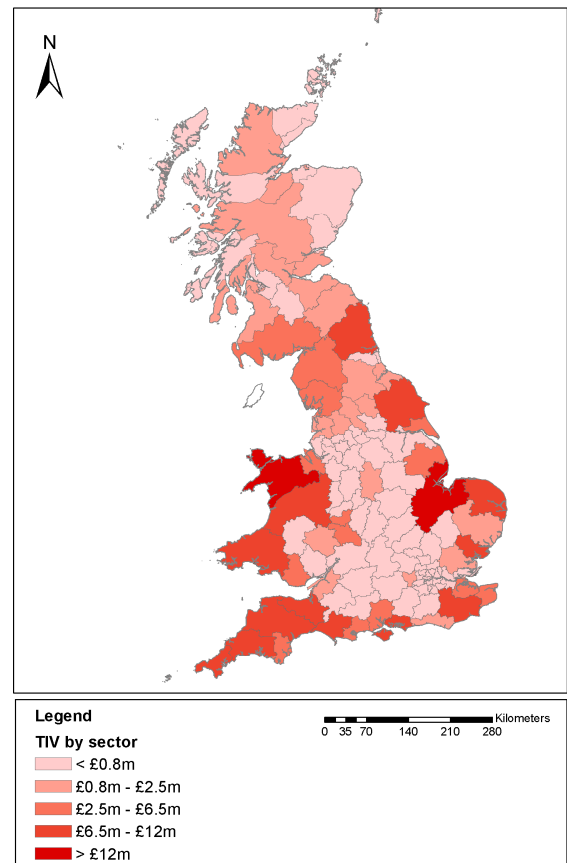


Figure 3.3 Compass Caravan Account Total Insured Value by postcode sector

3.3 Pricing risk to caravans

Catlin price their caravan policy using the RMS Inland Flood and RMS Wind and Storm Surge to calculate the AAL however Catlin currently take a conservative approach to pricing risk to the caravan account, adding 30% to 40% to the modelled losses to account for uncertainty.

Although Catlin provide the insurance cover they are not responsible for selling the insurance, this is done through an external company. The implication of this is that the information Catlin knows about the caravans to put into the Cat model is limited, in most cases only containing the site location at postcode level and the value of caravans, chalets, park homes and residential property at the site (Table 3.1). Various assumptions have to be made about the value of each unit, the total number of units at the site and the construction characteristics of each unit as discussed below.

Table 3.1 Data provided to Catlin about each insurance policy

Category	Description
Postcode	Usually given to 6 digits
Park name and address	The address is used for geo-coding if no postcode is given
Insured value of caravans, chalets, park homes, other structures	Total insured values for each structure type included in the policy
Total insured value	Sum of all structure types
Risk Reference	Reference number assigned to each policy

3.3.1 Unit value assumptions

Catlin has estimated the number of units at each site from the TIV based on the following assumed values (rounding down with the minimum number of units set to 1);

- Park Homes and chalets: £75,000
- Caravans: £20,000
- Other (residential): £125,000

The estimated number of units is used to calculate the deductible (excess) for each loss which Catlin specifies at £50 per unit.

A sensibility check was carried out on these assumptions using the value of individual units insured under the Compass Private Clients and Compass Direct schemes (rather than the per site values reported for the Compass Caravan scheme). Based on the insured value of 9432 individual caravans, the mean insured value was £19,352 (Table 3.2) indicating the assumed value of £20,000 is suitable. However there is a long tail to the distribution (Figure 3.4) with the maximum insured value reaching £117,500 (although it is possible that a single customer could insure more than one caravan under the same policy). Of particular note in the table below is that the mean insured value for park homes is more than double that for chalets. The two structure types are grouped together in Catlin's assumptions meaning that Catlin are likely to significantly underestimate the number of chalets on a site, especially as the minimum insured values are similar but there is a £90,000 difference in the maximum insured values. No data was available for other individual residential structures in the direct or private accounts.

Table 3.2 Summary of insured values of individual site structures in the Compass Private Clients and Compass Direct Schemes

Type	Number in data set	Mean insured value	Max insured value	Min insured value	Standard deviation
Caravans	9432	£19,352	£117,500	£2,500	£11,056
Chalets	1270	£39,990	£160,000	£7,500	£22,625
Park Homes	6363	£85,153	£250,000	£6,001	£31,357
Chalets and Park Homes combined	7606	£77,612	£250,000	£6,001	£34,463

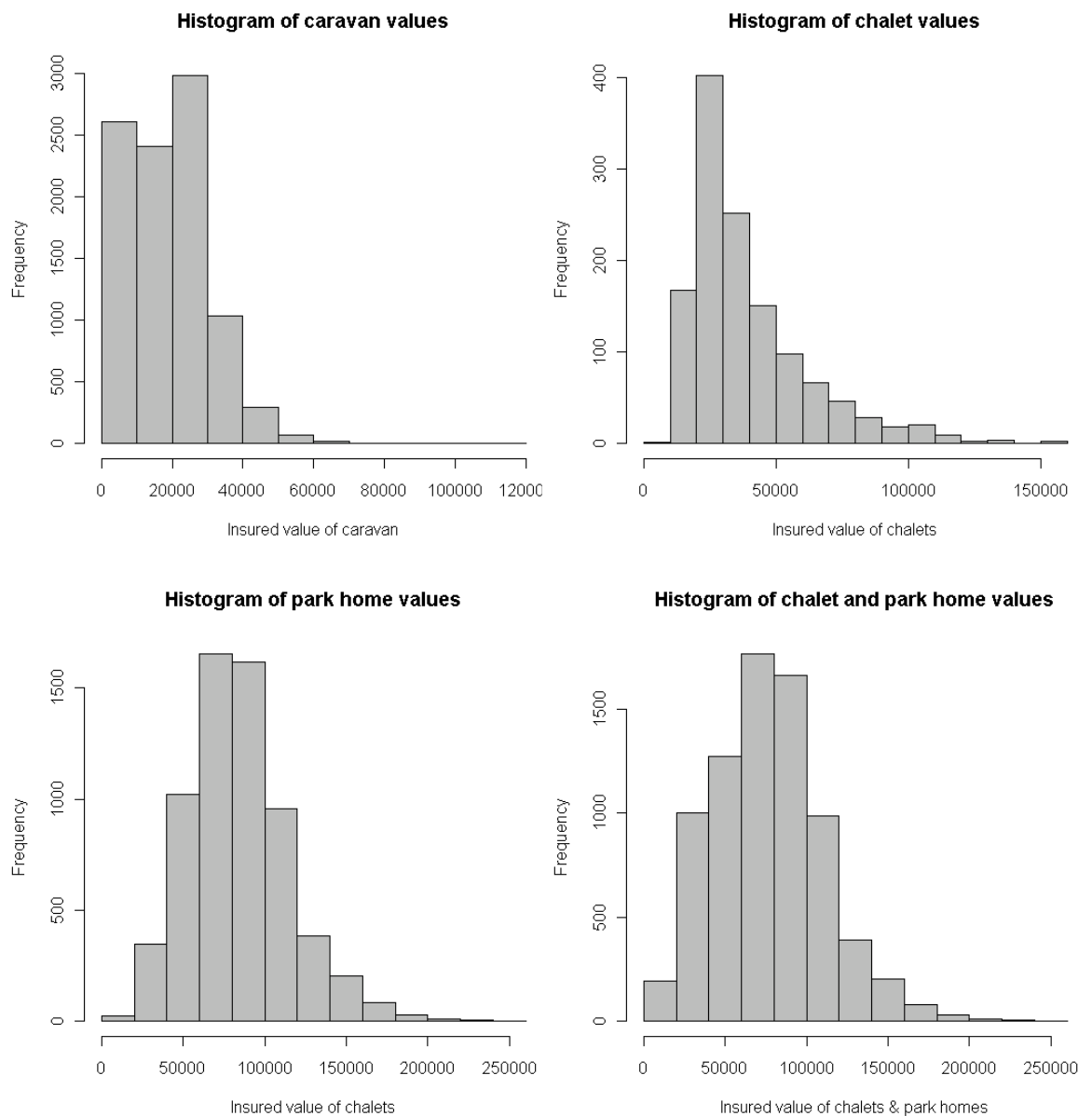


Figure 3.4 Histograms of insured values for each accommodation type in the Compass Caravan Account

McEwen *et al* (2000) conducted a review of the value of caravan site structures based on caravan sales websites and conversations with site owners. The results are shown in Table 3.3 and do not account for contents. Comparison of Table 3.3 with Catlin's assumed values also indicates that the assumed values are suitable although McEwen's data again confirms that combining park homes and chalets is likely to overestimate the number of chalets on a site. McEwen *et al*'s data are from 2000 and hence some account needs to be taken of inflation. A review of caravan prices in 2010 from internet sales sites reveals that the values for static caravans are still appropriate.

Table 3.3 Cost to buy new of different types of caravan site accommodation

Name	Cost to buy new	Description
Touring Caravan	£7000 - £15,000	Temporary
Static Caravan	£15,000 -£30,000	Semi-permanent
Mobile Home	£45,000 - £60,000	Prefabricated construction, built on park, more stable than static caravan but can still be removed if required
Chalet	£60,000 - £130,000	Wooded, semi-permanent structure

Source: McEwen *et al* (2000)

As well as the values, it is also possible to check the assumptions based on the number of units per site. Since it is difficult to identify if park structures are caravans, park homes or other residential buildings a check has been carried out comparing aerial photography and insured values for sites that can easily be delimited and which only have caravans and no other residential structures insured. It should be noted that not all caravans on a site are necessarily covered by the Compass Caravan account so in general the TIV per unit estimated from the photography is expected to be higher. A larger sample would be needed for conclusive results however Table 3.4 shows the results from five sample sites. There is a broad range of errors between the assumed and observed number of units which could be due to the inclusion of caravans not insured by Catlin, or because the site is a particularly high end site with a few valuable units rather than many cheaper units. In general, given the large standard deviation in caravan values, Catlin's assumptions produce a reasonable estimate of the number of caravans at each site especially when the interest is in the profile as a whole rather than individual units. The sensitivity of the damage and loss calculation to the unit value is assessed in Section 9.1.4.2.

Table 3.4 Comparison of Catlin assumed number of units on caravan sites with aerial photography for given sample site locations

Site location	From Catlin data		From aerial photograph	
	TIV (£1000)	number of units - assuming £20,000 per unit	Number of units	TIV - assuming £20,000 per unit (£1000)
Somerset	£2,273	113	146	£2,920
Cumbria	£1,107	55	28	£560
Essex	£2,077	103	347	£6,940
Devon	£1,128	56	76	£1,520
Fife	£6,894	344	516	£10,320
Fife	£1,054	52	55	£1,100

3.3.2 Unit construction and occupation assumptions

Within RMS RiskLink Catlin can set construction and occupation classes. Catlin specifies the construction type of park homes as “wood structure” and caravans as “unknown”. Where buildings are classified as “unknown” RMS RiskLink uses the occupancy to identify the type of building. There is no differentiation in RiskLink between mobile and static caravans. Catlin has coded the occupancy as “single occupancy summer houses” and “mobile homes” as appropriate. RMS RiskLink does provide a construction class for “manufactured / mobile homes” which could potentially be used to improve the damage calculations, however no details are available as to what assumptions this construction class makes and it is not currently available in the Windstorm model.

No information is specified about the split between buildings and contents insurance although both are covered. Normally this would be assumed to be around 60% buildings and 40% contents but as caravans are assumed to contain minimal possessions and most of the furnishings are part of the construction of the caravan, the buildings to content split for the portfolio has been assumed at 90% buildings and 10% content.

RMS RiskLink also allows additional information about buildings to be included through the use of modifiers such as the presence of basements or particular types of roof construction which makes properties more or less vulnerable during a catastrophic event. Catlin has not specified any modifiers for the Caravan account. However as Catlin do specify certain criteria before they will offer insurance (see Section 3.1), the modifiers could potentially be used to take account of this.

Catlin are aware of the importance of correctly specifying the unit construction and occupation types when modelling their exposure risk and have in the past carried out some simple sensitivity testing to identify the effect of varying the construction type and vulnerability of the caravans. Some of the options selected by Catlin were very extreme for example roof type as “thatched”, or occupancy type as “small marina.” Although this gives an impression of how sensitive the loss is to construction vulnerability, in reality it would not be sensible to model the caravans in this way. Results are presented in Figure 3.5 to Figure 3.6 for the most significant modification tested. Expected loss is standardised based on the 0.001 AEP (10 000 year) expected loss for each peril from the currently modelled construction class. Analysis of loss curves in this way can help understanding of the damage functions used in RMS. It should be noted that the exposure dataset used in Figure 3.5 and Figure 3.6 is different from the 2009 exposure dataset used in Figure 3.7 and Figure 3.8

The results show that the shape of the Occurrence Exceedance Probability (OEP) curve is similar for all construction and occupation types. The flood losses to mobile homes (as Catlin has coded them) are initially higher than for other construction and occupation types, and increases faster. This indicates a high vulnerability to flood damage. It is unknown what construction type RiskLink applies when the occupation is specified as mobile homes but comparing the modelled losses to the construction type wood, occupancy mobile homes curve indicates a more vulnerable construction type.

For flood losses the modifiers have a significant impact for example a 7% decrease in loss is expected for a 0.004 AEP event if the caravans are raised up to 1m above ground level, and a 15% increase in loss is expected for if there are large flood carried missiles. The flood missiles could be other caravans moved by the flood, site equipment or general flood debris such as trees in the flood water.

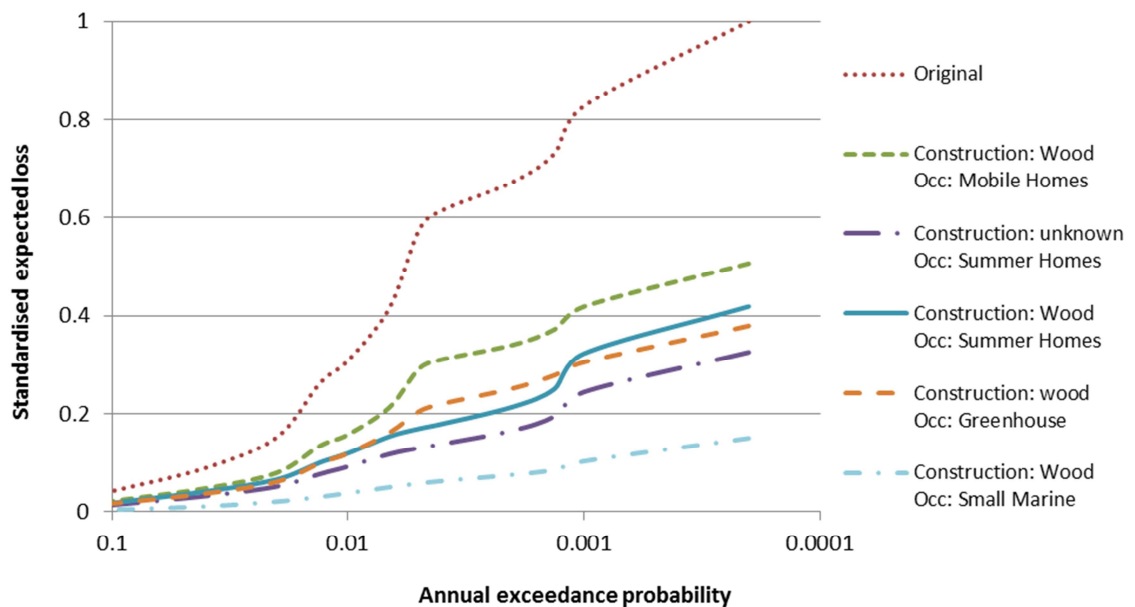


Figure 3.5 Results of previous Catlin analysis of the effect of changing construction and occupation class on flood losses

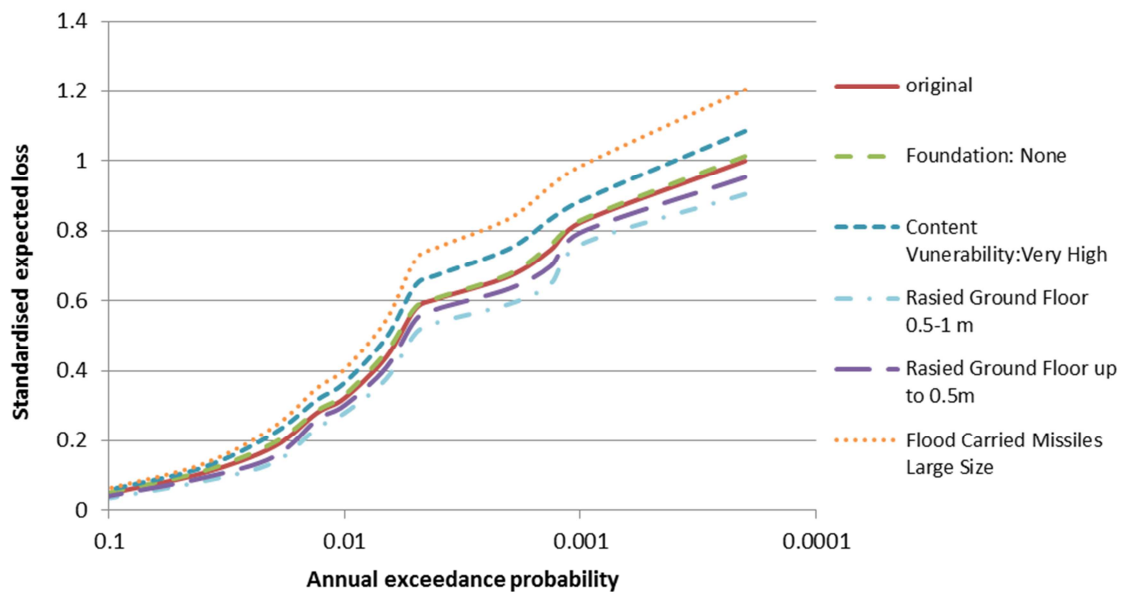


Figure 3.6 Results of previous Catlin analysis of the effect of changing vulnerability modifiers on flood loss

New sensitivity testing runs were made for this PhD by modelling Catlin’s exposure through RMS RiskLink for flood, wind, and combined wind and storm surge losses by comparing three scenarios:

1. As currently modelled, construction = “unknown”, occupancy = “mobile homes”
2. Construction = “unknown”, occupancy = “residential”
3. Assuming that a more representative coding for caravans could be occupancy = “mobile homes”, construction = “manufactured / mobile home”, floor level = up to 0.5m

Figure 3.7 and Figure 3.8 illustrate the high vulnerability of caravans under all perils compared to residential properties. It is also interesting to note that when the construction type is specified as “manufactured / mobile home” the vulnerability increases compared to Catlin’s current modelling values. This is most notable in the wind storm results since the effect of specifying the floor height at 0.5m above ground level reduces the flood losses for the other models. There is a step change in the loss curve around an AEP of 0.01 for flood losses which is not seen in the residential class. This is possibly indicative of a point in the damage function at which minor damage changes to major or irreparable damage. Further details of damage functions for caravans are discussed in Chapter 9.

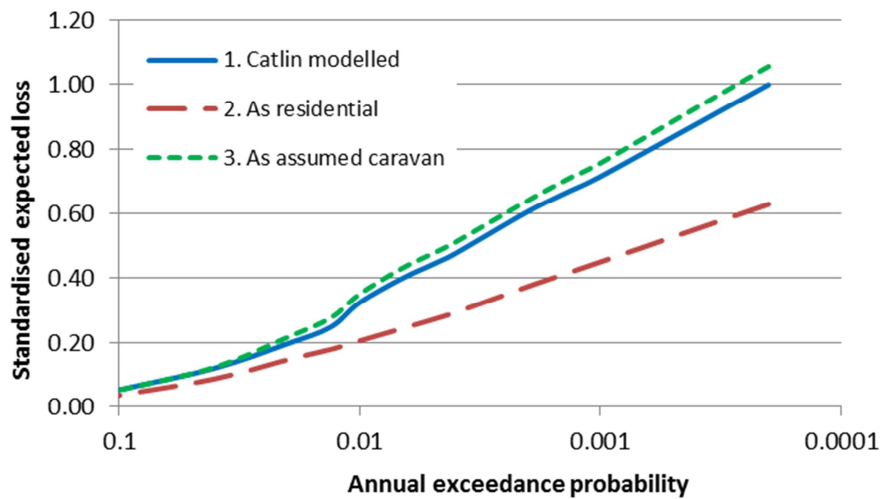


Figure 3.7 New sensitivity analysis of the effect of construction class on fluvial flood losses

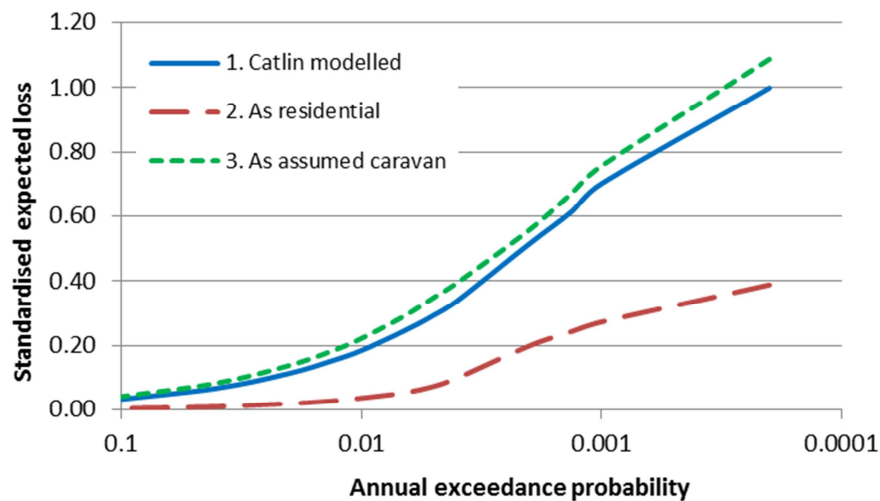


Figure 3.8 New sensitivity analysis of the effect of construction class on wind and storm surge losses

The various sensitivity tests presented in this section show that Catlin's assumptions for modelling caravans are suitable and give a conservative estimate of OEP when compared to other construction and occupancy types. Changing the construction to "manufactured / mobile home" would provide a more conservative modelling code. The RMS loss curves are particularly sensitive to the modifiers for flood losses, raising the ground flood level by 1m or specifying large flood missiles result in a 25% variation of the OEP. Catlin do not know this amount of detail about the individual units and sites, for example are the site structures such as fences and fuel storage, well situated or are they likely to become missiles during a flood event, are individual caravans raised above ground level or is there significant property stored beneath the caravan which would be damaged. Therefore it is difficult to use the modifiers

efficiently. Lack of knowledge about individual caravan construction therefore represents a major source of uncertainty in Catlin's ability to accurately estimate risk to its portfolio.

3.3.3 Location assumptions

The caravan site locations are specified as six digit postcodes. RMS uses these postcodes to geo-code the data before using it in the model. The geo-coding process matches the postcode to a known geographical unit within the model and assumes the site is located at the centre of this unit. The Compass Caravan account data has good geo-coding, 98.7% of sites are modelled based on postcode units, the remainder are modelled at city or CRESTA level (CRESTA zones are large aggregated areas used for insurance and re-insurance purposes).

The geo-coding means that a site is either modelled as flooded or not flooded based on whether the central point in the postcode unit is flooded. This method is standard across most Cat models and in most cases provides a reasonable approximation of location. However when considering caravans there are a number of particular considerations to take into account;

- Caravan sites are usually located in rural areas where the postcode units are large
- Caravan sites include multiple individual units, which for large sites may not all be represented by the postcode location of the site office
- The geo-coding assumption may result in an over or under estimation of risk where part of a site is flooded depending if the flooded area covers the centre of the postcode unit.

Figure 3.9 and Figure 3.10 illustrate the difference between the geocoded postcode locations and the observed spatial extents of the caravan sites for an inland location near Stourport-upon-Severn and for the Lincolnshire coastline near Ingoldmells. The coastal example illustrates a situation whereby the spatial extent of the site is much greater than the postcode point location, at its widest point the large concentration of sites in Figure 3.9 is 0.8km x 1.8km. The Stourport-upon-Severn example shows two sites where the point postcode location does not lie within the site outline. The largest discrepancy between the point location and the centre of the site is 0.4km. The sensitivity of damage to location assumptions is tested in Section 9.1.4.1.



Red stars show point postcode locations, yellow shading indicates site outlines

Figure 3.9 Discrepancies between caravan site postcode points and site outlines: Ingoldmells



Red stars show point postcode locations, yellow shading indicates site outlines

Figure 3.10 Discrepancies between caravan site postcode points and site outlines: Stourport-on-Severn

3.4 Past claims data

Insurance claims data from 2006 – 2009 were reviewed to identify the claims resulting from key events, and to identify any trends in the claims data. A review of claims data provides a useful addition to analysis of the observed hydro-meteorological event data, especially when carrying out a consequence based study. Both flood and wind storm events are reviewed due to the link between the wind and surge model.

Table 3.5 lists the information recorded for each claim. The claims data relating to caravans (reported as “Caravan Flood” or “Caravan Storm”) is reviewed in this section for both the number of claims and the total incurred loss. The number of claims can give an idea of how widespread an event is while the total incurred loss indicates the severity of the event. The value of loss for individual events is not reported due to data confidentiality. Losses are reported proportional to the total loss incurred between 2006 and 2009. This is calculated separately for flood and storm events.

Table 3.5 Information recorded for each claim in the caravan account

Category	Description
Claim reference	Claim reference
Policy holder	Name of policy holder, either name of individual or name of caravan site
Policy number	Policy number
Loss date	Date of the event
Claim description	Brief description of the claim e.g. “flood damage”, “storm damage to roof”
Catastrophe code	When a large event occurs it is assigned a code and all claims resulting from that event are coded the same. This allows for easy identification if re-insurance thresholds are reached.
Heading	Code identifying type of claim
Heading description	Description identifying type of claim e.g. “Caravan flood”, “Caravan storm”, “Chalet flood”, etc.
Claims paid	Amount awarded to the client
Fees paid	Fees paid by the client
Incurred loss	Claims plus fees

3.4.1 Quality of claims data

Catlin do not process claims directly and therefore do not keep their own claims record. The claims data available from the external company is poor and of limited use for a number of reasons;

- The detail of the event and resulting damage is limited, for example the record may just say “Flood” under description.
- Coding of events is unclear, the claim may be coded as “Caravan Storm” but the description refers to water damage. This could be due to errors in data coding, for

example a wind storm event causing damage to the caravan which results in water ingress by rainfall, or most importantly because there is no clear definition in the event coding between a wind storm event and a coastal surge event.

- Cross referencing between the claims event and the exposure dataset is difficult as the claim reference (Table 3.5) does not relate to the risk reference used by Catlin (Table 3.1). Therefore manual cross referencing must be used based on the name and address of the claimant and the addresses of the insured site however this does not always result in a direct match.
- There is no separation of claims from the four different accounts listed in Section 3.1.
- A site may make one claim for all affected units on the site or individual claims for each unit. This will affect the number of claims made per event.
- Once a site has been flooded, Catlin are unlikely to continue to provide insurance so the site may no longer appear in the portfolio. Analysis of records of past exposure portfolios is therefore required.

These factors make it difficult to identify the location of claims and to compare the claims data with the exposure database to establish the proportion of loss compared to insured value. In addition to these general inadequacies there is also evidence of poor reporting of the timing of events, particularly for wind storms which have possibly been grouped and recorded on 1st of the month.

Although a loss adjuster attends each site after a claim is received and makes more detailed reports of the damage, it was not possible to review the data from the loss adjusters as part of the project. Access to this data would have provided a more robust and detailed damage dataset to work with, and would have provided a useful dataset to validate the systems model with.

The following review makes the best use of the available data but should be viewed in light of the limitations of data quality, reliability and availability.

3.4.2 Review of past claims

In general the portfolio has performed well. During the large flood events of June and July 2007 only minimal losses, less than the estimated AAL of the combined Compass policy, were incurred. There have been no large scale coastal events over the past three years and given that the greatest concentrations of sites are located along the coast the portfolio performance may have been significantly different if a storm surge had occurred. The flood events that have occurred have resulted in a low number of high value claims. This is shown in Figure 3.11

which displays the proportion of total losses from flood and wind events over the claims period (2006 – 2009) sustained from each event. A 15% proportional loss on a given day means that 15% of the total flood losses from 2006 and 2009 were recorded on that date. Five key flood events, resulting in 49 claims, account for 76% of the total flood losses between 2006 and 2009. Details of the significant events over the claims period are listed in Table 3.6. This is in contrast to the five largest windstorms over the same period which accounted for 37% of the total wind storm loss but resulted in 875 claims. This is indicative of the vulnerability of caravans to flooding but is also a function of larger flood events being experienced over the past three years but no major windstorm events.

Table 3.6 Description of main flood events in the claims period 2006:2009

Event window	Description of event	Number of flood claims	Proportion of total flood losses
13th December 2006	Severe weather across Scotland with flooding in a number of areas (BBC News 2006)	5	14%
19th June 2007	Large inland flood event affecting the North East and the Northern Midlands (Environment Agency 2007)	15	15%
18^h July 2007	Large inland flood event affecting much of central England including the Rivers Severn, Warwickshire Avon, Bedford Ouse, Trent and Thames (Environment Agency 2007)	9	11%
10th March 2008	Combination of low pressure system and spring tide leading to coastal flooding, especially in the South West (BBC News 2008)	12	20%
10th November 2008	Strong winds and rain across South West and South Wales resulted in local flooding in South Wales (BBC News 2009)	8	16%

An initial aim of this thesis was to investigate if there is any correlation between extreme flood and wind events. A simple means of doing this is to look at the number of flood and wind claims resulting from the same event. There are 42 days with insurance claims for flood damage. The number of wind claims and associated damage occurring on the same day as these flood claims is shown in Figure 3.11. Only 13% of the losses due to wind events over the period 2006 – 2009 occur on the same day as flood events. Small scale wind claims are received throughout the year. This is a recognised issue when working with insurance claims data (Donat *et al.* 2011) and although localised small events do occur it is indicative of policy holders claiming even though there is no wind event. It was therefore expected that there would be some wind damage on each of the flood event days. There is one event on 10th March 2008 where there is a notable number of wind claims indicating a link between the wind and flood events. However it is more common in the dataset to see flood events which

have little corresponding wind damage such as June and July 2007. Two events where there are multiple wind claims but only one low value flood claim are 1st February 2008 and 1st January 2008, this could be a wind event with little corresponding flood damage although both these events occur on the first day of a month and could therefore be a function of poor data recording as discussed in Section 3.4.1.

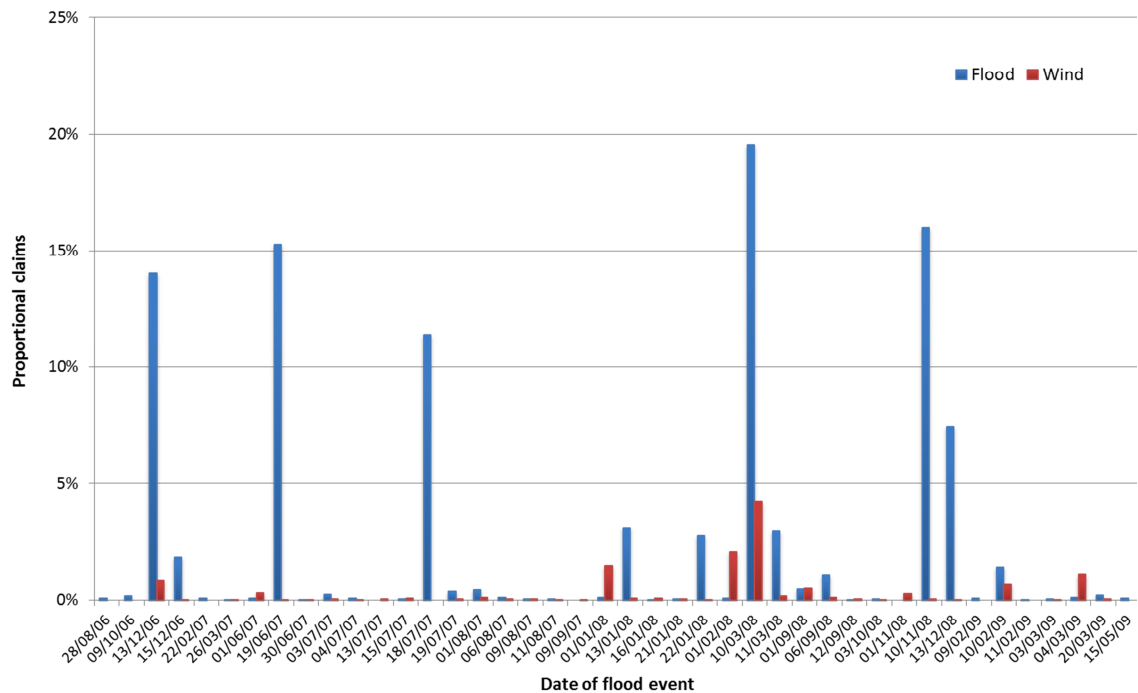


Figure 3.11 Proportion of claims between 2006 and 2009 occurring on the same day as flood events

3.4.3 Use of claims data

It was hoped that the past claims data would provide a useful means of both identifying preliminary trends in the claims data which could be investigated further to help understand exposure and to provide a means of validating the methodology. However given the concerns with data quality listed in Section 3.4.1 and the limited record length of only three years the use of the claims data is limited to the above qualitative review of the portfolio performance over the past three years.

Although the claims data does not show a significant correlation between flood and wind losses, it is acknowledged that a link does exist, particular between coastal flood events and windstorms as identified in the existing statistical research reviewed in Chapter 5. However in this thesis the focus is on risk from fluvial and coastal flooding only.

3.5 Sites at risk

A full review of Catlin's exposure was carried out to identify areas of high flood risk or with particular risk driving issues. Sites were deemed to be at risk if they were located within the Environment Agency Extreme Flood Outline (EFO) (Environment Agency 2009b). A map of the at risk sites is shown in Figure 3.12. It is not possible to model risk for all Catlin's caravan exposure within the PhD time frame. Instead a nested multi-site model has been developed which allows more detail to be included at particular sites of interest while still maintaining the national structure. Further discussion of the motivation behind a nested multi-site model is given in Chapter 4.

Risk clusters were identified around each caravan site, summing up the TIV within a 25km radius of the site. The clusters were then ranked by TIV to identify the highest risk areas, ensuring no overlap between the clusters. Four risk clusters were selected for inclusion into the multisite model based on:

- The value of assets at risk
- Achieving a balance of fluvial and coastal sites
- Accessibility of data
- Good spatial distribution of sites
- Links between risk processes across the cluster

The clusters selected are shown in Figure 3.12. Further reasons for selecting each cluster are detailed below. It is acknowledged that the EFO only considers fluvial and coastal flood risk and sites may also be exposed to pluvial flooding. Although pluvial flooding is modelled in RMS it is not considered as part of this thesis.

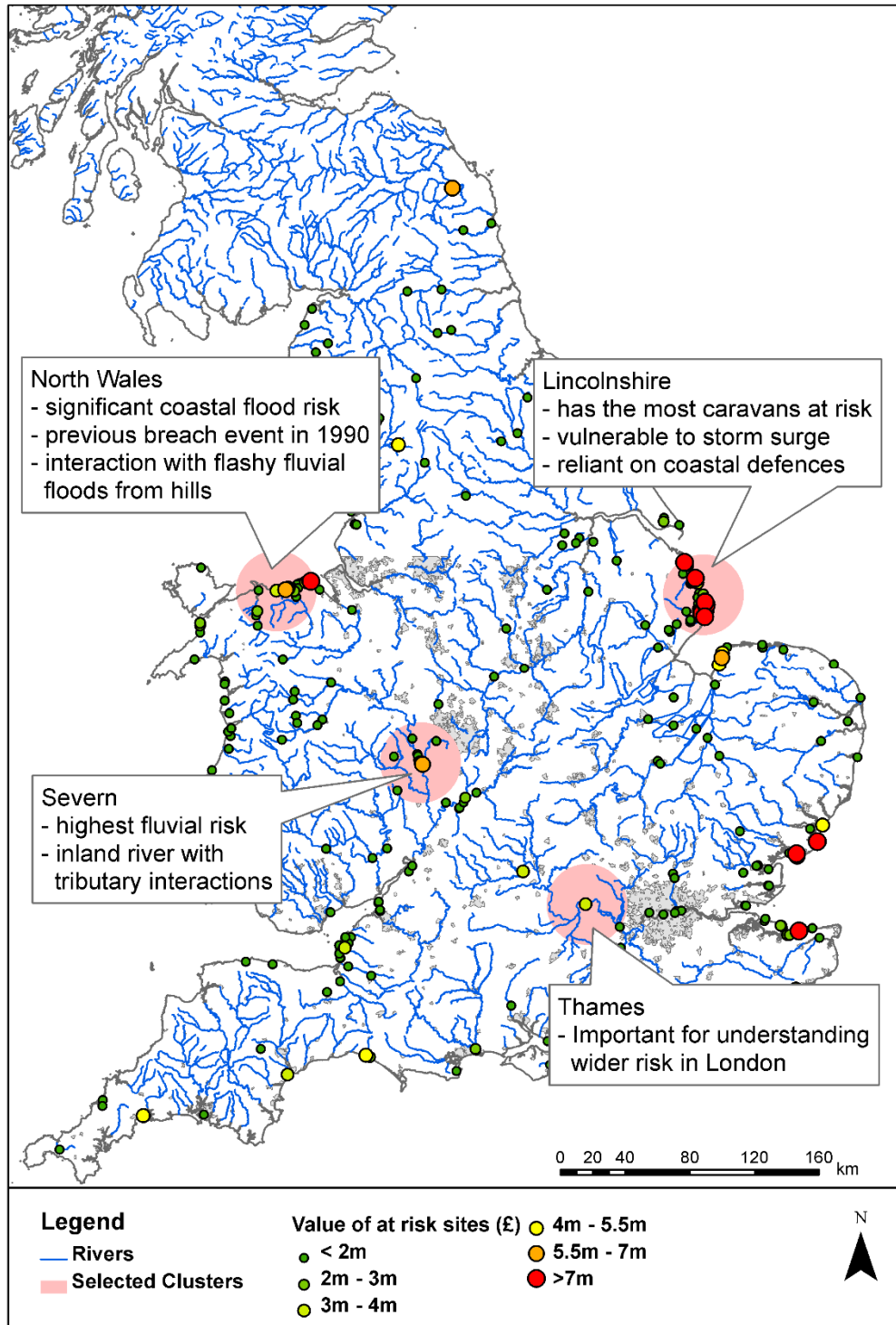


Figure 3.12 Selected risk clusters

3.5.1 Cluster 1. East Coast

The Lincolnshire coastline has the highest concentration of at risk caravan sites in the UK, 27.7 % of Catlin’s portfolio. The location and value of the sites is shown in Figure 3.13 and Table 3.7.

The area being considered is very low lying with 69 sites below sea level as shown in Figure 3.14. The area of low lying land extends approximately 10km inland before starting to rise. The flood risk is predominantly tidal and the area is particularly vulnerable to coastal surges in the North Sea. There are continuous flood defences along the coastline comprising of sea walls, flood banks and some natural dune defence systems. Some sites may also be at risk from flooding from small drainage channels behind the coastal defences which could back up during a high tide event if water is unable to discharge into the sea. The assessment of fluvial risk in this area is complicated as the low lying land is managed with a complex pumping system to promote drainage.

Two main areas of connected flood risk have been identified north of Skegness (Ingoldmells) and at Mablethorpe. A breach in the flood defences in either of these areas would result in rapid inundation of the low lying caravan sites, many of which form a continuous zone of caravan sites along the coastline, as shown in Figure 3.15.

Detailed information is available from the Environment Agency for the coastal flood defences in this area. This means that it provides a good case study for investigating the importance of correctly modelling flood defence reliability given the available data and heavy reliance on flood defences.

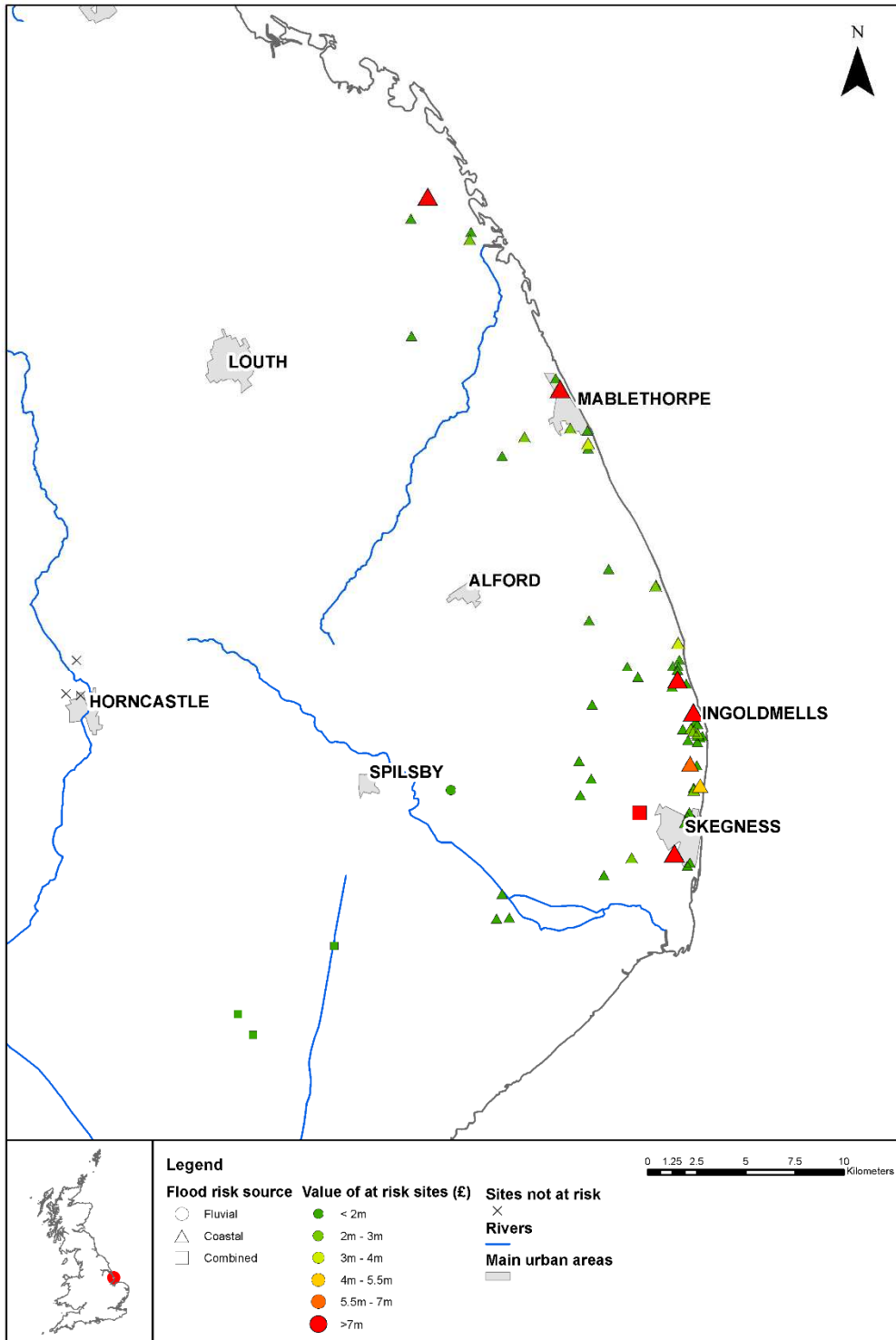


Figure 3.13 Total insured value of at risk sites: Lincolnshire coast

Table 3.7 Exposure risk summary: Lincolnshire coast

Number of sites at flood risk	Fluvial: 1	Coastal: 126	Combined: 4
Proportion of Catlin's portfolio at risk	27.7%		

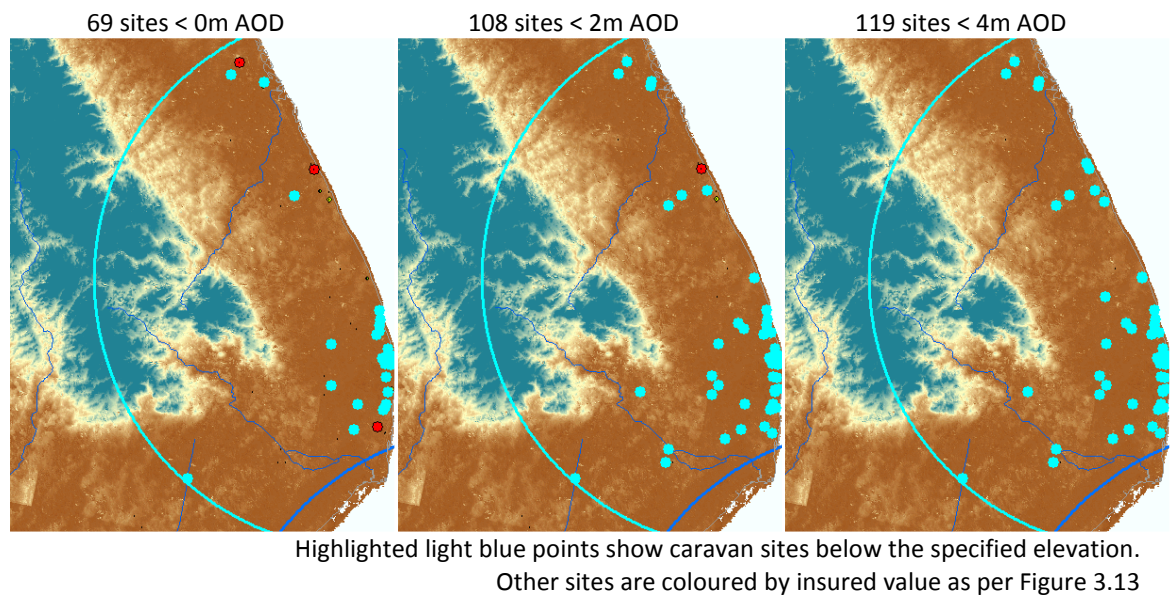


Figure 3.14 Lincolnshire site elevation



Figure 3.15 Spatial extent of multiple caravan parks at Ingoldmells

3.5.2 Cluster 2. North Wales

A large proportion of Catlin's risk is located in sites along the North Wales coast, with the concentration of risk second only to Lincolnshire. The location and value of the sites is shown in Figure 3.16 and Table 3.8.

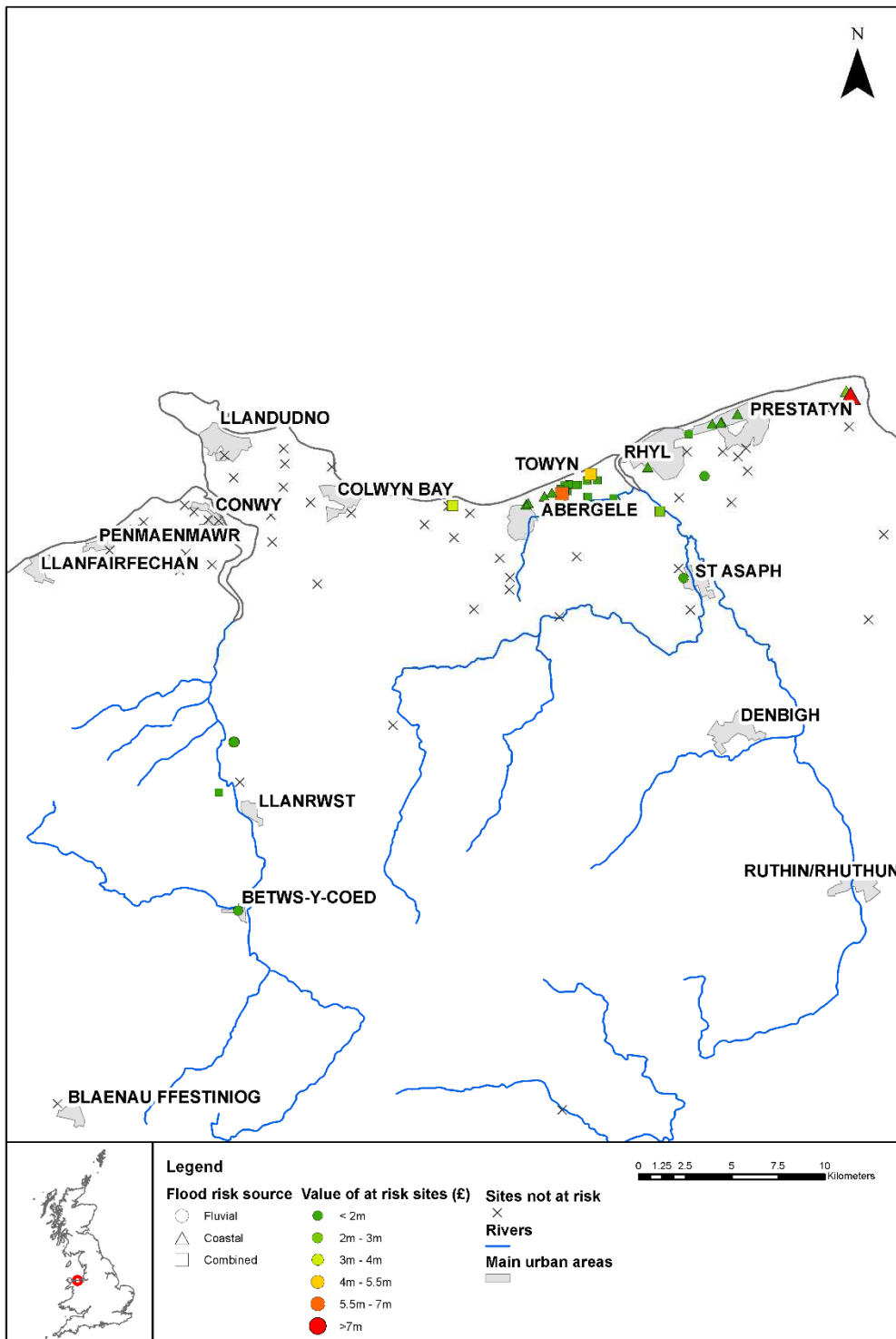


Figure 3.16 Total insured value of at risk sites: North Wales coast

Table 3.8 Exposure risk summary: North Wales coast

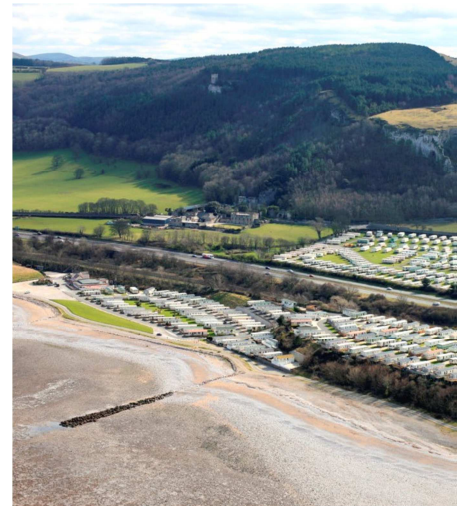
Number of sites at risk	Fluvial: 9	Coastal: 32	Combined: 42
Proportion of Catlin's portfolio at risk	11.1%		

Caravan sites in this area are at risk of coastal flooding and fluvial flooding from the River Clwyd. Many of the sites in this area are located along the sea front and are bounded on the inland side by the A55, the main transport link in the area, as shown in Figure 3.17.

There are flood defences protecting most of the urban areas consisting of flood walls and clay embankments. Similar to the East coast sites, most of the sites included in the North Wales cluster form a continuous line of caravan sites along the coastline (Figure 3.18)

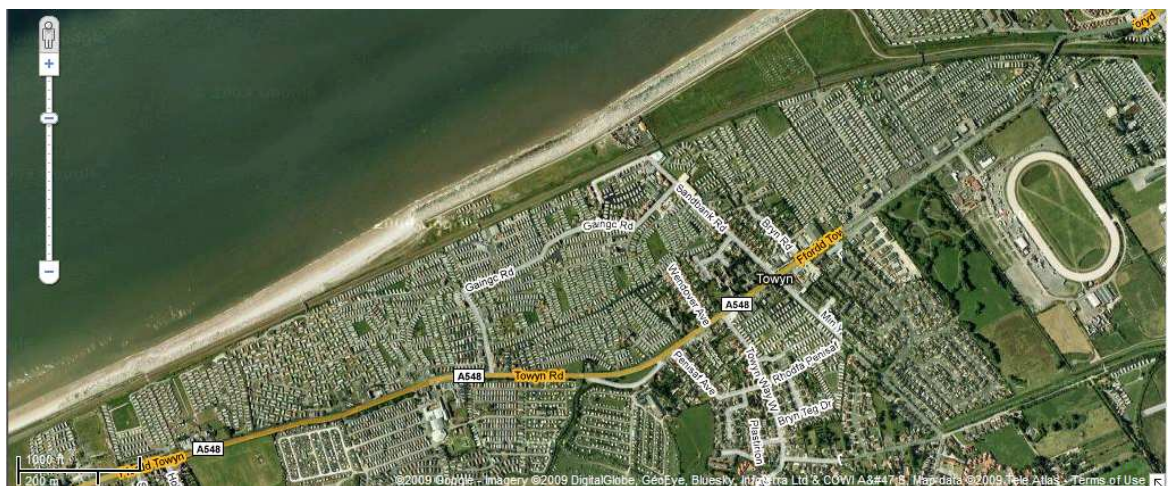
The greatest flood risk in this area is acknowledged by local experts to be tidal flooding around the Kimmel Bay area from where the River Clwyd meets the sea south to Abergele. A major flood was experienced in Towyn in 1990 when a combination of high sea levels, high tides and strong winds caused a breach in the flood embankments flooding 3000 properties. The flood lasted four days with successive high tides flowing through the breach. EA staff (personal communication) recall that many of the caravans came dislodged from their bases.

There are numerous small streams draining the low lying coastal area and anecdotal evidences from Conwy Council suggests that there is also some flood risk associated with the small stream running parallel to the coast however data are not available for these small scale features so they are not included in this analysis.



Source: North West England and North Wales Coastal Group (2008)

Figure 3.17 Caravan site at Abergyll



Source: Google maps

Figure 3.18 Continuous location of multiple sites along the North Wales Coast

3.5.3 Cluster 3. River Severn near Stourport-on-Severn

A cluster of caravan sites located in the River Severn catchment near Stourport-on-Severn provides the greatest concentration of sites at risk from fluvial flooding. The location and value of the sites is shown in Figure 3.19 and Table 3.9.

This area has been chosen as a suitable site to develop the methodology for fluvial dominated risks. This is an area at risk from fluvial flooding from multiple river systems including the Severn, the Leam and the Stour, all with different flooding regimes. It therefore provides a useful case study to investigate the dependence between flood risks on different rivers in the catchment system. Unlike the coastal sites where individual sites are located adjacent to each other, the fluvial sites in Worcestershire tend to be more spaced out, therefore requiring individual consideration of pathways in the S-P-R-C model.

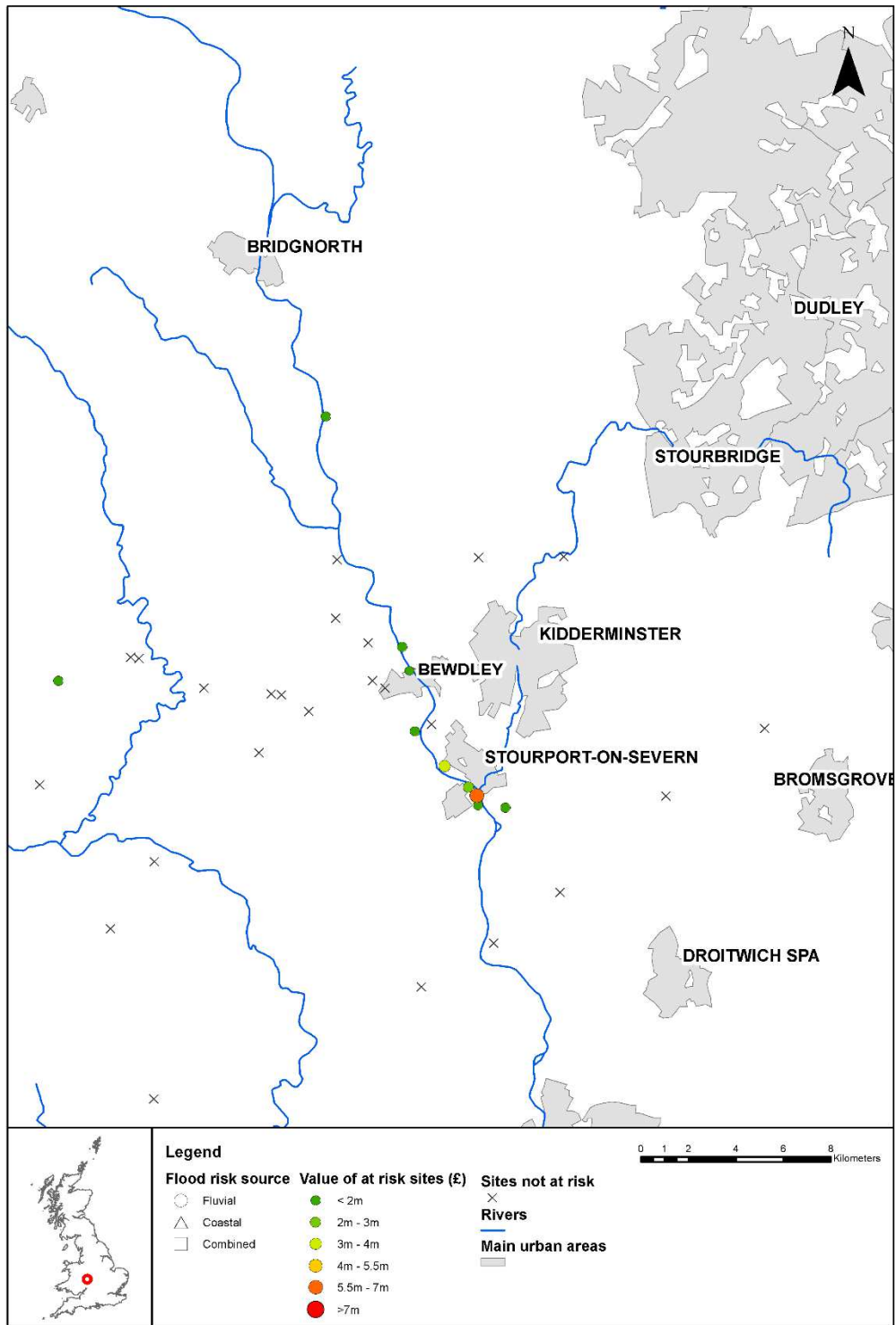


Figure 3.19 Total insured value of at risk sites: River Severn near Stourport-on-Severn

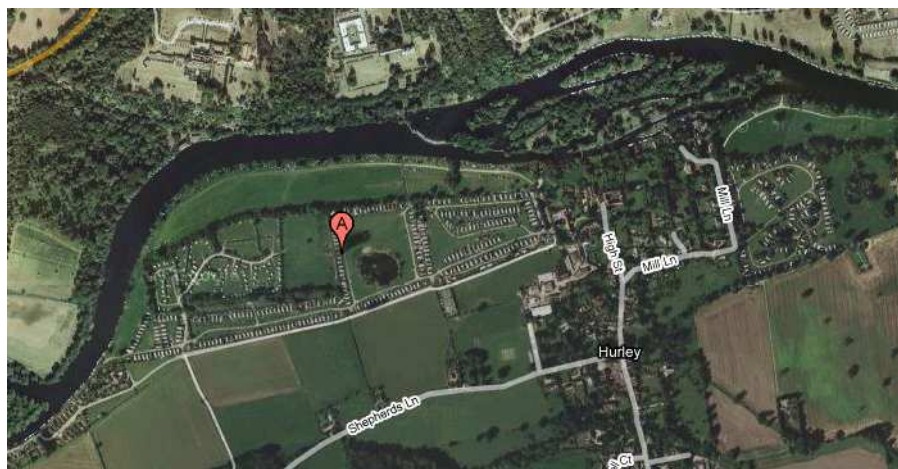
Table 3.9 Exposure risk summary: River Severn near Stourport-on-Severn

Number of sites at risk	Fluvial: 27	Coastal: 0	Combined: 0
Proportion of Catlin's portfolio at risk	3.3%		

3.5.4 Cluster 4. River Thames near Hurley

Flood risk in the River Thames catchment is receiving high levels of research and media attention at present and as such it is desirable to test the methodology in this area where it may have future application for other at risk assets. Two sites on the River Thames at Hurley have been identified as the initial focus of the analysis (Figure 3.21 and Table 3.10).

Flood risk at Hurley is fluvial from the River Thames. It is complicated by management of the weir system at Hurley. In contrast to the coastal sites, the main site at Hurley is spread out (Figure 3.20) potentially meaning that the whole site is unlikely to flood at the same time except in very large events.



Source: Google Maps

Figure 3.20 Caravan sites on the Thames at Hurley

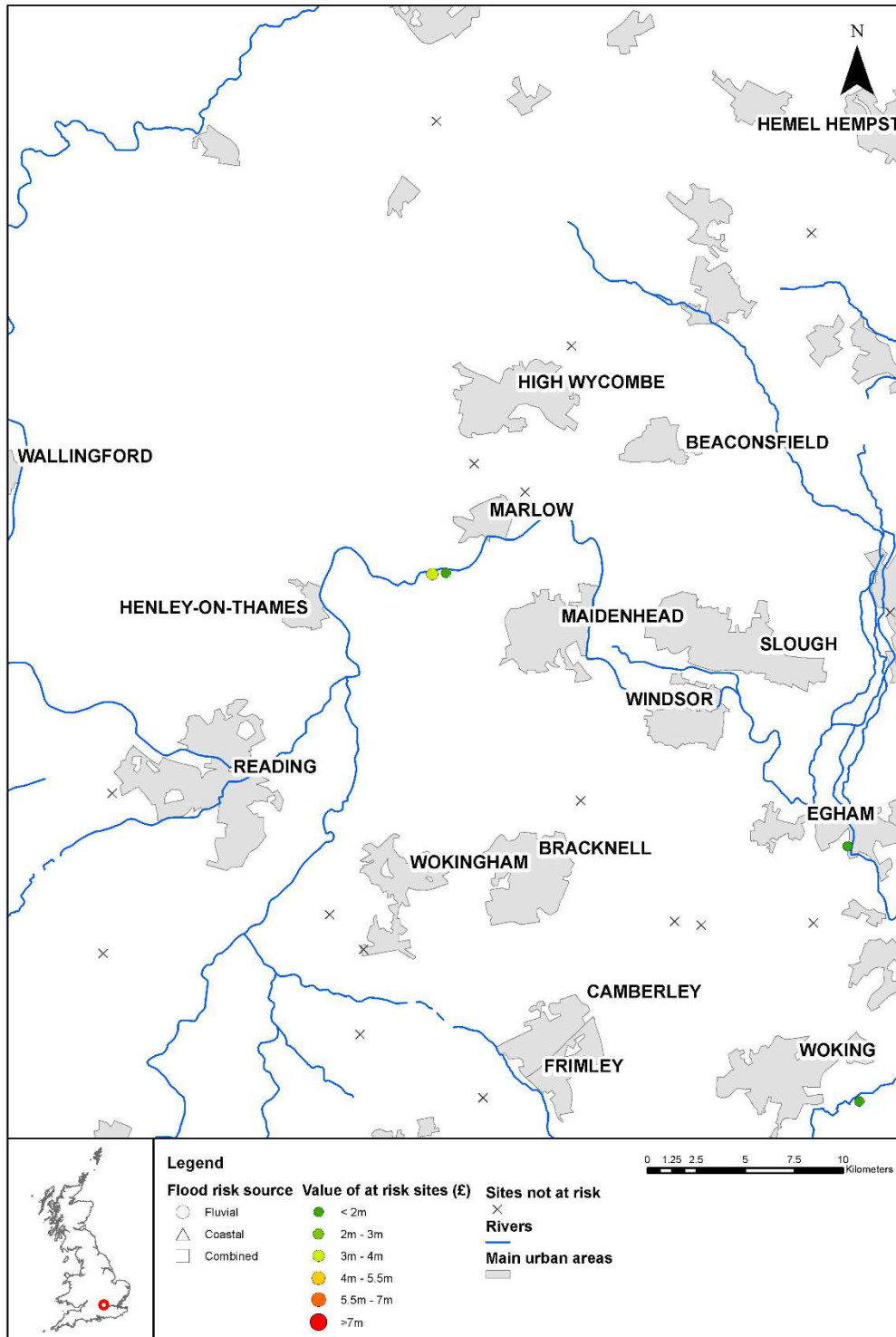


Figure 3.21 Total insured value of at risk sites: River Thames

Table 3.10 Exposure risk summary: River Thames

Number of sites at risk	Fluvial: 2	Coastal: 0	Combined: 0
Proportion of Catlin's portfolio	0.9%		

3.6 Summary of Catlin's caravan exposure

Catlin's exposure from the Compass Caravan account is high due to the large proportion of UK caravan stock covered and the clustering of sites in high risk locations along the coastline.

This chapter has illustrated that Catlin's assumptions regarding the construction and occupation classes used to determine loss in RMS RiskLink are suitable given the limited data available to validate the assumptions. However losses have been shown to be particularly sensitive to modifiers such as the floor height, which is concerning as Catlin do not know this level of detail about individual units. Further analysis of the sensitivity of risk estimates to the damage functions will be investigated in Chapter 9.

The main limitation to how much additional understanding can be gained regarding the damage to caravans during a flood event is due to the lack of detailed claims data. It is recommended that Catlin collect, as a minimum, cross referenceable data, and ideally, more detailed data from any future flood event to help understand if their assumptions regarding caravan vulnerability are suitable.

The remainder of this thesis focuses on risk to the four key clusters identified in this chapter;

1. Lincolnshire East Coast
2. North Wales Coast
3. River Severn near Stourport-on-Severn
4. River Thames near Hurley

Using these multiple nested sites allows a detailed process based understanding of risk from both coastal and fluvial sources to be developed which will help improve understanding of exposure risk across the portfolio as a whole.

4 A methodological framework for multi-site risk analysis

4.1 Modelling approach

As introduced in Chapter 2, the optimal approach to flood risk modelling is a systems based model that is transparent, adaptable, flexible, efficient and as simple as possible. This chapter sets out the proposed means of achieving this in the context of a risk based framework to help inform insurance portfolio analysis. The proposed model also has wider uses for flood risk management and could be applied to any spatially distributed receptor.

4.1.1 Systems based approach

The benefits of a generic systems based approach were summarised in Chapter 2. Figure 4.1 illustrates the components of the S-P-R-C model relevant to this thesis. Further details on the modelling of each component are given in Section 4.2.

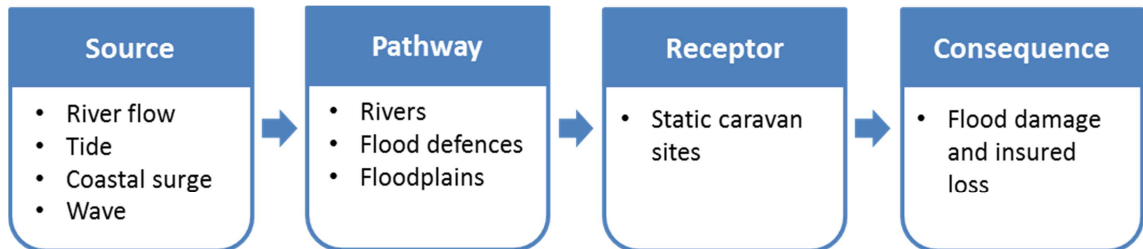


Figure 4.1 Components of system model as considered in this thesis

By considering each of these components separately a modular framework is developed. This allows explicit consideration of all of the important factors in the risk system and the links between them.

A modular approach allows for changes in one component of the system without having to change all components. This also means that additional components can easily be included, for example an additional source variable. A further advantage of a modular approach is that it enables each stage of the process to be validated independently. This is important when taking a whole system approach as validation of the end to end system model can be difficult as discussed in Section 4.4.

4.1.1.1 Sources

A brief synopsis of the causes of extreme weather in the UK was given in Chapter 1. The sources of interest in this thesis are extreme river flows and sea level. River flow has been selected in preference to rainfall as although in most cases the rainfall record is longer and has

a finer spatial resolution; using rainfall data incorporates an additional uncertainty through rainfall-runoff modelling. Using the flow data directly includes all of the spatially variable rainfall-runoff process. A constraint of using flow data is that it limits the use of the model for potential climate change analysis which is more naturally incorporated through the use of weather generators using rainfall as the primary variable (see Kilsby *et al.* 2007 for details). Although it is useful for insurance companies to have a long term view of how their risk exposure may change in the future, insurance pricing is carried out on an annual timeframe. Climate change is therefore not considered as a fundamental part of this research since providing the source data are up to date there is no requirement for explicitly modelling climate change impacts.

Extreme sea levels are a combination of the deterministic tide and stochastic storm surge, plus a wave component. The wave component is particularly important for defence overtopping but due to modelling complexities is often poorly represented in coastal analysis (Hawkes *et al.* 2002). These three variables are known to be correlated especially the wave and surge components in extreme events which are driven by meteorological forcing (Hawkes *et al.* 2002). Total water level can also be restricted by the tide due to the mediating effect of shallow water on wave height (Thomas and Hall 1992; Coles and Tawn 2005b). All three variables are considered in this thesis.

4.1.1.2 Pathways

The pathways are the routes by which water reaches the sites of interest. Here the main focus is the reliability of flood defences as this is likely to cause the greatest variability in flood risk.

Also considered as part of the pathway term is the link between extreme water levels observed at gauging stations and the extreme water level at the sites of interest. This requires the use of physically based transformation methods to convert offshore waves to inshore sea level and to interpolate from river gaging stations to ungauged locations.

Hydraulic modelling of the river section of interest is required to estimate the water levels at the defence structures from the river flow. Should overtopping or breaching occur, the final pathway is the floodplain, the topography of which can either prevent water reaching the receptors or encourage preferential flow routes for example along low lying ground or roads.

4.1.1.3 Receptors

The receptors considered in this thesis are static caravans as detailed in Chapter 3. The caravans are located on large sites across the UK, many of which are located near to water

bodies due to its scenic and recreational value. This results in clustering of exposure in certain areas, such as along the Lincolnshire coastline.

Due to the modular nature of the framework, the proposed methodology could be applied to other spatially distributed receptor. Examples might include electricity substations or transport infrastructure.

4.1.1.4 Consequences

The consequence of interest is insured loss. This is based on a flood damage model combined with a simple financial losses model. Due to their flimsy constructions, caravans are particularly vulnerable to flood damage since any amount of water ingress can quickly cause significant structural damage (Hall *et al.* 2000; McEwen *et al.* 2000). The development of caravan specific damage curves is discussed in Chapter 9. The damage functions could easily be changed to adapt the framework to a different receptor in the future.

4.1.2 Nested multi-site approach

The consideration of flood risk for insurance pricing or for other large scale flood risk management decisions requires analysis over national scales (or larger in other non-island nations). Computational it is not possible to carry out detailed analysis at the national scale therefore alternative solutions must be sought.

The RASP project (Hall *et al.* 2003) outlined a hierarchy of assessment methods for different scales of analysis. While this approach allows for increasing levels of detail to be included at smaller scales it does not support cascading of information from one level to the next. For example the most detailed level recommends continuous simulation of hydraulic loads, since this is not possible at a national scale, there is no consideration of wider scale dependencies in the detailed analysis.

The 'Spatial Coherences of Flood Risk' project (Keef *et al.* 2009a) produced a national scale assessment of spatial and temporal correlations in flood risk. This assessment mainly focused on correlations between extreme river flows at gauged locations and used an interpolation method (discussed further in Chapter 7) to provide data between the gauging stations. In recognition of the computational load of a national scale model the study outlined a relatively simplistic methodology by which the output from the statistical model could be used to assess the impact of extreme river levels on receptors (Keef *et al.* 2009a; Lamb *et al.* 2010).

The solution proposed in this thesis draws on both of the above ideas to develop a nested multi-site approach. In this way more detailed analysis can be carried out at the sites of

interest including consideration of defence failure and detailed inundation modelling while still maintaining a national structure and incorporating the broad scale spatial correlations between sites. This nested approach is similar to that used by the climate modelling community in Global Climate Models (GCM) to Regional Climate Model (RCM) downscaling where the output from large scale models provides the boundary conditions for more detailed regional models while maintaining the larger scale spatial structures. The proposed nested model structure is shown in Figure 4.2.

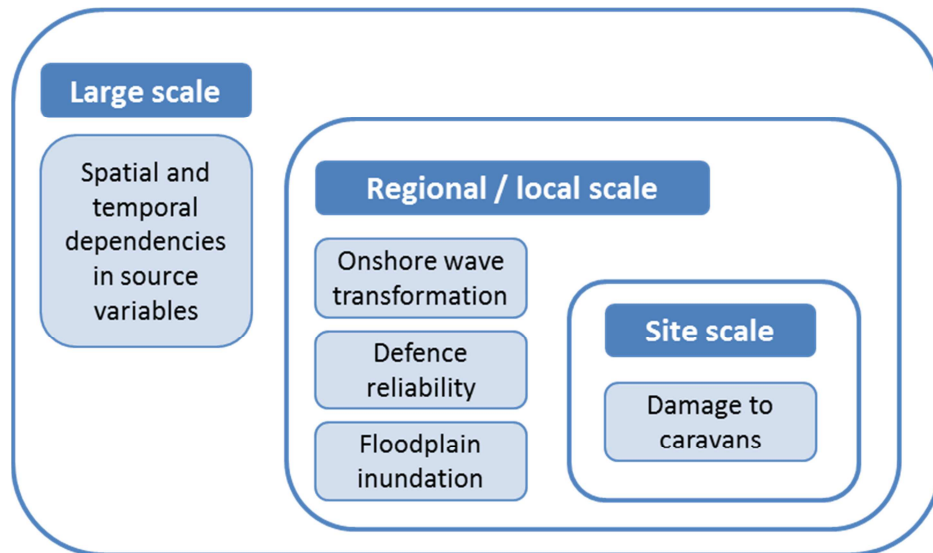


Figure 4.2 Nested framework structure of systems components

Rather than fitting the dependence model to a large national set of gauges, a smaller subset (referred to as the network) is selected consisting only of gauges connected to the sites of interest. By only using a subset of gauges it is possible to incorporate national scale spatial and temporal dependencies while restricting the dimensionality of the statistical dependence model to a realistic level for use in a risk based model. For example the UK National River Flow Archive contains a standard dataset of around 200 gauges (CEH 2009a). Using the conditional dependence model outlined in Chapter 5 with 200 gauges and 10,000 simulated events per gauge, 100 of which are likely to be extreme events over the 0.99 threshold leads to 20,000 simulation points per gauge and 4×10^6 for the full network when the conditional flow at all other gauges in the network is simulated from each conditioning gauge. To extend this to include temporal dependencies within a 7 day window of the conditioning extreme event leads to over 3×10^7 simulation points for the whole network.

Although not all these simulations would be carried through the full system model due to rejection sampling (See Chapter 6), it is immediately obviously that to extend the dependence

model to include the other variables of interest from the coastal gauges results in high computational costs. By using a nested approach and only including gauges located close to the sites of interest the large scale spatial and temporal dependencies are preserved without unnecessary computation cost. This is illustrated in Figure 4.3 for an example event (each dot represents a gauge in the network shaded by event magnitude). This also allows for inclusion of more gauges in the areas of interest for example to better incorporate loading patterns near tributary confluences.

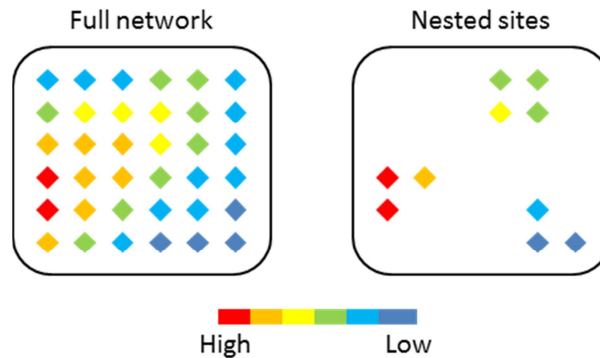


Figure 4.3 Illustration of how spatial dependence is maintained through the nested model

An additional benefit of reducing the number of gauging stations in the dependence model is that the probability of having missing data for any gauge in the network on any given day is reduced. The problem of missing data is discussed further in Section 6.3.5.1.

Maintaining the national dependence structure in the risk model is important for insurance applications since simultaneous losses across large areas are likely to result in large payouts. In contrast areas where the exposure is low make a minimal contribution to total losses, therefore there is limited additional benefit in including these areas in a risk model. This type of nested approach could also be useful for wider flood risk management for example in the 2007 floods temporary flood defences, support equipment and personnel were moved from one area to the other (Environment Agency 2007; Pitt 2008). Knowledge of the large scale spatial structure of flood events and the local impacts could provide a valuable tool for improving logistical risk management decisions such as these.

The key to a successful nested model is careful selection of the areas to include to maintain good coverage of the national structure while also including key areas with high risk exposure. Details of the process used to make this selection for this thesis were provided in Chapter 3.

4.2 Outline of the risk model

An overview of the proposed risk assessment framework is shown in Figure 4.4 illustrating the methodological flow from national level to local scale assessment. The methodology explicitly couples large scale spatial dependencies in extreme events with local scale dependencies in defence crest height, defence reliability and defence loading. The novel aspects of the methodology are in the nested model structure, the simulation of extreme events and consideration of the defence system. The methodological framework is outlined in Sections 4.2.1 to 4.2.7. More details of each component are discussed in the remaining chapters of this thesis.

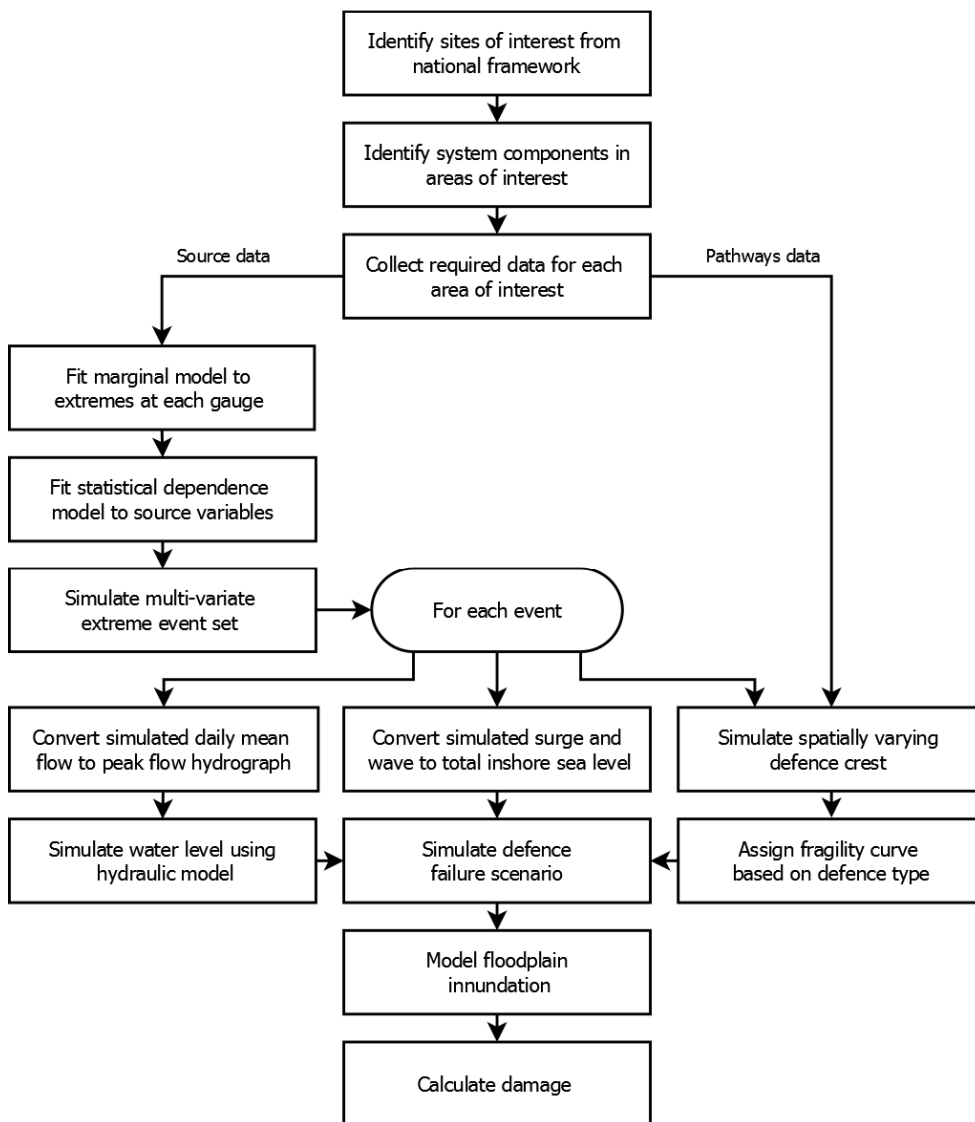


Figure 4.4 Overview of the risk assessment methodology

4.2.1 Sources input

For each event, i , daily mean flows are simulated at all the gauges in the network using a conditional dependence model. The total sea level is assumed to comprise of a tide, surge and

wave component. The tide component is modelled deterministically using the full tidal range at the sites of interest. The surge component is modelled using the conditional dependence model fitted to the skew surge from each event. The swell waves from the nearest wave rider gauge are also modelled using the conditional dependence model. The simulated vector of sources across the network, X_i , represents a large scale spatial event with probability, $P(X_i)$.

The local dependencies are then addressed at each site or risk cluster, s . The daily mean flow at the nearest gauge to the site is labelled q_i . The procedures for transferral to ungauged sites are discussed in Section 7.2.2. The daily mean flow is then converted into a peak flow and hydrograph, Q_i , such that;

$$Q_i = f(q_i, k_s) \quad 4.1$$

where k_s is the ratio of daily mean flow to flood peak specified for each site.

The combined coastal component at the site of interest is labelled z_i . This is then transformed to represent inshore wave heights (See Section 7.3 for details) at the site of interest such that,

$$Z_i = f(z_i, h_s) \quad 4.2$$

where h_s represents the local bathymetry between the wave rider and shoreline of interest.

4.2.2 Defence system

Consider a flood defence system with n sections, d_1 to d_n , characterised by their construction type and standard of protection. Any one of the defences can fail in one or more locations resulting in inundation of the floodplain. Within each defence section it is assumed that the crest height varies along the length of the defence. The degree of variation depends on the defence type and condition such that;

$$c_{j,i} = f(\text{defence type}, \text{defence condition}) \quad 4.3$$

Where c is the simulated crest height and resistance to load of any given defence, j . The combined vectors of crest height for the whole system is referred to as C_i .

4.2.3 Water level and overtopping

The water level is referred to as L_i through the modelled reach or shoreline, or $l_{j,i}$ at a particular defence section. Coastal water level is determined by inshore transformation of the simulated sea state from Equation 4.2. The fluvial water level is simulated using the hydraulic model for the specified flows and defence crest heights;

$$L_i = f(C_i, Q_i) \quad 4.4$$

Overtopping of defences is considered deterministically based on the modelled water level conditional on the simulation of the defence crest height. The probability of overtopping, $P(OT_i)$ depends on the probability of the extreme event, however due to the variation in crest height $P(OT_i|L_i = SOP) \neq 1$. Defence overtopping occurs when the water level at the defence is greater than the crest height. This can be defined throughout the model OT_i , or for individual defences, $ot_{j,i}$ or points within an individual defence, $ot_{j,y,i}$, where y is the chainage along the defence section from 1 to t .

$$OT_i = f(C_i, L_i) \quad 4.5$$

4.2.4 Defence failure

A defence is said to have failed if it has breached in one or more locations. Overtopping is considered directly via the modelled water level so failure only relates to breaching. The failure of defence d_j is labelled as event D_j . The non-failure of defence d_j is labelled as \bar{D}_j .

The probability of failure for any given event, $P(D_{j,i})$ is conditional on the loading variable, amount of overtopping, and defence reliability such that for any given defence;

$$P(D_{j,i}) = f(l_{j,i}, ot_{j,i}, r_{j,i}) \quad 4.6$$

This can be extended to consider any point along the defence;

$$P(D_{j,y,i}) = f(l_{j,y,i}, ot_{j,y,i}, r_{j,y,i}) \quad 4.7$$

Assuming that breaches are independent, the probability of breaches at locations $y=1$ and $y=2$ is;

$$P(D_{j,1,i}) \times P(D_{j,2,i}) \times P(\bar{D}_{j,3,\dots,t,i}) \quad 4.8$$

The probability of defence failure for any given load is defined using a fragility curve, giving the conditional failure probability $P(D_j|l_j)$, in this case the load is defined as the water level at defence j . The unconditional failure probability, $P(D_j)$ is given by;

$$P(D_j) = \int_0^{\infty} p(l_j)P(D_j|l_j)dl \quad 4.9$$

Where $p(l_j)$ is the probability density function of the water level, l , at defence j .

4.2.5 Sample probabilities of breach scenarios

A central assumption of the RASP methodology is that all defence sections are loaded at the same time (Hall *et al.* 2003). In practice this may not be the case due to the potential reduction in water level following an upstream breach, particularly in areas with significant floodplain storage (Apel *et al.* 2009).

An iterative sampling procedure is proposed to incorporate the dependence on previous upstream breaches for fluvial loading. Firstly the hydraulic model is run assuming no failures to give $L_{i,\overline{D_1,\dots,D_n}}$. Successive sequences of one or more defence breaches, D_{ss} , are sampled based on the conditional failure probabilities at each point in the defence $P(D_{j,y}|L_{i,\overline{D_1,\dots,D_n}})$ until $P(D_{ss}|L_{i,\overline{D_1,\dots,D_n}}) \rightarrow 0$. The hydraulic model is run for each sequence with a standard breach size and growth rate to provide water levels at each section including the impact of potential reduction in water level from upstream breaches. The probability of each failure sequence $P(D_{ss})$, is the product of the failure probability at each breach point $P(D_{j,y,i})$, for the modelled water level $l_{j,y,i,D_{ss}}$. One of the failure sequences, $D_{ss,i}$, is sampled from the probability distribution $p(D_{ss})$ for each event. Each breach in $D_{ss,i}$ is assigned a maximum width such that;

$$W_{ss,i} = f(L_i, \text{defence type, floodplain size and shape, timing of breach}) \quad 4.10$$

For coastal loading there is unlikely to be a reduction in total water level and the fluvial locations selected for further analysis in this thesis (see Chapter 3) do not contain significant storage behind levees. The above steps are therefore included for completeness if the methodology were to be applied in different areas in the future, however they have not been tested in this thesis.

By not considering the sequential failure probabilities there is no need for iterative model runs and the probability of each failure sequence $P(D_{ss})$, is the product of the failure probability at each breach point $P(D_{j,y,i})$, for the modelled water level $L_{i,\overline{D_1,\dots,D_n}}$.

4.2.6 Damage conditional on event

For each event, X_i , for the specified defence state variables, C_i , $D_{ss,i}$, and $W_{ss,i}$, the hydraulic model is run to calculate water level in the channel and flows onto the floodplain. A raster based floodplain inundation model is used to calculate flood depths across the floodplain. Using caravan specific depth damage curves these floodplain depths are converted to loss estimates at each site using a simple financial model, and summed together to give the loss across the portfolio conditional on the event. Loss conditional on event is denoted φ_i .

4.2.7 Calculating risk

As discussed in Section 2.2, risk is commonly defined as the probability of an event multiplied by the consequence (Equation 4.11)

$$R = \int f(\alpha) V(\alpha) d\alpha \quad 4.11$$

where $f(\alpha)$ is the joint probability function and $V(\alpha)$ is the damage function.

$F(\alpha)$ is established empirically assuming a large enough sample size such that:

$$\alpha_i = \frac{1}{\sigma} \sum_{s=1}^k X_s > x_{i,s} | X_{1,\dots,s-1} > x_{i,1,\dots,s-1} \quad 4.12$$

where σ is the sample size, s is the closest gauge to the site or risk cluster, k is the total number of gauges in the system, x is the simulated value at each gauge for event i , and X is a vector of all simulated values at each gauge. The event probability is established from the probability at the gauging stations ($P(X_i)$). $V(\alpha)$ is the damage function which is a sum of damage sustained at all sites of interest for the event. This is equivalent to φ_i .

One way of evaluating this integral is by Monte Carlo integration, based upon η Monte Carlo samples from $f(\alpha)$, in which case:

$$R \approx \frac{1}{\eta} \sum_{i=1}^{\eta} C(\alpha) \quad 4.13$$

This thesis has also considered the effect of flood defence systems in modifying the probability of flooding. In the simplest instance, for a system of n flood defence sections, there are $t=1, \dots, 2^n$ possible system states, each of which has a probability of failure which is conditional upon the loading variables, written $P(D_{ss,t}|\alpha)$. In this case the risk is calculated as follows:

$$R = \int \sum_{t=1}^{2^n} f(\alpha) V(\alpha) P(D_{ss,t}|\alpha) d\alpha \quad 4.14$$

and the Monte Carlo estimate is:

$$R \approx \frac{1}{\eta} \sum_{i=1}^{\eta} \sum_{t=1}^{2^n} V(\alpha) P(D_{ss,t}|\alpha) \quad 4.15$$

If the event probabilities are calculated on an annual scale, and damage are calculated in terms of insured losses then AAL can be used as the risk metric. The EP curve can be constructed by plotting the conditional event probability against event loss for all simulated events.

4.3 Data sources

A major consideration of a full system based model is the large amount of data required. The multisite approach restricts this to specific areas, however the range of data needed is still considerable. Table 4.1 lists the main data components required for the systems based model outlined in Section 4.2 and identified potential data driven limitations. Further details of each data set are given in the signposted chapters.

Table 4.1 Data requirements for a system based model

Model component	Data required	Source	Data format	Known limitations	Further details
Source (Fluvial)	Concurrent flow data for river reaches of interest	Centre for Ecology and Hydrology (CEH) National Rivers Flow Archive (NRFA)	Daily mean flow (DMF) at each gauging station	Limited number of extremes in record. Gauges not necessarily located near caravan sites. DMF doesn't provide flood peak.	Chapter 5 Chapter 6 Chapter 7
Source (coastal)	Concurrent still water level including tidal and surge components for coastlines of interest	British Oceanic Data Centre (BODC) UK Tide Gauge Network	15 minute to hourly predicted and observed sea level	Limited number of extremes in record. Gauges not necessarily located near caravan sites.	Chapter 5 Chapter 6 Chapter 7
Source (coastal)	Concurrent significant wave heights for coastlines of interest	Centre for Environment, Fisheries and Aquacultural Science (Cefas) Wavenet network	Wave height, period and direction at up to 30 minute resolution	Wave data recorded at offshore buoys, requires transformation to near shore	Chapter 5 Chapter 7
Pathway	River channel dimensions	Environment Agency Lidar	Raster tiles at 2m resolution	Interpolation required below water level.	Chapter 7
Pathway	Flood defence location, type and height	Environment Agency National Flood and Coastal Defence Database (NFCDD)	GIS files of defence location and other available data	Poor spatial resolution of data. Limited data for defence reliability analysis.	Chapter 8
Pathway	Floodplain geometry	Environment Agency Lidar	Raster tiles at 2m resolution		Chapter 7
Receptor	Location and value of caravan sites / units	Catlin exposure database	Postcode locations of total insured value at each site	Number / value of individual units at any given site is not known. Postcode location may not be suitable.	Chapter 3 Chapter 9
Receptor	Damage functions for caravans	Catlin historic claims Cat model EP curves Multi-Coloured-Manual (MCM) Expert knowledge	Depth-damage curve	Commercial sensitivity of Cat model damage functions Limited caravan specific data. Generalisation of curves.	Chapter 3 Chapter 9

4.4 Consideration of uncertainty

Inherent to any systems based risk model are a large number of potential sources of uncertainty. These can be aleatory uncertainties due to variability in input variables or epistemic uncertainties stemming from a lack of knowledge and understanding of the processes involved. There are considerable difficulties in validating complex flood risk models which incorporate deterministic and probabilistic components and there is limited published work looking at this problem (Environment Agency, 2012b).

Several approaches have been established to try to identify the contribution of different sources of uncertainty in systems risk models for example Dawson et al (2008) used sensitivity analysis to attribute risk to different components of the system while Hall et al (2011) outline a Bayesian approach to the problem which incorporated prior knowledge about the ability to model different components within the system model to estimate the relative contribution to uncertainty of different components.

Some of these uncertainties including event definition, quality of defence data, breaching processes and spatial distribution of caravan units will be assessed as part of the modelling process. Others such as the potential errors in 1D hydraulic models or the accuracy of DEM data are assumed an inherent part of flood modelling and are not considered further.

Existing work on uncertainties in flood risk models can be used to rank the potential significance of sources of uncertainty in a systems based risk model. Uncertainty around the extreme value statistics are generally assumed to be much larger than other factors (Apel *et al.* 2004). This provides justification for omitting many of the additional sources in an uncertainty analysis. Apel *et al.* (2004) found the second major source of uncertainty in their model was in the breach module due to poor knowledge of breaching processes and defence properties. High sensitivities to breaching were also identified by Muir Wood *et al.* (Muir-Wood and Bateman 2005; Muir-Wood *et al.* 2005) as the critical component in RMS' coastal flood risk models

Based on past experience and existing preconceptions, Catlin (Personal Communication) assume that there are large errors in the calculation of flood damage from the depth-damage curves used in Cat models. The risk assessment is also likely to be influenced by the location assumptions surrounding the positioning of caravans. This is reflected in the output of the NaFRA 2005 which was found to be particular sensitive to property floor level (Environment Agency, 2012b).

The critical sources of uncertainty may change for different magnitude events, for example for a large event that substantially overtops the flood defences, the consideration of breaches may not have as significant an effect on the resulting flood depths as for a smaller event where there would be no flooding without a defence breach.

4.5 Informing decision making

The focus of this thesis is to develop a research framework that can be used to help explore some of the issues facing insurers. Through discussion with Catlin, and with reference to the emerging issues facing wider flood risk management, a set of output questions have been established. The key issues fall into two categories; investigating the spatial and temporal dependencies in flood driving events (Section 4.5.1), and identifying which components of the risk model the resulting risk estimates are most sensitive to, and hence where future improvements in modelling or increased awareness for risk pricing are needed (Section 4.5.2).

The level of detail used in this thesis, for example the “average” caravan construction value used in the depth-damage curves, is not sufficient for making insurance pricing decisions directly. Rather the framework is used to identify the relative importance of different components and to investigate high level spatial structures such as the dependence between flood driving events. The proposed framework itself is a robust structure that includes all important risk driving sources, therefore by incorporating additional detail into the model components, the framework could be used by insurance companies, or for other detailed flood risk assessment purposes in the future.

4.5.1 Investigating the spatial and temporal dependences in flood driving events

The use of a statistical model to incorporate the spatial and temporal dependencies in source variables into the risk model allows for the importance of this component to be explicitly investigated. In particular the following questions are of interest:

- If there is a large event at location A what is the probability that there will also be a large event at location B and do these probabilities change as events get more extreme?
- How important is the event definition (or assumed event duration) to the risk estimate over different spatial scales?
- Is there a significant correlation between extreme fluvial and coastal events and how much impact does including this correlation have on the risk estimate?
- How important is the contribution to risk from fluvial and coastal events?

4.5.2 Identifying critical components of the risk model

Cat models are essentially black boxes where the end user has limited ability to investigate individual components in the model. Therefore where assumptions are made about the modelling of each component it is difficult to identify the impact each of these assumptions has on the final risk estimate. By using a systems based risk model it is possible to run multiple scenarios and identify the sensitivity of the risk estimate to changes in individual components. Key components that will be investigated are:

- The shape of the damage curve and the point at which write off is assumed to occur.
- The spatial distribution of individual caravans across a site.
- The consideration of flood defences including correctly specifying input data and investigating the importance of breaching.

4.6 Summary of methodological framework

This chapter has provided an overview of the proposed methodological framework for risk assessment. It has demonstrated how each component in the S-P-R-C system will be investigated both individually and as part of the system framework. Further details of each of the components are discussed in the remaining chapters of this thesis. Each chapter provides a review of existing work in the area and details of the modelling carried out in this project. Chapter 9 illustrates how the methodological framework can be used to produce risk estimates to help inform risk based decision making, particularly for the insurance industry.

In reference to the five criteria for a flood risk model as set out in Section 2.5 the proposed methodology can be seen to be:

- Transparent as each component and the links between them is individually considered. All relevant assumptions are outlined and where the assumptions used in previous methodologies appear restrictive these have been identified and investigated.
- Adaptable as the structure of the framework is such that if any component changes in the future, for example a new defence is built or longer data records of input sources become available, the relevant component can be re-run to account for this change (all subsequent stages would also need to be recalculated). Similarly if improved data becomes available the framework can be modified to take account of the improvement. For example if better data on flood defence crest height and strength becomes available in the future, the simulation of spatially varying defence properties can be removed and the improved data used directly.

- Flexible as the focus of the framework can be changed as required. Here the main focus is on the spatial and temporal dependencies in the driving source of risk and the consideration of flood defence failure. In the future if there was more interest in the damage functions more work could be done in this area and the consequences component improved while still maintain the rest of the model structure. However it should be born in mind that improving one component significantly more than the rest of the model relies on the uncertainties in the model as a whole being small enough to support more detail in particular areas.
- Efficient as the nested model approach enables the input data required and number of model runs to be reduced to just consider the areas of interest while still maintaining a national structure.
- Simple as although some individual components of the methodology are complicated (such as the statistical dependence model) the overall framework is clearly visible throughout as illustrated in Figure 4.4. Consideration has been given to the best means of communication the results with end users and a simplistic interactive tool developed that allows end users to explore the system and relevant uncertainties.

5 Multi-variate spatial extremes

5.1 Defining “extreme”

The definition of extreme is dependent on the context. The media coverage of extreme events often verges on sensationalism, largely because “extreme weather makes news” (Nature 2011, p131) and sells newspapers (Hudson 2011). Another difficulty is that what is classed as extreme changes over time. Bryan Utteridge, head of flood defence at the EA, commented during the 1998 floods in Evesham “we’ve seen nothing like this in living memory” (cite BBC News 1998) however nine years later the floods of 2007 exceeded the 1998 water level by 300mm (Environment Agency 2007). One problem is that there is often increased funding for studies into extremes immediately following major events. This leads to biased analysis as the datasets used inevitable show the largest events occurring at the end of the record (Coumou and Rahmstorf 2012).

The statistical definition of an extreme event is an event that exceeds some pre-specified threshold or is the largest (or smallest) in a specified set of observations (Coles 2001). Studying extremes is of cross disciplinary interest from the meteorological extremes central to this thesis through to financial and medical applications. With climate change models predicting an increase in extreme weather events in the future it is becoming increasingly important to understand and predict extreme events.

Studying extremes presents some unique difficulties as by definition there are not many events to base analysis on; in the UK flow records at most sites are less than 40 years long (Robson and Reed 1999). In addition, a particular interest is in estimating the probability of events more extreme than anything that has occurred before which requires extrapolation beyond the existing data. Multi-variate extremes present additional difficulties as it is necessary to define extreme events at multiple sites and identify which observations belong to the same underlying event. The area over which the event is classified also affects the extremeness, as the most extreme events tend to be very localised (see Section 1.2.1).

The remainder of this chapter begins by outlining the meteorological conditions that cause extreme events in the UK (Section 5.2). It then moves on to consider the established statistical methods used to model single sites and multi-variate extremes (Section 5.3) and the practical issues involved in their use for applied studies. The final Section (5.4) outlines the requirements of the statistical model for the sources component of the system model developed in this thesis, and justifies the use of the conditional dependence model of

Heffernan and Tawn (2004) for this purpose. The application of the conditional dependence model to this thesis is discussed further in Chapter 6.

5.2 Extreme events in the UK

5.2.1 What causes extreme events in the UK?

As identified in Chapter 1, flooding presents the greatest climatic risk in the UK. The UK has a temperate climate with wet winters and dry summers. Location within the UK affects the dominant weather systems experienced and the type of catchment and antecedent conditions affect runoff processes leading to spatial variation in the flooding climate. There are known relationships between inputs. Mid-latitude cyclones bringing rainfall to the UK cause sea level to rise due to the effects of low pressure at the centre of the cyclone. The associated wind from the cyclone drags the sea water in a similar direction as the wind causing a surge in sea levels coinciding with the heavy rainfall event (Svensson and Jones 2002). These interactions are discussed further in Section 5.2.2.

It is useful to have a basic understanding of the physical components of extreme events before considering how to model them. A brief overview of fluvial and coastal extremes is given in Sections 5.2.1.1 and 5.2.1.2.

5.2.1.1 Fluvial extremes

Rainfall events

Precipitation in the UK arises from three main sources; frontal systems, convective instabilities (thunderstorms) and orographic uplift (Barrow and Hulme 1997). There is a distinct precipitation gradient with more rain in the west caused by orographic uplift and frequent frontal systems blowing in from the Atlantic. The difference can be up to five times the annual total, however in summer the rainfall totals are similar across the country due to higher frequencies of thunderstorms in the south east (Barrow and Hulme 1997).

The classification of rainfall events as extreme depends on both the amount of rainfall and the event duration (Collier *et al.* 2002). Convective events result in intense rainfall for a short period of time which can lead to flashy localised flooding. The spatial dependences for convective events are usually low (see Section 5.2.2). Frontal events affect larger areas and lead to less intense rainfall over a longer period of time which can lead to widespread flooding.

Using rainfall records and other historic sources, Collier *et al.* (2002) identify 50 extreme UK rainfall events from convective, orographic and frontal sources. Figure 5.1 shows the distribution of event type illustrating both the acknowledged timing for different event types,

with convective storms dominating the summer months and frontal systems being most prevalent through the autumn, and the generally accepted trend for the most extreme events in the UK to be localised convective storms. The variation in total rainfall for this set of extreme rainfall events is shown in Figure 5.2.

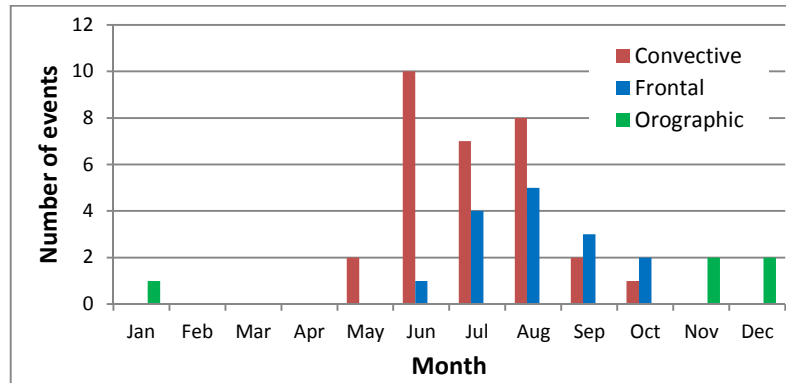


Figure 5.1 Number and type of extreme rainfall events by month as identified by Collier et al (2002)

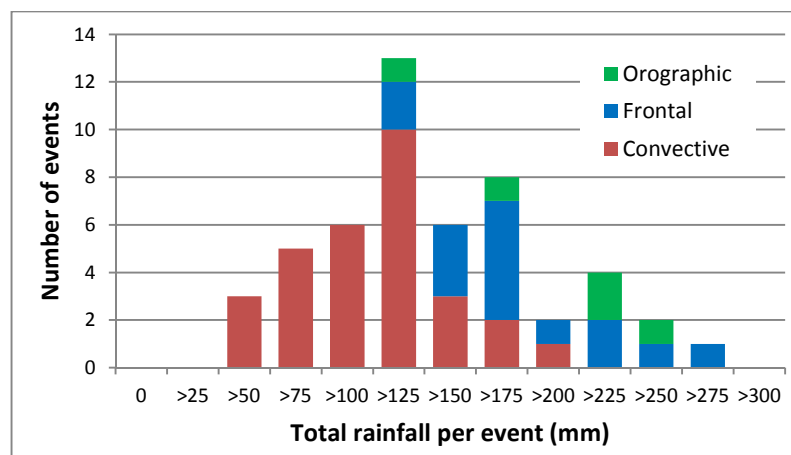


Figure 5.2 Rainfall totals by type of extreme event as identified by Collier et al (2002)

Different types of rainfall events produce different responses depending on the catchment characteristics (see Ledingham 2011) and antecedent conditions. As discussed in Section 5.2.2, how a catchment responds to rainfall influences the strength of the spatial and temporal correlations during flood events. For this reason, for a flood risk study such as this, it is easier to use flow data directly as this removes the uncertainty associated with rainfall run off modelling (see Section 4.1.1.1).

Historic events

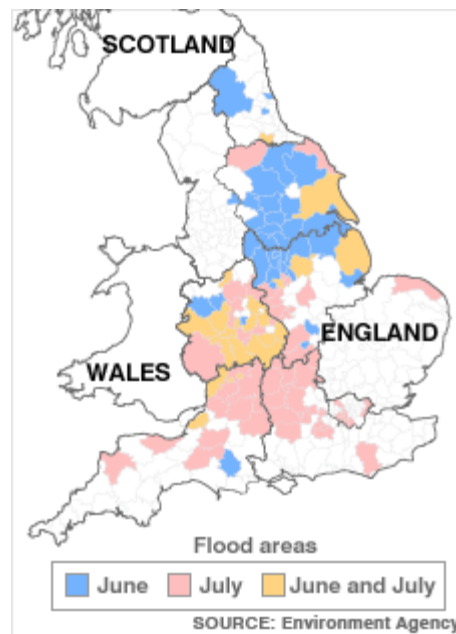
Recent significant, large scale, fluvial events in the UK include the floods of Easter 1998, Autumn 2000 and Summer 2007. All three of these events occurred due to changes in the normal weather patterns resulting in unseasonal amounts of rainfall. Prior to these events the

benchmark flood was in 1947 when a rapid thaw combined with heavy rainfall caused extensive flooding across the UK. Many of the flood levels experienced in 1947 have been exceeded by subsequent events.

In April 1998 prolonged, slow moving and heavy rainfall was experienced across in a band across the Midlands from Evesham in the south west and the Wash to the north east. The wettest areas experienced over 75mm of rainfall in a 24 hour period. This rain fell on previously saturated soil and caused widespread flooding. River levels rose rapidly at a speed around twice as fast as had been previously recorded, 42000 properties were flooded causing insured losses of £500 million (Met Office 1998; Horner and Walsh 2000).

Again in autumn 2000 pre-saturated ground conditions from an unusually wet summer and the wettest autumn in England since records began (Climatepredictions.net) led to widespread flooding. The period from September to November saw a series of widespread and prolonged rainfall events with seasonal frontal weather systems tracking across the UK further south than usual. The worst affected regions were the South East, Wales and Yorkshire. Around 10000 properties were flooded with losses estimated to be £1billion. The extended duration and widespread nature of the flooding was more significant than the magnitude of flows in many cases. The local response was complex with different areas flooding at different times and some flooding more than once over the autumn (Climatepredictions.net; Marsh and Dale 2002).

The 2007 floods were a result of unusual weather conditions with a combination of warmer sea temperatures and the Jet Stream located further south than usual bringing heavy, unusually long rainstorms over southern and central parts of the UK. The exceptionally wet May to July period caused the ground to saturate and reservoirs to fill up, leading to widespread flooding in late June and early July. As well as river flooding, the 2007 event caused widespread surface water flooding from the intensity of the rainfall. There were two main events; the period of June 24th -25th saw flooding in South Yorkshire and Hull then on July 19th a slow moving depression caused heavy rainfall over south-east England onto already saturated ground causing flooding along the Rivers Avon, Severn and Thames. In total 13 people lost their lives, approximately 48,000 households and nearly 7,300 businesses were flooded and over £3bn of insured losses occurred (Environment Agency 2007; Pitt 2008). A map of the areas affected in Summer 2007 is shown in Figure 5.3. The emergency response to the 2007 floods was compromised due to the unprecedented scale of affected locations with Pitt referring to it as the “largest peacetime emergency since World War II” (Pitt 2008).



Source: Environment Agency (cite BBC News 2007)

Figure 5.3 Map of areas affected by the summer 2007 floods

5.2.1.2 Coastal extremes

The still water level at the coast comprises of two main components, the deterministic tide, which can be predicted based on the relative positions of the earth, moon and sun, and the non-tidal residual, or surge component, which is meteorologically driven. The combination of these two components is shown in Figure 5.4. The highest water levels are observed when a strong positive surge occurs at the same time as a high tide. The seasonal variation in water level is relatively low. The largest surges tend to occur in winter while the largest tides are most often observed in spring and autumn (Dixon and Tawn 1999). Further details of the driving forces behind the tidal and surge components are discussed below. The still water level may be further increased by waves.

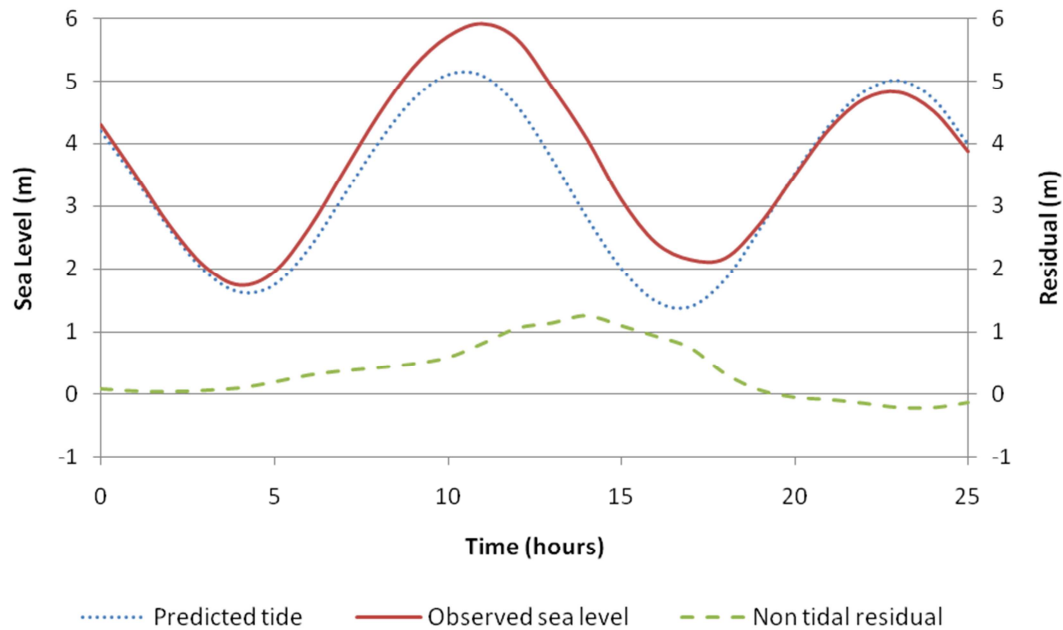


Figure 5.4 Components of still sea level

Tide

The tide is caused by the gravitational forces of the moon and the sun. In the UK there is a semi-diurnal tidal cycle lasting on average 12 hours and 25 minutes meaning there are two high tides per day. The physics behind predicting the tide are well understood (for details see Pugh 2004) and allow for accurate forecasting of the predicted tide at any given location well into the future.

The maximum tidal ranges, known as Spring Tides, occur when the sun and moon are aligned at new and full moons every 14.8 days. There are also longer term tidal cycles which should be considered. The most important are the 18.61 year lunar nodal cycle, which is caused by the difference between the earth and moons position relative to the sun, and the 8.85 year cycle of lunar perigee, which peaks when the moon aligns closest to the earth in its elliptical orbit. In practice the lunar perigee cycle has a quasi 4.4 year peak due to the positioning of the sun during the cycle (Pugh 2004; Haigh *et al.* 2011). In the UK the lunar perigee cycle is dominant (2011), the highest tides are therefore expected when this cycle peaks, next forecast to be in 2015. Using data records shorter than these significant tidal cycles is likely to lead to under or over estimation of the tidal sea level depending where in the cycle the data originates from.

Surge

The surge component is the difference between the observed water level and the predicted tide. During an extreme event this is normally termed the storm surge, and at other times it is often referred to as the non-tidal residual. Unlike the tide, storm surge is not easily predictable

in advance and depends on a combination of atmospheric pressure and wind drag. The impact of the meteorological driving forces on the observed water level is further influenced by the water depth and the shape of the coastline, with the greatest effects seen in shallow water.

The atmospheric pressure changes the pressure forces acting on the sea surface. Extra tropical cyclones (ETCs) travelling over the ocean with a deep low pressure system at their centre cause the sea level to rise beneath the low pressure. Theoretically a decrease in atmospheric pressure of one millibar will produce an increase in sea level of one centimetre. Pugh (2004) suggests in a typical year the extra tropical atmospheric pressure ranges between 980mb and 1030mb which when compared to the standard atmospheric pressure of 1013mb results in sea level changes between +0.33m and -0.17m. The surge formed by the atmospheric low then propagates towards the coastline. Surges can also be produced by strong winds which cause wind drag along the water surface. This is known as the locally generated surge.

The effects of both the wind drag and atmospheric pressure surges are greatest over shallow seas. The effects are also enhanced when the surge is travelling into an enclosed or narrowing area. The worst case surge scenario would be a low pressure system leading to storm conditions with very high onshore winds, especially if the storm was blowing into an enclosed sea at high tide (Haslett 2000).

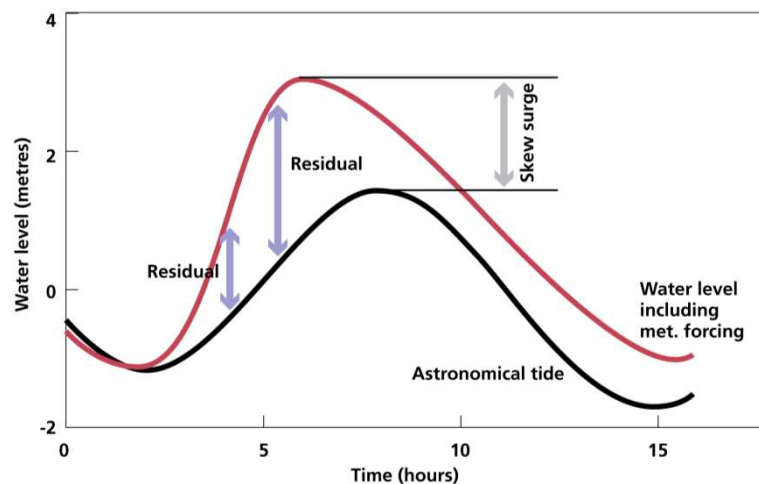
The North Sea is particularly susceptible to storm surges (Haslett 2000; Pugh 2004). This is because of its location as ETCs travelling across the North Atlantic cross the northern entrance to the North Sea; its shallow depth as pressure gradients develop between the deep Atlantic Ocean and the shallow shelf waters of the North Sea; and its shape becoming shallower and narrower towards the south. The travel time of a storm surge between the Forth Estuary in Scotland and the Thames Estuary is around nine hours (Pugh 2004).

Skew surge

Statistical modelling of extreme sea level using the combination of tide and surge is difficult due to timing issues. Correctly modelling the timing of peak tide and peak surge is important, for example a large storm surge occurred in the UK during November 2007 however the impact of this event was low as the peak of the surge occurred at low tide (JBA Consulting 2007). The interaction between surge and tide, especially in shallow water, means that the maximum surge residuals tend to occur at low to mid tide as the tide rises (Horsburg and Wilson 2007).

An alternative method is the concept of skew surge. Skew surge is the difference between the maximum observed sea level and the maximum predicted tide from the nearest tidal cycle, as

illustrated in Figure 5.5. Using skew surge avoids having to account for the tide-surge interaction as skew surge is independent of the tide height (Keef *et al.* 2009a). Skew surge is used in preference to the surge residual in many recent studies on coastal flood risk including, UKCP09 (UK Climate Projections 2009), and the EA Coastal Flood Boundary Conditions project (McMillian *et al.* 2011a) and Spatial Coherences of flood risk project (Keef *et al.* 2009a). For these reasons skew surge is used as the basis of analysis in this thesis.



Source: UK Climate Predictions (2009)

Figure 5.5 Calculating skew surge

Waves

Waves are produced by wind blowing over open water. While the wind is still actively forming the waves they are known as wind waves. Once formed, waves can continue to travel hundreds of kilometres without the active intervention of the wind. These waves are then known as swell. Swell waves are generally more damaging to coastal defences than wind waves as they have a longer period and greater power. A longer period increases the run-up and wave overtopping compared to wind waves of an equivalent height (Environment Agency 2011b). As a wave travels towards the coastline it is affected by local bathymetry and water depth.

The consideration of waves is particularly important as during storm surge events the waves can impact coastal defences above the designed height and may overtop the defence causing damage to the rear face (Wolf and Flather 2005). This is especially relevant on exposed coastlines such as in Lincolnshire. In many cases the consideration of waves in coastal flood risk studies is limited. This is largely due to the complexity of including waves and the lack of easily useable datasets. The EA (Environment Agency 2011b) has recently published guidelines

for the inclusion of waves in coastal studies so there may be improvements in this area in the future.

Historic events

The worst historic coastal flood in the UK occurred in January 1953 when a major storm surge hit the East Coast, causing multiple defence breaches, flooding 24000 homes and causing the loss of 300 lives (Spalding 1953). The storm originated from a low pressure system located off the Iceland coast. The depression then travelled southwards and centralised itself in the North Sea between Aberdeenshire and Southern Norway. At its lowest point the depression measured 966mb and the resulting surge was amplified as it travelled southwards along the East Coast. At the same time a high pressure ridge was building in the Atlantic causing steep pressure gradients which led to winds of up to Force 10 piling up the water and waves up to 8m high (Met Office 2011b). The surge took 9 hours to travel from Northumberland to the Isle of Thamet. Luckily the surge did not correspond with the high tide in the UK (Snell 1953). While this reduced the peak water levels, it did mean that levels remained high for an extended period of time.

Another event of interest occurred in February 1990 on the North Wales coast. A low pressure system, recording 947mb at its lowest point (Met Office 2011c) moved southwards from Greenland to the UK. This resulted in strong winds in the Irish Sea creating exceptionally high waves and a storm surge of 1.5m (Williams 2010). The arrival of the low pressure system coincided with the highest spring tides of the year and led to the highest recorded water levels for the North Wales coast. In Towyn this led to the failure of the sea defences and flooding of nearly 3000 properties (NGfL Cymru 2011) and caravan parks (see Figure 5.6).



Source: Bowen and Pallister (2001)

Figure 5.6 The Chester to Holyhead railway and flooded caravan site at Towyn during the 1990 event

5.2.2 What known relationships exist between extreme events?

The above discussion has illustrated that extreme events are caused by a number of different weather conditions. When different variables respond to the same weather conditions they can be considered meteorologically dependent (Hawkes *et al.* 2008, p328), however the

physical response also depends heavily on the local topography and geology (Svensson and Jones 2002; 2004; Keef *et al.* 2009b).

The degree of dependence is related to the type of extreme event. Frontal events tend to affect large areas of the UK simultaneously and therefore display widespread spatial dependence. The most extreme rainfall totals are often from convective storms which are very localised meaning that the dependence changes as events get more extreme (McSweeney 2007; Johnson 2008; Keef *et al.* 2009b). The influence of the type of storm event also means that the spatial dependence has seasonal variability as localised, convective storms are more common in the UK in summer than winter (Keef 2006). The inverse is true of coastal events where the surge driving cyclonic events are more frequent in winter and the interactions with the deterministic tides means the relationship between extreme sea levels and wave height is strongest for the most extreme events (Hawkes *et al.* 2002). An added complication is that these correlations are likely to change in the future as the climate changes. This section presents the main findings from previous studies of dependencies in extreme events in the UK.

Building on the work of Keef (2006) in her thesis, Keef *et al.* (2009b) investigated the dependence between extreme river flows and precipitation (see Section 5.3.3 for details of their methodology). They found large scale spatial dependence structures in extreme rainfall events which they attribute to topography. The spatial dependence in rainfall was found to be higher in the southeast than in the mountainous northwest. Keef *et al.* (2009b) suggest a possible reason for this is that orographic precipitation varies at the same spatial scale as topography. An example of the output is shown in Figure 5.7. The map was produced using the spatial dependence measure introduced in Section 5.3.3.5, using a 30km radius and a 55 year return period. The dots on the map show each gauging station, shaded by the probability that if the rainfall at one station exceeds a 55 year event what is the probability that other gauges within a 30km radius will also experience an extreme event. The dependencies in the extremes were found to be lower than the rest of the data and to fall rapidly to zero.

The spatial dependencies in flow were shown to be greater than for precipitation (as illustrated in Figure 5.8 using the same spatial dependence measure as for rainfall). Keef *et al.* (2009b) suggest this is because flow represents an areal averaging of response compared to the point rainfall measurements. The flow results however do not show the same NW to SE dependence characteristics. Keef *et al.* (2009b) conclude that a major factor determining the dependence in river flows is catchment characteristics, where similar catchment occur together the dependence is high but where catchment characteristics vary over a small distance a decrease in spatial dependencies is seen for example where highly permeable

catchments in the SE are located next to less permeable ones or where the storage capabilities of lakes and reservoirs in the catchment affect response such as in Western Scotland.

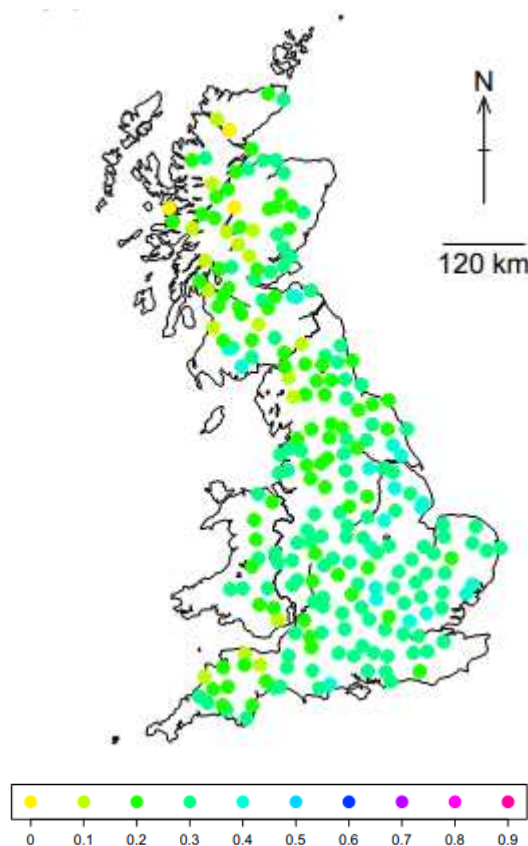
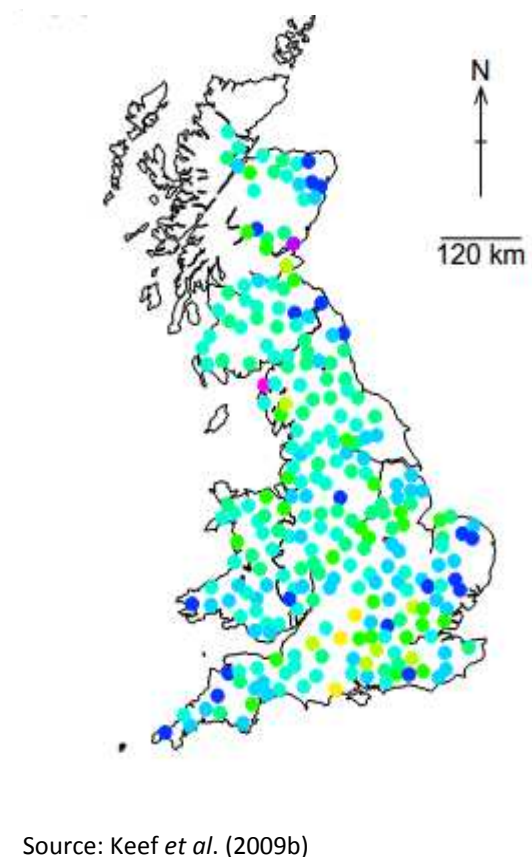


Figure 5.7 Spatial dependence in rainfall for a 55 year event over a radius of 30km



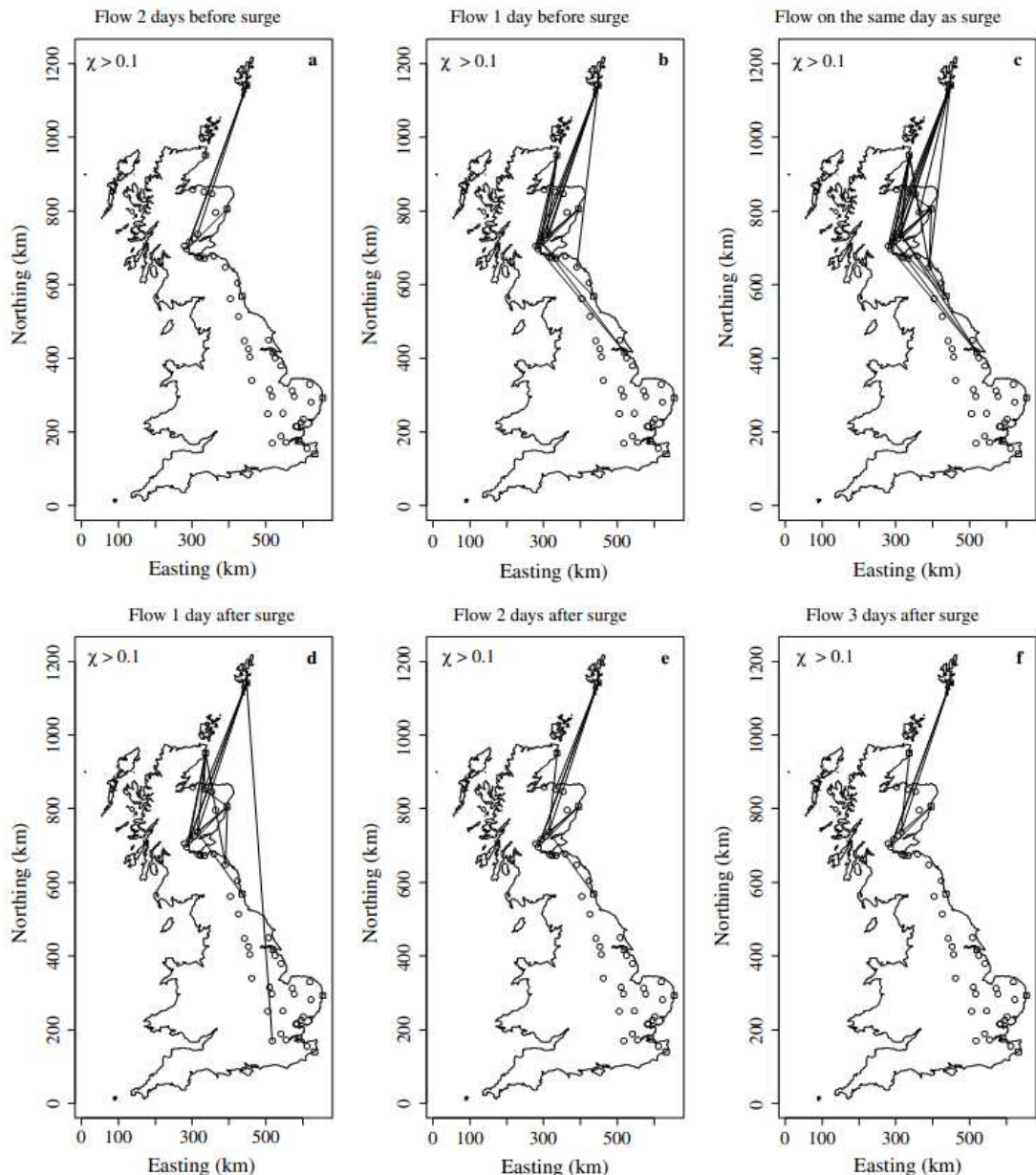
Source: Keef *et al.* (2009b)

Figure 5.8 Spatial dependence in river flows for a 50 year event over a radius of 30km

The importance of catchment characteristics in determining spatial dependence between extreme events was also identified in the earlier work by Svensson and Jones (2002; 2004) who looked at river flows, rainfall and storm surge around the UK coast using the pairwise dependence measure χ presented in Section 5.3.2.2. They found that the highest dependence between surge and flow is found in hilly areas with a southerly to westerly aspect as these areas respond faster to rainfall. Using rainfall data to help interpret their findings they conclude that the surge-flow dependence can vary greatly over short distances due to different catchment responses for example due to catchment area or geology. They also observe that the type and direction of cyclonic activity is important and found that rivers showed stronger dependence to surges that occurred north of them than south (Figure 5.9).

Svensson and Jones also considered the temporal dependence between variables and note that the dependence is greatest for flows and surges occurring on the same day and remains high for lags of up to one day (Figure 5.9). They also looked at the seasonal variation in the process and found that the flow-surge dependence on the East and West Coasts is strongest in

winter but north of Wales it is stronger in summer. The reasons for this are suggested to be seasonal changes in the rainfall-runoff relationship and to the metrological conditions causing storms. Events on the East Coast are generally caused by cyclones passing NW of Scotland which are most frequent in winter. However Keef *et al* (2009a) do not consider seasonality due to the short record lengths when observations are split into seasons. Given that Svensson's and Jones method cannot be extended beyond the observed data (see Section 5.3.2.2) their seasonal observations should therefore be taken with caution.



Lines connect station pairs with χ exceeding 0.1 (Source: Svensson and Jones 2002, p1163)

Figure 5.9 Dependencies between river flow and sea surge for different time lags on the East Coast

Previous work on the spatial dependence structure of sea levels around the UK was carried out by Dixon and Tawn (1994; 1995; 1997) using the revised joint probability model (RJPM, see Section 5.3.2.2). They concluded that while extreme tides are relatively frequent; the greatest concern was extreme surges occurring at the same time as extreme tides. They found that the surge variability was greatest on the East Coast and more consistent on the West Coast. In areas of shallow water around the coast, the most extreme water levels were caused by different combinations of surge and tide (Dixon and Tawn 1994);

- For Lerwick to Immingham - high tide combined with moderately extreme surges;
- For Cromer to Dover and Heysham to Portpatrick - extreme surges occurring on a high tide;
- For Newlyn to Holyhead and Ullapool to Stornoway - high tidal level combined with a moderate surge.

Hawkes and Gouldby *et al* (2002) conducted further analysis of coastal water levels around the UK, including wave height which is known to have a significant impact on defence overtopping. In general they found that waves and water level are usually partially dependent, displaying a moderate correlation which varies around the coastline, however the dependence between surge and wave height is often masked by the tide which is not meteorologically driven. They conclude that on the East Coast “strong northerly winds produce both surges and high waves, but there tends to be a time lag between the occurrence of the peak values of the two variables.” The West Coast shows little time lag between surges and waves but “wave conditions tend to include higher swell component unrelated to the local weather conditions.” (Hawkes *et al.* 2002, p242). Unlike rainfall and flow events, they observe that the most extreme sea conditions show a higher dependence than more commonly occurring conditions. This is likely to be due to the increased influence of the tide under less extreme conditions.

Hawkes *et al* (2002) also acknowledge the importance of local scale conditions on total water level, for example the interaction with currents in shallow water, however this is not explored further in their analysis and is unlikely to be possible in any analysis carried out at a national scale.

Figure 5.10 provides a geographical summary of the dependencies in rainfall, flows and sea level identified in previous research by Keef *et al* (Keef 2006; Keef *et al.* 2009b), Svensson and Jones (2002; 2004) and Hawkes *et al* (2002).

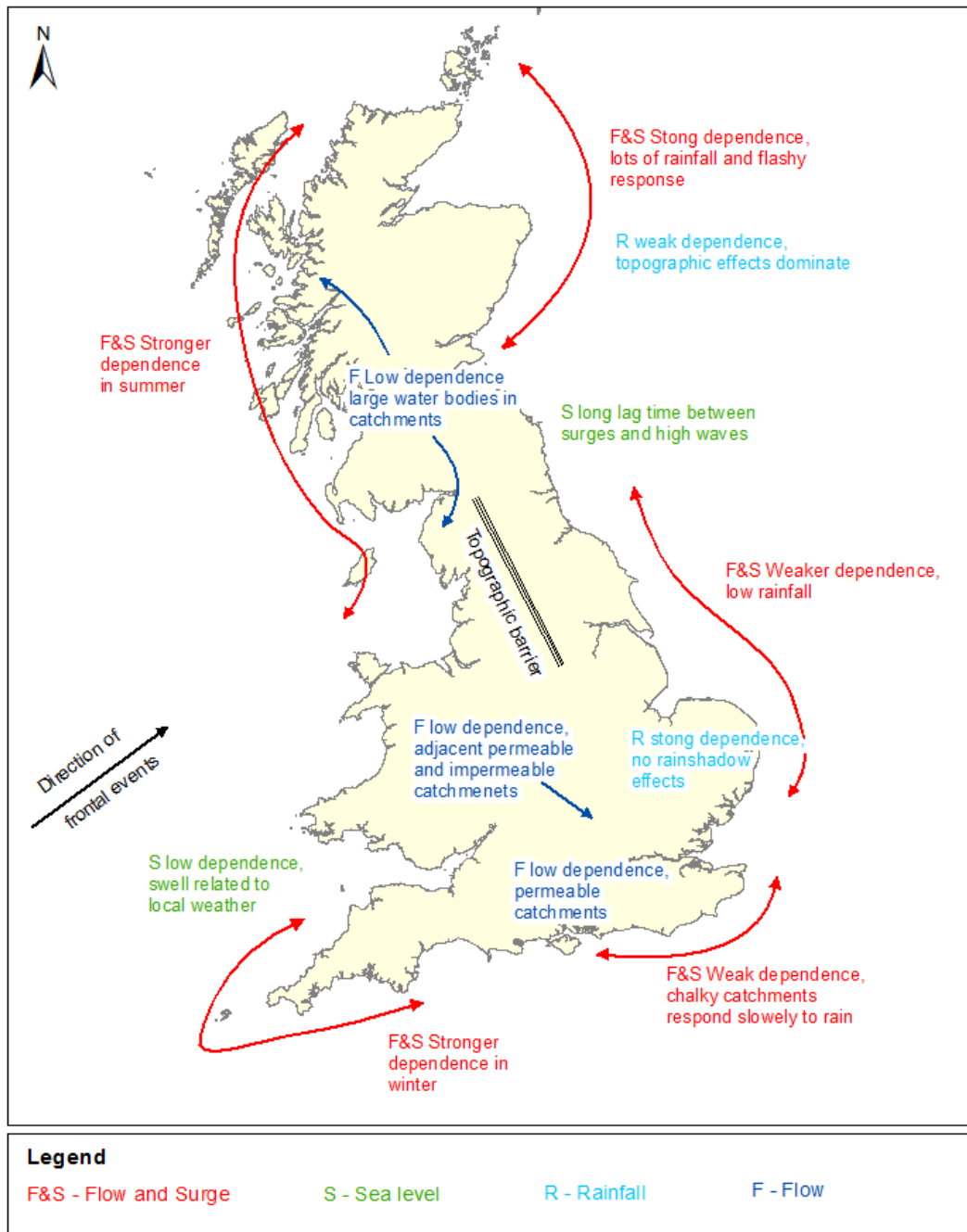


Figure 5.10 Summary of past research on spatial dependencies of UK extreme events

5.3 Modelling extreme events

Modelling multi-variate extreme events requires consideration of the event at each individual location and the relationship across different locations and time steps. Hawkes *et al* (2008) recommend that meteorological dependence is best studied using statistical modelling. They suggest “the essential elements of a joint probability extremes assessment are the distribution of each variable, the extreme values of each variable, and the dependence for each variable pair coupled with a method to combine all this information in a meaningful way” (P329).

Statistical modelling of events at individual sites can be achieved using a number of methods based on the principles of Extreme Value Theory (EVT). The most common include the Generalised Extreme Value Distribution (GEV), Generalised Pareto Distribution (GPD) and the R largest methods. These three methods are summarised in Appendix A as well as the Generalised Logistic method (GL) which is common in engineering studies in the UK since it is recommended for use by the Flood Estimation Handbook (FEH, Robson and Reed 1999). The popularity of different methods depends on both their statistical robustness and suitability for the required purpose as well as political motivations (see Griffis and Stedinger 2007a; 2007b; 2008; 2009 for an interesting discussion on the issues involved in selecting a suitable extreme value distribution of modelling floods in the USA). It is assumed that readers have a basic understanding of statistics and EVT. For those that require an introduction to the subject Coles' (2001) informative text book on extreme value theory is recommended.

As well as the core methods themselves, analysis of meteorologically driven extremes requires consideration of the natural clustering of extreme values in time. To meet the assumptions of EVT, data must be de-clustered before they can be used in a statistical model. The available methods for doing this are reviewed in Section 5.3.2.

Statistical modelling of events across different spatial and temporal scales requires modification of the standard EVT methods. Numerous statisticians and hydrologists have developed methods to do this, many of which are reviewed by Hawkes *et al* (2008). There are two approaches, either the statistical approach of developing a method with a simulated or simplified data set or an engineering driven approach of fitting a model to a real dataset. There are pros and cons to each method. The first allows the development of a sophisticated, generic approach however modifications are often required when applying the method to real data sets. The mathematics involved are often highly complex and present difficulties in both understanding for practical end users of the method and high computational loads. These issues often result in a long lead time between methods being first published and their general uptake by the hydrological community. The latter approach is often driven by an end user problem and as such has a much shorter time frame between inception and application. However in order to achieve this, the statistics involved may be less robust and the method less suitable for use in a wide range of applications due to the need to meet a number of initial assumptions.

The methods reviewed in Section 5.3.2.2 tend towards the engineering, end user based approach but still have a strong statistical basis. Reviewed methods include simple distance

based correlation methods, the χ dependence measure of Svensson and Jones (2002; 2004) and improved $\bar{\chi}$ method of Coles *et al* (1999), the Joint Return Period Method (JRPM) of Dixon and Tawn (1995; 1999) and the conditional dependence model of Heffernan and Tawn (2004), applied to fluvial, pluvial and coastal extremes by Keef *et al* (2009a; 2009b).

The modelling framework in which methods are applied is also significant, for example using a Bayes framework allows the user to include their existing knowledge of the processes of interest within the statistical model which can be useful in improving efficiency by constraining the parameter optimisation within a specified range. This is touched on further in Section 5.3.4.

The final stage of modelling extreme events is to acknowledge that all models have their limitations and will not be a true representation of the process of interest. To this ends an assessment of the uncertainty in the statistical model is required as discussed in Section 5.3.4.

5.3.1 Extreme value theory

EVT is a special type of statistical modelling that deals with extreme events and addresses the difficulties of limited observations and extrapolation beyond observed data (Coles 2001). The GPD model is used in this thesis, a summary of which is provided below. The reason for selecting the distribution was because it had previously been used successfully by Keef *et al* (Keef *et al*. 2009a; Keef *et al*. 2009b; Keef *et al*. 2009c) however it is acknowledged that other distributions could have been used in its place and a summary of the strengths and weaknesses of different methods is provided in Appendix A. Extreme value theory is based on the central assumption that above a certain threshold data are asymptotic, meaning they tend towards some absolute value. If this is not the case an alternative statistical model should be sought. The assumption that hydrological events are asymptotic causes some disagreement amongst hydrologists, some of whom disagree that the distribution of extreme floods can be bounded. This is a disagreement that has been ongoing since Gumbel first started working on estimating the return periods of floods in the 1940s. Further discussion can be found in Katz *et al* (2002). Here it is assumed that the extremes of interest are asymptotic and EVT is valid.

EVT also assumes that data are independent identically distributed (IID). In many meteorological cases this is not the case due to temporal sequencing of events therefore pre-processing is required to de-cluster the data as described in Section 5.3.2.1.

The extreme variables of interest in this study, river flow, storm surge and wave height, are all continuous variables and therefore the probability distribution for each variable is defined by a probability distribution function;

$$F(x) = Pr\{X \leq x\} \quad 5.1$$

Using peaks over threshold data (with the threshold defined as u) and the GPD, the probability distribution for the Peaks over threshold (POT) data described using three parameters, the location parameter, μ , the scale parameter, σ , and the shape parameter, ε as shown in Equation 5.2. The shape parameter is dominant and when ε equals zero the distribution takes a different form as given by Equation 5.3.

$$H(y) = 1 - \left(1 + \frac{\varepsilon y}{\tilde{\sigma}}\right)^{-1/\varepsilon} \quad 5.2$$

$$\text{where: } \tilde{\sigma} = \sigma + \varepsilon(u - \mu)$$

$$H(y) = 1 - \exp\left(-\frac{y}{\tilde{\sigma}}\right) \quad 5.3$$

5.3.1.1 Defining thresholds

A central requirement of any EVT model is establishing the threshold at which events can be considered extreme. This process is seen by some statisticians to incorporate a potentially subjective component to the model. The following example explores the issues of threshold definition when using the GPD model.

For a series of independent variables, X_1, X_2, \dots, X_n extreme events are defined as those of the X_i which exceed some defined high threshold, u . The threshold must be set high enough that the GPD is a good model for the POT series. The threshold can be selected either using exploratory techniques before the model is fitted or by testing the stability of the parameter estimates following fitting the distribution for a range of thresholds. The former of these is based on the fact that the mean of the excesses ($X_i - u$) is a linear function of $u : u > u_0$, where u_0 is the minimum threshold at which the assumptions of the GPD are met (and hence will also be met at any higher threshold, u). Therefore above a threshold u_0 , if the plot of mean excess against u (termed the mean residual life plot) is approximately linear the GPD can be seen to provide a valid approximation to the excesses distribution. The downside of this method is that it can often be difficult to interpret the mean residual life plot, therefore Coles (2001) recommends using both methods in parallel.

Figure 5.11 shows an example of a mean residual life plot for DMF data at Kingston on Thames. Interpretation of this plot would suggest a suitable threshold for the GPD at around $u = 150$ m^3/s . However a scatter plot of the data (Figure 5.12) suggests that $150\text{m}^3/\text{s}$ is a particularly low threshold as the average number of exceedences per year at this threshold is 39.

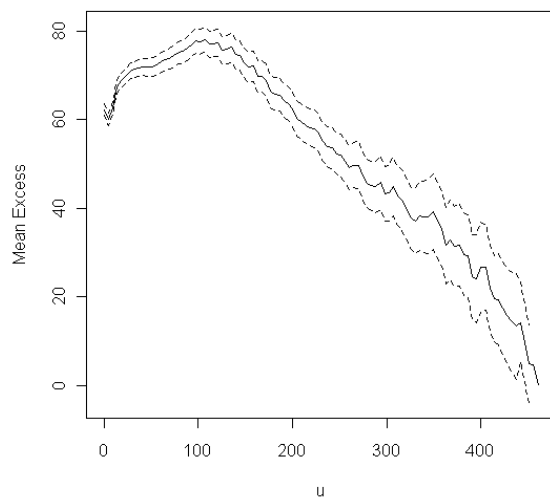


Figure 5.11 Example mean residual life plot for Kingston upon Thames flow data

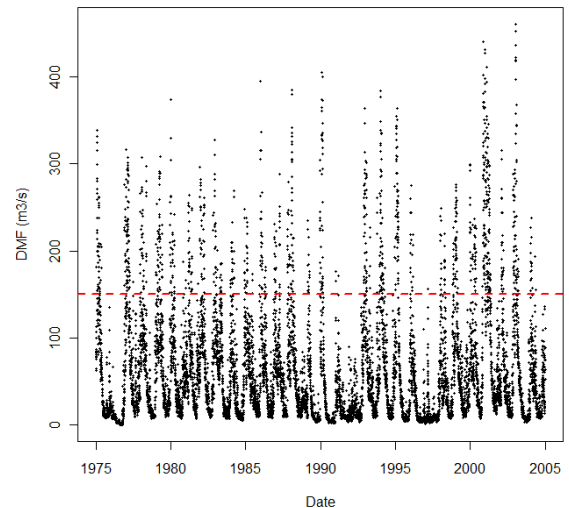


Figure 5.12 Scatter plot of Kingston on Thames daily flows by year

Given the concerns raised above about the initial threshold selection and the advice of Coles (2001) to use both methods in parallel, the POT analysis was repeated using several thresholds and the parameter stability reviewed. The results are shown in Table 5.1 which suggest a more suitable threshold of $250 \text{ m}^3/\text{s}$, this equates to a total of 326 exceedances with an average of 10.9 exceedances per year. Table 5.1 also shows the problem with increasing the threshold too high. For a threshold of $350 \text{ m}^3/\text{s}$, both the shape parameter and 1% AEP estimate are considerably different from the other thresholds. This is because there are only 44 exceedances above $350 \text{ m}^3/\text{s}$, an average of 1.5 events per year resulting in an increase in parameter variability.

Table 5.1 Parameter stability assessment for a GPD model fitted to DMF at Kingston on Thames for multiple thresholds

Threshold (m^3/s)	1% AEP return level (m^3/s)	Shape parameter
150	469	-0.251
200	471	-0.243
250	474	-0.022
300	474	-0.240
350	461	-0.457

5.3.2 Dependence structures

For environmental variables, particularly the ones of interest in this thesis, the assumption of independence is invalid. Data can be dependent on previous observations in the sequence, for example high river flows on one day increases the probability of high flows on the following day; related to other variables, for example high rainfall and river flows are likely to occur simultaneously during a storm event; or spatially dependent, for example a high sea level recorded at one coastal location is likely to be seen in neighbouring stations.

The primary issue is to identify what defines an event. When looking at single sites the most common ways of doing this are to either specify a fixed time window, for example the insurance industry define events as lasting seven days, or to specify a threshold which once the observations fall below the event is classified as over. These definitions form the basis of the de-clustering methods discussed in Section 5.3.2.1. When looking at multiple locations or different variables the definition of an event is complicated as it may take time for the meteorological system driving the event to travel across all the locations, or there may be a lag in the physical appearance of the event for example as flood flows travel downstream. Sections 5.3.2.2 and 5.3.3 introduce several methods and statistical constructs that go some way towards addressing these issues for multi-variate spatial dependence.

5.3.2.1 Temporal dependence

Stationary Processes

If flows at a particular location are high on any given day, it is likely that flows will also be high on the preceding or following day. This temporal structure is known as a stationary process and violates many of the assumptions of EVT.

A stationary process is one where for a random process X_1, X_2, \dots, X_n any given set of integers $\{i_1, \dots, i_k\}$ and any integer m , the joint distribution of $(X_{i_1}, \dots, X_{i_k})$ and $(X_{i_1+m}, \dots, X_{i_k+m})$ are identical. Therefore X_i can be dependent on previous values however this dependence must be consistent throughout the dataset, meaning trends such as seasonality are not included when assuming stationary. Processes may also be termed as weak stationary processes when the mean and variance for any subset of the sequence are identical even if the joint distributions are different.

Both the GEV and GPD models can still be applied to stationary processes allowing for some small adaptations for example de-clustering of extremes in the POT series. A simple example is illustrated here for sea level data at Southend 1988 to 2000.

The 25 highest sea levels for the years 1997 to 2000 are shown in Figure 5.13. Two things are immediately obvious from the scatter plots, firstly the peak water levels have a seasonal cycle, mainly occurring between September and April. Secondly many of the events occur on the same day or adjacent days. This means that the events are dependent on the same storm surge and therefore form a stationary sequence with the peak tide level more likely to be high if the preceding level was also high. Ignoring the seasonality the focus of this example is on removing the dependence between events.

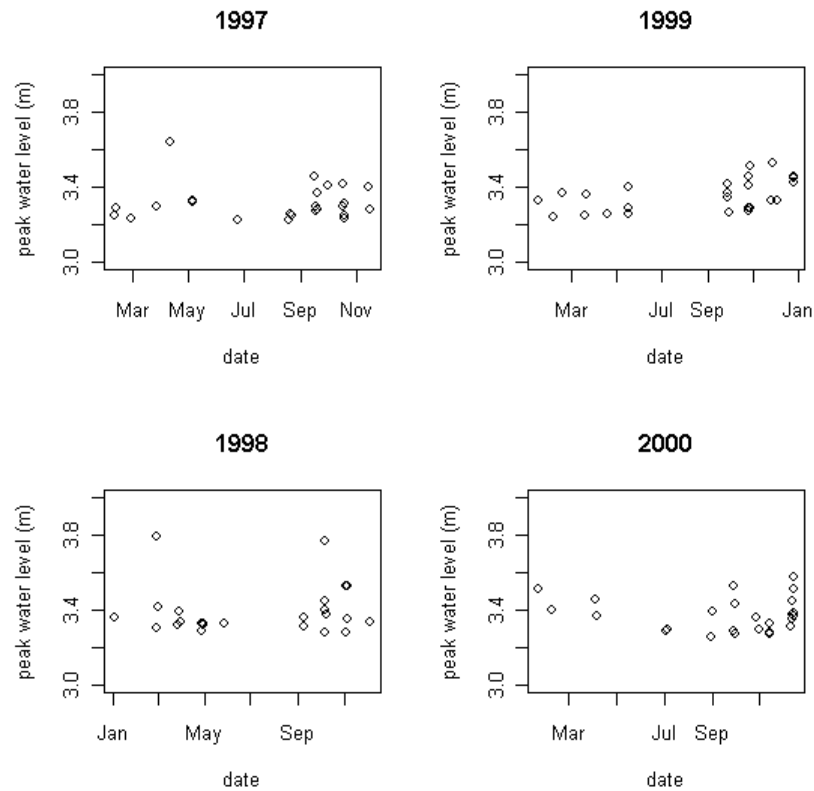


Figure 5.13 Peak sea levels at Southend 1997 - 2000

The rank ordered data series for each year was de-clustered using the following algorithm;

1. Select the date of the largest event
2. Check all smaller events and remove from the data set if the event is within two days of the selected event
3. Repeat for the next (none removed) largest event, until all events have been checked.

Reproduction of the plots for the 25 largest events from 1998 to 2001 shows that the 25 largest events no longer occur during the same storm surge event (Figure 5.14).

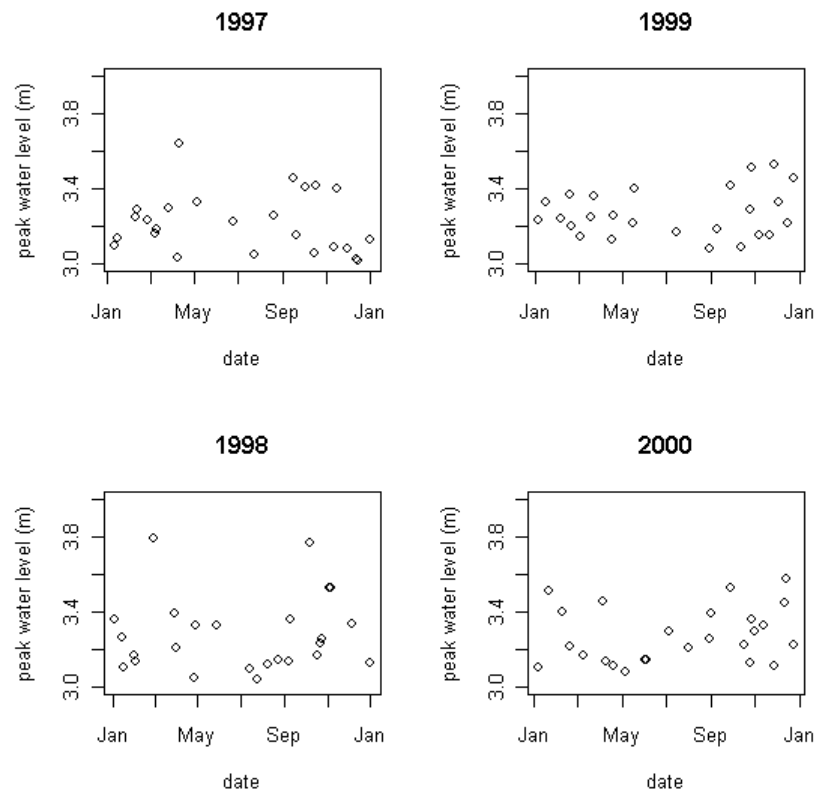


Figure 5.14 De-clustered peak sea levels at Southend 1997 - 2000

The disadvantage of de-clustering in this way is that the de-clustering method reduces the number of observations available to fit the model to from 730 to 112. The seasonality of the events is also less defined. While the largest events are still maintained in the sequence, so are much lower peak levels, making the choice of thresholds increasingly important.

There are several variations on data based de-clustering methods discussed in the literature. The most prevalent of which are reviewed by Nadarajah (2001). The simplest is to assume that each event is of a standard length and select the maximum value from within this moving time window, as applied above (see Tawn 1988). This is the approach taken by Keef *et al* 2009a) in existing applications of the Heffernan and Tawn (2004) conditional dependence model. An alternative approach which allows for more variability within the event, is to define an event as having ended once a certain number of occurrences fall below a specified threshold (as per Smith 1989; Coles 2001). This is termed a “fixed termination time approach” by Walshaw (1994) or “runs de-clustering” by Smith and Weissman (1994) and in the R software. More complex approaches include Smith’s (1984) development of parametric models fitted to the data to estimate the time between independent events.

The first stage in de-clustering time series data is to define the period of time over which peaks at the subject site are dependent and belong to the same event. This can either be defined by

the user or from the data. For example within the insurance industry an event is defined as seven days. This definition is easy to understand and apply however the arbitrary window of seven days does not account for potential variability in catchment response. A more physically robust definition can be established from the data itself. For example Keef *et al* (2009a; 2009b) test the time period over which the value of $P(X_{t+\tau} > v_p | X_t > v_p)$ changed for values of τ up to 50, for v_p equal to the 0.99 probability threshold at gauge X (See Section 5.3.3.3), and used this to define a suitable de-clustering time window.

De-clustering of continuous data to extract an independent series of flood peaks is an essential, but seemingly arbitrary, process in applying extreme value models. The choice of de-clustering method is important as the method used can introduce bias into the results. A balance needs to be found between maintaining enough data to fit the statistical model while ensuring an independent time series. There is no clear consensus as to which method is best. Smith (1989) comments of his parametric modelling approach that it offers no improvements over using simpler methods, while Smith and Weissman (1994) suggest that runs de-clustering reduces the bias compared to a time window method and allows for more variability within the event. Their observation is based on a theoretical discussion and is not proven with meteorological data however the application in Section 5.3.3.6 further illustrates the suitability of runs de-clustering for use with variable meteorological data. Fawcett and Walshaw (2006) argue that using any form of de-clustering incorporates bias into the results and therefore propose bypassing de-clustering methods entirely and using Markov chains to incorporate the temporal dependence structure in the data. While de-clustering is a useful tool for applications where the cluster behaviour is important, statisticians seem able to provide justification for using most available de-clustering methods based on their aims and objectives.

Markov Chains

Markov chains provide a means of further defining the dependence behaviour of a random process. A first order Markov Chain process is defined where the value of X_i depends on X_{i-1} . More complex k^{th} order Markov Chain models can be defined where the value of X_i depends on the most recent k observations. Furthermore the dependence on previous values in the chain can diminish as distance increases, thereby allowing for the influence of recent events in the series to have a greater effect than distant events. Markov chains are explored further in Section 8.4 as a means of representing spatially varying defence crest heights.

Non-stationary sequences

Non-stationary occurs when processes change systematically through time for example seasonal changes in the weather or long term trends such as rising sea levels. If systematic

trends do persist in the data it is important to model them as accurately as possible, especially when extrapolating beyond the observed data as any biases may be amplified (Coles 2001). EVT methods can be adapted to incorporate non-stationary dependence (see Walshaw 1994; Coles 2001).

5.3.2.2 *Multivariate dependence*

Multivariate dependence structures exist between multiple sites recording the same variable (this may also be referenced to as spatial dependence), or between different variables recorded at the same or multiple locations.

It is particularly important that dependence is correctly estimated when studying extremes, especially when extrapolating beyond the observed data. Dependence in the tails can take two forms, asymptotic dependence where high values of both variables occur together or asymptotic independence where the probability of the most extreme values occurring together is zero. Two variables may not be dependent but can still display positive extremal association if the joint extremes of the two variables occur more often than if they were independent. If the sum of two variables is of interest, for example the maximum tide level and maximum surge, assuming them to be independent when they are not leads to under estimation of the maximum value (Keef *et al.* 2009a).

In the following sections various methods of dealing with multivariate dependence structures are presented, the most sophisticated of which is the Heffernan and Tawn conditional dependence model explained in Section 5.3.3. This method is particularly attractive as it is able to deal with changing dependencies as events get more extreme.

Distance based correlation coefficients

Meteorological data are known to be spatially dependant, for example if it rains in one location it is more likely to also rain in other neighbouring locations. A simplistic method of accounting for this is to correlate by distance as illustrated using rainfall data from the Thames catchment (as shown in Figure 5.15). The distance correlation coefficients between each pair of gauges were calculated, the results for four example gauges are shown in Figure 5.16. Each of the four gauges is highly correlated with the gauges located closest to it and the degree of correlation decreases with distance between the gauges.

The analysis was repeated for extreme events over a threshold, taken as 25% of RMED (the median annual maximum rainfall) which resulted in an average of 10 events per year being retained. As shown in Figure 5.17 the correlation coefficients are much lower, decreasing to <0.2 compared with 0.5 for the full event set. This provides a good example of the changing

dependencies as events get more extreme and illustrates the importance of localised storm events in the South East of England.

However rainfall does not depend on distance alone and may be further influenced by other factors such as distance to the sea, site elevation and rain shadow effects. Multivariate dependence therefore often requires more detailed analysis than distance alone.

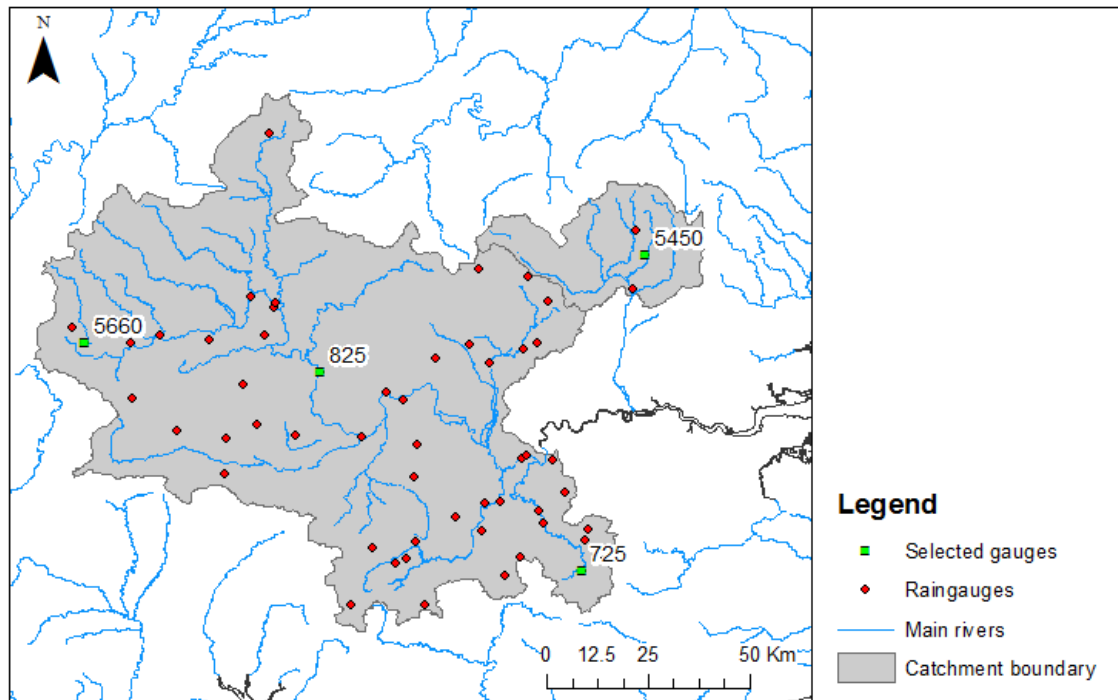


Figure 5.15 Location of raingauges in the Thames catchment

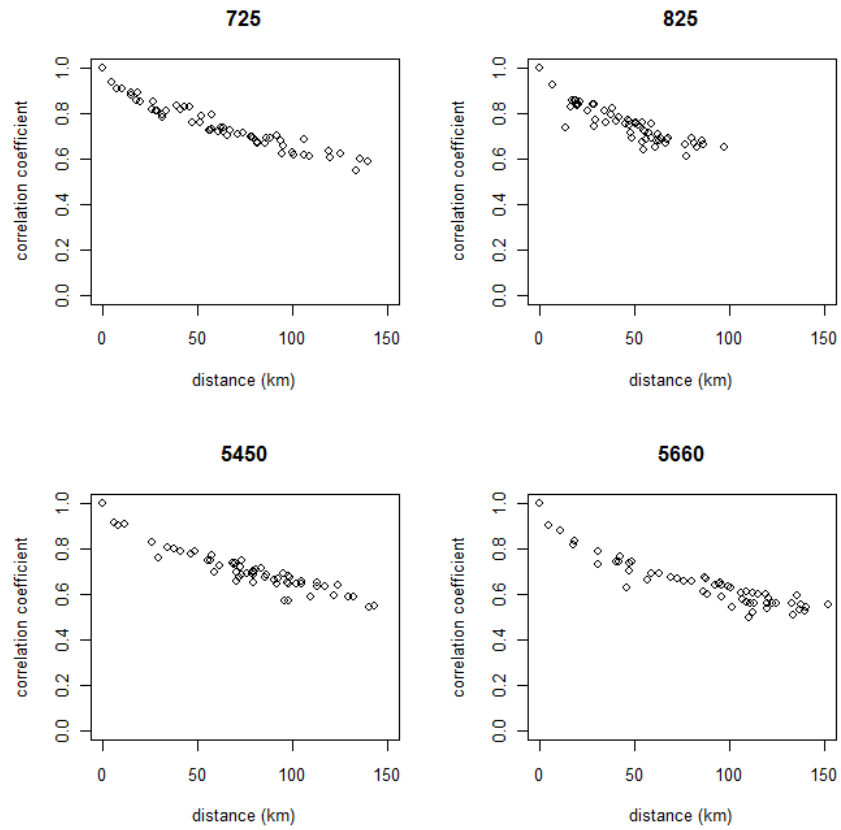


Figure 5.16 Thames rain gauges distance correlation coefficients

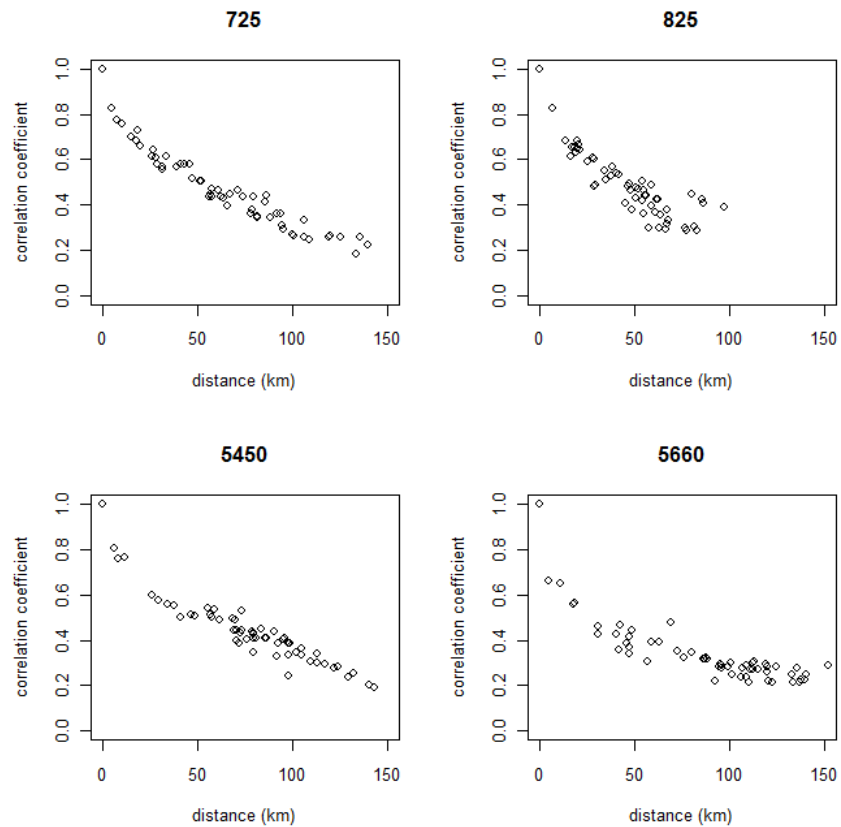


Figure 5.17 Thames rain gauges distance correlation coefficients for extreme events

Joint probability models

Sea level is an example of a multivariate problem with dependence components (see Section 5.2.1.2). To fully describe sea level a joint probability model of the deterministic tide and stochastic storm surge is required. One means of doing this is the revised joint probability method (RJPM) used by Dixon and Tawn (1995; 1999). In the RJPM the distribution of the annual maximum still water level in year i is:

$$G_i(z) = \left\{ \prod_{t=1}^T F_{Y,i|X}(z - X_t | X_t) \right\}^{\theta_t N/T} \quad 5.4$$

Where $F_{Y,i|X}$ is the distribution of the surge, Y , in year i conditional on the tide X . X_t is the hourly tide level and T and N are the number of hours in a nodal tidal cycle and year, and θ_t is the extremal index of the still water level series. The choice of $F_{Y,i|X}$ is an important feature of the model as this accounts for the tide surge interaction. This is discussed further in Dixon and Tawn (1999).

The RJPM model has been shown to offer significant advantages over standard GEV models, particularly in areas where the tide surge interaction is high due to non stationarity in the tide data (Dixon and Tawn 1999). The RJPM was used by Dixon and Tawn (1994; 1995; 1997) in their detailed study of extreme sea levels around the UK after being found to be the most suitable method for sites with at least 5-10 years of data. This study remains the most comprehensive review of extreme sea levels in the UK to date.

Coles and Tawn (2005a; 2005b) also formulate a joint probability model to account for tide and storm surge such that for a multivariate random variable which is a vector of random variables $X = (X_1, \dots, X_k)$. The joint distribution function of X is given by;

$$F(x) = \Pr\{X_1 \leq x_1, \dots, X_k \leq x_k\} \quad \text{Where } x = (x_1, \dots, x_k) \quad 5.5$$

The joint density function for continuous random variables, X_i is;

$$f(x) = \frac{\partial^k F}{\partial x_1 \dots \partial x_k} \quad 5.6$$

The covariance of variables X and Y , having joint density function $f_{X,Y}$ is;

$$\text{Cov}(X, Y) = \int_{-\infty}^{\infty} \int_{-\infty}^{\infty} \{x - E(X)\} \{y - E(Y)\} f_{X,Y}(x, y) dx dy \quad 5.7$$

The dependence between components can therefore be defined with the correlation coefficient;

$$\text{Corr}(X, Y) = \frac{\text{Cov}(X, Y)}{\sqrt{\text{Var}(X)\text{Var}(Y)}} \quad 5.8$$

An alternative means to deal with the relationship between tide and surge is to use the concept of skew surge as detailed in Section 5.2.1.2.

Dependence measure χ and $\bar{\chi}$

The dependence measure χ describes the probability that one variable (U) is extreme, given that the other variable (V) is also extreme based on a user specified threshold, u . Values of $\chi=1$ signify asymptotic dependence and values of $\chi=0$ signify asymptotic independence or negative dependence. χ is calculated as;

$$\chi(u) = 2 - \frac{\ln \Pr(U \leq u, V \leq u)}{\ln \Pr(U \leq u)} \quad 5.9$$

The dependence measure χ , forms the basis of Svensson and Jones' (2002; 2004) work on estimating the dependence between sea surge, river flow and precipitation around the UK. An example application is developed here showing the use of χ for characterising asymptotic dependence between rainfall and flow data for an area in Worstershire on the River Severn. This area corresponds to one of the caravan risk clusters identified in Chapter 3. In this area there are three different main river systems, the Severn, the Leam and the Stour, all with different flooding regimes so it is useful to understand how processes on one river system relate to another. The main river in this area is the River Severn which has its headwaters in mid Wales. It is therefore expected that the dependence between the River Severn flow gauge, 54001, and the rain gauges will be low. The gauges are detailed in Figure 5.18, Table 5.2 and Table 5.3.

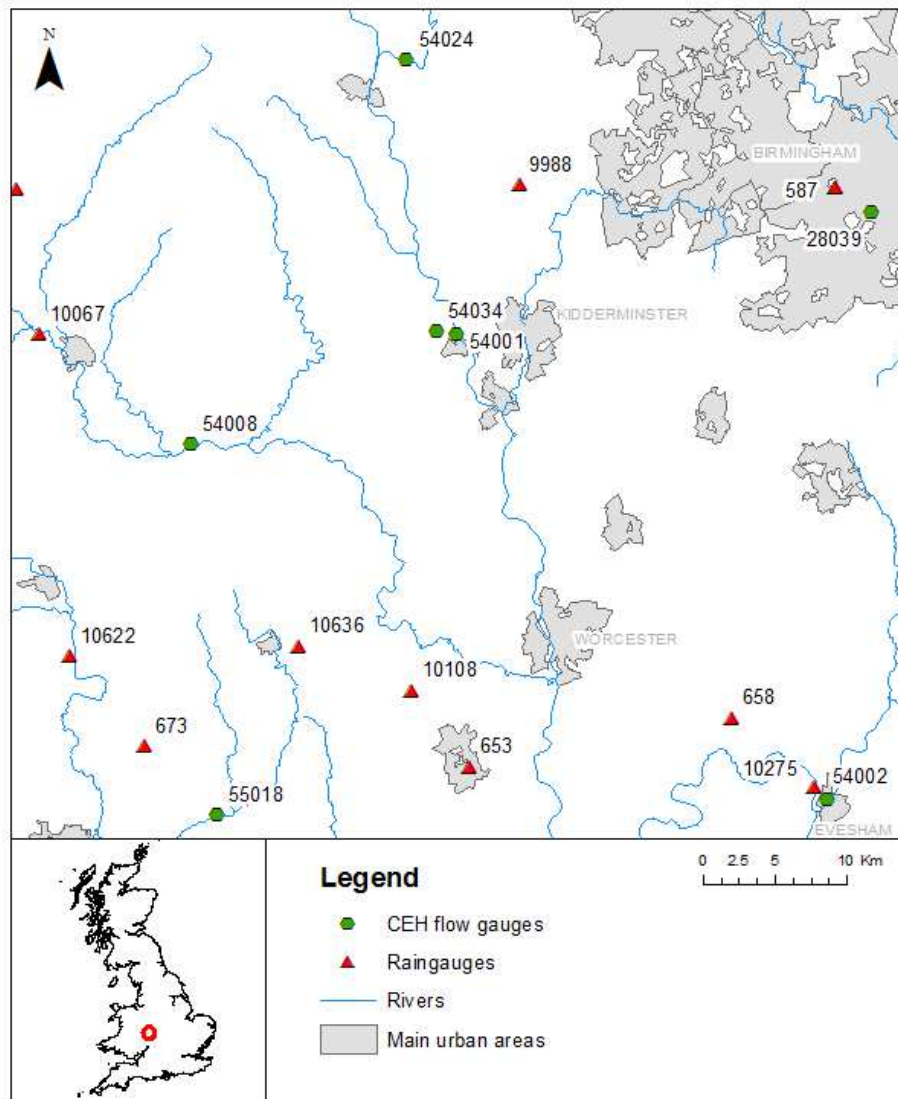


Figure 5.18 Location of sample rain and flow gauges around the Severn risk cluster

Table 5.2 Rain gauges near the Severn risk cluster

SRC Number	Station Name	Start date	End date
10638	Bromyard, Down House	2/1/1961	31/12/2006
9988	Enville	2/1/1961	1/08/2005
10108	Old Storridge	2/4/1963	31/12/2006
635	Malvern	2/1/1900	31/12/2006

Table 5.3 Flow gauges near the Severn risk cluster

Number	Station Name	Start date	End date
54001	Severn at Bewdley	1/1/1921	31/12/2006
54008	Teme at Tenbury	1/1/1956	31/12/2006
54024	Worf at Burcote	1/1/1969	31/12/2006
54034	Dowles Brook at Oak Cottage	1/1/1971	31/12/2006

The first step is to set a suitable threshold, u , above which the observations can be considered extreme. As the magnitude of U and V may differ, the threshold, u , is defined using the non-exceedance probability for individual observations of U and V . The annual maximum non-exceedance probability, a is;

$$a = Pr(\text{Annual maximum} \leq x) \quad 5.10$$

where x is the magnitude of the variable. It relates to the return period, T , as $T - 1(1/a)$ and can be defined using the POT sequence;

$$a = \exp\left(-\frac{i - 0.5}{N}\right) \quad 5.11$$

Where N is the number of years of observations and i is the rank of the POT series.

The value of a needs to be low enough to allow sufficient data points to exceed it and high enough to be considered extreme. In their study, Svensson and Jones found that using an annual maximum non-exceedance probability of greater than 0.5 resulted in values of χ that tended to zero as there were no threshold exceedances. They used a threshold of $a=0.1$ which means that the annual maximum will exceed this threshold in 9 out of 10 years.

Specifying $a = 0.1$, The value of i was calculated as;

$$i = N(-\ln(a)) + 0.5 \quad 5.12$$

The i^{th} value of the declustered POT sequence was extracted for each gauge record to form the thresholds (x^* and y^*) shown in Table 5.4. Since the distributions of the variables of interest are unlikely to be the same, the data and the specified thresholds are transformed to uniformity on $[0,1]$.

Table 5.4 Rain and flow gauge threshold for the χ dependence measure

Rain gauge threshold (mm)				Flow gauge threshold (m^3/s)			
10636	9988	10108	653	54001	54008	54024	54034
23.0	21.6	23.6	23.3	266.8	78.1	4.7	3.3

Equation 5.9 is calculated by counting the number of observation points (X,Y) such that;

$$Pr(U \leq u, V \leq v) = \frac{\text{Number of } (X,Y) \text{ such that } X \leq x^* \text{ and } Y \leq y^*}{\text{Total number of } (X,Y)} \quad 5.13$$

And

$$\ln Pr(U \leq u) = \frac{1}{2} \ln \left(\frac{\text{Number of } X \leq x^*}{\text{Total number of } X} \cdot \frac{\text{Number of } Y \leq y^*}{\text{Total number of } Y} \right) \quad 5.14$$

The results are shown in Table 5.5. As would be expected, the rain gauges show the strongest correlation with each other and a much lower correlation with the flow gauges due to the influence of additional catchment processes. In some cases it can be assumed that the flow and rain gauges show asymptotic independence, for example between 54024 and 9988.

Table 5.5 Dependence measure χ for all pairs of gauges around the Severn risk cluster

		Rain gauges				Flow gauges			
		10636	9988	10108	653	54001	54008	54024	54034
Rain gauges	10636	1	0.461	0.677	0.625	0.329	0.265	0.075	0.215
	9988	0.461	1	0.405	0.518	0.337	0.235	0.009	0.106
	10108	0.677	0.405	1	0.742	0.275	0.216	0.074	0.174
	653	0.625	0.518	0.742	1	0.026	0.130	0.117	0.181
Flow gauges	54001	0.329	0.337	0.275	0.026	1	0.489	0.598	0.448
	54008	0.265	0.235	0.216	0.130	0.489	1	0.503	0.476
	54024	0.075	0.009	0.074	0.117	0.598	0.503	1	0.377
	54034	0.215	0.106	0.174	0.181	0.448	0.476	0.377	1

Although variables may be asymptotically independent, $\chi=0$, there may still be some dependence within the extremes in the form of positive extremal association which it is important to understand (Keef *et al.* 2009a). In addition there is some uncertainty around the value $\chi(u)$ for high thresholds. To describe this issue formally consider Figure 5.19, taken from Coles *et al.* (1999), which shows that for higher values of u , the values of $\chi(u)$ converge towards 0 i.e. as the threshold is raised and the events being considered become more extreme the dependence is less. For values of $\chi(u) > 0$ the convergence is abrupt as $u \rightarrow 1$ meaning that $\chi(u)$ is considerably greater than zero for values of u close to 1 and hence estimates of $\chi(u)$ may appear positive and constant for asymptotically independent variables (Coles *et al.* 1999). The joint survivor measure $\bar{\chi}$ (Equation 5.15) presented by Coles *et al.* (1999) is used to provide additional information on the dependence structure in these cases.

$$\bar{\chi}(u) = \frac{2 \ln Pr(U > u)}{\ln Pr(U > u, V > u)} - 1 \quad \begin{array}{l} \text{Where } -1 \leq \bar{\chi} \leq 1 \\ \text{for all } 0 \leq u \leq 1 \end{array} \quad 5.15$$

Estimation of both χ and $\bar{\chi}$ provide pairs of summary measures $(\chi, \bar{\chi})$ such that $(\chi > 0, \bar{\chi} = 1)$ signifies asymptotic dependence and χ can be used as a measure of the strength of dependence, and $(\chi = 0, \bar{\chi} < 1)$ signifies asymptotic independence with $\bar{\chi}$ determining the strength of extremal association (Coles *et al.* 1999).

Figure 5.20 shows the added clarity of using this approach compared to χ in Figure 5.19.

Without the use of the additional measure $\bar{\chi}$, Keef *et al.* (2008b) suggest that the analysis of dependence by sea surge, river flow and precipitation by Svensson and Jones (2002; 2004) is of

limited value as it cannot be compared to other dependence estimates as variables may be classified as dependent instead of the alternative classification of asymptotic independence with extremal association.

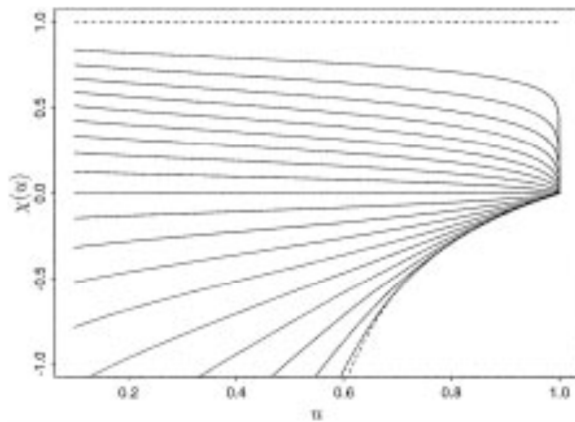


Figure 5.19 Dependence measure $\chi(u)$
as $u \rightarrow 1$

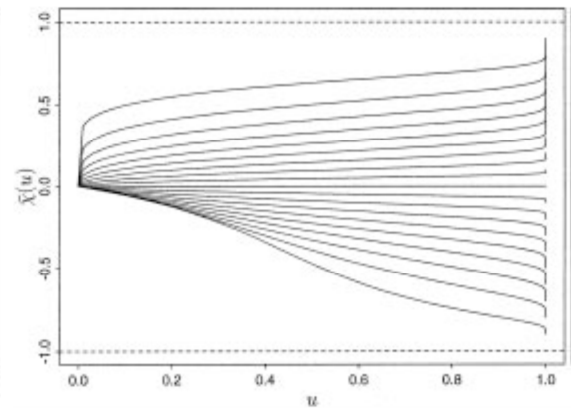


Figure 5.20 Dependence measure $\bar{\chi}(u)$
as $u \rightarrow 1$

Source: Coles *et al* (1999)

Since all the values of χ in Table 5.5 are > 0 , $\bar{\chi}$ has been estimated for all the gauge pairs (Table 5.6). In all cases $\bar{\chi}$ is > 0 but < 1 confirming the previous findings that the rain and flow gauges show some degree of asymptotic dependence but are not completely dependent and identifying χ as a suitable measure for describing the dependence structures. The weak dependence between 54024 and 9988 is again highlighted, given that $\chi \approx 0$ and $\bar{\chi} \approx 0$, it can be concluded that this pair is asymptotically independent and shows near independence under the assumption of independence. The pair 54001 and 653 also shows near independence under both measures.

Table 5.6 Dependence measure $\bar{\chi}$ for all pairs of gauges near the Severn risk cluster

		Rain gauges				Flow gauges			
		10636	9988	10108	653	54001	54008	54024	54034
Rain gauges	10636	1	0.300	0.512	0.455	0.197	0.152	0.039	0.120
	9988	0.300	1	0.254	0.350	0.202	0.133	0.004	0.056
	10108	0.512	0.254	1	0.590	0.159	0.121	0.039	0.095
	653	0.455	0.350	0.590	1	0.013	0.069	0.062	0.100
Flow gauges	54001	0.197	0.202	0.159	0.013	1	0.324	0.427	0.288
	54008	0.152	0.133	0.121	0.069	0.324	1	0.336	0.313
	54024	0.039	0.004	0.039	0.062	0.427	0.336	1	0.232
	54034	0.120	0.056	0.095	0.100	0.288	0.313	0.232	1

A more complex method for analysis of spatial structures in extremes is detailed in Section 5.3.3.

5.3.3 A conditional dependence model for multivariate extremes

Many of the existing extreme value models available in the literature are based on the assumption that variables are either asymptotically independent or asymptotically dependent (see Section 5.3.2.2). While this is attractive as it reduces model complexity, it reduces the choice of variables that can be used and the distance over which the model can be assumed to be valid. For example while flows in the same catchment may be asymptotically dependent, the same assumption cannot be made for river flows over the entire country.

Heffernan and Tawn (2004) proposed a more flexible model that is able to account for both asymptotically dependent and independent data and can model the changes in dependences as events get more extreme. The model describes the distribution of $Y | X$ given that X is large for independent, identically distributed data without missing values (Keef *et al.* 2009a), where X is a vector of data from a single gauge and Y is a matrix of data at all other gauges in the network. The model is particularly useful for extremes as the model describes the relationship between variables based on the residuals. The residuals are independent of the size of the conditioning variable and therefore the model can be used to extrapolate beyond the range of the data through statistical simulation. This is an additional benefit when compared to alternative methods such as Svensson and Jones' (2002; 2004) work with the dependence measure χ , which are empirical. The conditional dependence model can theoretically be applied to any number of variables over variable time lags providing flexible scope for the scale of analysis. Due to computational memory limitations Keef *et al.* (2009a) suggest a practical limitation of 50 variables (or site) with time lags of +/- 5 time steps.

Heffernan and Tawn (2004) originally demonstrated the model using air quality data but it has since been used extensively for fluvial and coastal flood risk analysis by Keef *et al.* in the UK (Keef 2006; Lamb *et al.* 2009; Keef *et al.* 2009a; Keef *et al.* 2009b; Keef *et al.* 2009c; Lamb *et al.* 2010). The following description of the model is based on the above references, a discussion meeting with Lamb, Keef and Tawn held at Newcastle University in December 2008 and subsequent personal communication.

5.3.3.1 The method

The method separates the marginal and dependence characteristics and models them separately through the use of a Copula. For an introduction to copulas readers are referred to Nelsen (2006). The benefit of using Copula functions is that the marginal and dependence characteristics can be separated, therefore reducing the dominance in the tails of variables with a large scale compared to variables with smaller scales (Keef *et al.* 2008a).

The copula function works by separating the joint distribution into m marginal distributions and a joint distribution function, C (Keef *et al.* 2009b). The Copula is the function which assigns the value of the joint distribution function to each pair of values (Nelsen 2006), meaning that the joint distribution function of X given in Equation 5.16 can be represented by Equation 5.17.

$$F(x) = \Pr\{X_1 \leq x_1, \dots, X_k \leq x_k\} \quad \text{Where } x = (x_1, \dots, x_k) \quad 5.16$$

$$C\{F_1(x_1), \dots, F_m(x_m)\} \quad 5.17$$

There is a unique Copula for each multivariate distribution. Keef *et al.* (2009a; 2009b; 2009c) use a Gaussian copula for their work on rainfall and fluvial extremes. It is acknowledged that this may not be the most appropriate copula for studying extremes (see AghaKouchak, Bardossy *et al.* 2010) however it was not realistic to consider changes to the core of the dependence model as part of this thesis

Within the conditional dependence model the marginal characteristics are modelled using a standard GPD (although theoretically other extreme value distributions could be used). As the model is primarily concerned with modelling extreme events, the distribution below the threshold is assumed to follow an empirical distribution, $\tilde{F}_{X_i}(x)$. This results in the marginal model for F_{X_i} shown in Equation 5.18 where u_{X_i} is the high threshold for variable X_i , $i = 1, \dots, d$, and β_i and ε_i are the GPD scale and shape parameters respectively.

$$\hat{F}_{X_i}(x) = \begin{cases} 1 - \{1 - \tilde{F}_{X_i}(u_{X_i})\} \{1 + \varepsilon_i(x - u_{X_i})/\beta_i\}^{\pm 1/\varepsilon_i} & \text{For } x > u_{X_i} \\ \tilde{F}_{X_i}(x) & \text{For } x \leq u_{X_i} \end{cases} \quad 5.18$$

The data are then transformed to Gumbel marginal using the probability integral transformation shown in Equation 5.19 to allow comparison between variables of different magnitudes.

$$Y_i = -\log[-\log\{\hat{F}_{X_i}(X_i)\}] \quad 5.19$$

The central motivation of the model is that there are some vector normalising functions $a(x)$ and $b(x)$ such that;

$$\Pr\left(\frac{Y - a(x)}{b(x)} \mid X = x\right) \rightarrow G(z) \quad \text{as } x \rightarrow \infty \quad 5.20$$

With the condition that;

$$\lim_{z_j \rightarrow \infty} G_j(z_j) = 1 \quad \text{For all } j, j=1, \dots, d \quad 5.21$$

So there is no mass at $+\infty$ in any margin.

Assuming that the limiting relationship 5.20 holds exactly for all values of X above a suitably high threshold, v_p , with the probability p of being exceeded, the random variable Z can be expressed as equation 5.22 when $X = x$ with $x > v_p$.

$$Z = \frac{Y - a(x)}{b(x)} \quad 5.22$$

Z is independent of X and has distribution function G , therefore allowing simulation beyond the range of the data. Theory suggests that there should always be some threshold, v_p , above which the independence of Z and X is an appropriate assumption.

The dependence model can then be given as a multivariate semi parametric regression model of the form;

$$Y = a(x) + b(x)Z \quad 5.23$$

For multivariate cases the distribution of Z_j is estimated as;

$$Z_j = \frac{Y_j - a_j(x)}{b_j(x)} \quad \text{For } j=1, \dots, d \quad 5.24$$

Heffernan and Tawn (2004) identified the characteristics of the normalising functions $a(x)$ and $b(x)$ for various different distributions. They found that the functions were special cases of the parametric family;

$$\begin{aligned} a(x) &= ax + I_{\{a=0, b<0\}}(c - d \log(x)) \\ b(x) &= x^b \end{aligned} \quad 5.25$$

Where a , b , c and d are vector constants such that $0 \leq a_j \leq 1$, $-\infty \leq b_j \leq 1$, $-\infty \leq c_j \leq \infty$ and $0 \leq d_j \leq 1$, and I is an indicator function.

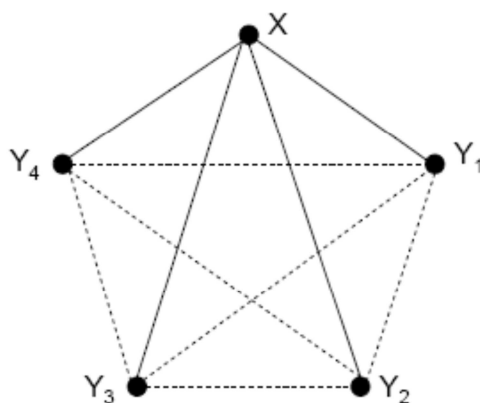
The parameter a describes the overall strength of dependence between the two variables. Larger values of a indicate stronger dependence. The b parameter describes how the dependence changes as events get more extreme. For positive values of b , the variance of $Y|X = x$ increases as x increases, therefore small values of Y can only occur with large values of X if b is large. The dependence between Y_j and X can be formally classified as follows (Keef *et al.* 2009a);

- If $a_j=1$ and $b_j=0$ then Y_j and X are asymptotically dependent, else Y_j and X are asymptotically independent;
- If $0 < a_j < 1$ or $b_j > 0$ then the variables exhibit positive extremal dependence;
- If $a_j = d_j = 0$ and $b_j \leq 0$ then the variables exhibit extremal near independence;
- If $a_j = 0, d_j < 0$ and $b_j < 0$ then the variables exhibit negative extremal dependence.

In practice, for most flood risk applications it is possible to assume that the variables exhibit either asymptotic dependence or asymptotic independence with positive extremal association (Keef *et al.* 2009a). In this case $c = d = 0$, giving the normalising functions as;

$$a(x) = ax \quad b(x) = x^b$$

The a and b parameters do not capture all of the dependence between the Y_j variables. The additional dependence is modelled non-parametrically through the Z_j parameter. Keef *et al.* (2009a) illustrate this using Figure 5.21.



Solid lines indicate dependencies modelled parametrically, dashed lines indicate dependencies modelled non-parametrically (Source: Keef *et al.* 2009a, p42)

Figure 5.21 Diagram of modelled spatial dependencies in the conditional dependence model

5.3.3.2 Estimating parameters and residuals

Equation 5.23 is fitted by assuming that each independent random variable Z_j is from a normal distribution with mean μ_j and standard deviation σ_j . Combined with the assumption of Equation 5.20, the mean and standard deviation of the variables $Y_j | X = x, x > v_p$ can then be specified as;

$$\mu_j(y_j) = a_j y_j + \mu_j x^{b_j} \quad 5.26$$

and;

$$\sigma_j(y_j) = \sigma_j x^{b_j} \quad 5.27$$

The parameters are estimated by minimising Function 5.28 with respect to $\mu_j, \sigma_j, a_j,$ and b_j .

$$\sum_{t=1}^{T_j} \left[\log\{\sigma_j x^{b_j}\} + \frac{1}{2} \left\{ \frac{y_j - a_j x - \mu_j x^{b_j}}{\sigma_j x^{b_j}} \right\}^2 \right] \quad 5.28$$

where T_j is the number of observations of y_j when $x > v_p$.

The estimated residuals at time t can then be defined as;

$$\hat{Z}_{j,t} = \frac{y_{j,t} - \hat{a}_j x_t}{x_t^{\hat{b}_j}} \quad 5.29$$

Where \hat{a} and \hat{b} are the values of a_j and b_j that minimise Function 5.28.

Keef (personal communication) found that the Nelder-Mead optimisation method was the most suitable for use with the conditional dependence model however it does not provide the ability to constrain parameter estimates. The optimisation method is also sensitive to the initial starting value of the parameters. To overcome these problems several additional steps have been built into the optimisation by Keef to help improve the stability of the model. R code to apply these steps was provided by Keef for use in this thesis. The model is also known to be unstable if there are less than 30 occurrences of Y when $X > u$, therefore Keef's optimisation method produces null values if this criteria is not met.

5.3.3.3 Consideration of temporal dependencies

There are two areas where consideration of temporal dependence is vital when fitting the conditional dependence model, firstly to establish a series of independent peaks at each sites and secondly to incorporate the time lag between peaks occurring at different sites.

At site temporal dependence

Based on the moving window de-clustering method (see Section 5.3.2.1), Keef *et al* (2009a; 2009b; 2010) investigated how the empirical estimate of $P(X_{t+\tau} > u | X_t > u)$ changed for values of τ up to 50, where τ is the time lag between events in days. This allowed identification of the temporal dependence structure at each gauge. In general they found that the at site temporal dependence in the extremes is lower than in the main body of the data. Plotting the dependence against catchment characteristics showed a clear link between temporal dependence and Base Flow Index (BFI), with higher BFI values maintaining temporal dependence over longer time periods. Although for some high BFI catchments the dependence remained high at a lag of 5 days, for most sites, Keef *et al* conclude a time window of ± 5 days sufficiently defined an independent event. The DMF data was therefore de-clustered using a moving window of ± 5 days from the highest peak event as described in Section 5.3.2.1. The analysis of Keef *et al* is repeated in Figure 5.22 using a dataset of 145 of the standard CEH DMF gauge network to represent a variety of catchment characteristics. The data set used was created for calibrating and validating the DMF to peak flow methods presented in Chapter 7.

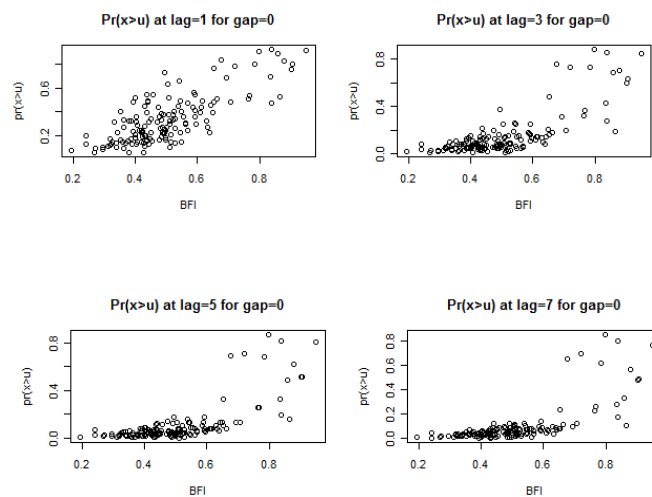


Figure 5.22 Relationship of conditional dependence measure $\Pr(X_{t+\tau} > u | X_t > u)$ with BFIHOST

The temporal dependence structure of the data set is clearly visible including the decaying dependence at lags of 5 days compared to 1 day for catchments with a BFI of < 0.7 . However for catchments with BFI values of > 0.7 there is little change in the temporal dependence

structure up to lags of 7 days. This indicates that peak flow events in the baseflow dominated catchments have a duration of more than the 10 day window adopted by Keef *et al.* Another significant concern with the window based method is that although the dependence falls, there is still a 20% chance that $x_{t+5} > u \mid x_t > u$ for catchments with BFI between 0.5 and 0.7. Analysis for this thesis (See Section 6.3.3) has shown that this could have a significant impact on the fit of the conditional dependence model and hence the resulting simulated data. As such an alternative de-clustering method is presented in Section 6.3.3.

Between site temporal dependence

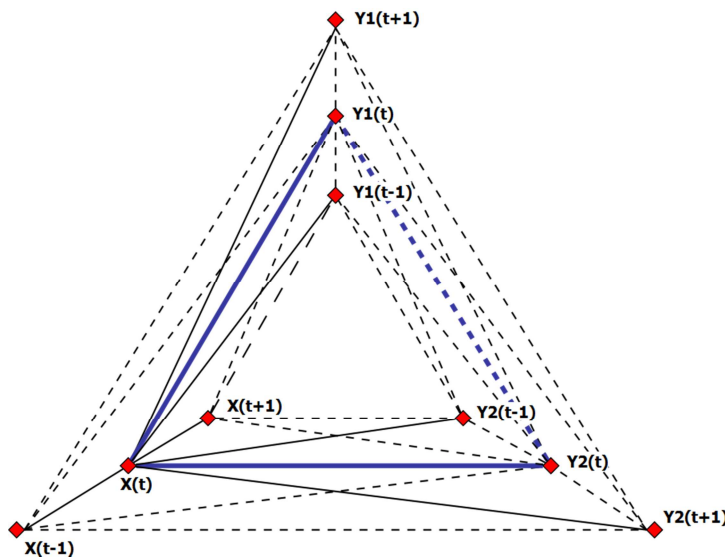
When modelling multiple sites it is unlikely that the event peaks will occur at the same time. Therefore consideration of the time period for which events at multiple sites can be assumed simultaneous is required.

The pure travel time between flood peaks provides a useful means of visualising the impact of temporal dependence between sites on the same river or coastline, however in terms of the conditional dependence model, it is more useful to consider when probability of large events occurring at any two sites within a given lag (τ) peaks. This measure is termed by Keef *et al* (2009a) as $P^{(\tau)}(p)$ and is calculated as:

$$P^{(\tau)}(p) = P(Y_{t+\tau} > v_p \mid X_t > v_p) \quad 5.30$$

Keef *et al* (2009b) found that for their data set of 256 UK DMF gauges, $P^{(\tau)}(p)$ peaked at 96% of the flow gauge pairs for $|\tau_{max}| \leq 3$. A suitable τ value for coastal data is investigated in Section 6.3.3.2.

Keef *et al* (2009a) illustrate the inclusion of multiple time lags into the conditional dependence model using Figure 5.23. The solid lines indicate dependencies modelled parametrically through the a and b parameters. The dependencies shown by the dashed lines are modelled semi-parametrically through the residuals, Z . The bold blue lines are directly equivalent to those shown in Figure 5.21 and incorporate no time lag.



Modified from Keef *et al* (2009a, p45)

Figure 5.23 Modelling temporal dependence in the conditional dependence model

5.3.3.4 Simulating from the conditional dependence model

One of the main advantages of the conditional dependence model is that it is possible to use the model to simulate data beyond the range of the observations using the fitted parameter values. The process of doing this is as follows;

1. New values of X are simulated from the fitted GPD distribution in Equation 5.19 (X_{sim})
2. The simulated X_{sim} data are converted to Gumbel margins as described in Equation 5.20
3. A matrix of Z values (Z_{sim}) the same length as X_{sim} is generated by resampling (with replacement) from the observed Z . The same event is used to provide the Z_{sim} value for all gauges.
4. Values of Y are simulated by applying Equation 5.23 using the fitted values of a and b and Z_{sim} for all time lags up to τ .
5. The simulated Y values (Y_{sim}) are on the Gumbel scale, they can be converted back to real values by rearranging Equations 5.18 and 5.19

Keef *et al* (2009a; 2009b; 2009c) use the conditional dependence model to simulate flood peaks at multiple sites belonging to the same event (henceforth referred to an event peak simulation). It is also possible to use the conditional dependence model to simulate full time series. This is explored further in Chapter 6. Keef *et al* (2009a) found that using this process directly resulted in too many extreme events being simulated compared to the observed data.

Therefore simulations are only kept in the sample if X_{sim} is more extreme than the associated values in Y_{sim} .

5.3.3.5 Measures of spatial dependency

Keef *et al* (2009a) propose two summary dependence measures that can be used with the simulated data from the conditional dependence model. Firstly Equation 5.31 describes the probability that Y is greater than a given threshold given that X is above the threshold.

$$P_j(p) = \Pr(Y_j > u_p | X > u_p) \quad 5.31$$

This is difficult to use as a summary measure as it provides a result set for each gauge which are time consuming to compare. However it does provide useful information about the behaviour of individual gauges.

The second more general summary measure Keef *et al* use is the expected proportion of gauges in Y over a given threshold given that $X > u$:

$$N(p) = \frac{E(\#\{j \in \Delta: Y > u_p\} | X > u_p)}{\#\{j \in \Delta\}} \quad 5.32$$

This measure can be applied over a specified search radius or the full gauged network. It is useful for identifying the spatial structure of extreme dependencies and forms the basis of Keef *et al*'s (2009b) assessment of spatial dependencies in fluvial flows, the results of which were discussed in Section 5.2.2.

5.3.3.6 Practical issues

The conditional dependence model was originally demonstrated for a small air pollution case study. When using the conditional dependence model with large spatial data sets of meteorological events there are a number of practical issues which arise due to the availability and suitability of the data. Some of these issues have been addressed by Keef *et al* (2009a; 2009b; 2009c), some still require further work and some are unique to the nested multi-site model presented in this PhD and therefore have not been considered previously.

Data requirements

To fit the conditional dependence model across all gauges in the network concurrent data at each gauge is required. Ideally continuous data would be used however taking an example gauge with 20 years of 15 minute flow data this equates to over 700,000 data points to analyse. Scaling this up to a moderate network of gauges soon results in an unmanageable amount of

data. To overcome these issues Keef *et al* (2009a; 2009b; 2009c) use daily mean flow data as input to the conditional dependence model. This provides one data value per day for each gauge, however the daily time step limits the application of the model for flood risk inundation modelling where a peak flow is required as input to the hydraulic model. Methods for overcoming this limitation are presented in Chapter 7.

Missing data

The nature of environmental data in the UK is such that there are periods of time when data records are not complete, for example gauges are put out of service for a period of time or there are problems with the gauging station structure or recording equipment. The requirement for concurrent data sets at all gauges means missing data restricts the application of the conditional dependence model.

Keef (2006) developed a means of using the conditional dependence model to re-simulate the missing data based on the assumption that the available data can provide information about the missing data. The model is fitted to the available observed data and then the missing data is infilled for days when at least one observed gauge exceeds u using the fitted values of a and b to simulate the missing data. Z values for the infilled data are generated from the conditional distribution of the observed Z values by assuming a multivariate normal copula (2009a).

While this approach is elegant, the computation involved in applying this infilling technique is significant and the process is not transparent to a none statistically trained end user. In light of these limitations a number of alternative infilling methods and investigated in Section 6.3.5.1.

De-clustering data

Keef *et al* de-cluster their data series using the moving window method detailed in Section 5.3.2.1. While testing this methodology a problem was identified that once the data had been de-clustered in this manner there were some occurrences where the lagged sequence produced flows at $t \neq 0$ which were greater than at $t=0$.

Take the example shown in Figure 5.24 for gauge 54001 for February 1946 plotted on a Gumbel scale. The moving window de-clustering method takes the highest flow in the sequence. In this case 8.5 on day 14 (X_1, t_0), and then remove all $x > u$ for $-5 < t < 5$. This removes the second peak, on day 9, from the de-clustered series. The next remaining highest flow value (X_2, t_0) occurs on the day preceding the removed day 9 peak. When the conditional dependence model is then fitted to the full series of time lagged data conditional on X_2 , the time series shows a higher flow at day X_2, t_1 . This effect is then reproduced in the simulated time series and causes uncertainty in the estimates of the a and b model parameters since the

conditional dependence model assumes that the flow at X_i, t_0 is the peak value in any given event. This problem is not identified by Keef *et al*, probably because it only becomes apparent when simulating time series of data at the conditioning gauge which has not previously been tested.

The underlying question is whether these two events are independent peak events or whether they are part of the same event and hence only the maximum of the two peaks should be retained. Arguably this is a research topic in its own right and much discussion of these types of questions is available in the statistical literature. It is however possible to address this issue through the use of runs de-clustering rather than the moving window approach. Runs de-clustering requires identification of the threshold, u , and the number of occurrences below the threshold, r , which signals the start of a new event (see Section 5.3.2.1). This method, which is recommended by Coles (2001), provides a more robust alternative to the moving window approach as it ensures only the peak events are included in the conditional dependence model. Application of runs de-clustering for use in the conditional dependence model is discussed in Section 6.3.3.

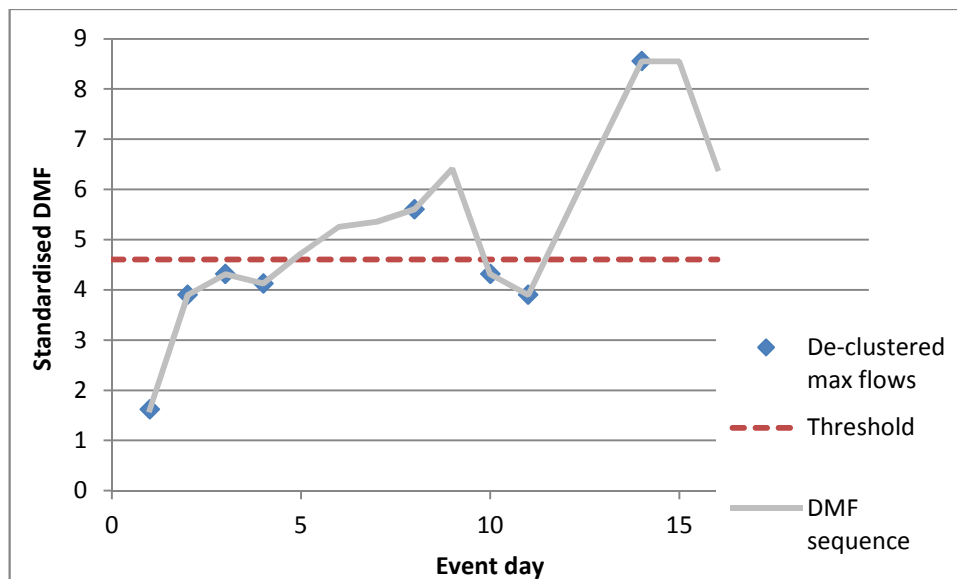


Figure 5.24 Temporal inconsistencies in moving window de-clustering method

Downstream sensibility tests

The negative log likelihood function (See Section 5.3.3.2) checks the suitability of the parameter estimates for each gauge pair but it does not explicitly check the suitability across the whole set of gauges. Keef *et al* (personal communication) have assumed that the negative log likelihood function will ensure physically realistic flows across the whole network.

For a small to moderate sized network such as used in this application it is possible to check if the simulated flows are physically realistic by establishing sensibility rules such that the upstream peak flow cannot exceed the downstream peak flow, and that the upstream peak must occur before the downstream peak.

In the application of the conditional dependence model discussed in Chapter 6 there are no paired gauges on the same watercourse to apply a sensibility check to, however prior testing of the model to an example case study in South Wales and the Midlands showed that the sensibility rules were met for simulated flows at gauges on the Rivers Severn, Avon and Usk, indicating that the model fitting procedures do insure physically realistic simulations.

5.3.4 *Uncertainty in statistical models*

The statistical modelling of extremes necessitates consideration of uncertainty for reasons that have already been identified in this chapter; there are limited observations and hence the data are only a sample of the possible values that could be observed; the interest is often in extrapolating beyond the range of the data; the data measurements themselves can be subjected to uncertainty; and, in the face of climate change and continuing human development, we cannot assume that past observations provide a suitable basis for predicting the future. Therefore these issues need to be explicitly considered in the analysis.

The assessment of uncertainty in statistical methods largely depends on the modelling framework in which the analysis has been made. Engineering based approaches are often closely related to the empirical data and incorporate limited physical knowledge, therefore uncertainty estimates from these types of method are possible using bootstrap methods of uncertainty (Anderson 2009).

Max stable models (for example see Smith 1990) and hierarchical models (see Fawcett and Walshaw 2006) are model based, that is they assume that there is some form of underlying influence or model structure that can be used to better represent the process of interest. Anderson (2009) observes that this means the assumption in the models are explicit and possible to test. He comments that estimates of uncertainty are possible, however the estimates are conditional on the model and therefore if the model is wrong then the uncertainty estimates are also wrong.

Taking a Bayesian approach to statistical modelling means including other prior sources of knowledge in the analysis for example known physical constraints such as the maximum possible value, understanding of related processes, and historical evidence that there is no observed data for such as anecdotal accounts (Coles and Tawn 1996). Bayesian analysis may

also sometimes proceed on the basis of “non-informative” priors, a method which is used to reduce bias in the model. Taking a Bayesian approach, for example as Coles and Tawn have done for rainfall data (Coles and Tawn 1996) and coastal surges (Coles and Tawn 2005b) can provide a means for reducing uncertainty due to the scarcity of extreme data by providing a means of increasing input data supply.

5.3.4.1 Measurement error

Statistical methodology is reliant on large external data sets and therefore it is not always possible to check the reliability of observations. The uncertainty due to measurement errors can be minimised by using good quality data sets from reliable sources (see Section 4.3). Initial graphical checks can be carried out to identify any very large or very small values and any significant trend changes can be investigated for example by checking for changes in the gauge history such as relocation or changes in the rating curve for flow gauges.

5.3.4.2 Statistical modelling error

Uncertainty in the statistical model used can arise due from the setting of the threshold for extremes and from the parameter estimation in the fitted model arising as the data used to fit the model are only a sample of the possible values that could be observed. The issues surrounding threshold selection have previously been discussed and the uncertainty here can be estimated from analysis of the parameter variability around the threshold. The uncertainty in the fitted model can be estimated using bootstrap methods as illustrated by Heffernan and Tawn (Heffernan and Tawn 2004).

Bootstrapping methods involve generating multiple samples of data and using the variability within these samples to estimate the overall variability. The process is as follows (see Davison and Hinkley 1997; Keef, Lamb *et al.* 2009a);

1. Generate a univariate sample of identically distributed data, X , of size n , and estimate the parameters of interest, θ , from X
2. Resample X with replacement from the modelled distribution to obtain a bootstrap sample X^* , also of size n
3. Calculate $\hat{\theta}$ from X^*
4. Repeat B times to obtain sample $\hat{\theta}^B$ of $\hat{\theta}$ of size B
5. Assess the variability of θ for example by calculating the 95% confidence intervals.

This process can be extended to consider multivariate data where $X = (X_1, \dots, X_d)$ by resampling the vector observations X_i , $i=1 \dots n$ to maintain the dependence between observations. This is

the method which is used by Heffernan and Tawn (2004) however as identified by Keef *et al* (2009a) this method does not preserve the temporal dependence such as seasonality and short term dependencies in the data series. Instead they use a block bootstrapping method which divides the data into blocks before resampling. The size of the blocks is chosen to maintain the temporal dependence but also to allow a large number of potential combinations in each sample. For meteorological data which displays strong seasonal trends a suitable block size is one year. It is assumed that the data in each block is independent of other blocks. Keef (2006) investigated this for fluvial data and found that specifying yearly blocks starting on 1st August when most rivers are in the middle of their dry season provided a means of minimising the dependence between flood events in consecutive blocks. Keef *at al* assume that the same annual break point is also suitable for coastal data but do not investigate this further.

As well as sampling uncertainty due to finite datasets, the choice of statistical model also leads to potential uncertainty which can be difficult to identify. For example Dixon and Tawn (1999) identified that using the RJPM produced significantly different results than the standard EVT model for certain sites however this problem had not previously been identified due to the particular sites that had been selected for previous analysis not having high tidal variations. It is relatively common practice for modellers to compare their results to previous studies or trial multiple methods allowing assessment of the robustness of the model choice. A more formal approach is outlined by Draper (1995) who used Bayesian model averaging to establish uncertainty bounds around results from a suit of possible models. There is no evidence of this approach being applied in an extreme value setting however it would be a useful study to compare the relative uncertainty from model choice and data quality in the extremes.

5.3.4.3 Assumptions of stationarity

There are increasing arguments that the concept of stationary is no longer valid within water resources research due to changes in catchment and river management and climatic forces meaning that hydrological patterns are not the same from year to year (Milly *et al.* 2008). The ability of past observations to provide a suitable means of predicting the future therefore depends on the time period over which predictions and management decisions are to be made.

Flood risk studies often try to account for potential changes due to climate change by providing some permutations of their results including future changes. The means of doing this has improved recently with the publication of UKCP09 (UK Climate Projections 2009) which explicitly contains a series of possible future climate scenarios embodying the inherent uncertainty in climate change modelling.

What is often not so well addressed in flood risk investigations is the assumption that data records are assumed to provide a stationary picture of the historic flooding regime at a particular gauge. Recent research by Lane (2008) has highlighted that the UK climate cycles through flood rich and flood poor periods and therefore depending on when the gauge record begins the trends identified within the data set will vary. This is in addition to other short term changes such as channel erosion and human influence on flooding regimes. In general this has a greater effect on fluvial data, while sea level is known to be rising around the UK, this is due to climate change and isostatic movement and other processes are unlikely to be significant. As these effects are not well understood at a national level it is difficult to quantify them in a study of this type although it is important to be aware of these issues throughout the analysis.

5.4 Selection of suitable statistical method to provide a robust ‘Sources’ component for the system model

The choice of model for a particular problem should be as simple as possible. Models can be evaluated by assessing how much of the variance is explained by one model compared to another which can be used to justify a more complex model however it should be remembered, as voiced by Coles (2001), that “the model is required as a description of the process that generated the data, not for the data themselves, so it is necessary to assess the strength of the evidence for the more complex model structure.” Using this framework it is important to have a thorough understanding of the processes being studied and not just the data themselves, hence the importance of the discussion of what causes extreme events in the UK in Section 5.2. As well as being as simple as possible it is important that the model is fit for purpose and does not violate the assumptions of extreme value theory.

The final section of the chapter establishes the modelling requirements for this thesis and evaluates the suitability of the methods presented in this chapter. The statistical model that has been chosen to provide the event simulation for the sources component of the risk model is the conditional dependence model of Heffernan and Tawn (2004). The reasons for this choice are given in Section 5.4.1.1.

5.4.1 Modelling requirements

To assess the suitability of a model or method it is first essential to assess the modelling requirements. In this thesis, the aim of the modelling is to estimate the probability of large scale floods simultaneously affecting different areas or from different sources. A set of modelling criteria for this thesis have been established (influenced by the criteria used by Keef *et al.* 2009a). The statistical model should;

- Consider multiple variables and locations and be flexible in allowing more detail to be incorporated around sites of interest
- Incorporate spatial and temporal dependence structures such as lag times between gauges and a suitable event definition for use in the insurance application
- Describe the dependence in the extremes
- Describe the changes in dependence as events get more extreme
- Incorporate data that are not extreme
- Allow extension to full event simulation rather than just event peaks
- Be suitable for use in an end user focused application

5.4.1.1 Method selection

Following a review of the available EVT methods, where suitable data exists a POT based statistical method is preferable in this case to block maxima or r largest as it provides the most efficient and consistent use of available data, however care is needed to select a robust threshold. The POT series is generally thought to provide a more complete picture of the flood regime at any particular site than annual maximum (Walshaw 1994; Robson and Reed 1999), however using POT methods often results in added model complexity due to the need to consider event clustering.

The analysis of temporal dependence structures in Section 5.3.2.1 and Section 5.3.3.6 highlight the importance of correctly defining events before applying an extreme value model. For environmental extremes which display natural variability due to different event types or catchment characteristics, a runs de-clustering method has been shown in Section 5.3.3.6 to provide the most robust means of de-clustering data prior to further statistical analysis. The definition of the r value is application specific and discussed further in Chapter 6. For multivariate analysis it is also necessary to specify a lag time over which observations at different gauges can be assumed to be from the same event. Keef *et al's* (2009a; 2009b; 2010) method for accounting for this was illustrated in Section 5.3.3.3 where it was shown that for most catchment pairs in the UK a lag of five days was appropriate. Similar analysis is repeated in Chapter 6 for coastal data.

In light of the review of available methods given in Section 5.3 and given the demonstration of its practicable ability in Keef *et al's* (2009a) work on spatial coherences of flood risk for the Environment Agency, the conditional dependence model of Heffernan and Tawn (2004) is used to provide a strong statistical basis for the risk modelling in this study. The conditional dependence model meets many of the modelling requirements listed in 5.4.1 in that it can be

used for any number of variables and can characterise dependence over a full range of event magnitudes and correlation structures. It can be used for event or time based applications and explicitly incorporates spatial and temporal dependence patterns. Theoretically any suitable model could be used to characterise the marginal dependence structure in the extremes, however as discussed above the GPD model is thought most suitable in this case as this is the model that was originally used by Heffernan and Tawn (2004) and Keef *et al* (2009a; 2009b; 2009c).

A disadvantage of the Heffernan and Tawn (2004) model is that it is theoretically complex and therefore presents challenges for communicating risk to the end user. Practical concerns have been raised about the model suggesting that the model's complexity restricts its use to those with professional connections to Heffernan and Tawn, or with very strong statistical backgrounds. There is some evidence of the conditional dependence model being used by researchers with no obvious connection to its original authors (for example Mendes and Pericchi 2009). This PhD should serve as evidence of an applied use of the conditional dependence model by someone with limited formal statistical training. Theoretical criticisms have also been made over the development of the multivariate structure from pairwise datasets. However the flexibility of the model and strength of the results produced by Keef *et al* (2009a; 2009b; 2009c) for flood risk analysis demonstrate its suitability for use in analysis of meteorological extremes and it is used here to provide a robust statistical underpinning to the sources component of the risk model.

6 A Multisite conditional dependence model for the selected risk clusters

6.1 Introduction

This chapter builds on the theoretical discussion of the conditional dependence model presented in Chapter 5 and illustrates how the model has been used to simulate events for the source component of the systems based risk model outlined in Chapter 4. Firstly the availability of suitable data sets is reviewed (Section 6.2.1) leading to the development of a gauged network in Section 6.2.2. Section 6.3 discusses the pre-processing required to generate a consistent data series across multiple gauges for fluvial and coastal data, including calculation of skew surge and de-clustering. Consideration is then given to fitting the conditional dependence model to the processed data including infilling missing data (Section 6.3.5.1) and the simulation of event peaks and time series (Section 6.3.6). Finally, in Section 6.4, the simulated data set is used to review the spatial and temporal dependence structures across the selected risk clusters. The conversion of the simulated events to the physical components that cause flooding is discussed in Chapter 7.

The conditional dependence model is also used as a means of representing the relationship between skew surge and wave heights however some modification of the model was required to achieve this which is discussed independently in Chapter 7.

6.2 Establishing a gauged network for selected risk clusters

6.2.1 Data sources

Hawkes *et al* (2008, p325) suggest that “data selection and preparation are probably the most important elements of extreme analyses”. Ideally the data set used for statistical analysis of extremes needs to be as long as possible to ensure multiple extreme events are recorded. For multivariate analysis long overlapping data sets are required. The observation frequency should be appropriate for the variable of interest; average monthly rainfall totals are of limited use for studying pluvial flooding which can occur on a timescale of minutes to hours. For a receptor focused study such as this it is important to balance the requirements of long and reliable record lengths with selecting gauges located close to the sites of interest to provide an accurate reflection of conditions at the receptors.

In the UK the most readily available source of extreme flow data is the Environment Agency HiFlows-UK database (Environment Agency 2010a). This is the data set recommended for use in FEH analysis (Robson and Reed 1999). This data set is restrictive as it only provides annual maximum and POT series which are of limited use for correlation analysis. An alternative to

using annual maximum or POT data is to use continuous data series which allows analysis of data when the event is not extreme at all gauges, when used on a national scale this it is likely to result in un-manageable data sets (See Section 5.3.3.6). Instead processed data can be used such as daily mean flows which are available from the National Rivers Flow Archive (NRFA) ran by the Centre for Ecology and Hydrology (CEH). DMF data provides a necessary compromise between requiring concurrent data for all sites while still maintaining a manageable data set. However further calculation is required to estimate the flood peak required in the fluvial risk model from the DMF data. This issue is discussed further in Chapter 7.

For coastal flood risk, observed sea level and predicted tide are available from British Oceanographic Date Centre (BODC). The data are available at 15 minute intervals. Pre-processing of the data is required to convert it into a comparable format to the DMF data and maintain a manageable data size (see Section 6.3.1). Wave data at a half hourly resolution, was downloaded from the Centre for Environment, Fisheries and Aquaculture Science (Cefas) WaveNet project (Cefas 2009). Again pre-processing is required to generate a comparable daily wave height. The statistical modelling of wave height is discussed separately in Chapter 7.

6.2.2 Selection of gauged network

Using the clusters identified in Chapter 3, a list of available gauges for fluvial, tidal and wave data was compiled.

The NRFA provides a standardised set of daily flow data for around 200 gauges across the UK freely available to download from the NRFA website (CEH 2009a). This dataset formed the basis of the gauge selection however where data gaps occurred additional gauges were identified in the areas of interest and requested from NRFA. In addition to the daily mean flow data, The Environment Agency HiFlows-UK database (Environment Agency 2010a) was reviewed and suitable gauges extracted. The POT data from HiFlows-UK is used for the DMF to peak flow conversion detailed in Section 7.2.1.

NRFA updated its database to include 400 sites in November 2011 (CEH 2011). Many of the relevant sites from this extended database are included in this PhD as they were requested from NRFA before the release of the new database, however due to the timing of the release a full review of the extended database has not been carried out.

For coastal risk still water data was obtained from the British Oceanographic Date Centre (BODC) network of tide gauges (BODC 2009) which provided predicted tide height and observed water level with a frequency of up to 15 minute intervals. Wave data was

downloaded from Cefas. The decision to use observed wave data rather than hindcast data is discussed in Section 7.3.3.

Once a list of available gauges had been identified, each gauging station was reviewed for its suitability for inclusion in the model. Given the nested site approach of this study it was possible to do this individually for each station rather than using generalised selection criteria. The review criteria were;

- **Location**

Does the location of the gauging station add value to the risk model? For example is it located on the same watercourse as a caravan site or does it provide useful 'donor' data?

- **Record length**

Is the record length at the site sufficiently long to allow fitting of the GPD and conditional dependence model? Keef (Personal Communication) suggests a minimum record length of 30 years however in some cases this restriction has been relaxed for particularly well located sites and for wave gauges where the record length is relatively short for all stations.

- **Reliability at high flows**

Sites were assumed suitable for high flows if they were rated as suitable for QMED estimation by HiFlows-UK. For stations without a HiFlows-UK classification, a review was made of available information from NRFA about the performance of the site.

- **Additional influences**

Are there any artificial influences such as reservoirs, pumping stations or flood defence schemes that affect the flow regime at the gauging station or is the site located in an area where the event may be enhanced, for example tidal gauges in estuaries? This is most important where the degree of influence changes over the period of record.

The following sections review the available gauges for each risk cluster area. A map of the gauge locations for each cluster is provided along with tables listing the characteristics of the potentially useful gauges. The core gauges which are used direct in the conditional dependence model are listed in Table 6.8. The remaining gauges are used to provide additional data to support the DMF to POT conversion, to infill missing data, or to help interpolate between gauging stations to estimate events at sites of interest.

6.2.2.1 East Coast

Fluvial

Risk on the East coast is mainly from the sea, although the Great Eau and particularly the Lymn could potentially cause fluvial flooding. Gauges on both watercourses are suitable for inclusion

in the model. Since the conditional dependence model is based on the relative positions of the event rather than the actual value, the potential bypassing at 29009 is not a major concern as the relative magnitude of the event will be maintained.

Table 6.1 Details of available East Coast fluvial gauges

Gauge ref.	Watercourse	Location	Catchment area (km ²)	Record length (years)	POT data	Comments
29002	Great Eau	Claythorpe Mill	77.4	48	yes	Bypassed at very large flows
30004	Lymn	Partney Mill	61.6	49	yes	No spot gaugings at high flows
29003	Lud	Louth Weir	55.72	42	yes	
30011	Bain	Goulceby	64.11	38	yes	Weir non modular at high flows

Coastal

There are two tide gauges to the north and south of the risk cluster. Both of these gauges have reliable data.

There are four waveriders in the vicinity. West Silver Pit, Northwell and Blackney Outfall have very short record lengths (less than 1.5 years) and have changed ownership during their lifetime which could result in inconsistencies in data recordings. Dowsing, although located further offshore provides a longer consistent data record and is therefore used to provide data on wave conditions for the East Coast.

Table 6.2 Details of available East Coast coastal gauges

Gauge ref.	Location	Type	Record length (years)
IMM	Immingham	Tide gauge	58
CRO	Cromer	Tide gauge	38
62289	Dowsing	Waverider	7.5
62040	West Silver Pit	Waverider	0.5
62041	Northwell	Waverider	1.5
62042	Blackney Outfall	Waverider	1.5

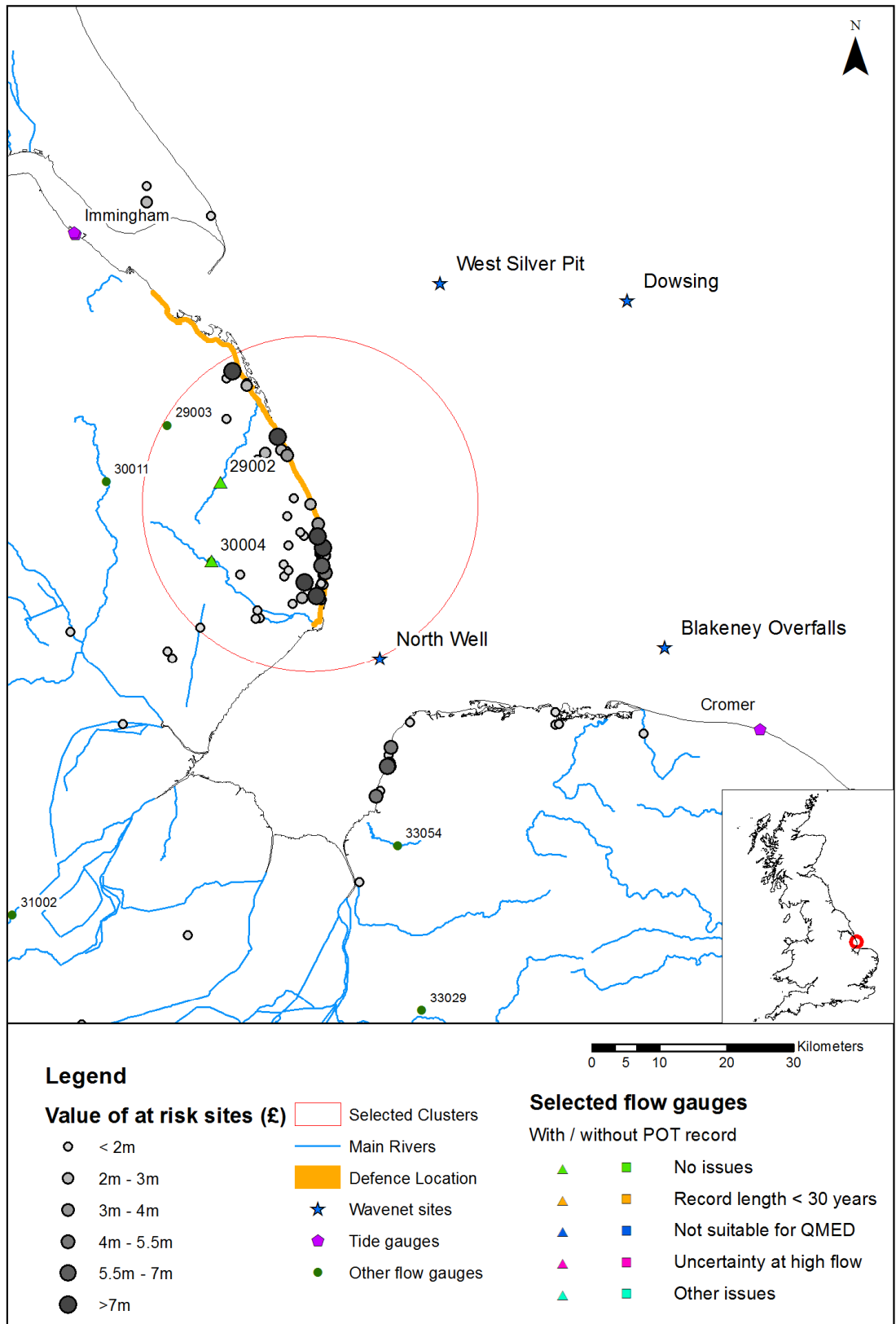


Figure 6.1 Gauging station locations: East Coast

6.2.2.2 North Wales

Fluvial

The North Wales cluster consists of two catchments, the Conwy which is gauged at 66011 and the Clwyd and Elwy system which has a series of gauges. Given that there are only three low value caravan sites on the Conwy, this river system is not modelled as part of this project however the Conwy gauge is included as it has a long record length and may provide useful data for infilling missing data at the other gauges. The best located gauges for the Clwyd and Elwy are 66025 and 66002 however these sites have short record lengths which do not overlap therefore 66001 and 66006 provide useful alternatives. Another advantage of using 66001 over 66025 is that it includes POT data.

Table 6.3 Details of available North Wales fluvial gauges

Gauge ref.	Watercourse	Location	Catchment area (km ²)	Record length (years)	POT data	Comments
66001	Clwyd	Pont-y-Cambwll	404	51	yes	
66025	Clwyd	Pont Dafydd	430.8	14	no	Short record
66011	Conwy	Cwm Llanerch	344.5	47	yes	
66002	Elwy	Pant yr Onen	220	14	yes	Short record
66006	Elwy	Pont-y-Gwyddel	194	38	yes	

Coastal

There is considerable coastal risk in North Wales to sites located near Towyn and extending East towards Rhyl and Prestatyn.

Interpolating between the tide gauges at Llandudno and Liverpool provides details of the still water conditions. Although LLA appears to have a long record, there are considerable periods of missing data (see Figure 6.6). The gauge at Holyhead is included as it can provide useful data for infilling the significant missing records at Liverpool and Llandudno. The waverider bouy in Liverpool Bay is used for wave conditions.

Table 6.4 Details of available North Wales coastal gauges

Gauge ref.	Location	Type	Record length (years)	Comments
LIV	Liverpool	Tide gauge	20	Short record length
LLA	Llandudno	Tide gauge	40	Significant missing data
HOL	Holyhead	Tide gauge	47	
62287	Liverpool Bay	Waverider	8	

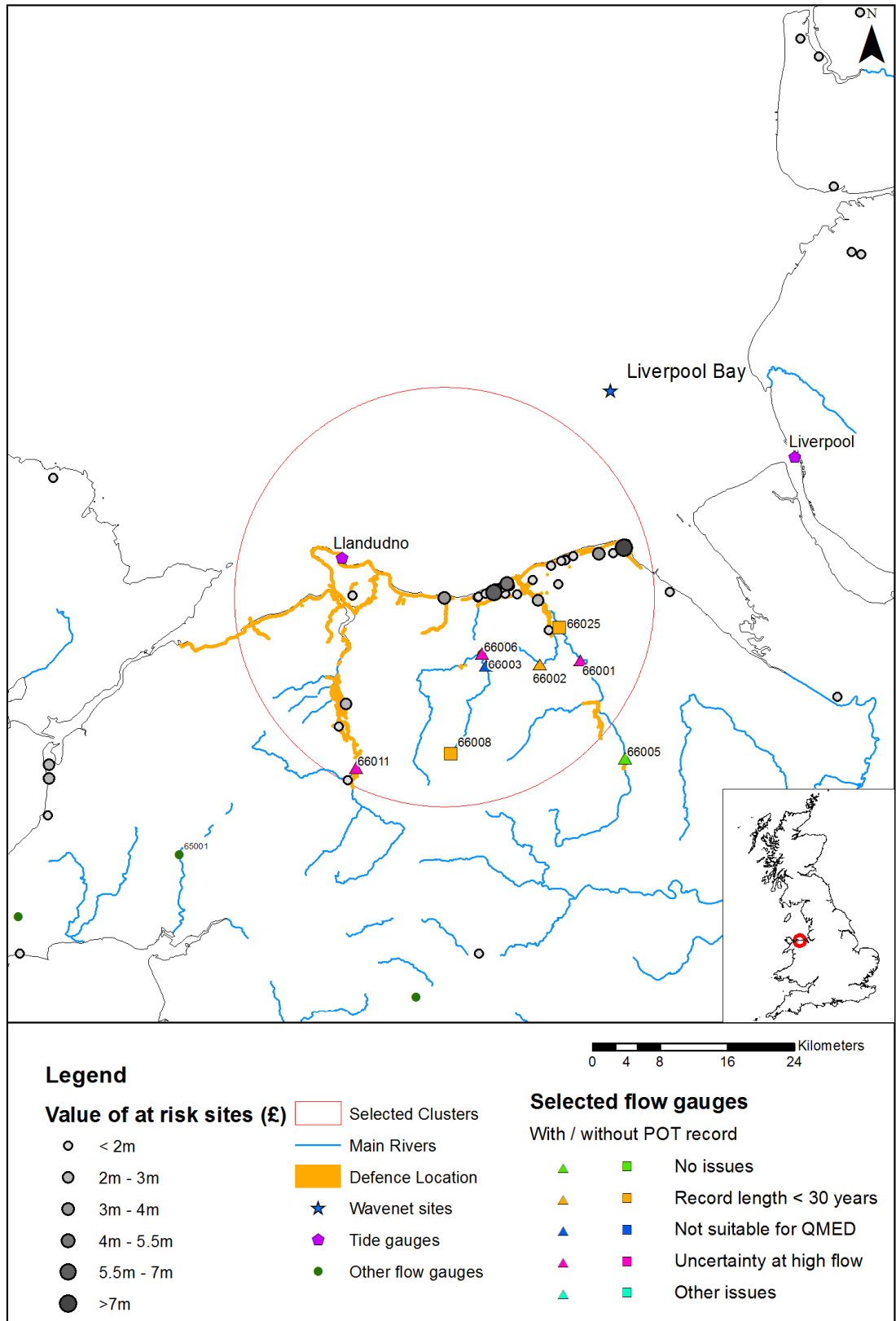


Figure 6.2 Gauging station locations: North Wales

6.2.2.3 Midlands – The River Severn

Fluvial

The primary concern in the River Severn cluster is to model risk at the caravan sites located around the Severn-Stour confluence. The most suitably located gauges for this area are 54034, 54001 and 54006. Unfortunately there is no downstream gauge on the River Severn except 54032 which includes flows from the River Teme and is tidally influenced. Gauge 54032 also has the potential to be influenced by high tides and by tidal gates on the River Avon at Tewksbury. In light of these difficulties no downstream gauge will be used and the flows at the downstream extent of the hydraulic model will be estimated by area scaling of the simulated upstream flows for the combination of the three rivers (see Section 7.2.2).

Table 6.5 Details of available River Severn fluvial gauges

Gauge ref.	Watercourse	Location	Catchment area (km ²)	Record length (years)	POT data	Concerns
54034	Dowles Brook	Oak Cottage	40.8	40	yes	
54001	Severn	Bewdley	4325	90	yes	
54032	Severn	Saxons Lode	6850	39	yes	Bypassing at high flows. Affected by high tides
54006	Stour	Kidderminster Callows Lane	324	57	yes	Flood alleviation scheme built in 2003
54063	Stour	Prestwood Hospital	89.9	36	no	
54029	Teme	Knightsford Bridge	1480	39	yes	

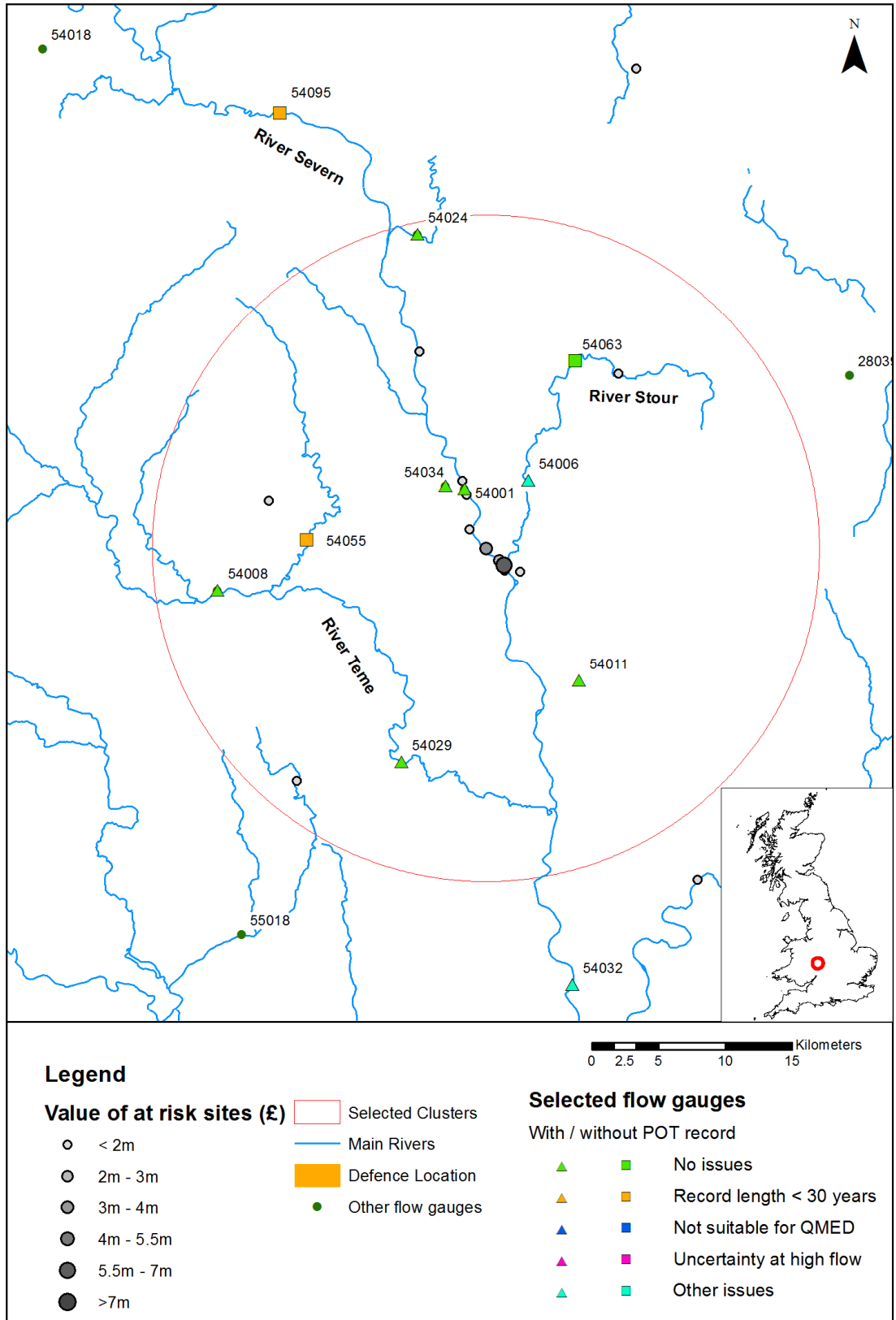


Figure 6.3 Gauging station locations: River Severn

There is an additional complication with the gauged data for the River Stour as a flood alleviation scheme was built between gauges 54006 and 54063 in 2003 (Wyre Forest District Council, 2008) to protect Kidderminster from floods up to a 1% AEP event by restricting flows leaving the storage area to $27\text{m}^3/\text{s}$ (Environment Agency 2010a), events larger than the design standard will overspill the culvert.

The impact of this scheme means that flows prior to 2003 will potentially be higher than those recorded after the flood alleviation scheme, effectively reducing the useable record length to eight years.

A review of the observed DMF and POT data at gauges 54006 and 54063 for POT events shows that the average ratio of flows between the two sites is affected by the scheme, especially for the most extreme events which are attenuated in the flood storage area between the two gauges (Table 6.6) however there is no clear trend to this relationship for all events (Figure 6.4). There is only one event prior to 2003 large enough to be affected by the flood alleviation scheme, this was in December 1981 when a DMF of $26.2\text{m}^3/\text{s}$ was recorded at gauge 54006. This is close to the culvert capacity, therefore if the alleviation scheme had been in place it would have probably reduced the peak flow but had minimal impact on the daily mean. Based on these observations and given the requirement for long concurrent data records, it is deemed sufficient to use the full data record at 54006 without modification for the flood alleviation scheme.

Table 6.6 Ratio of DMF peaks between 54006 and 54063 before and after the installation of the flood alleviation scheme in 2003

	Average ratio of peak DMF 54006 / DMF 54063	
	All events	Events above Q99 threshold at 54034
Pre flood alleviation scheme	2.05	1.34
Post flood alleviation scheme	1.92	1.10
All events	2.01	1.25

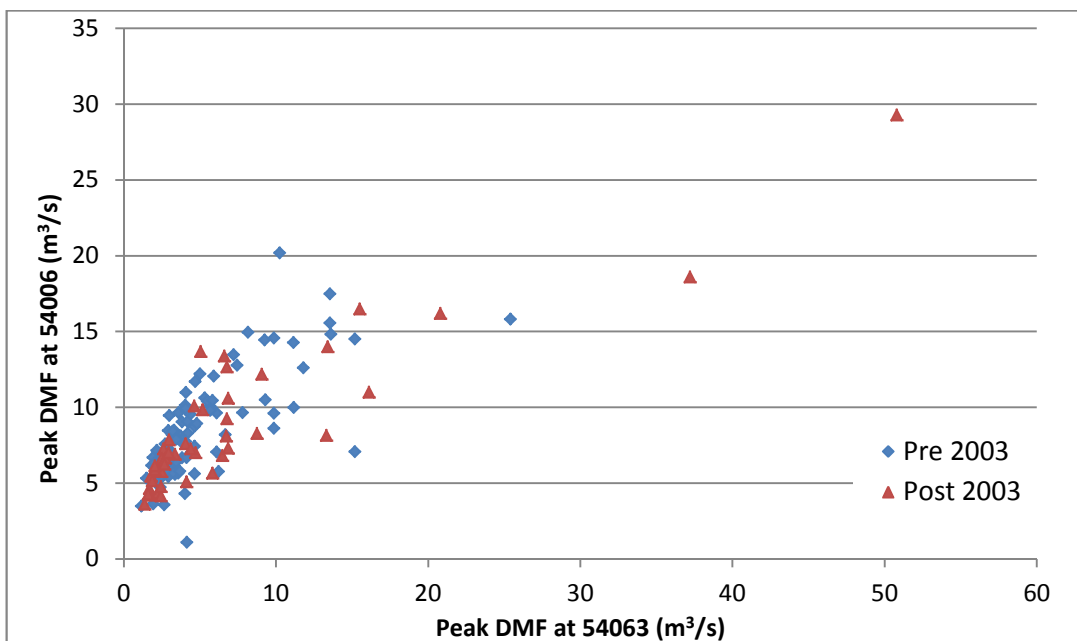


Figure 6.4 Relationship between gauges 54006 and 54063 for POT events before and after the installation of the flood alleviation scheme in 2003

6.2.2.4 The River Thames

Fluvial

In the Thames cluster gauges 39138, 39130 and 39009 are well located for the sites of interest. However the record length at these sites is short (between 11 and 22 years), in addition the observation period for 39009 is 1959-1982 which provides a very limited period of overlapping record. On the Thames itself sites 39072, 39001 and 39002 provide long record lengths although there are multiple tributary interactions between 39002 and the caravan sites of interest and a very large difference in catchment area between all three sites. In light of the added complication of including multiple tributaries, a single gauge will be used to provide estimates for the Thames, 39072 at Royal Windsor Park. The only gauged tributary between 39072 and the sites of interest is the Wye. This is a small groundwater dominated catchment (Environment Agency 2010a) and unlikely to have a major influence on flows in the River Thames. There are no POT data available at 39072 therefore 39002 will be used as a donor site to estimate peak flows as described in Section 7.2.

Table 6.7 Details of available River Thames fluvial gauges

Gauge ref.	Watercourse	Location	Catchment area (km ²)	Record length (years)	POT data	Concerns
39007	Blackwater	Swallowfield	354.8	58	Yes	
39016	Kennet	Theale	1033.4	49	yes	Possible groundwater

A Multisite conditional dependence model for the selected risk clusters 6

Gauge ref.	Watercourse	Location	Catchment area (km ²)	Record length (years)	POT data	Concerns
39138	Loddon	Twyford	751.8	12	No	interaction Short record length
39022	Loddon	Sheepbridge	164.5	44	Yes	Some bypassing at high flows
39023	Wye	Bourne End	137.3	47	Yes	
39002	Thames	Days Weir	3444.7	72	Yes	
39009	Thames	Bray Weir	6915.3	22	No	Short record length
39130	Thames	Reading	4633.7	17	No	Short record length
39072	Thames	Royal Windsor Park	7046	31	no	
39001	Thames	Kingston	9930.8	111	yes	Early record probably inaccurate

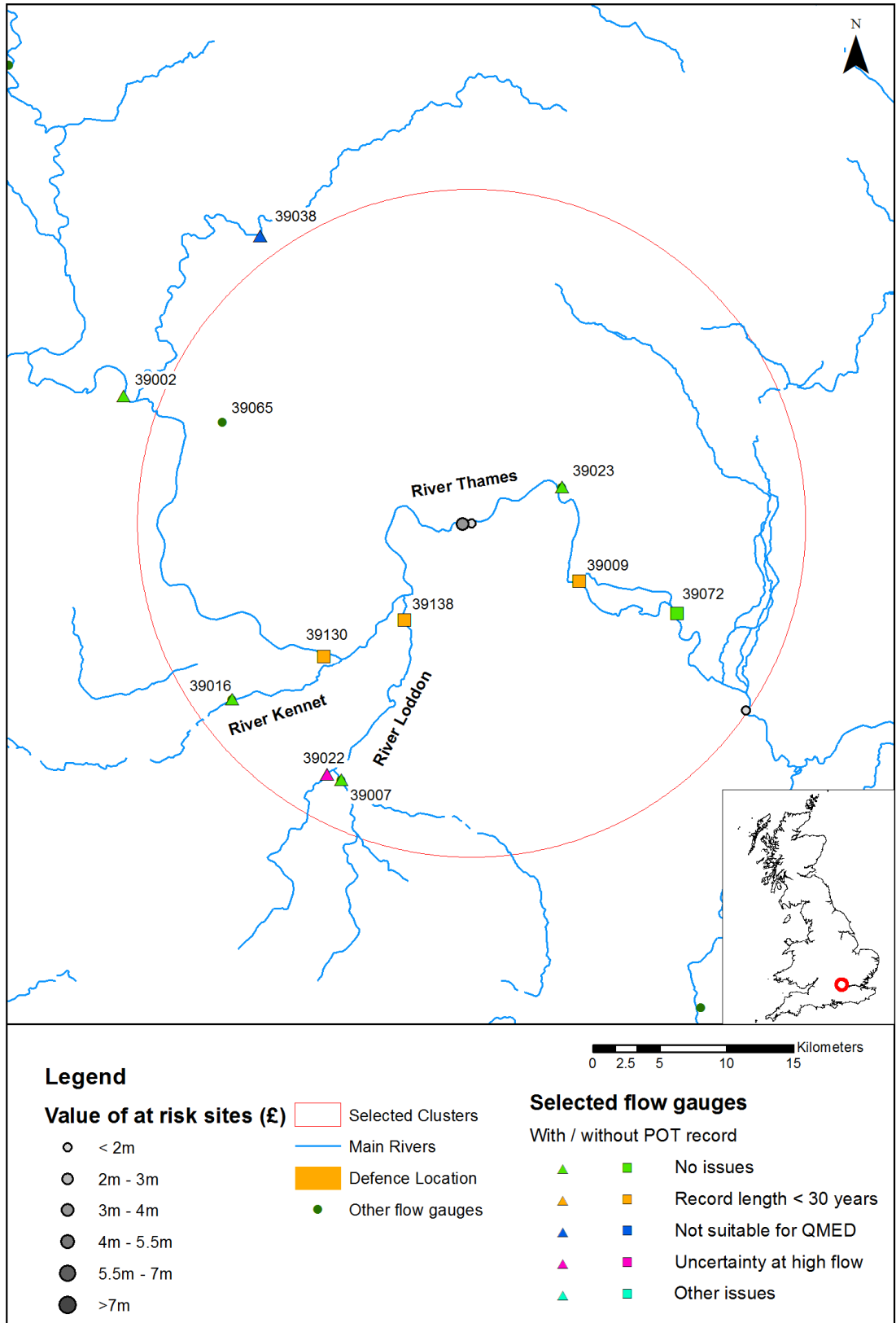


Figure 6.5 Gauging station locations: River Thames

6.2.2.5 Gauges used in conditional dependence model

The fluvial and tidal gauges which will be used directly for simulation of extreme events for the risk model are identified as core gauges in Table 6.8. The remaining gauges in Table 6.8 are used to infilling missing data (see Section 6.3.5.1) and to support the interpolation methods outlined in Chapter 7.

The conditional dependence model requires long concurrent data records without missing data. As shown in Figure 6.6, all core gauges have 31 years of data from 1979 to 2010 without significant periods of missing data except the North Wales coastal gauges at Llandudno and Liverpool. The degree of missing data for the fluvial gauges is minimal. For coastal gauges missing data presents more of a potential problem. The procedures for dealing with missing data are discussed in Section 6.3.5.1.

Table 6.8 Selected gauges for use in conditional dependence model

Gauge ref	Cluster	Location	Start date	End date	Record length (years)	Main purpose
30004	East Coast	R. Lymn	01/01/1962	31/12/2010	49	Core
IMM	East Coast	Immingham	01/01/1953	31/12/2010	58	Core
CRO	East Coast	Cromer	01/01/1973	31/12/2010	38	Core
29002	East Coast	R. Great Eau	01/10/1962	31/12/2010	48	Infill
29003	East Coast	R. Lud	05/07/1968	31/12/2010	42	Infill
30011	East Coast	R. Bain	01/08/1971	31/12/2010	39	Infill
66001	North Wales	R. Clwyd	01/10/1959	31/12/2010	51	Core
66006	North Wales	R. Elwy	01/01/1973	31/12/2010	38	Core
66011	North Wales	R. Conwy	01/06/1964	30/11/2011	47	Infill
LIV	North Wales	Liverpool	01/01/1991	31/12/2010	20	Core
LLA	North Wales	Llandudno	31/12/1970	31/12/2010	40	Core
HOL	North Wales	Holyhead	01/01/1964	31/12/2010	47	Core
54034	Severn	Dowles Brook	01/01/1971	31/12/2010	40	Core
54001	Severn	R. Severn	01/01/1921	31/12/2010	90	Core
54006	Severn	R. Stour	01/10/1953	31/12/2010	57	Core
54063	Severn	R. Stour	01/08/1972	31/12/2008	36	Infill
54029	Severn	R. Teme	01/04/1970	31/12/2010	39	Infill
39001	Thames	R. Thames	01/01/1900	31/12/2010	111	Infill
39002	Thames	R. Thames	01/10/1938	31/12/2010	72	Infill
39072	Thames	R. Thames	20/7/1979	31/12/2010	31	Core

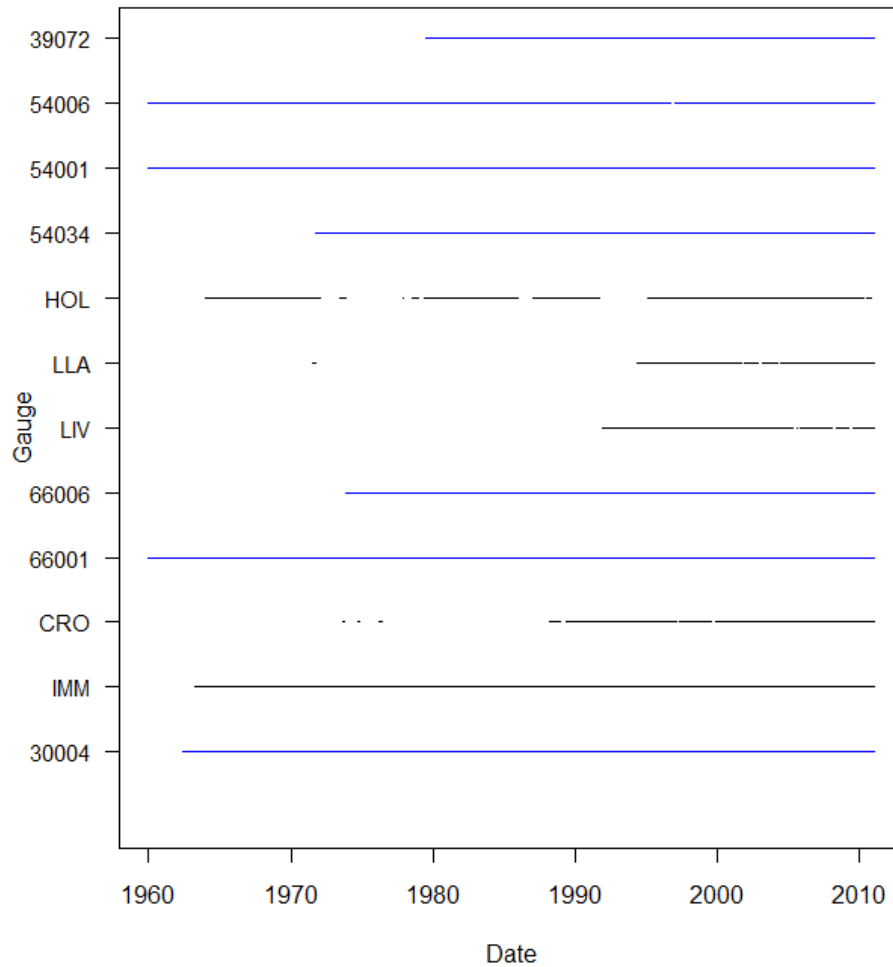


Figure 6.6 Period of record for core gauges

6.3 Development of a multisite conditional dependence model for the gauged network

6.3.1 Calculating daily maximum skew surge

Pre-processing is required to convert sea level observations into daily maxima skew surge to be used with the DMF data.

The data sets available from BODC give the observed sea level and the tidal residual (observed sea level minus predicted tide). The data are coded by BODC to mark improbable values, null values, and, interpolated values. Improbable values were removed to minimise errors.

Interpolated values were retained due to the requirement for concurrent data (this was assumed to be more reliable than using the infilling technique in Section 6.3.5.1). The predicted tide for each time step was calculated as the observed sea level minus the residual.

In the UK the tidal cycle is 12.25 hours. The highest water level and predicted tide height were found by searching for the highest value within three hours of the estimated time of high tide for each cycle. More sophisticated methods were tested including using the aggregate function

in the R package “zoo” (Zeileis and Grothendieck 2005) to extract the highest value over a given time window. However this method produced unreliable results, possibly due to missing data within the tidal cycle.

The skew surge (see Section 5.2.1.2) for each tidal cycle was calculated by subtracting the highest observed water level from the predicted high tide. Due to differences in the timing of tides around the UK, it was not possible to use the tidal cycle data to generate a concurrent series across all gauges. The zoo aggregate function was used to extract the daily maximum skew surge, thus providing a concurrent dataset that is comparable to the DMF data used for the fluvial sites. Where only one of the two potential high tides of any given day is recorded this was taken as being the daily maximum. Using daily maximum skew surge in this way creates some difficulties when assigning a tide event to the generated skew surges as identified by Keef *et al* (2009a) but results in a conservative estimate of the combined water level. The resulting daily maximum skew surges at each gauging station are shown in Figure 6.7.

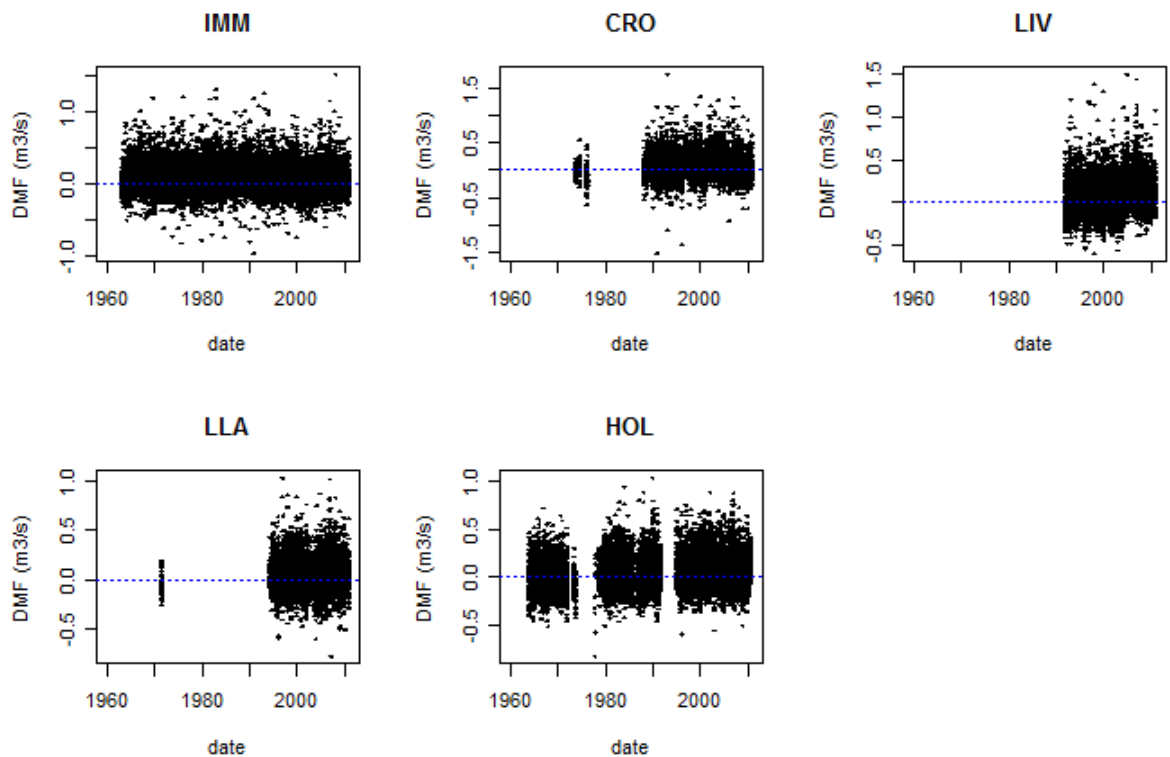


Figure 6.7 Daily maximum skew surge at selected gauges

6.3.2 Sensibility tests for selected data

The suitability of the gauging stations was reviewed in Section 6.2.2. Prior to use in the statistical model a sensibility check was made of the observed data at each of the selected

sites. The full data time series was plotted and a visual assessment of the data made. No significant outliers were identified. The results of the sensibility tests are provided in Appendix B.1.

In addition, pairwise plots of the observed data were plotted to identify the expected model results. The plots for the core gauges are shown in Figure 6.8. This plot provides an initial indication of the importance of considering multisite dependence, as dependence structures are evident between fluvial and coastal gauges in North Wales (66001, 66006, LIV, LLA and HOL), and broad scale spatial dependences between sites in the Midlands (54001), North Wales (66001) and the South East (39072).

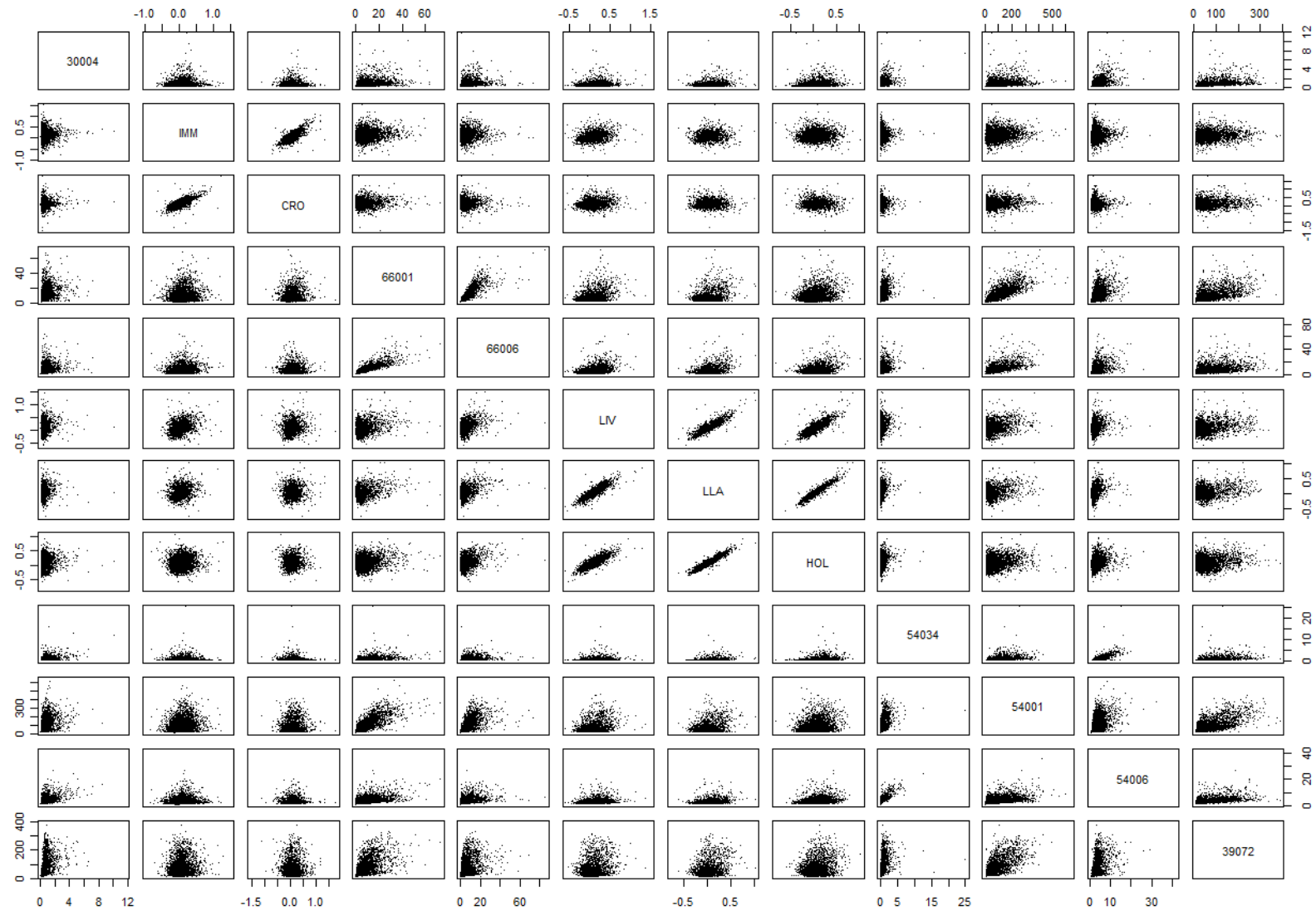


Figure 6.8 Pairwise plots of observed DMF and skew surge data for all core gauges

6.3.3 De-clustering

The review of available de-clustering methods presented in Chapter 5 identified that the most suitable method for de-clustering meteorological data was runs de-clustering which allows for varying response times at different sites due to local conditions. The de-clustering of DMF and skew surge using runs de-clustering is discussed below.

6.3.3.1 Fluvial

Identifying a suitable threshold, u , and cluster interval, r , are to some extent arbitrary (Smith 1989) and suitable limits are likely to interact with each other. In theory values could be identified from the point at which the parameters of the GPD and conditional dependence model stabilise. However because both of these models have multiple, interacting parameters it is difficult to accurately identify where this point is. To overcome this problem, Keef *et al* (2009a) use the empirical estimates of the $P(X_{t+\tau} > u | X_t > u)$ to estimate suitable time windows for extracting peak events (See Section 5.3.3.6). The value of $P(X_{t+\tau} > u | X_t > u)$ for a range of cluster intervals is shown in Figure 6.9 for the validation dataset of DMF gauges.

Since the value of $P(X_{t+\tau} > u | X_t > u)$ tends rapidly towards zero when runs de-clustering is applied, a comparison with the number of event peaks retained using the window based de-clustering method of Keef *et al* (Figure 6.10) were used to maintain stability in the fit of the conditional dependence model. Although it is acknowledged that there is some interaction between u and r , u has been set at the 0.99 quantile throughout to maintain consistency with the conditional dependence model.

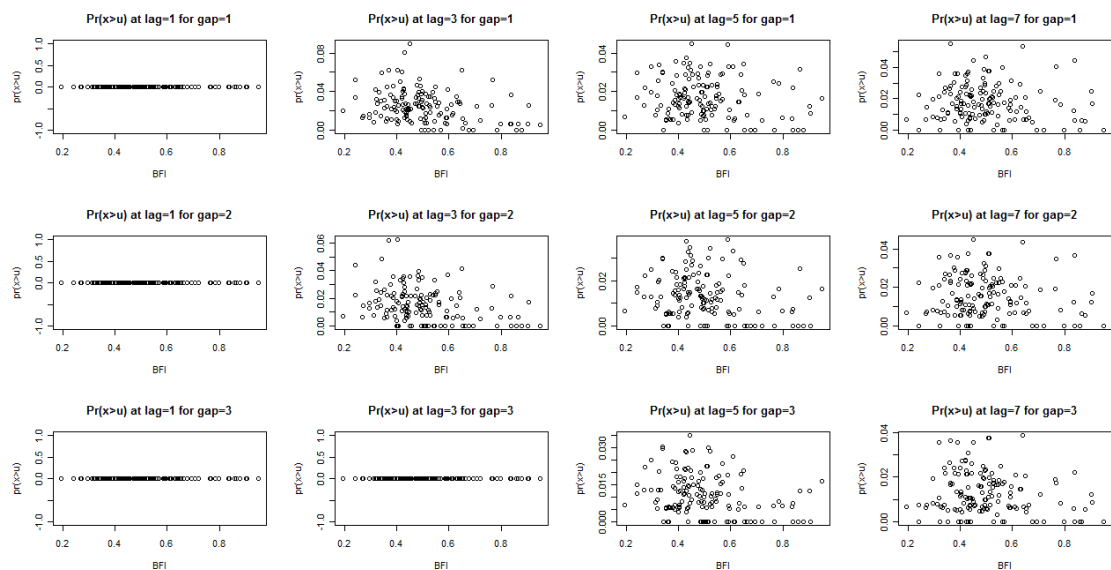


Figure 6.9 Identification of suitable de-clustering interval by comparing $\Pr(X_{t+\tau} > u | X_t > u)$ with BFIHOST for a range of r values

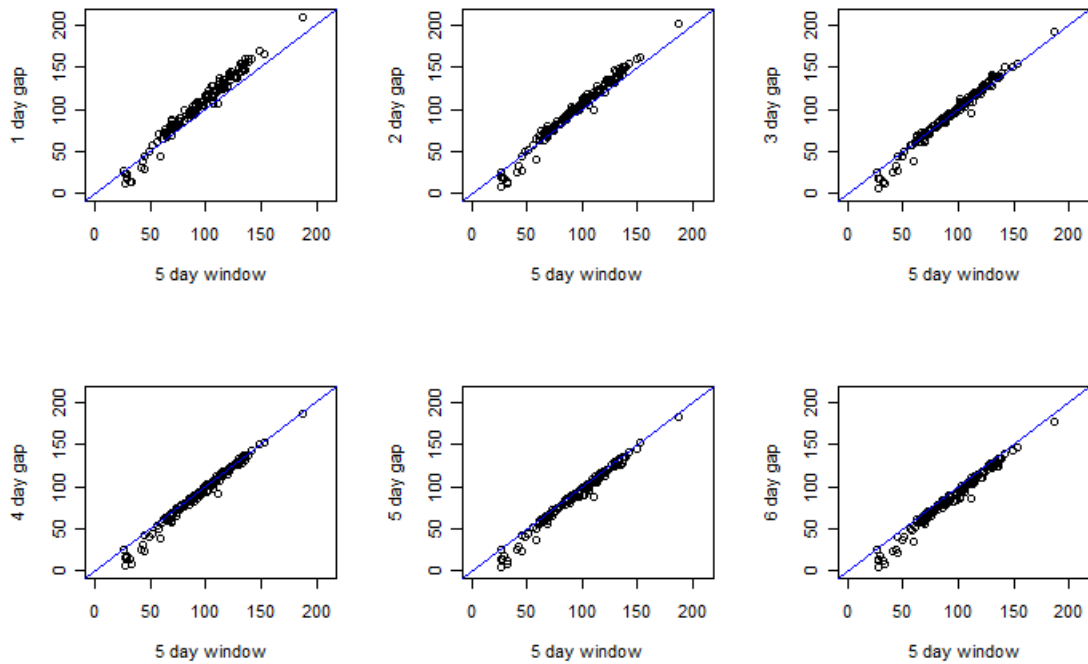


Figure 6.10 Comparison of number of events retained by runs and moving window de-clustering methods

As shown in Figure 6.9, the probabilities of concurrent events occurring in the data series are very low using the runs de-clustering method, irrespective of the value of r chosen. This suggests that for all catchment types, once the flow drops below the threshold, it is unlikely to rise again within a short time frame. The method itself is therefore not sensitive to the choice of r , however r does have some notable effects on the number of events retained as shown in Figure 6.10. Values of $r \leq 2$ result in more events being retained than Keef *et al*'s five day moving window method and values of $r \geq 6$ result in fewer events being retained. Using a value of $r = 1$ is not recommended due to the potential event classification uncertainty from data errors.

The conditional dependence model assumes that the conditioning peak is the maximum within the event. As discussed in Section 6.3.6.1, the event duration used in this study is 10 days (a lag of five days either side of the flood peak) to allow for incorporation of the full temporal dependence structure between different sites. Therefore although an r value of three would be sufficient at individual sites, an r value of five has been used to remove the probability of secondary flood peaks within the five day event lag.

Despite the difficulties in establishing a suitable value of r , de-clustering in this manner insures that only the peaks are retained and therefore removes the inconsistencies identified in Figure 5.24, therefore the runs method is considered the best approach for use in this application.

Figure 6.9 also shows that the runs de-clustering method removes the dependence with BFIHOST values shown in Figure 5.22. This is because peak events in baseflow dominated catchments tends to be of long durations, therefore using the runs de-clustering method allows incorporation of varying event lengths in different catchment types.

For practical reasons the threshold at gauge 39072 was lowered from 0.99 to 0.98. This was because although 39072 meets the requirement of 30 years of data and had more than 30 events above the Q99 threshold, due to the slow response of the catchment after de-clustering the number of extremes fell to less than 30 meaning 39072 could not be used as a conditioning gauge in the dependence model. The additional uncertainty from lowering the threshold was thought to be less than using an alternative site on the Thames further away from the receptors of interest, for which there is a greater than 2500km² difference in catchment area (See Table 6.7).

6.3.3.2 Coastal

The characteristics of storm events around the UK coastline (discussed in Section 5.2.1.2) mean that there is unlikely to be significant temporal clustering over periods longer than a few days. Repeating the analysis of Section 6.3.3.1 for daily skew surge, Figure 6.11 shows that the value of $P(X_{t+\tau} > u | X_t > u)$ falls to approximately 5% for lags of more than one day at Immingham, Cromer and Liverpool, however it remains high for lags up to three days at Holyhead and Llandudno.

Figure 6.12 shows that this dependence structure is removed when the r value is larger than the dependence lag. Based on this analysis an r value of three would again be suitable for de-clustering skew surge at individual sites but has been increased to five to provide consistency with the fluvial de-clustering method and meet the criteria of the conditional dependence model. This value ensures temporal correlations at all sites are removed prior to fitting the GPD model and provides consistency with the fluvial model. Table 6.10 provides the number of events retained in the data set for different r values. There is no major jump in number of events retained at any value of r which suggests that the GPD fit will not be overly sensitive to the run time used.

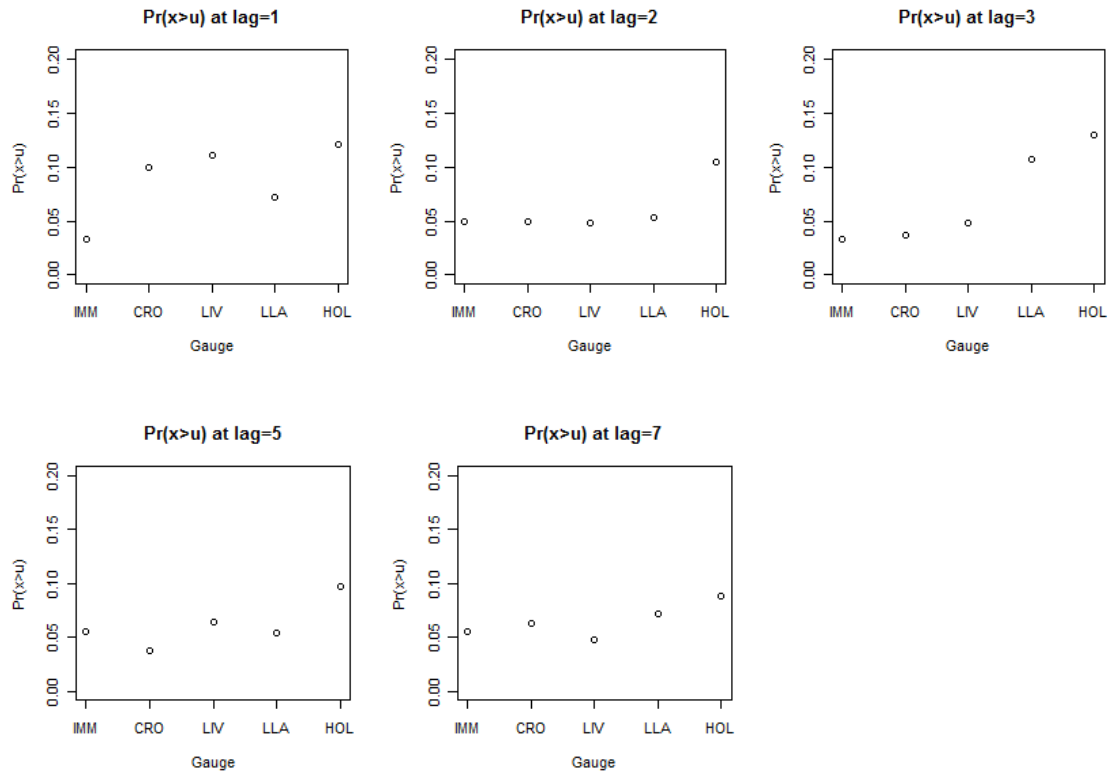


Figure 6.11 Conditional dependence measure $\Pr(X_{t+\tau} > u \mid X_t > u)$ at coastal gauges for a range of time lags

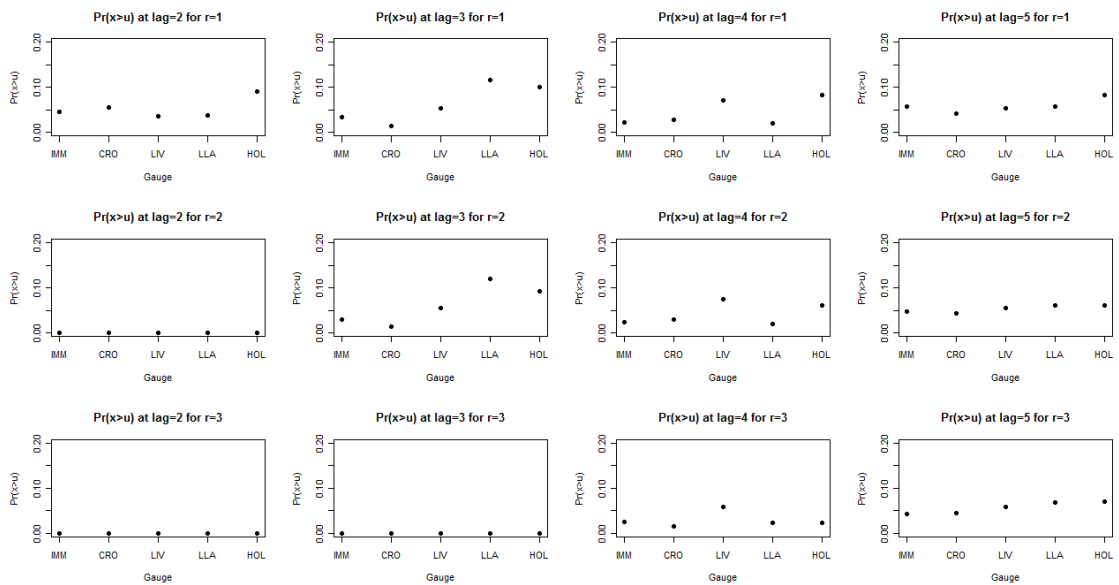


Figure 6.12 Identification of a suitable coastal de-clustering interval by comparing $\Pr(X_{t+\tau} > u \mid X_t > u)$ at different time lags with a range of r values

Table 6.9 Number of retained extreme events after de-clustering skew surge data for a range of r values

Site	All data	De-clustered data $r =$			
		1	2	3	4
IMM	181	175	167	161	157
CRO	80	72	68	67	65
LIV	63	56	54	51	46
LLA	56	52	50	44	43
HOL	124	109	98	85	80

6.3.4 Fitting the GPD model

A GPD model (see Section 5.3.1) was fitted to the maximum available record length of de-clustered data at each gauge between 1960 and 2010 using the `gpf.fit` function in the R package `ismev` (Coles and Stephenson 2010). The period 1960 – 2010 was chosen to maximise the use of available data while maintaining a consistent climatic period across all gauges.

The threshold was taken as the 0.99 quantile throughout except for gauge 39072 (see Section 6.3.3.1). The model fit and threshold stability were reviewed to assess the stability of the model over a range of possible thresholds using the R function `gpd.fitrange` (also available from the `ismev` package) and found to be suitable at all gauges. Plots of the GPD fit and threshold stability are shown in Appendix B.2. The fitted GPD parameters are shown in Table 6.10 with standard errors shown in brackets.

Table 6.10 Fitted GPD parameters for selected network

Gauge ref	Threshold (u)	Scale (σ)	Shape (ϵ)
30004	2.70	0.03 (0.09)	1.41 (0.18)
66001	32.60	-0.13 (0.12)	11.22 (1.81)
66006	26.92	0.02 (0.12)	10.93 (1.74)
54034	3.18	0.26 (0.12)	1.43 (0.22)
54001	297.30	0.08 (0.14)	60.93 (11.66)
54006	10.52	0.01 (0.07)	3.83 (0.43)
39072	214.00	-0.1 (0.17)	45.21 (10.87)
IMM	0.62	-0.05 (0.08)	0.17 (0.02)
CRO	0.69	-0.09 (0.11)	0.24 (0.04)
LIV	0.68	-0.11 (0.18)	0.25 (0.06)
LLA	0.53	-0.09 (0.19)	0.15 (0.04)
HOL	0.51	-0.19 (0.09)	0.15 (0.02)

The uncertainty in the fit of the marginal model can be identified from the confidence bounds which can be calculated using the R function `gpd.parameterCI` from `ismev` or in the `extRemes` package. Confidence intervals are shown in the plots of GPD fit in Appendix B.2 and illustrate

wide uncertainty bounds beyond the range of the data. Example confidence intervals for a 1.3 AEP event are tabulated in Table 6.11. The 1.3 AEP event was chosen as this is the threshold for providing insurance cover.

Table 6.11 Confidence intervals for the GPD model fit at a 1.3 AEP event

Gauge	Best estimate	95% confidence interval	
		Lower bound	Upper bound
54001	580.1	500.5	878.0
39072	363.7	326.4	545.9
IMM	1.43	1.29	1.84
LIV	1.47	1.22	1.50

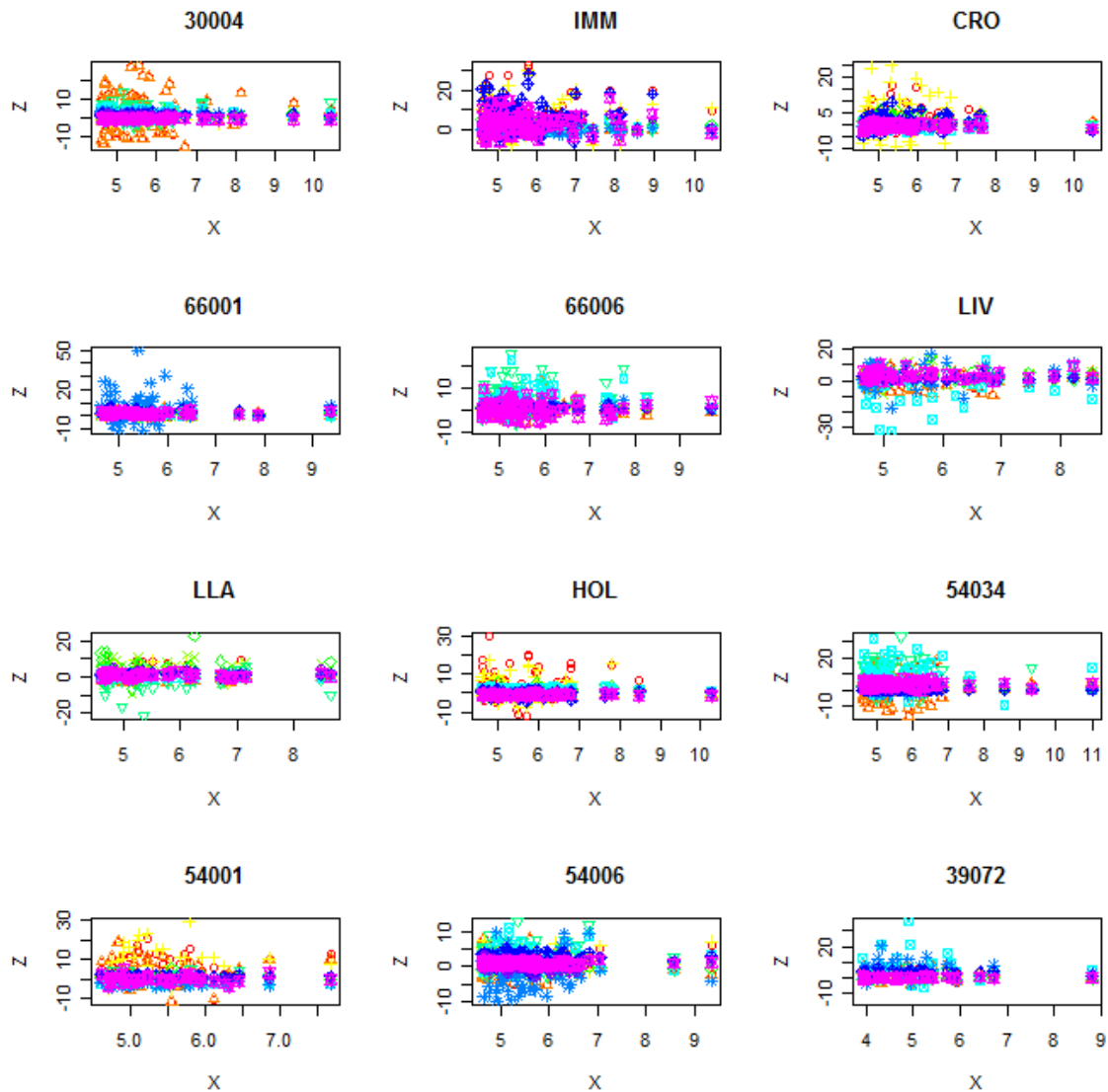
6.3.5 Fitting the conditional dependence model

The data were transformed to uniform margins using the semiparametric model given in Equation 5.18 and the fitted values of u , σ , and ϵ given in Table 6.10.

The conditional dependence model was fitted as described in Section 5.3.3.2 for an event window of up to ten days. The minimisation of Function 5.28 was carried out using the inbuilt Nelder-Mead optimisation function in R (optim, R Development Core Team 2009) and code supplied by Keef to implement the optimisation constraints outlined in Section 5.3.3.2. Using lags of up to ten days allows for increased flexibility in the event simulation as discussed in Section 6.3.6, although it is acknowledged that the strength of the dependence structures is likely to weaken at the extremes of this range.

The model requires concurrent data of at least 30 years and concurrent data on a minimum of 30 extreme days for each conditioning site. Review of the periods of record shown in Figure 6.6 identifies that the longest period of concurrent data available is from 01/01/1979 – 31/12/2010. This period was largely determined by the limited coastal data record for North Wales as the gaps in coastal data at Holyhead limit the potential to infill data at Liverpool and Llandudno (see Section 6.3.5.1) and the record length at site 39072. The conditional dependence model was fitted to observations from 01/01/1979 – 31/12/2010.

A crucial check of the suitability of the conditional dependence model is to check that Z is independent of X (Keef *et al.* 2009a). As shown in Figure 6.13 for Z 's at time lag 0, this criterion is satisfied for all the core sites.



Each conditional gauge is plotted using a different colour and plotting symbol

Figure 6.13 Evidence of independence of Z and X in the conditional dependence model

6.3.5.1 Dealing with missing data

By infilling data the maximum possible use of all observed data can be made. It is shown by Keef (2006) that infilling the missing data improves the estimation of extreme dependence structures compared to simply removing it. Concurrent data are only required for events where at least one gauge in the network is extreme. There are 782 days between 1979 and 2010 when this occurs. As illustrated in Table 6.12, the coverage of fluvial data for these “extreme days” is good with a maximum of 13 missing days at 39072. The coverage of coastal data is more sporadic, with only Immingham providing comprehensive coverage over all but 18 extreme days.

Table 6.12 Number of days when core gauges have missing data 1979 - 2010

Gauge	Number of missing days	Number of missing days when at least one gauge is extreme	Percentage of missing days when at least one gauge is extreme
30004	66	3	0.4
66001	0	0	0.0
66006	70	1	0.1
54034	2	1	0.1
54001	0	0	0.0
54006	91	8	1.0
39072	200	13	1.7
IMM	312	18	2.3
CRO	3861	230	29.4
LIV	5410	313	40.0
LLA	6174	405	51.8
HOL	2280	158	20.2

Note: the table is calculated on the day of the conditioning peak. It is assumed that the distribution of missing data throughout the event will be the same as on the peak day

Limiting the size of the network to the areas of interest rather than applying the model across a UK network of gauges as per Keef *et al* (2009b; 2009c) restricts the impact of missing data as the extreme days display more temporal coherence. This has implications for how periods of missing data are dealt with in the data set. Keef (2006) proposes a generic method which uses the conditional dependence model to infill the periods of missing data. While this is elegant, the computation involved in applying this infilling technique is significant and the process is not transparent to end users without statistical training. Therefore a number of alternative methods were tested including:

- Quantile mapping which is used extensively in the Low Flows literature (World Meteorological Organisation 2008) as a means of infilling DMF data
- Standard regression models fitted to both the full data range or just the extremes
- Use of additional covariates such as rainfall data, antecedent conditions and catchment characteristics as proposed by Ledingham (2011)
- A simplified pair-wise version of the conditional dependence model

Although quantile-quantile mapping was developed in the low flows literature, it is possible to modify the methodology for use with high flows. This is discussed in more detail in Chapter 7 where the methodology is also considered as a means to interpolate flows to ungauged sites. For infilling missing data, the method is restrictive as it assumes a direct correlation between two sites and therefore cannot incorporate natural variability in the data.

Using standard regression models was found to work well for sites with strong correlations. Unlike the quantile mapping method, some natural variability is retained through the residual

term, however where the correlation is low the residual term becomes dominant. An advantage of using a standard regression model over the conditional dependence model is that the regression model can be fitted to all data and therefore the closest gauge can be used as the donor site regardless of whether it experienced an extreme event during the period of missing data, although this may result in a poorer fit in the extremes.

Ledingham's (2011) rainfall and antecedent conditions methodology has potential advantages in extending and infilling the observed flow data due to the availability of rainfall data over a longer time period and denser network, however it was found to be computationally demanding compared to the other methods. It is restrictive as it was designed to simulate independent flood peaks and therefore cannot be used to infill complete hydrographs, it is fitted to POT data and therefore conversion to DMF is required before the infilled data can be used in the conditional dependence model and finally it is not possible to use this method with coastal data.

The method chosen for use in this project was a simplified version of the conditional dependence model. During testing this was found to perform better than the standard regression model for sites with moderate to weak extremal association and approximately the same for sites with strong extremal association. A major advantage of using a version of the conditional dependence model is that it fits naturally with the existing model structure.

Selection of suitable donor sites

The first stage of the infilling missing data methodology is to select suitable donor sites that can be used to provide information about the missing data. Ideally for fluvial sites the donor site would be connected to the missing data site that is the same water flows through both locations and would be nearby to preserve the spatial dependence structure. Recently the use of distance between catchment centroids has been promoted as a method of identify suitable donor sites for estimation of QMED in ungauged locations (Kjeldsen 2008). Catchment centroids are preferred over distance between gauging stations as they prioritise nested catchments and locations where the catchment headwaters are situated nearby (Keef *et al.* 2009a). The core gauged network was extended to include all gauges in Table 6.8 where the pairwise concurrent data record was greater than 30 years long for the purposes of infilling.

Where possibly fluvial sites were used to infill other fluvial sites and coastal sites other coastal sites since the characteristics of the event are assumed to be more similar at sites of the same type. Donor sites were ranked by inverse distance weighting. The distance between each pair of catchment centroids was calculated using the centroid location from the FEH CD-ROM 3

(CEH 2009b), and the distance between each pair of coastal sites was taken as the distance along the coastline between the two sites. Where no same type site experiences an extreme event, coastal and fluvial sites have been paired. The distance between coastal and fluvial sites was taken as the direct distance between the two sites.

Infilling missing data

The difference between this method and the one used by Keef (2006) is that the simulation of missing data only takes into account one other gauge rather than all available gauges. This removes the requirement to use a copula to fit a multivariate normal distribution function to the residuals. Since the underlying motivation of the infilling method proposed by Keef is based on a bivariate result (Keef 2006), the simplification to a bivariate case is assumed appropriate here. The implication of this simplification is that the true conditional distribution across all gauges is not taken into account. This is likely to be most significant where the relationship between the paired gauges is weak or the spatial distribution of the network is sparse. However in most cases the amount of missing data is small and hence the contribution to uncertainty from the infilling method is small.

The conditional dependence model was fitted as described in Section 5.3.3.2 using all available data from 1960 – 2010. The data period was extended for the purpose of infilling to make maximum use of all available observed data for each gauged pair and allow the model to be fitted for marginal gauges with 30 or less paired observations between 1979 and 2010. Extending the data period further than this was deemed unsuitable due to issues of potential non stationary in the data over extended time frames. The residuals at each time step, $\hat{Z}_{j,t}$, were estimated using Equation 5.29.

For each missing date, the closest donor site (Y_j) which experienced an extreme event within 10 days of the missing date (x_t) was selected and the missing data infilled conditional on the peak event, $y_{j,s}$, where s is the date of the peak event and r is the lag from the event peak and a and b are the fitted model parameters at each r , such that:

$$X_{s+r} = a(y_{j,s}) + b(y_{j,s})z_{sim} \quad 6.1$$

where z_{sim} is resampled from the observed data with replacement as described in Section 5.3.3.4. The infilling methodology is illustrated in Figure 6.14.

Figure 6.15 illustrates the fit of the infilled data compared to observed data. Some variability is expected between the observed and simulated events due to the random sampling of z values. Although the results shown in Figure 6.15 do not show a good fit between observed and simulated events, the simulated events are representative, if not realistic. Table 6.14 shows

that the use of infilled data, even using the simplistic approach used in this study, serves to improve the fit of the conditional dependence model compared to using observations alone. The complete infilled time series for the core gauges in Table 6.8 are shown in Appendix B.3.

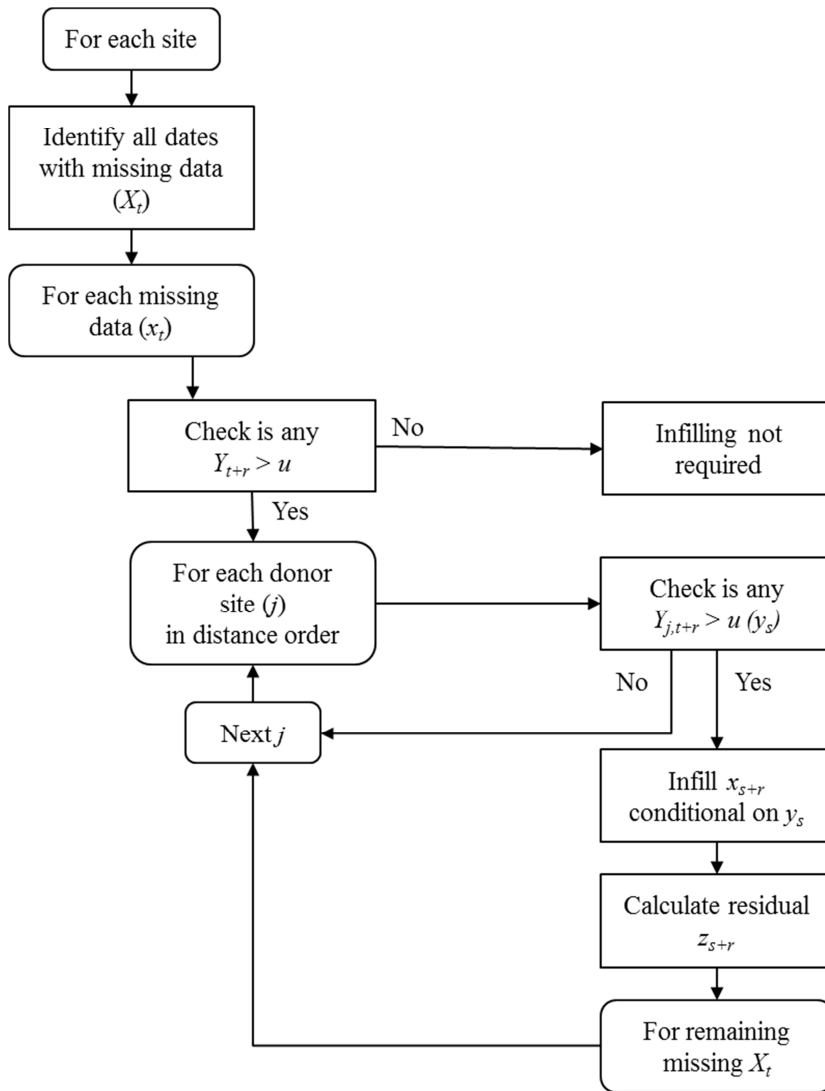
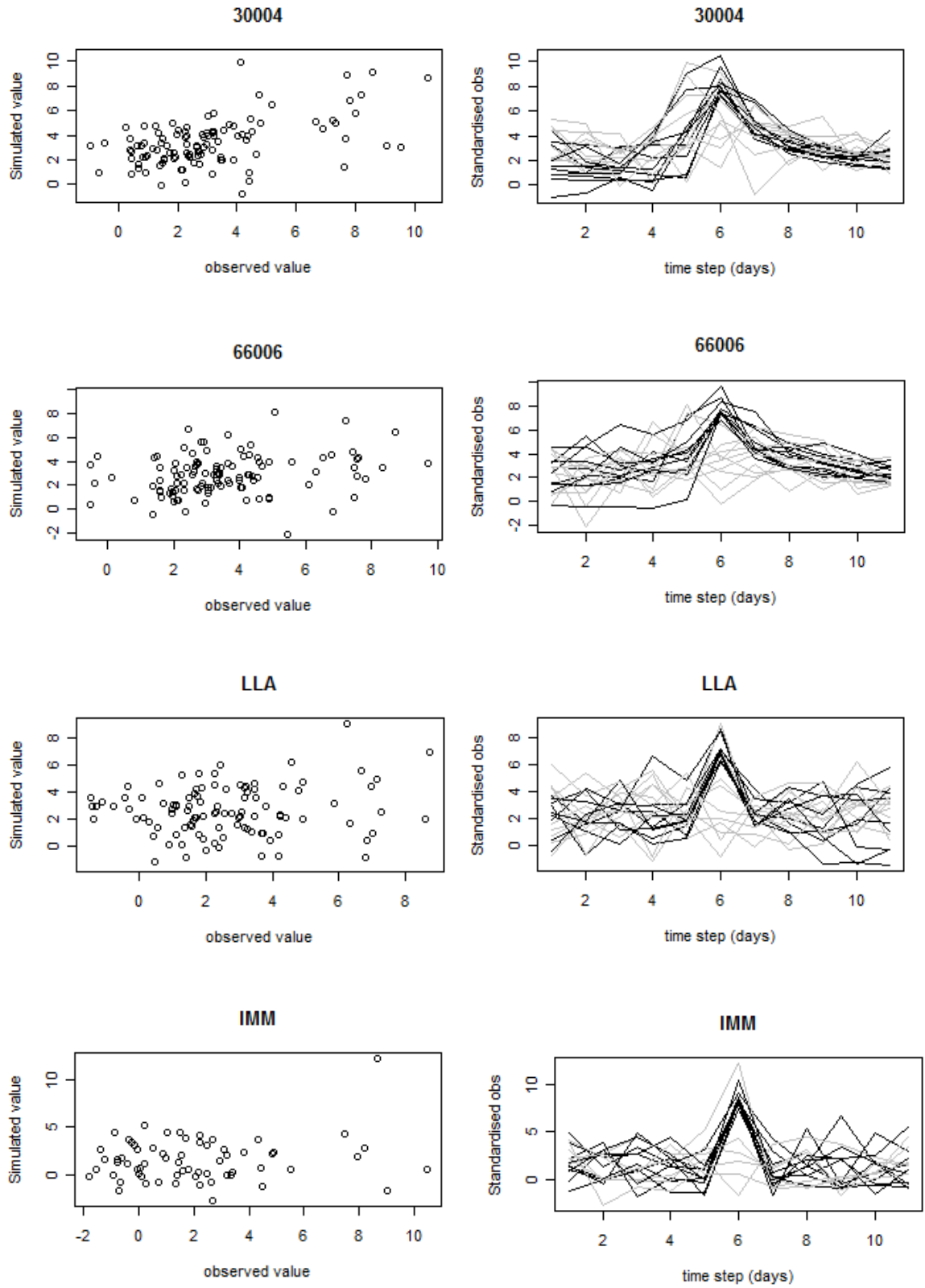


Figure 6.14 Diagram of the infilling process



Plots on the left show the observed peaks plotted against the equivalent simulated peaks. Plots on the right show the daily time series for the ten largest events at each site. Black lines are the observed data and grey lines are the equivalent infilled data for the same event.

Figure 6.15 Example of infilled coastal event peaks and time series

6.3.6 Event simulation

The observed data sets are extended using the five step simulation procedure in Section 5.3.3.4. The R Package *evd* (Stephenson 2001) was used to simulate data from the specified GPD model. Event peaks were extracted from the simulated conditional data for lags of up to five days. The specification of the event lag is discussed in Section 6.3.6.1.

For systems based analysis of risk it is also useful to consider events on a time series basis, for example extended durations of high water levels are more likely to result in defence breach than high water that only occurs for a limited time. The simulation methodology can be extended to include full time series by retaining all simulated times rather than only the event peak (Section 6.3.6.4.).

In total 30000 events (including full event hydrographs and storm surge cycles) were simulated to provide a large event sample to support Monte Carlo sampling in the risk model as discussed in Sections 6.3.6.5 and 4.2.7.

6.3.6.1 Specification of event lag

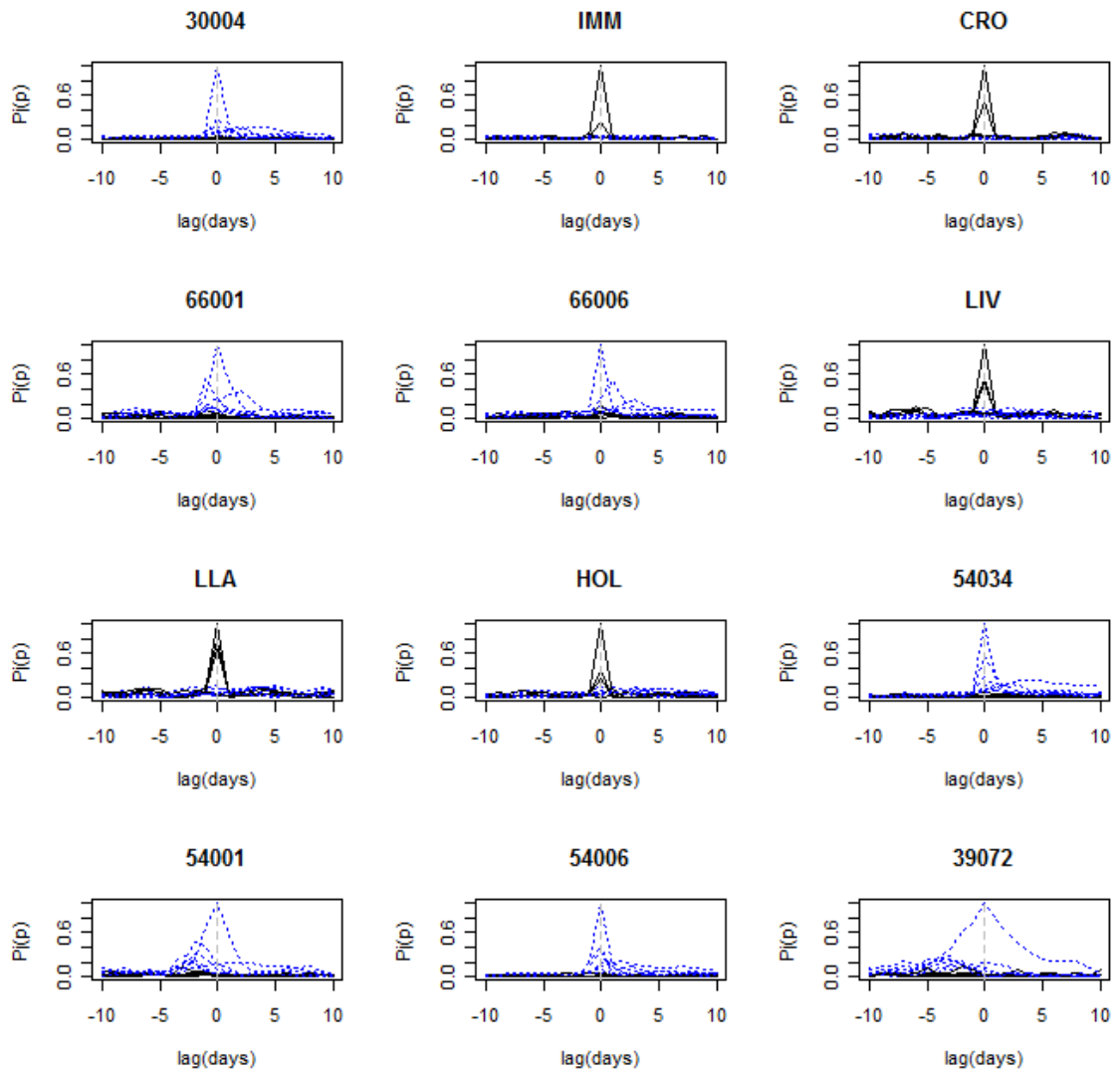
The event lag used should be long enough to include peak probability of large events at different sites. Keef *et al* (2009b) (see Section 5.3.3.3) found that for most fluvial sites the probability of peak events occurring peaked for lags of up to three days. Their analysis is repeated in Figure 6.16 for the probability of pairs of fluvial-fluvial, fluvial-coastal, and coastal-coastal sites used in this study for observed data exceeding the Q99 threshold.

Coastal sites, on the same coastline, are shown to display no time lag between peak events. The three day lag used by Keef *et al* (2009b) is shown to be appropriate for most fluvial sites except for 39072 on the Thames which show a 20% chance of flood peaks occurring at more upstream sites up to five days before peak it peaks. This is due to the difference in catchment size between the gauges used in this study. The same effect is also evident on the Severn (54001). The temporal correlation between fluvial and coastal sites is very low.

Increasing the lag time beyond five days would allow for the potential of including additional independent events, for example the events conditional on LIV indicate a previous extreme event seven days before the condition peak. Although the probabilities of peak events occurring at lags of more than five days remains around 20% for some sites, the peak probabilities all fall within five days, therefore five days has been taken as the maximum event lag in this study.

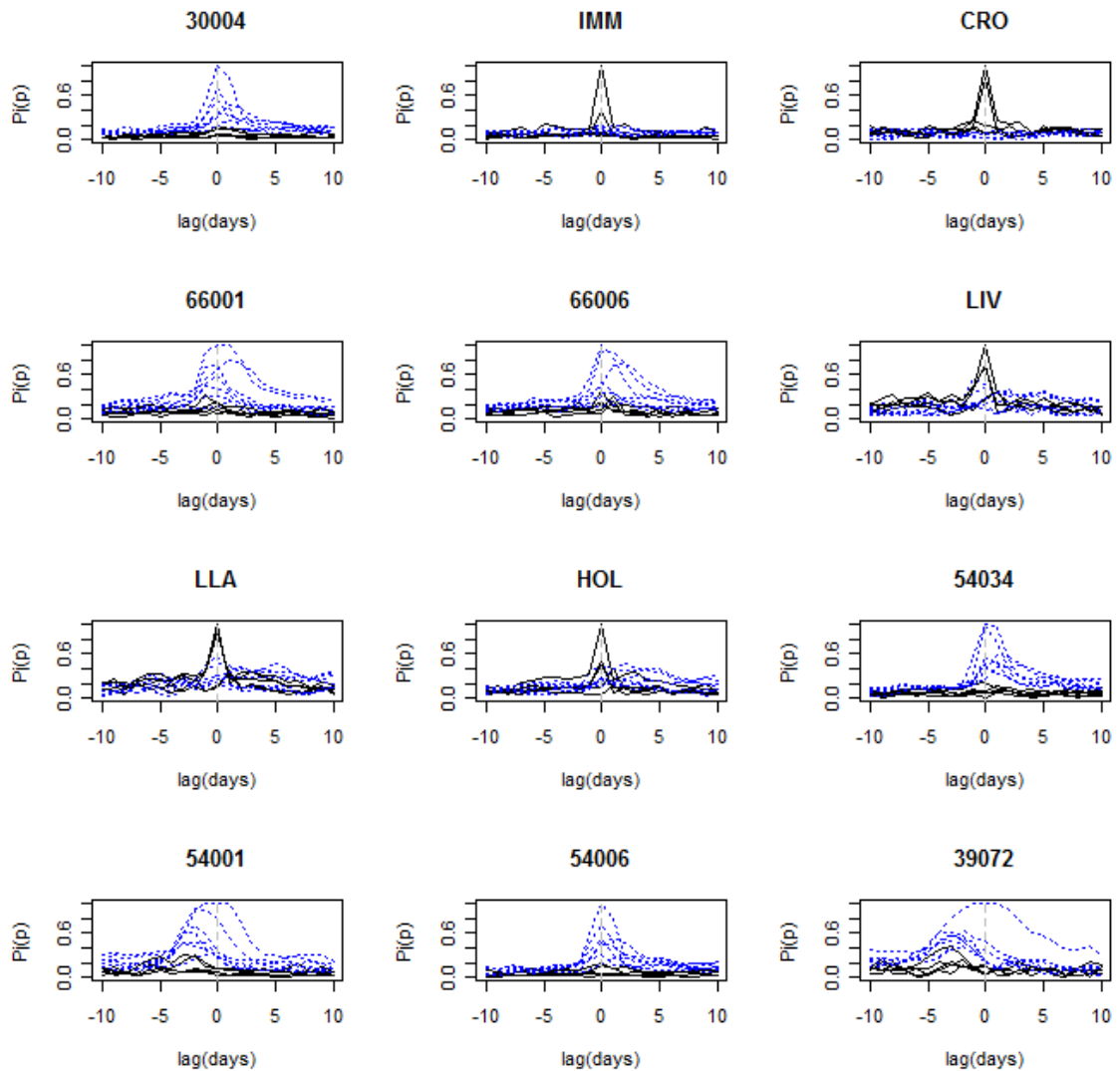
Figure 6.17 shows the same temporal dependence measure for less extreme events at the dependent site (here taken as the 95th quantile) which may still make a contribution to risk, especially over a wider area. Figure 6.17 illustrates that although the dependence remains high for a longer period of time, and there is evidence of higher dependencies between fluvial and coastal sites, especially in North Wales, the five day lag is sufficient to incorporate these additional features.

It should be noted that the lag of five days leads to an event window of ten days. This is longer than the insurance industry standard of seven days. In practice a large event is required to trigger an insurance claim window, and hence the seven days would normally include the largest event at the beginning and any subsequent losses on the following days. The probability of peak events occurring seven days after the main event peak is shown to be very low, therefore the five day lag includes all significant risk following the trigger event and can be assumed comparable to a seven day window.



Blue dotted lines are fluvial sites, black solid lines are coastal sites. The site which reaches a probability of 1 at lag 0 is the conditioning site plotted against itself.

Figure 6.16 Temporal extreme dependence between gauge pairs ($p=Q99$)

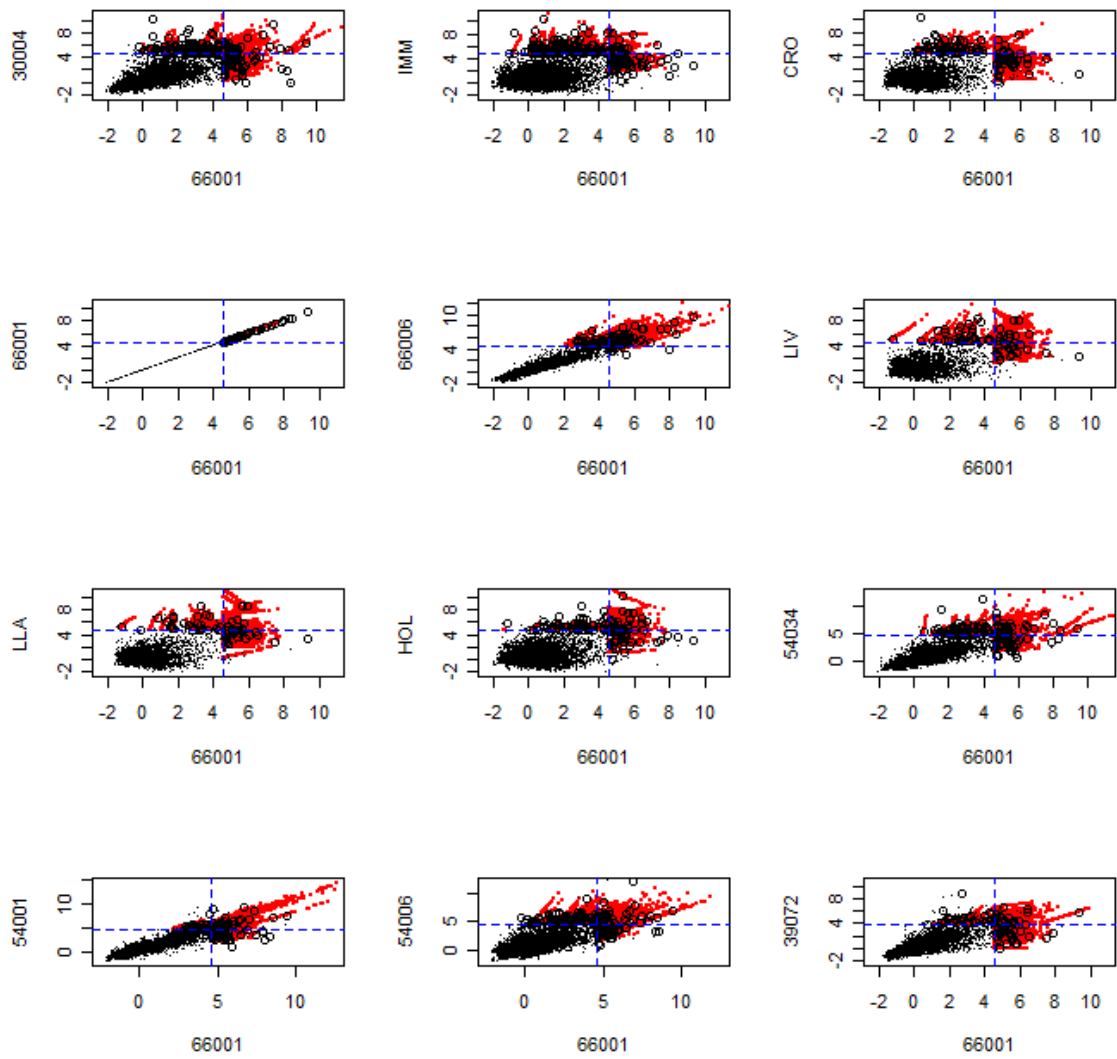


Blue dotted lines are fluvial sites, black solid lines are coastal sites. The site which reaches a probability of 1 at lag 0 is the conditioning site plotted against itself.

Figure 6.17 Temporal extreme dependence between gauge pairs ($p=Q95$)

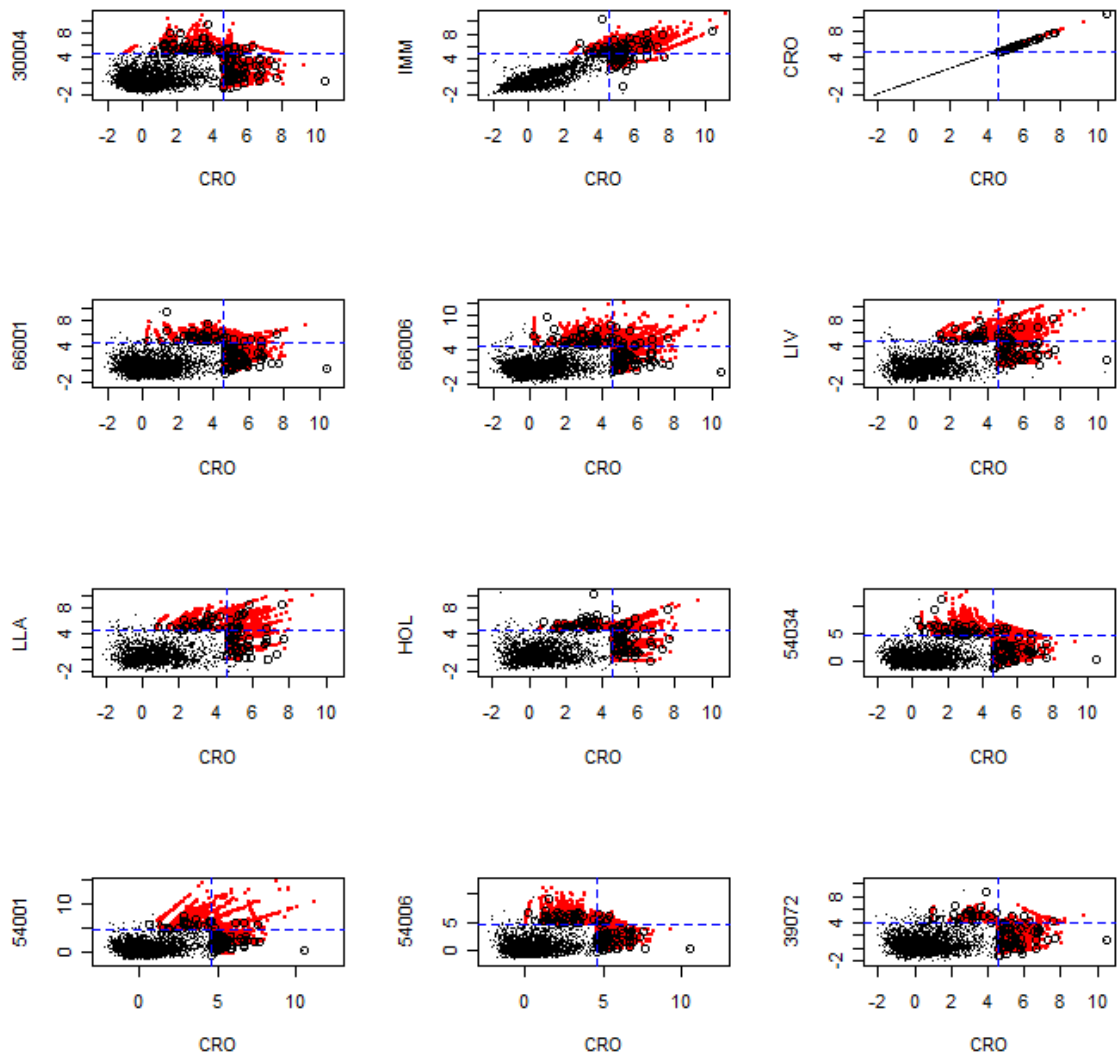
6.3.6.2 Event peak simulation

Keef *et al* used the conditional dependence model to simulate flood peaks at multiple sites belonging to the same event (henceforth referred to as event peak simulation) by retaining the maximum value in Y_{sim} . Figure 6.18 and Figure 6.19 show the simulated event peaks compared to the observed data extracted from Y_{sim} for lags of up to five days conditional for both coastal and fluvial gauges. The figure demonstrates the ability of the conditional dependence model to represent a range of dependence characteristics in the extremes from a strong extremal association, for example 66001 and 66006 or IMM and CRO, through to the weak correlation of CRO with most fluvial gauges. The banding of simulated events at some sites, for example CRO and 54001 is due to the short record length restricting the number of Z_s to resample from.



Black open circles are the observed de-clustered peaks, red filled circles are the simulated peaks, black dots are all observed data

Figure 6.18 Comparison of simulated and observed peaks for 66001 and all core gauges



Black open circles are the observed de-clustered peaks, red filled circles are the simulated peaks, black dots are all observed data

Figure 6.19 Comparison of simulated and observed peaks for CRO and all core gauges

6.3.6.3 Rejection sampling

Any set of simulated events should reflect the distribution of times when each gauge is extreme. Keef *et al* (2009a) found that to ensure the correct number of peak events at each site was maintained a form of rejection sampling was required in the simulation procedure. The proportion of times each conditioning gauge is the event maxima in the simulated data set should be equivalent to the true proportion of times each site experiences the event maxima. The event maximum is defined on the relative size of the event at each site compared to the threshold at each site on a standard scale. This can be estimated by simulating a large number of events conditional on each site in turn. The proportion of times that each gauge site is the event maxima will be representative of the true proportion of events (Keef *et al*. 2009a). Table

6.13 shows the results from a large sample using 2000 simulated events from each conditioning gauge.

In addition, it is assumed that the value at the conditioning gauge is the maximum value over all sites (Keef *et al.* 2009a) therefore events are removed from the simulated sample where this criteria is not met. This criteria requires considerably redundancy in the simulated data set as for the event set of 24000 simulated using 2000 conditioning events at each site, only 28% of the simulated events were retained in the sample after rejection sampling.

The final sample set is constructed such that the proportion of maxima events at each site (given in Table 6.13) was maintained, for example for a sample of 100, 10 events would be simulated conditional on 30004, nine events would be conditional on IMM and so forth.

Table 6.13 Percentage of relative event maxima over 5 day lag at each site from a sample of 24000

30004	IMM	CRO	66001	66006	LIV	LLA	HOL	54034	54001	54006	39072
9.8	8.9	7.3	3.2	11.1	11.7	10.7	11.2	8.2	2.9	6.8	8.3

6.3.6.4 Event time series simulation

In an extension to the event peak simulation, the conditional dependence model can also be used to produce full event hydrographs and storm surge cycles by retaining all time lags in Y_{sim} . At site X_i the flood peak is simulated from the GPD distribution at time t . The conditional time series is then simulated from the Heffernan and Tawn model for $\tau \neq 0$ conditional on $X_{i, t=1}$. At sites $X_{j, t=+/-\tau}$ the conditional time series is simulated from $X_{i, t=1}$. A block of residuals is resampled for the Z values of length 2τ to maintain consistent characteristics within each event.

Although this extension allows the model to be used to simulate time series, this should still be thought of as an event based simulation. The conditional dependence model is based on the assumption that at least one gauge in the network is extreme. The time series of flows at all other gauges can be simulated from this point however there is a limit at which the dependence between $X_{i, t=1}$ and $X_{j, t=+/-\tau}$ decays and can no longer be accurately simulated. The method can therefore only model one peak event and cannot incorporate long term rises and falls in the hydrograph. In light of these concerns, time series simulation has been restricted to lags of up to five days in keeping with the event definition (Section 6.3.6.1). Examples of simulated time series are shown in Figure 6.20 demonstrating the ability of the conditional dependence model to incorporate the temporal dependence in a range of different situations, for example a strongly dependent coastal case IMM | CRO, a weakly dependent coastal pair

HOL | IMM, a weakly dependent fluvial and coastal pair IMM | 66001, a slowly responding fluvial pair 54001 | 30004 and a fast responding fluvial pair 66006 | 66001.

The scale at which time series simulation is possible from DMF data in the UK is limited as for many catchments daily data are not detailed enough to reflect the full event hydrograph (Robson and Reed 1999), this limitation is discussed in more detail in Chapter 7. However an additional advantage of simulating time series in this way is that the simulated flows on the anterior and posterior days can be used to estimate the hydrograph shape, which as discussed in Section 7.2.1 widens the choice of peak flow estimation methods available.

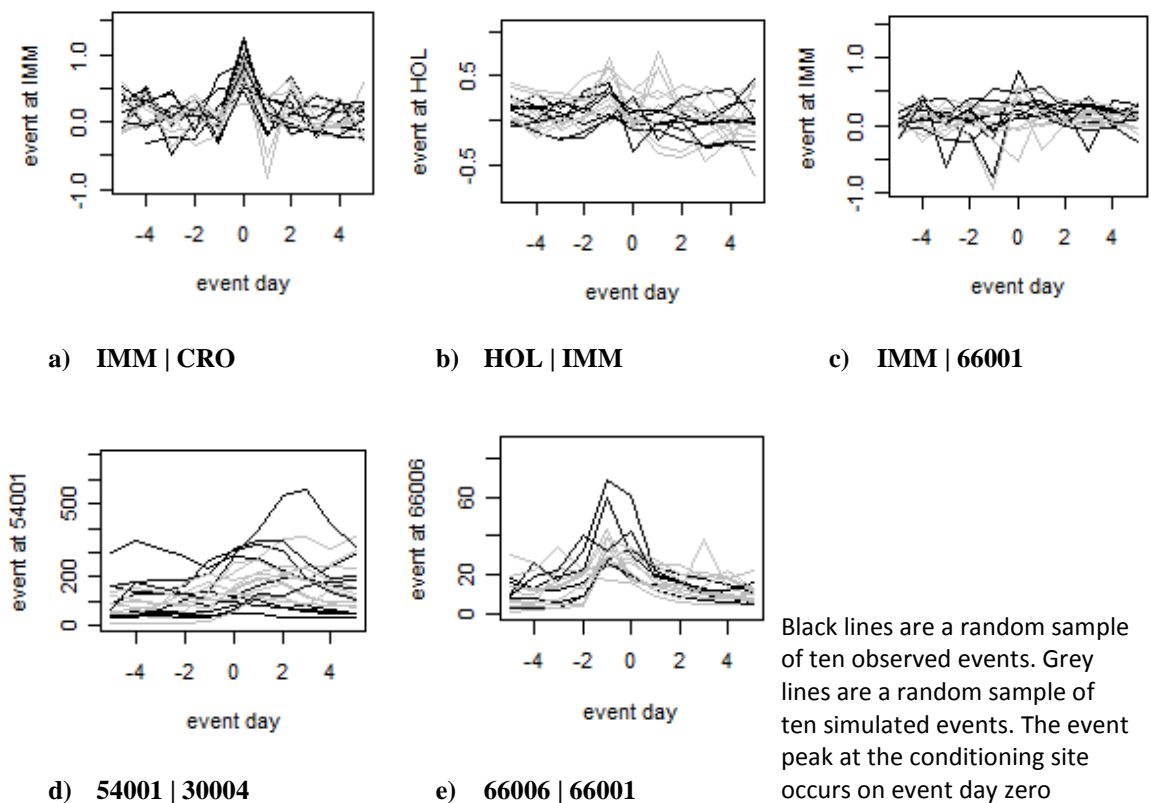


Figure 6.20 Example DMF and skew surge simulated time series compared to observed

6.3.6.5 Sample size

Monte Carlo sampling is used as the framework for risk analysis in this thesis. There is limited guidance in the literature on the recommended size of Monte Carlo sample.

The sample size should be large enough so that the uncertainty associated with the Monte Carlo simulation is small, however the sample size that is needed to achieve this depends of the purpose of analysis. In their example demonstration of using the conditional dependence model for four river flow stations in Scotland, Keef *et al* (Keef *et al*. 2009c) use a Monte Carlo sample of 500 runs. In Lamb *et al*'s (2010) outline of using the conditional dependence model

to assess the risk of flooding, events equivalent to a record length of 800 years are generated. At their stated average occurrence rate of 6.25 events per year, this is a sample of 5000 events. In Lamb *et al*'s proof of concept report for the Environment Agency Spatial Coherences of Flood Risk project (Lamb *et al.* 2009), a Monte Carlo sample of 10000 events is used to investigate flood fluvial risk in the NE region while the coastal example used 800 years of simulated record for the North Sea used to generate 122 samples of the three day sea level maxima. Other similar flood risk studies which have used Monte Carlo simulation include Apel *et al* (2009) who found that using a sample of 10^5 synthetic flood events produced stable results up to return intervals of 10^4 years.

The Flood Estimation Handbook (CEH 1999) recommends a record length of five times the return period of interest for robust estimation of extremes. For a 0.1% AEP event this equates to 20000 simulated events (assuming an average occurrence rate of 4 per year). To allow for the rejection sampling procedure (Section 6.3.6.3), 6500 conditioning events were simulated conditional on each of the 12 core gauges. 30000 conditioning events were retained in the final sample set. This sample size is equivalent to those used previously in the model by Keef and Lamb *et al* (Lamb, Keef *et al.* 2009; Keef, Lamb *et al.* 2009a; Keef, Svensson *et al.* 2009b; Keef *et al.* 2009c) but is much smaller than that used by Apel *et al* (2009) in their risk based study.

The computational demands of the inundation and breaching model are greater than the conditional dependence model. Therefore a large set of extreme events can be generated which is sampled from in the later stages of the system risk model.

6.3.7 Contribution of simulation procedure to uncertainty

Uncertainty in the simulated events set stems from two main sources; limitations on the observed data quality and length, and the assumptions embodied in the statistical model. A brief summary of the contribution of these two components to statistical modelling uncertainty is provided here. A systems based risk model of this type incorporates multiple sources of uncertainty throughout the system. The relative contribution to uncertainty in flood risk estimation from the statistical model is discussed in Section 9.4.

6.3.7.1 Data driven uncertainties

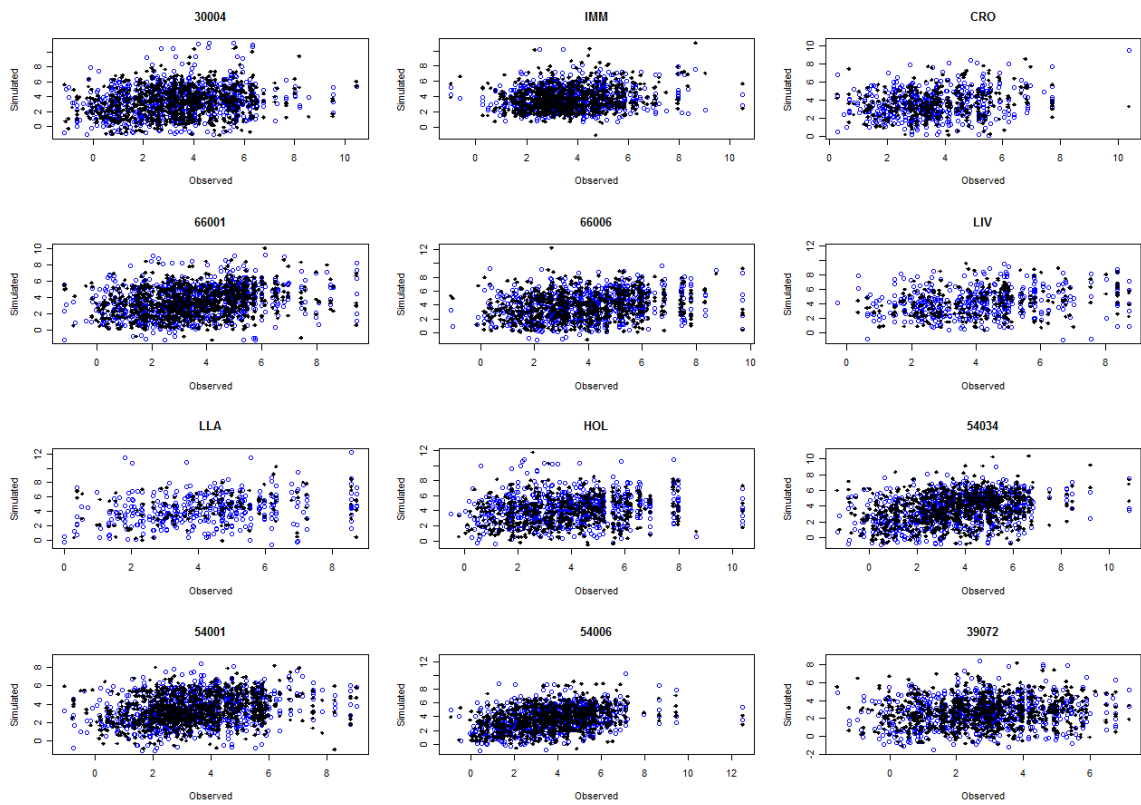
A trade-off is required between using only high quality long gauged data series and the requirement to use gauges near to the sites of interest. Using better quality data sets located further away from the receptors may reduce uncertainty in the statistical model but will lead

to increased uncertainties in the estimation of peak events at the sites of interest (see Section 7.2).

Short record lengths present problems for all extreme value analysis, in particular for multi-site analysis long concurrent records are required. Potential uncertainties from using short record lengths to fit the GPDs have been minimised by extending the record length to include longer data sets at individual gauges which are not possible to use in the concurrent data set.

The data quality at all sites was reviewed prior to inclusion in the statistical model (See Section 6.2.2). Most of the fluvial gauges in this study are part of the NRFA standard DMF data set (CEH 2009) which includes quality checked long records deemed by CEH to be suitable for use in flow analysis.

Aside from record length, the biggest contributor to data driven uncertainty is the missing data. In order to make maximum use of all available data and hence reduce uncertainties from short record lengths, missing data in this study has been infilled using the methodology outlined in Section 6.3.5.1. The missing data methodology produced realistic values for data gaps but as shown in Figure 6.15 is not able to accurately predict observed events. For fluvial sites the proportion of missing events is low (see Table 6.12) and therefore the contribution to uncertainty from infilling is low compared to the additional benefits from increasing the available concurrent record length. For coastal events however the amount of missing data is up to 50% at LIV and LLA. The model was fitted with and without infilled data and the root mean squared errors (RMSE) between the 1001 observed event peaks and equivalent simulated events peaks calculated (Table 6.14). As illustrated in Figure 6.21 there is no noticeable difference in the simulated events using infilled and non-infilled data other than that the infilled data enables the generation of a larger number of events due to the increase data enabling the model to be fitted to more gauge pairs. Whilst some variability is expected due to the random sampling of z values, the RMSE (Table 6.14) showed that the model fit is the same or improved by increasing the concurrent record length through infilling.



Blue circles show simulated events from infilled data.
Black diamonds show simulated events from observed data only

Figure 6.21 Comparison of simulated event peaks using infilled and non-infilled data

Table 6.14 RMSE of peak events simulated from conditional dependence model using infilled and observed data

	30004	IMM	CRO	66001	66006	LIV
Observed data only	3.90	4.00	3.92	3.97	4.29	4.53
Including infilled data	2.34	4.00	1.85	3.97	2.33	4.53

	LLA	HOL	54034	54001	54006	39072
Observed data only	4.71	4.34	4.12	3.86	4.18	3.20
Including infilled data	2.15	4.30	2.33	3.86	2.00	3.17

6.3.7.2 Modelling assumptions

A statistical model is one of many possible representations of reality. Here the conditional dependence model is assumed to provide a robust representation of the dependence between sites during extreme events and the GPD model a suitable representation of the marginal characteristic at each gauge.

The GPD model is shown to have a good fit to the observed data within the observation domain and is known to be a suitable model for the representation of environmental extremes (as discussed in Section 5.3). Table 6.10 provides a quantification of the standard error from

the GPD parameter estimation. The plots in Appendix B.2 indicate that there are wide uncertainty bands when using the fitted distribution for large return periods. This is standard for all extreme models due to a lack of data in the extremes.

The identification of thresholds, de-clustering run time and event duration, add a subjective element to the statistical model. In this case the suitability of the threshold was checked for each site and found to provide a stable estimate of the GPD parameters (See plots in Appendix A.6.3) and the run time was carefully selected to represent the physical characteristics of the observed events (See Section 6.3.3).

The use of the conditional dependence model to represent fluvial and coastal extremes is well documented in the literature and can therefore be assumed to be a suitable model for use in this study. In Figure 6.18 to Figure 6.20 it is shown that the conditional dependence model is able to represent the full range of dependence characteristics across the sites of interest. Table 6.14 shows the RMSE of peak events simulated conditional on all 1001 independent extreme events in the observed data series at the core gauges. Some variability is expected between the observations and the simulated values at each site due to the random sampling of the residual term however in general the dependence model is found to be a suitable model choice. The use of the model in previous high profile studies into dependences in extreme events in the UK also adds credibility to its use here.

6.4 Spatial and temporal dependences in simulated extreme events

The use of the conditional dependence model to simulate a large number of extreme events allows for better analysis of the dependence structure between sites by increasing the record length and allowing consideration of a wide range of events and extension to events more extreme than those available in the observed time series. The final section of this chapter reviews the spatial and temporal dependence structures seen in the simulated event set.

All gauged pairs displayed positive extremal association (with $0 < a < 1$ or $b > 0$), supporting the assumption by Keef *et al* (2009a) that in most flood risk applications it is suitable to use a simplified version of the Heffernan and Tawn (2004) conditional dependence model with $c=d=0$ (see Section 5.3.3.1 for further details).

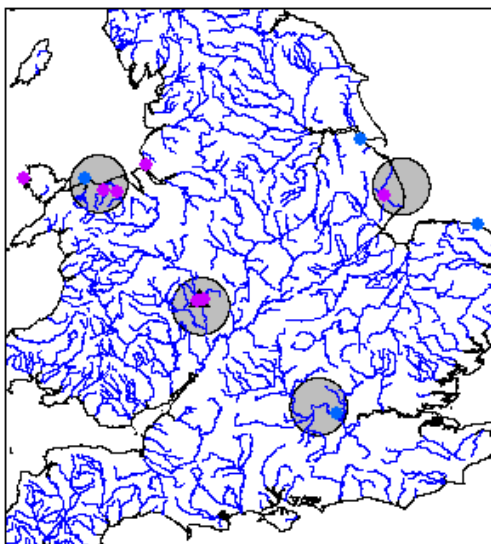
The spatial dependence between individual gauges can be investigated by applying Equation 5.31 to the simulated event peak data as shown in Figure 6.22 conditional on three example gauges, 54001 on the Severn, 66001 on the Clwyd and the tide gauge at Holyhead (which are shown as black triangles). These sites were selected as they demonstrate some interesting spatial dependence characteristics. The threshold at the conditional site is varied to show the

changing dependency patterns as events get more extreme. Equivalent plots for the core gauges are included in Appendix B.4.

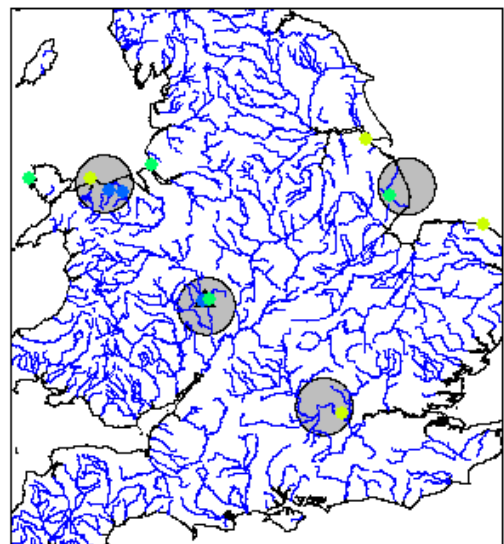
The results for 54001 show that a strong spatial dependence is maintained for events which experience their largest peak at 54001, even for the most extreme events. This is due to the large scale nature of flood events that affect the River Severn, and, in the case of the fluvial gauges in North Wales, is a feature of the close spatial proximity between the catchment headwaters. There is also a moderate dependence between fluvial floods on the Severn and extreme coastal events in North Wales which suggests that flood risk on the Severn can be driven by large scale weather systems which may also contain a coastal component.

In contrast 66001 is located in a smaller catchment and as such the spatial dependence between 66001 and other gauges in the network is low, except for the neighbouring gauge 66006 on the River Elwy. What is interesting is that the spatial dependence between peak events occurring at site 66001 and the nearby coastal gauges at Holyhead, Llandudno and Liverpool is higher than the dependence between peak coastal events (shown here at Holyhead) and associated fluvial floods at 66001. This indicates that if a fluvial even occurs in North Wales it is more likely to occur within an event that also results in coastal flooding than a large coastal event which is more likely to occur independently.

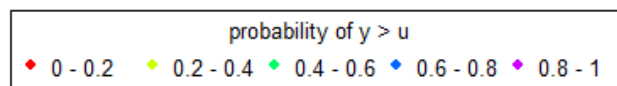
Probability of $y > 0.95 \mid 54001 > 0.99$



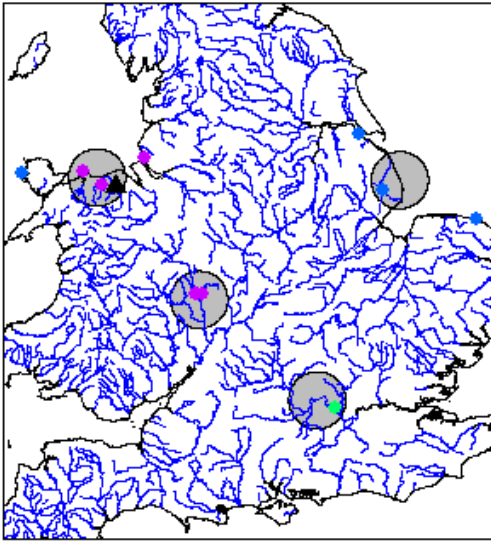
Probability of $y > 0.99 \mid 54001 > 0.99$



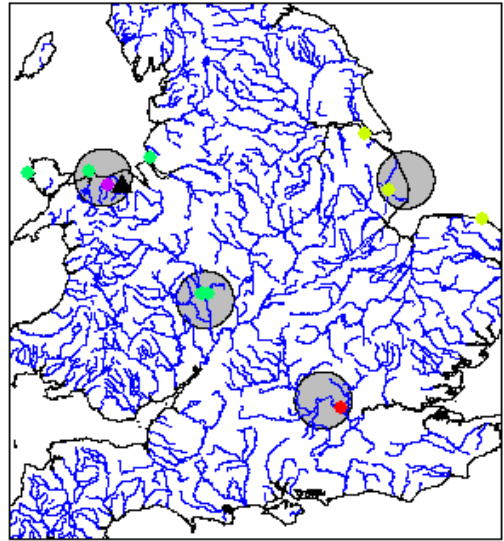
Named conditioning gauge (u) is marked with a solid black triangle



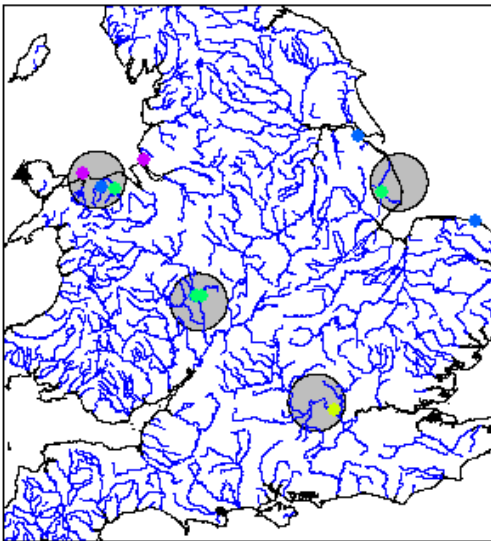
Probability of $y > 0.95 \mid 66001 > 0.99$



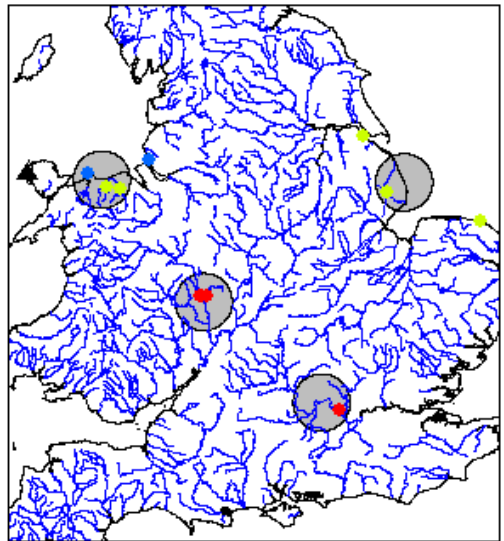
Probability of $y > 0.99 \mid 66001 > 0.99$



Probability of $y > 0.95 \mid \text{HOL} > 0.99$



Probability of $y > 0.99 \mid \text{HOL} > 0.99$



Named conditioning gauge (u) is marked with a solid black triangle

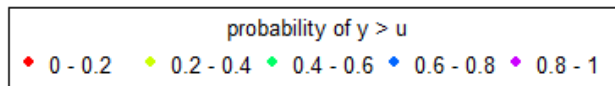


Figure 6.22 Spatial conditional dependency maps: probability of $y > u \mid x > Q99$

The second more general summary measure that can be used is the expected proportion of gauges in Y over a given threshold given that $x > u$ (Equation 5.32). Plotting this data graphically (Figure 6.23) allows identification of areas with high spatial dependence between extreme events. The most extreme events are shown to be very localised, with only 54001 on

the Severn and 66001 in North Wales showing an expected proportion of more than 0.4 other gauges likely to also exceed the Q99 level. For less extreme dependent events, at the Q95 and Q90, more spatial dependence is evident. The coastal gauges are shown to have a lower spatial dependence than the fluvial gauges, although this is possibly a result of the network architecture.

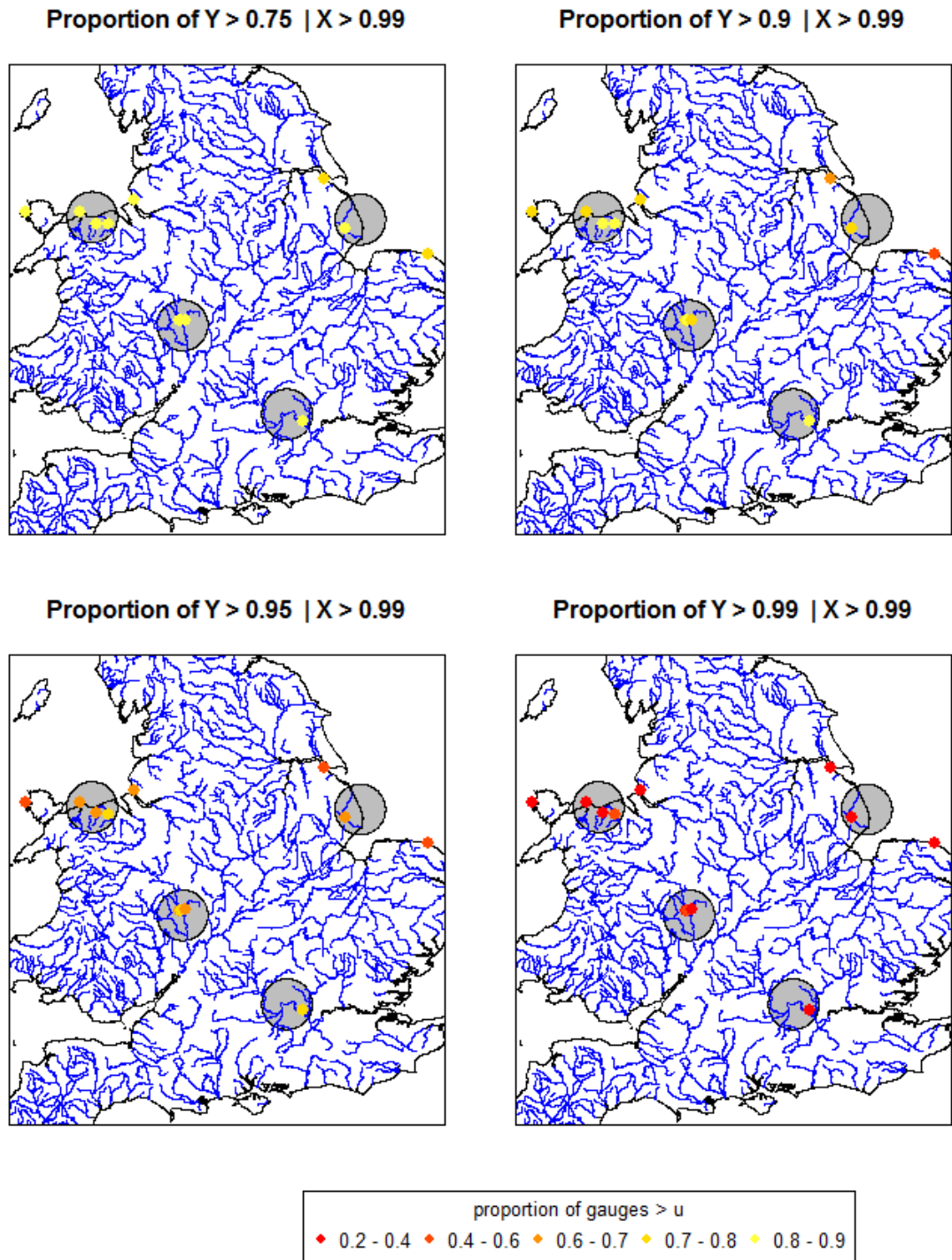


Figure 6.23 Spatial conditional dependency maps: expected proportion of gauges in $Y > u \mid X > Q99$

The results shown in Figure 6.23 are slightly skewed because there is an uneven spread of gauges across the study area, therefore in most cases, in locations where the density of gauges is higher, the spatial dependence structure will appear stronger. Since coastal gauges are shown in Figure 6.22 to be more correlated with other coastal gauges, having less coastal gauges in the network will also make the dependence between coastal gauges appear lower. To overcome these problems the network was split into subsets and the analysis repeated.

For fluvial and coastal differentiation this can be achieved by separating the calculation into the proportion of fluvial gauges in Y and the proportion of coastal gauges in Y which are above the threshold for events at any given conditioning gauges as shown in Figure 6.24. This reaffirms the observation that the spatial dependence is strongest in North Wales where extreme events at both the fluvial and coastal gauges are shown to have a strong relationship with other coastal gauges. In general it is shown that the dependence between pairs of coastal gauges is stronger than pairs of fluvial gauges. This is expected due to the additional variation in fluvial events caused by catchment processes. Separating the network in this way still does not entirely remove the artefact of the network structure as the spatial dependence on the East Coast is shown to be lower than in North Wales but there are three nearby gauges in North Wales and on the East Coast there are two gauges located further apart. This is a limitation of using a sparse gauges network and should be born in mind for all similar analysis of this type.

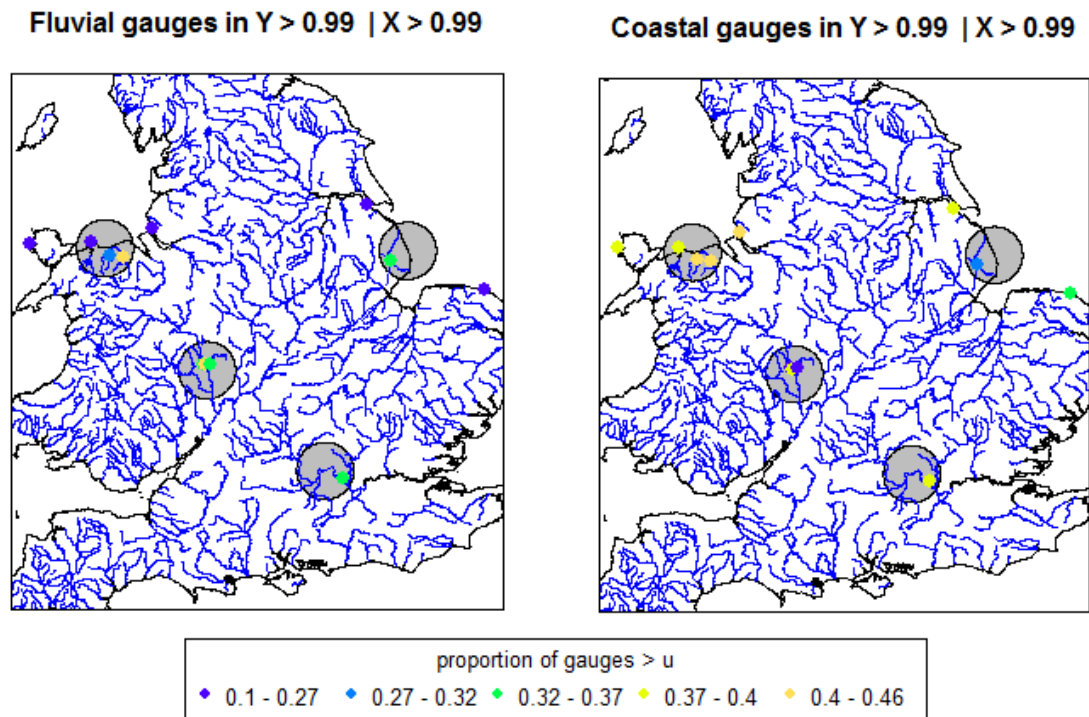


Figure 6.24 Spatial conditional dependency maps: expected proportion of gauges in $Y > Q99 \mid X > Q99$ by gauge type

For the clusters the calculation is more difficult due variations in the number of gauges in each cluster. Therefore an alternative measure is used which calculates the number of clusters with gauges $> u$ for each conditioning gauge. The results are shown in Figure 6.25 and Figure 6.26 for dependent events above the Q95 and Q99 threshold. The plots should be interpreted as follows; for a conditioning extreme event at site 39072 on the Thames, three clusters are expected to have 50-99% of their associated gauges experience an event peak $> Q95$, whereas at the Q99 level this drops to only one cluster.

In all cases at least one other gauge in the same cluster as the conditioning gauge experiences an extreme event. This shows that within the clusters there is a strong dependence structure. There is a significant fall in dependence between the Q95 and Q99 threshold, this is most evident in the bottom left plot in Figure 6.25 and Figure 6.26. Only the fluvial sites 54001, 39072, and 66001 maintain a weak dependence across clusters at the Q99 level (as discussed in reference to Figure 6.22).

For details of which clusters contribute to the expected number of clusters with gauges $> u$ analysis of the probability plots shown in Figure 6.22 and Appendix 6.6 is required. For example 39072 is shown to have a strong dependence with sites in the Severn cluster so this is likely to be the cluster that experiences 50-99% of its associated gauges $> Q99$ threshold for a conditioning event at site 39072. Again this cluster based measure does not totally remove the influence of the network structure as the Thames cluster can only have 0% or 100% of its gauges experience an extreme event.

The gauges used in this study are restricted to the risk clusters of interest. For consideration of more general spatial dependence characteristic of extreme fluvial events in the UK using this method readers are directed to Keef (2006) and Keef *et al.* (2009b). As summarised in Section 5.2.2.

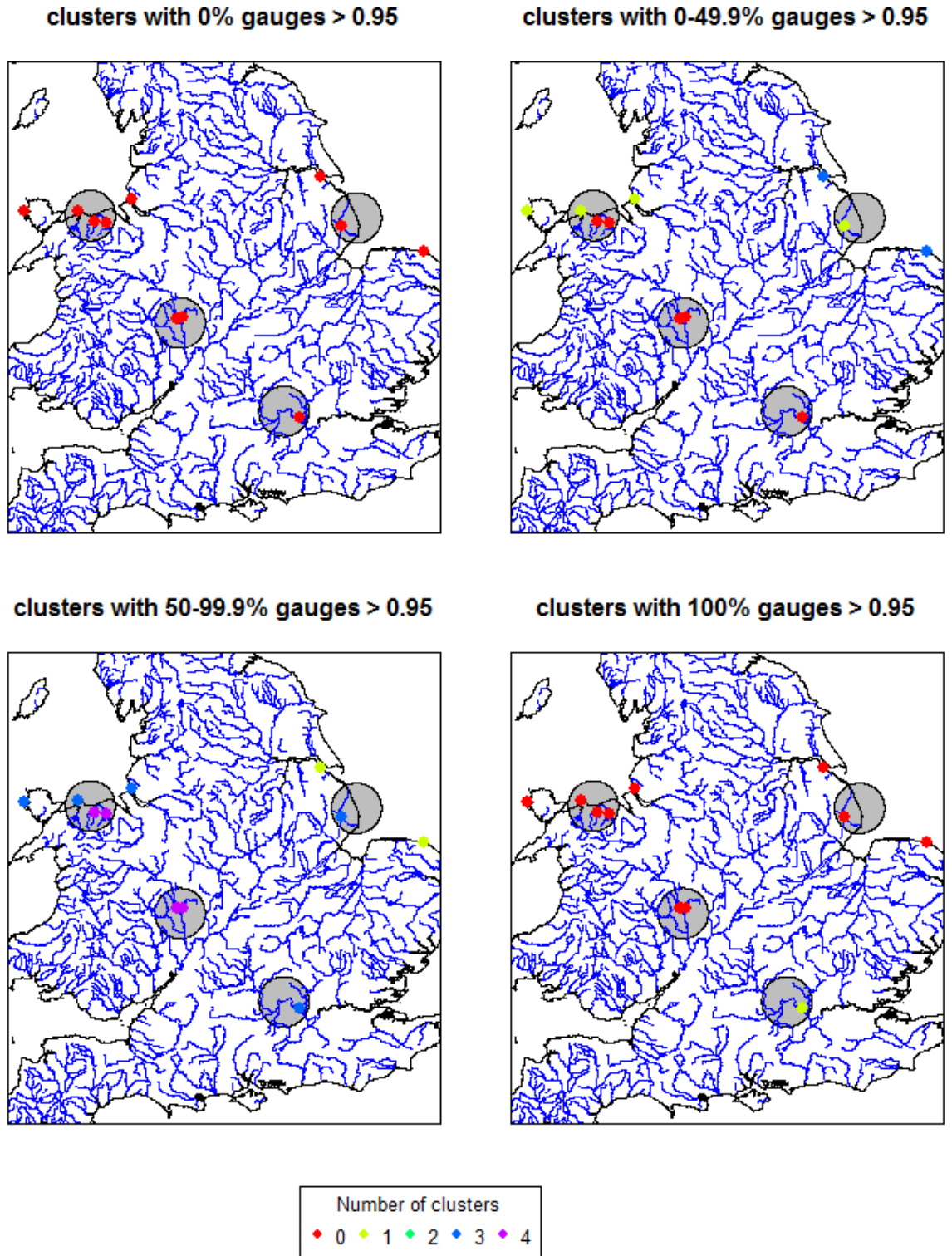


Figure 6.25 Spatial conditional dependency maps: expected number of clusters with gauges > Q95 | X > Q99

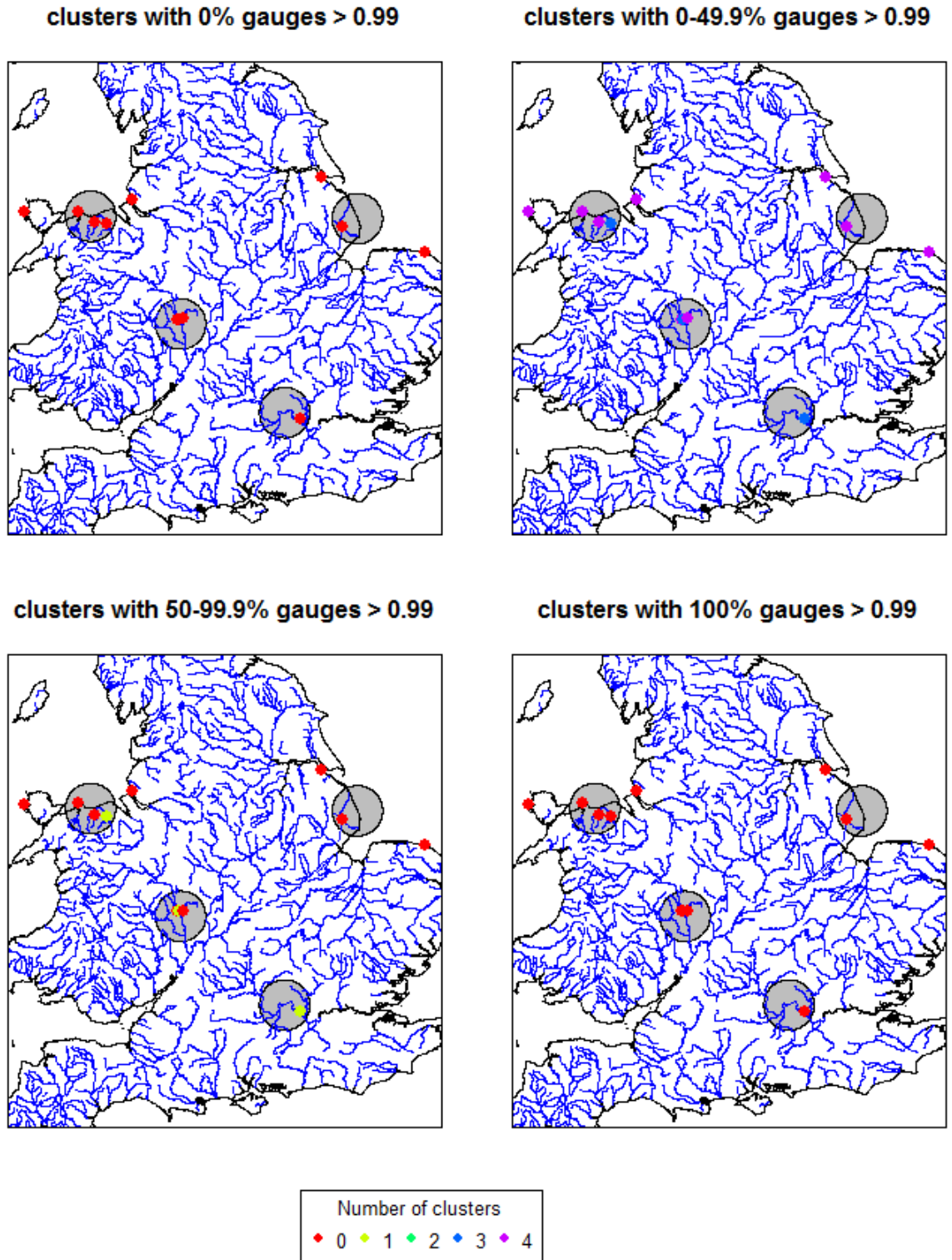


Figure 6.26 Spatial conditional dependency maps: expected number of clusters with gauges > Q99 | X > Q99

6.4.1 Summary of dependence structures in each of the risk clusters

6.4.1.1 East Coast

Although known to be vulnerable to extreme coastal events, the correlation between the East Coast cluster and other gauges is low. For Catlin this is a positive result as it suggests that they would be unlikely to sustain a large loss on the East Coast at the same time as losses from elsewhere in the country. However the dependence between Immingham and Cromer, even though the distance along the coastline between them is 465km, is relatively strong. This is indicative of the vulnerability of the whole coastline to storm surge events travelling through the North Sea.

6.4.1.2 North Wales

The gauges in North Wales demonstrated the strongest dependence structures between fluvial and coastal events and across large spatial scales with the other clusters. The fluvial-coastal dependence was shown to be strongest for extreme fluvial events which are likely to also have a strong coastal component. This presents a particular concern for flood risk in the area due to the risk of access routes along the narrow coastal plains and steep river valleys being flooded simultaneously.

The close proximity between the headwaters of the River Severn and the Rivers Elwy and Clwyd mean the dependence between fluvial events in North Wales and the Severn is high. This could result in large losses distributed over a large area for Catlin if an extreme event was to affect these two correlated areas.

6.4.1.3 Severn

As discussed above, extreme events in the Severn cluster show close similarities to events experienced in North Wales. Events on the Severn itself are also shown to be correlated with events on the Thames.

Within the Severn cluster, although the gauges are located in different catchments with different response characteristics, the probability of all three gauges experiencing the most extreme event type ($u > Q99$) within a five day event lag is moderate ($>50\%$). This is a concern as the many of the caravan sites in the area are located around the confluence of the three rivers.

6.4.1.4 Thames

Only one gauge was included in the Thames cluster due to the lack of suitable located reliable gauges (see Section 6.2.2.4). This made it difficult to identify large scale dependence structures

due to the influence of the network architecture meaning that spatial dependences appeared lower in the Thames as there were fewer nearby gauges. Evidence of dependence with the River Severn was seen as both rivers are large, slowly responding catchments. The temporal dependence for the Thames is also high with events staying high for long periods of time. This is a significant concern as longer duration floods are likely to cause more damage.

6.5 Chapter conclusions

This chapter has detailed the development of the statistical method to provide the underlying event simulation for the sources component of the systems model. The available data were reviewed in Section 6.2 and a suitable gauged network corresponding to the risk clusters selected.

The conditional dependence model introduced in Section 5.3.3 was applied to the selected gauged data. The adaptation of the model for use in this thesis was discussed including modification of the de-clustering method used by Keef *et al* (2009a) to use runs de-clustering, which was found in Section 6.3.3 to be more suited for use with naturally varying environmental data. Consideration was also given in Section 6.3.5.1 to dealing with the requirement for concurrent data across all gauges in the network and a simplification of the infilling methodology proposed by Keef (2006) was presented which is more accessible to the non-statistically trained end user. In Section 6.3.6.4 the use of the dependence model to simulate time series of DMF and skew surge over the full duration of the extreme event was presented. This is an extension to previous applications which have used the conditional dependence model for event peaks over a given event time frame.

The extreme event set for use in the systems risk model was developed in Sections 6.3.4 to 6.3.6, including consideration of rejection sampling and time series simulation. These events will be processed further in Chapter 7 to develop a set of peak water levels for use in the inundation model. Consideration of potential uncertainties in the statistical model was made in Section 6.3.7. It is concluded that although uncertainty is inherent in any form of statistical model the conditional dependence model provides a robust means of simulating a variety of dependence conditions between fluvial and coastal sites. The greatest source of uncertainty, common to all statistical extreme analysis, is the lack of data, which is particularly important in this case as concurrent records are required across all gauges in the network. Section 6.3.7.1 illustrated that although some stations experience considerable periods of missing data during the observation period, the infilling methodology proposed is able to reduce the modelling error compared to using observed data alone. Uncertainty could be reduced in the future by repeating the analysis with longer record lengths, in particular for the coastal sites.

Finally in Section 6.4 the spatial and temporal dependencies between the selected gauges in the risk clusters were reviewed highlighting many of the trends in extremes identified by previous studies (see Chapter 5) including the localised nature of the most extreme events. Findings of particular interest to this study were highlighted in Section 6.4.1 and include the dependence between fluvial and coastal events in North Wales, large scale spatial dependencies between North Wales, the Severn and the Thames regions and the relative independence of events on the East Coast.

It has been shown the structure of the gauged network has a strong effect on the visible spatial dependence structures. This should be born in mind by anyone designing future studies of this type and highlights the importance of maintaining a high quality data set of extremes across the UK to ensure data are available at locations of interest in future studies.

7 Statistical and physical modelling of water level

7.1 Extreme events at the receptors

The processes outlined in Chapters 5 and 6 simulate daily mean flows for fluvial gauges and skew surge for coastal gauges. This provides a means of representing the extremeness of an event but it does not reflect the full physical components of the event at the receptors.

Additional transformation and modelling steps are required to represent the event at the sites of interest rather than the gauging station and to incorporate the full temporal dimensions of the event rather than just the peak flow or skew surge.

For fluvial models this includes interpolation between gauges to estimate the peak DMF at the sites of interest and converting the simulated DMF into a peak flow and hydrograph. The processes for doing this are discussed in Section 7.2. For coastal sites, details of the tide and wave height are required to represent the total water level impacting on the flood defences. The variation of the tide, surge and wave components throughout the event also needs to be captured as well as interpolation between gauges to represent the conditions at the sites of interest. The simulation of the multiple components of coastal water levels is discussed in Section 7.3.

Throughout this chapter the FEH physical catchment descriptors (PCDs) are used as specified in the FEH CD-ROM V3 (CEH 2009). A list of the PCD descriptions is provided in Table 7.1.

Table 7.1 Definition of FEH Physical Catchment Descriptors

Descriptor	Definition
AREA	Catchment drainage area (km ²)
BFIHOST	Base Flow Index derived from the HOST soil classification
DPLBAR	Mean of distances between each node on IHDTM grid and the catchment outlet (km), Characterises catchment size and configuration
FARL	Index of flood attenuation attributable to reservoirs and lakes (fraction)
FPEXT	Flood plain extent
PROPWET	Proportion of time when Soil Moisture Deficit was equal to, or below, 6mm during 1961-90
SAAR	Average annual rainfall in the standard period (1961-90) (mm)
URBEXT2000	Extent of urban and suburban land cover in 2000 (fraction)

7.2 Fluvial water levels

7.2.1 Estimating peak flow from DMF

To use DMF for flood risk assessment it is essential to understand the relationship between DMF and flood peak. In all cases the flood peak will be larger than the DMF however the difference depends on the catchment response. For rapidly responding catchments the ratio between DMF and flood peak is large. This reduces as the catchment response slows down since the flood hydrograph makes a greater contribution to the DMF as shown in Figure 7.1. In most catchments there is a strong relationship between DMF and peak flow as shown in Figure 7.2 for 145 gauges across the UK (see Section 7.2.1.2). Hence it is possible to model this relationship.

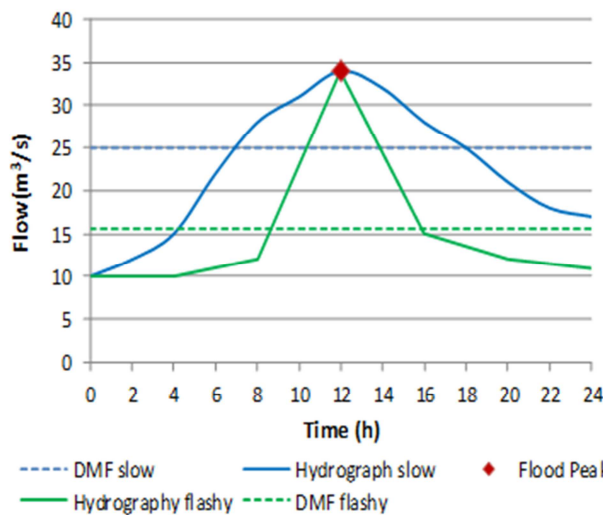


Figure 7.1 Effect of hydrograph shape on POT:DMF ratio

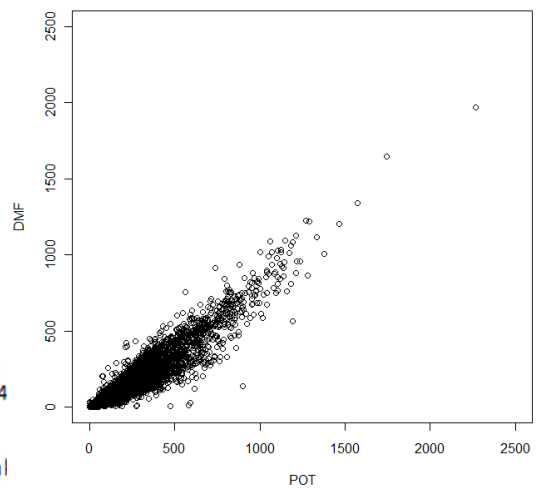


Figure 7.2 Relationship between DMF and POT for UK gauges

7.2.1.1 Existing DMF to peak flow methods

The UK is relatively unique in that there is good temporal and spatial coverage of continuous flow gauges. In other countries often the only readily available dataset is DMF data therefore research has been carried out into establishing relationships between DMF and flood peaks.

Fill and Steiner (2003) provide a comprehensive review of the existing methods. There are two main approaches to the problem, either establishing a relationship based on PCDs such as area, or using the shape of the hydrograph from the posterior and anterior days to estimate the peak flow. Several methods using both approaches are outlined below. There is no evidence to suggest that any of these methods have been tested in the UK.

Methods based on catchment characteristics

The oldest method was developed by Fuller (1914). Working in the USA he proposed that the peak flow (Q_{max}) could be estimated from the DMF (Q) based on catchment area (A) using Equation 7.1.

$$Q_{max} = Q(1 + 2.66A^{-0.3}) \quad 7.1$$

His original sample consisted of a broad range of catchments ranging in size from 3.06 km² to 151,592 km². The strength and ease of applicability of his method is evident in its take up by other hydrologists who have either used it in its original form or modified the coefficients for individual hydrological and climatic regions. A list of the variations is provided by Fill and Steiner (2003), no applications are documented in the UK.

A further modification is to use additional catchment characteristics. One example is that of Silva and Tucci (1998), working in Brazil, who propose a regression based model where the ratio of DMF to peak flow (C) is based on catchment area (A), length of river (L), slope of river (D) and time of concentration (T);

$$C = aA^b L^c D^d T^e \quad 7.2$$

Where a, b, c, d and e are the regression coefficients. Their study is of limited use in this instance since the paper is written in Portuguese, the data set used is not strictly a DMF data set and their results failed to provide evidence of a definitive relationship. However the concept of using a regression model based on catchment characteristics to incorporate more variability between catchments than area alone is a valid one and is explored further below.

Methods based on hydrograph shape

The second approach is based on the theory that the peak flow can be estimated using the ratio of maximum DMF and DMF on the posterior and anterior days, an idea originally pioneered by Langbein in 1944 and Linsley *et al* in 1949 (cit. Fill and Steiner 2003). A more recent application is that of Sangal (1983) who, assuming a triangular hydrograph shape from the posterior (Q_1) and anterior (Q_3) days flows around the maximum DMF (Q_2), estimated peak flow as;

$$Q_{max} = \frac{4Q_2 - Q_1 - Q_3}{2} \quad 7.3$$

Sangal originally developed this method in Canada and it has since been applied in Brazil. One limitation of this approach is that it assumes the flood events lasts for more than 24 hours. For

many small catchments this is unlikely to be the case and results have shown that for catchments of less than 1000 km² the method produces peak flows of up to 50% higher than observed values (Fill and Steiner 2003).

Fill and Steiner (2003) modified Sangal's method to incorporate more detail about the hydrograph shape for individual catchments using;

$$Q_{max} = \frac{0.8Q_2 + 0.25(Q_1 + Q_3)}{k} \quad 7.4$$

where k is a correction factor based on the hydrograph shape factor, x and ϵ is the error term .

$$x = \frac{Q_1 + Q_3}{2Q_2} \quad 7.5$$

$$k = 0.9123x + 0.3620 + \epsilon \quad 7.6$$

In their case study in Brazil this was shown to provide significant improvements to Sangal's method however it is computationally more demanding as a regression analysis is required to establish k for each catchment.

7.2.1.2 Development of method for use in the UK

The three established methods were tested for UK data and compared to the observed flood peaks. The results are shown in Table 7.2. The data set used to test the applicability of DMF to flood peaks methodologies is comprised of 217 standard DMF gauges from CEH (CEH 2009) and POT data from the Environment Agency HiFlows-UK dataset (Environment Agency 2010a). The data were checked for suitability and separated into a calibration and validation set comprising of 145 gauges with both DMF and POT data, as detailed in Appendix C. The results show that all three methods perform reasonably well for UK data across the whole calibration data set.

Table 7.2 Goodness of fit of published DMF to peak flow conversion methods for UK data

Method	Nash-Sutcliffe	RMSE	Bias
Fuller	0.92	0.36	-0.01
Sangal	0.92	0.32	-0.07
Fill & Steiner	0.86	0.39	-0.24

Following initial testing of the methods, further optimisation of the coefficients was carried out for UK data. A detailed description of the process is provided in Appendix C. The results

showed that sensible improvements could be made by optimising the parameters, for example the optimised Sangal coefficients place more importance on the peak DMF than the anterior and posterior days. This corresponds to relatively short UK river systems having a peakier flood response than the larger basins of Canada and Brazil where this method has previously been applied. There is a small improvement in the fit between observed and simulated flood peaks using the optimised method, except for the Fuller method which shows a decrease in the efficiency measures. The lower efficiency for the validation dataset is largely due to a weaker correlation between DMF and flood peak at the validation gauges compared to the calibration data set as illustrated in Appendix C.3.

Table 7.3 Goodness of fit of optimised DMF to peak flow conversion methods for UK data

Method	Nash-Sutcliffe		RMSE		Bias	
	Cal.	Val.	Cal.	Val.	Cal.	Val.
Fuller	0.93	0.89	0.56	0.00	-0.22	-0.24
Sangal	0.92	0.90	0.32	0.45	0.10	0.09
Fill & Steiner (original with UK <i>k</i>)	0.89	0.86	0.34	0.48	-0.01	-0.01
Fill & Steiner (optimised with no <i>k</i>)	0.92	0.90	0.32	0.44	0.12	0.12

The final approach tested was to develop a multiple regression model linking the ratio between DMF and peak flow (*C*) to PCDs. The regression model was built by systematically testing combinations of the FEH PCDs. Consideration was paid to the complexities of developing a hydrological regression model as discussed in the FEH vol. 3 (Robson and Reed 1999) and the potential for cross correlations between the variables leading to model equifinality.

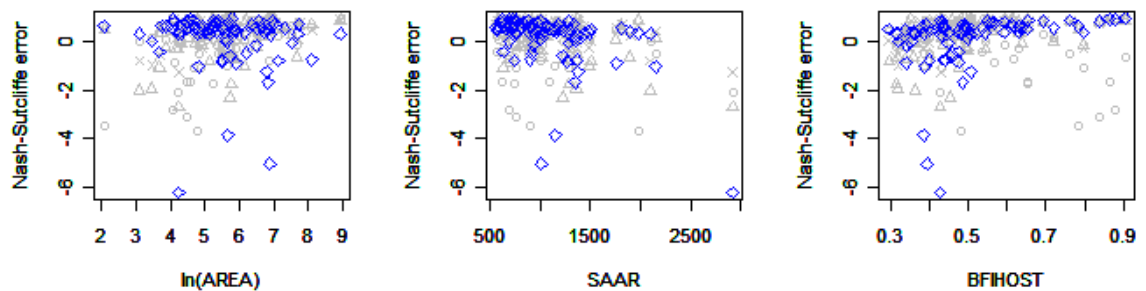
The proposed regression model is given in Equation 7.7 and the model efficiency results in Table 7.4. Across the full data set the regression model performs less well than any of the other models tested except for the un-optimised Fill and Steiner method. However when the results are viewed for individual catchments the regression model is comparable the other methods except for three outlying catchments (Figure 7.3).

The regression analysis identified a possible reason for the poor performance of the Fuller simple area method. DPLBAR was found to be a more useful descriptor than AREA as it incorporates information about both the catchment area and its shape and stream network configuration which is important in determining the shape of the hydrograph.

$$C = 0.0005SAAR - 1.6317BFIHOST + 5.1176FARL + 4.6215URBEXT - 0.0058DPLBAR \quad 7.7$$

Table 7.4 Goodness of fit of DMF to flood peak multiple regression model

	Nash-Sutcliffe		RMSE		Bias	
	Cal.	Val.	Cal.	Val.	Cal.	Val.
Regression model	0.89	0.86	0.38	0.58	-0.11	-0.16



Blue \diamond = regression Grey \circ = Fuller, Grey \times = Sangal, Grey Δ = Fill and Steiner

Figure 7.3 Goodness of fit of DMF: flood peak multiple regression model compared to other methods

7.2.1.3 Proposed DMF to peak flow conversion method for use in the UK

This section has presented four possible methods of transforming DMF data into flood peaks. Overall the optimised Sangal method (as given in Equation 7.8) produces the smallest errors between modelled and simulated data. This method is therefore used to transform the simulated DMF into flood peaks. An additional advantage of the Sangal approach is that it preserves the simulated temporal dependence structure from the conditional dependence model by estimating a peak flow dependent on the DMF at the posterior and anterior days.

$$Q_{max} = \frac{4.2Q_2 - 0.9Q_1 - 0.9Q_3}{2.3} \quad 7.8$$

The methodologies developed in this chapter use POT data as the source of peak daily flow. The relationship between DMF and peak daily flow for less extreme events is likely to be different due to the flatter shape of the daily hydrograph, however, given that flooding is unlikely for events that do not exceed the threshold, Equation 7.8 is assumed to hold for the full range of DMFs. The methods have been tested using a large scale UK dataset and therefore the results are applicable for any UK location.

7.2.2 Interpolating flow to ungauged sites

Due to difficulties in finding long reliable gauged records to fit the conditional dependence model to (See Chapter 6), the simulated flows are not necessarily located at the sites of interest. Therefore when using the model to simulate inflows for flood risk assessments an additional step is required to interpolate flows from the gauging stations to the sites of interest, henceforth referred to as the subject sites.

Flow estimation at ungauged sites is an on-going research area in hydrology (Sivapalan *et al.* 2003). Ideally the subject site and donor gauging station would be located nearby in nested catchments with the same water flowing through them. In this case flows at the subject site can be interpolated by using a simple rescaling method, such as by area. In some cases the subject site can be located on an ungauged tributary or in an adjacent catchment which makes the interpolation to the ungauged subject site more difficult.

The interpolation methods presented in this chapter are based on the premise that by applying some form of transfer function (fn) the simulated flow at the gauging station (Q_A) can be used to estimate the corresponding flow at the subject site (Q_S), as in Equation 7.9.

$$Q_S = fn Q_A \quad 7.9$$

In most cases research has focused on estimation of particular characteristics of the flow regime for example QMED and flood frequency curves in the FEH, and flow duration curves in the low flows literature. Keef *et al* (2009a) use a statistically based standardisation method using the Gumbel distribution. The decision by Keef *et al* to use a statistically based standardisation method was partly motivated by the lack of clear evidence of a strong correlation between physical catchment descriptors and the spatial dependence properties of extreme flows (Keef *et al.* 2009b). Secondly, physically based methods require more data to be collected about the subject catchments and can be more computationally expensive, for example if pooling groups need to be derived. Therefore a statistically based method offers a more practical alternative for the large scale study undertaken by Keef *et al.* In comparison the site based approach taken in this PhD offers more scope for including detail at the sites of interest.

An alternative solution identified by Keef *et al* (2009a), was to introduce covariates into the conditional dependence model to enable it to be used in completely ungauged catchments. This is very computationally demanding and it is difficult to define quantitative relationships between catchment descriptors and the parameter of the dependence model. Keef *et al* therefore reject this approach, and no further consideration of it is given in this project.

7.2.2.1 Existing interpolation methods

Scale by catchment area

The simplest method of simulating time series data is to scale by area using the standard format given by the World Meteorological Organisation (2008);

$$Q_S = fn \left(\frac{A_S}{A_A} \right) Q_A \quad 7.10$$

Where A_S and A_A are the areas of the subject and donor catchments accordingly. For simple area scaling the fn function is normally set to 1 although other factors could be included for example the ratio of average annual rainfall is sometimes used to incorporate the influence of differences in rainfall (World Meteorological Organisation 2008).

Although this method is simple to apply, it is limited by its simplicity as flood flows are likely to be influenced by multiple interacting catchment characteristics. However for nearby connected sites an area scaling method offers a robust and efficient means of transferring flow estimates.

Scale by QMED

An alternative to using the flow duration curve approach is to standardise by QMED;

$$Q_S = QMED_S \left(\frac{Q_A}{QMED_A} \right) \quad 7.11$$

QMED can be estimated at the analogue site using gauged POT or AMAX data and at the subject site using catchment descriptors as outlined in the FEH (Robson and Reed 1999; Kjeldsen *et al* 2008). Using QMED rather than catchment area allows for inclusion of some local influence through the local estimate of QMED. However QMED is a stationary measure of the flow response in the target catchment and does not incorporate the potential variation in the ratio of flood flows to QMED between the target and subject sites.

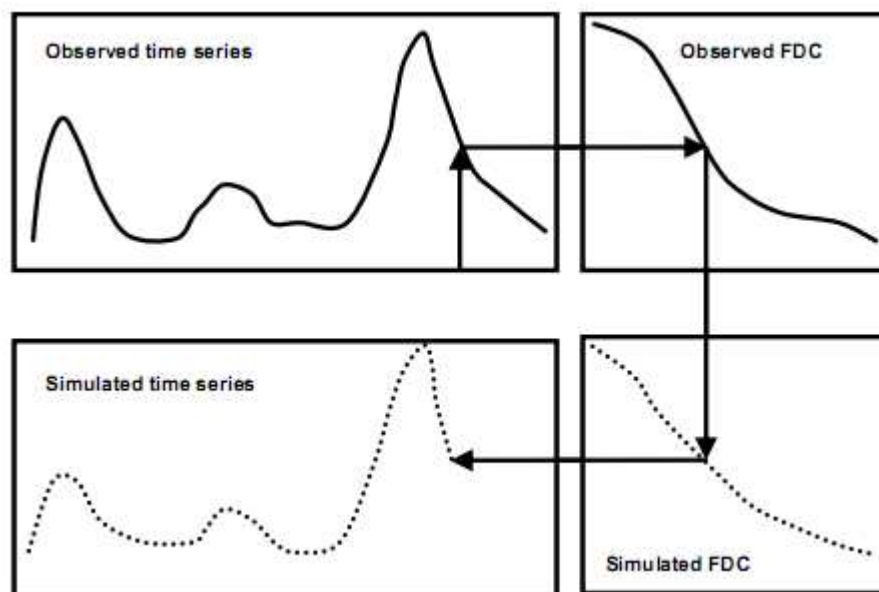
Equipercntile method from growth curves

Within the low flows literature the equipercntile method is often used as a robust method of infilling gaps in time series data (for example see Harvey *et al.* 2010). Flow duration curves are established for the gauged analogue site using the DMF record, and for the ungauged site using the region of influence approach within the Low Flows software (Holmes *et al.* 2002).

The time series at the ungauged location can then be simulated as shown in Figure 7.4.

The advantage of this method over the simple area based method is that the dependence characteristics of the flood event are maintained by sampling the exceedance probability from the analogue catchment while the actual DMF includes the influence of the local catchment through the local flow duration curve.

The same principles can be applied using Flood Growth Curves estimated in the Winfap-FEH software as described in the Flood Estimation Handbook Vol. 3 (Robson and Reed 1999). The use of this method is computationally demanding as the simulated DMFs must be transformed to peak flows prior to interpolating to the ungauged site, and secondly pooling groups need to be established for the subject and analogue sites (of which there could be several for each subject site). This is particularly onerous when the subject site is located on the same river as the analogue sites, in which case it may be more appropriate to use a simple area or QMED scaling method. Although it is acknowledged that the equipercenile growth curve interpolation method could be particularly useful for time series interpolation, the difficulties in testing the method in the absence of a concurrent series of peak flow data meant it was not possible to test the method sufficiently for inclusion in this project.



Source: World Meteorological Organisation (2008, p86)

Figure 7.4 Illustration of the equipercenile technique to simulate time series at ungauged site

Catchment centroids

Keef *et al's* (2009b) investigation into the importance of catchment descriptors on the spatial dependence of flow identified the distance between centroids as the most important factor. Recent work on updating the FEH procedures (Kjeldsen *et al* 2008) has also identified distance

between centroids to be a more important factor in the estimation of QMED from analogue stations than other catchment descriptors. The advantage of using distance between catchment centroids rather than between the sites is that more weight is given to nested catchments than adjacent ones.

The weighted average of distance method used by Keef *et al* (2009a) is given in Equation 7.12.

$$X = \frac{\sum_{i=1}^N X_i d_i^{-1}}{\sum_{i=1}^N d_i^{-1}} \quad 7.12$$

Where d_i is the geographical distance between catchment centroids for site i and the site of interest X . And X_i is the DMF on the Gumbel scale at site i .

Shared catchment area

An alternative method trialled by Keef *et al* (2009a) was a shared catchment area method as shown in Equation 7.13 where the subject site flow is calculated from the upstream and downstream donor gauges. X_{UP} and X_{DOWN} are the DMFs on a Gumbel scale at the upstream and downstream stations respectively and A_{UP} and A_{DOWN} are the catchment areas.

$$X = X_{DOWN} + (X_{UP} - X_{DOWN}) \left(\frac{A_{DOWN} - A}{A_{DOWN} - A_{UP}} \right) \quad 7.13$$

If there are multiple upstream gauges, A_{UP} becomes the sum of all upstream catchment areas and X_{UP} a weighted average of all upstream flows.

$$X_{UP} = \sum_{k=1}^{n_{UP}} \frac{X_k A_k}{A_{UP}} \quad 7.14$$

Initial testing by Keef *et al* (2009a) indicated that there was little difference in the performance of the catchment centroids and shared catchment area methods, however later application to the northeast of England suggested that the catchment centroids method performed slightly better. In addition the catchment centroids method is preferable because it can be applied to any location whereas the shared catchment area method is dependent on the existence of a connected donor station upstream or downstream of the subject site. Only the catchment centroids method is considered further in this thesis.

7.2.2.2 Selection of suitable donor and analogue gauges

Prior to application of any of the above methods suitable donor sites need to be identified. Common criteria for doing this include consideration of distance between locations and catchment similarity (Kjeldsen *et al.* 2008; Keef *et al.* 2009a).

The Flood Estimation handbook identifies suitable sites for inclusion into pooling groups based on catchment similarity. The PCDs used are AREA, SAAR and BFIHOST (see Table 7.1). As part of the update to the FEH method, Kjeldsen *et al* (2008) developed a new weighting method for selecting pooling group catchments (Equation 7.15) which removed BFIHOST, and added FARL and the new descriptor FPEXT. These two additional variables provide information on the flashiness of response based on storage in the catchment from both lakes and reservoirs and on the floodplain during extreme events.

$$SDM_{ij} = \sqrt{3.2 \left(\frac{\ln AREA_i - \ln AREA_j}{1.28} \right)^2 + 0.5 \left(\frac{\ln SAAR_i - \ln SAAR_j}{0.7} \right)^2 + 0.1 \left(\frac{FARL_i - FARL_j}{0.05} \right)^2 + 0.5 \left(\frac{FPEXT_i - FPEXT_j}{0.04} \right)^2} \quad 7.15$$

The distance measure, SDM, and the individual PCDs are considered as measures of catchment similarity. FARL and FPEXT are not included individually as they only provide information on a small factor of the overall catchment response. In addition, work by Ledingham (2011) identified that PROPWET can be a useful indicator of catchment response as it incorporates the significance of antecedent conditions on catchment response. Catchments with a high value of PROPWET are more likely to experience high flow events due to the inability of the soil to soak up additional rainfall.

7.2.2.3 Testing of methods for interpolation to ungauged sites

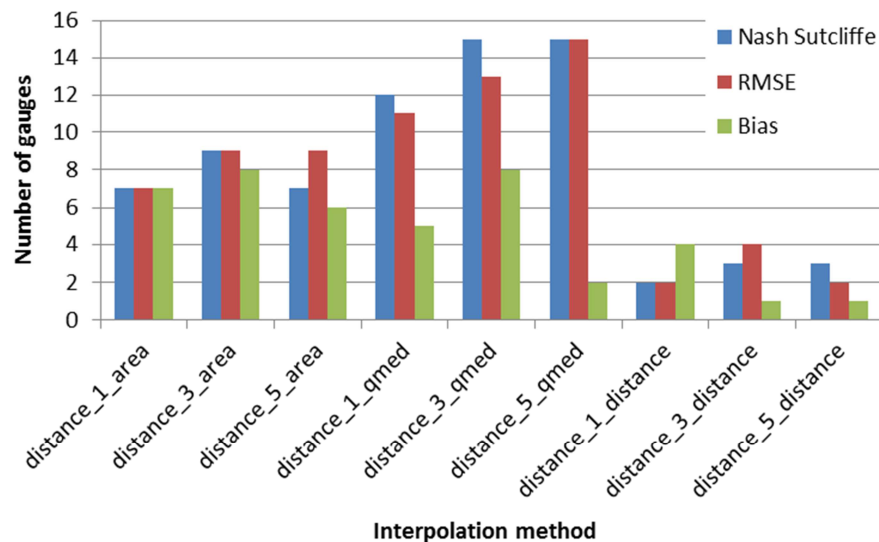
Potential interpolation methods were tested for use in this thesis using the dataset of 145 DMF gauges introduced in Section 7.2.1.2, however the selection of a suitable method was hampered by two problems. Firstly a continuous set of flood peak data was not practical for use in this study and converting to peak flows resulted in uncertainties in the dataset which varied from gauge to gauge. The interpolation methods were therefore only tested using the available DMF data rather than flood peaks. Secondly the spatial distribution of gauges in the sample dataset was large meaning when testing the methods using a jackknife approach, the distances between gauging stations were considerably larger than the distances between gauging station and subject site to which the method will ultimately be applied to.

Three interpolation methods were investigated; scaling by catchment area, scaling by QMED and Keef *et al*'s catchment centroids method. As the interest is in peak flows, the data at each gauge was de-clustered as described in Section 6.3.3 and the peaks at the subject site used as a proxy to identify extreme events. It is acknowledged that when applying the method the

peak event will occur at the donor site, however this was the only way to identify a consistent set of event peaks for use across multiple donor sites. The Nash-Sutcliffe coefficient, the RMSE, and the bias were calculated between the observed and simulated data at each gauge.

Potential donor sites were identified by minimising the distance between centroids, AREA, SAAR, BFIHOST, PROPWET and SDM. To preserve the spatial dependence structure, potential donor sites selected from PCDs were restricted to within 100km of the subject site catchment centroid. For each criteria the closest, three closest and five closest gauges were identified. Where more than one donor site was used all sites were given equal weighting. Detailed results for the best method at each gauging station are given in Appendix C.7.

Selecting donor sites by distance between catchment centroids provided the best fit in over 50% of cases. For donor sites selected by distance between catchment centroids, Figure 7.5 shows the number of gauges for which each tested interpolation method provided the best fit. The QMED criteria produced the best fit over the largest number of gauges. There is little change between the number of donor sites used however three sites provides a lower bias at more sites. For all donor site selection methods, interpolating by QMED also provides the best fit in over 50% of cases.



Interpolation methods are listed as “search criteria_number of donor gauges_interpolation method”

Figure 7.5 Number of gauges for which each tested ungauged site interpolation method provided the best fit with observed DMF

The Nash-Sutcliffe efficiency test provides the most useful means of comparison as it is standardised across all gauges. In half of the gauges the best fitting interpolation method

produces Nash-Sutcliffe values less than one meaning that the interpolation method is worse than simply taking the mean value at the donor site. This is a concern as it suggests that none of the methods are suitable, however the dataset used to test the interpolation methods is sparse with the average distance between the nearest gauge pairs being 21km but ranging up to 74km. In reality the gauges used in the conditional dependence model (as listed in Table 6.8) are located as near as possible to the sites of interest, therefore it is assumed that the interpolation methods will perform better than for the test dataset which is not sufficient to develop a methodology for interpolation to ungauged sites. Whereas the AREA and QMED scaling method allows for inclusion of individual catchment properties in the estimation of flow at the ungauged sites the catchment centroids interpolation method uses only the distance between sites. This is potentially why it performs poorly in this test case as the distances between gauges is large and therefore the gauges in the test dataset do not respond in similar way to the same event.

Proposed interpolation to ungauged sites method

In the absence of detailed dataset to develop a robust interpolation method for ungauged sites it is proposed to use the QMED scaling method. This method performed best for the test dataset and offers a good compromise between a simple approach and incorporating known characteristics of the flow response at the subject site through the use of QMED. The choice between number of donor sites to use is location specific. Where the model inflow point occurs on an ungauged tributary with multiple tributary confluence between the inflow point and the simulated gauging stations, up to three donor sites can be used to introduce natural variability into the results. Where the model inflow point is situated close to the simulated gauging station only one donor site will be used.

QMED is estimated at the ungauged model inflow points from catchments descriptors and modified using the nearest donor gauges as recommended by Kjeldsen *et al* (2008). The QMED values for each of the model inflow points are given in Appendix C.8.

7.2.3 Event Hydrographs

A full hydrograph is required for hydraulic modelling. Although the conditional dependence model can be used to simulate event time series (See Section 6.3.6.4) the model is fitted to DMF data and, for most catchments in the UK, DMF is not detailed enough to represent the full event hydrograph (Robson and Reed 1999).

7.2.3.1 Single site event hydrographs

A standard means of producing a flood hydrograph is to borrow a standard hydrograph shape from a rainfall-runoff methodology which creates a hydrograph from catchment descriptors based on time to peak (CEH 1999). The standard 1% AEP year hydrographs produced using the ReFH Rainfall-Runoff method (Kjeldsen 2007) at gauges 54001 and 66001 are shown in Figure 7.6 and Figure 7.7. In particular at 66001, a small flashy catchment, the event hydrograph is shown to rise and fall within a 20 hour period, the details of which would not be captured in the daily data.

An advantage of using a rainfall-runoff model to produce a flood event hydrograph is that the method can be applied at any location by extracting the PCDs from the FEH CD-ROM and does not require gauged data. The limitation of this approach for use in a systems based risk model is that it can only produce one standard hydrograph shape. In most cases flood events can occur from a variety of different scenarios. For floodplain inundation modelling the flood volume is particularly important as different event types are likely to have different volumes of flow.

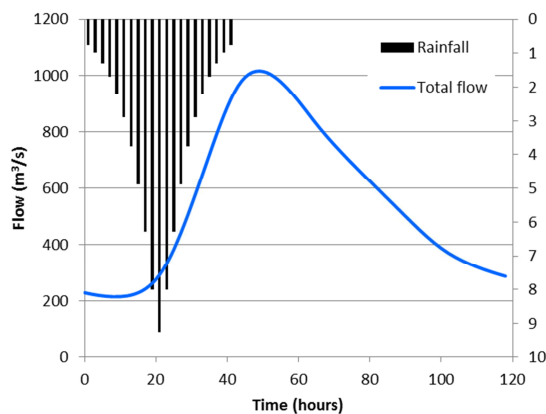


Figure 7.6 ReFH design hydrograph: 54001

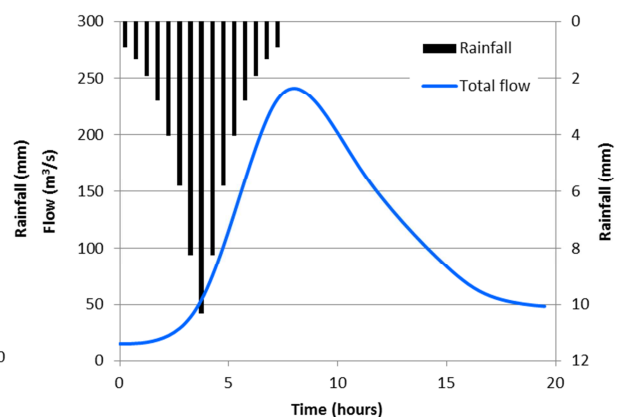


Figure 7.7 ReFH design hydrograph: 66001

Apel *et al* (2004; 2006) and Vorogushyn (2009) present a method to synthesise standard hydrograph shapes using Wards Clustering which they then use to sample a range of realistic input hydrographs within a Monte Carlo framework. This method is attractive for use in a systems based model as it allows consideration of the full range of flood driving events, however when tested for use with the catchments included in this study it was found that the DMF data did not provide sufficient detail to capture flood events in the smaller catchments. Therefore the simple method of using standard hydrograph shapes from the ReFH-Spreadsheet is used to provide input hydrographs for the hydraulic model (See Section 7.2.4). The hydrographs are scaled to match the peak flow estimated in Section 7.2.1. The Wards

Clustering method was found suitable for surge shapes and is described in more detail in Section 7.3.1.

7.2.3.2 Multi-site event hydrographs

Whilst the flood event itself may only last for several hours, the event based nature of the systems risk model requires consideration of the relative lags between sites to investigate the potential interactions around tributaries. The event time series simulation from the conditional dependence model allows incorporation of the relative timing of events at different tributaries.

Simulated DMFs outside of the range of the ReFH hydrograph are scaled by the ratio between the simulated event peak DMF and the estimated peak flow. It is acknowledged that the ratio between DMF and flow at any point in time may not be the same as the ratio between DMF and the peak flow however this simplification is used here as it is assumed that lower flow events will not produce flooding. An example of the process is given in Section 7.2.5.

The interface between the event hydrograph and the simulated DMFs shows a reduction in river flow immediately before and after the event. This is because the ReFH rainfall-runoff hydrograph assumes the river is at base flow before and after the event whereas in reality flows will depend on the antecedent conditions. Example simulated hydrographs for the Severn cluster are shown in Appendix C.8.

7.2.4 Physical modelling of river levels

1D hydraulic models have been used to route flow through the river sections of interest and to convert the simulated flood flows to water level. Models were constructed using the hydraulic modelling software ISIS. Due to the combination of limited data availability for the purpose of this project and the requirement for fast, stable hydraulic modelling simplified model cross sections were generated from the available 2m LiDAR data. The available data for construction of the hydraulic models are listed in Table 7.5.

Table 7.5 Available data for hydraulic river modelling

Item	Comments
Existing hydraulic models	An ISIS model of the River Severn exists but it is currently being updated by the Environment Agency and therefore not available for use. Short sections of existing river model were provided by the Environment Agency in North Wales however these did not fully cover the reaches of interest
Cross section survey	Not available – currently being re-surveyed by Environment Agency for the River Severn and no sections available for other areas
Topographic data	2m LiDAR obtained from Environment Agency
Map data	Ordnance Survey 1:50,000 maps obtained from DigiMap

In the absence of cross section data simplified cross sections were estimated from LiDAR data assuming a standard trapezoidal channel shape as follows;

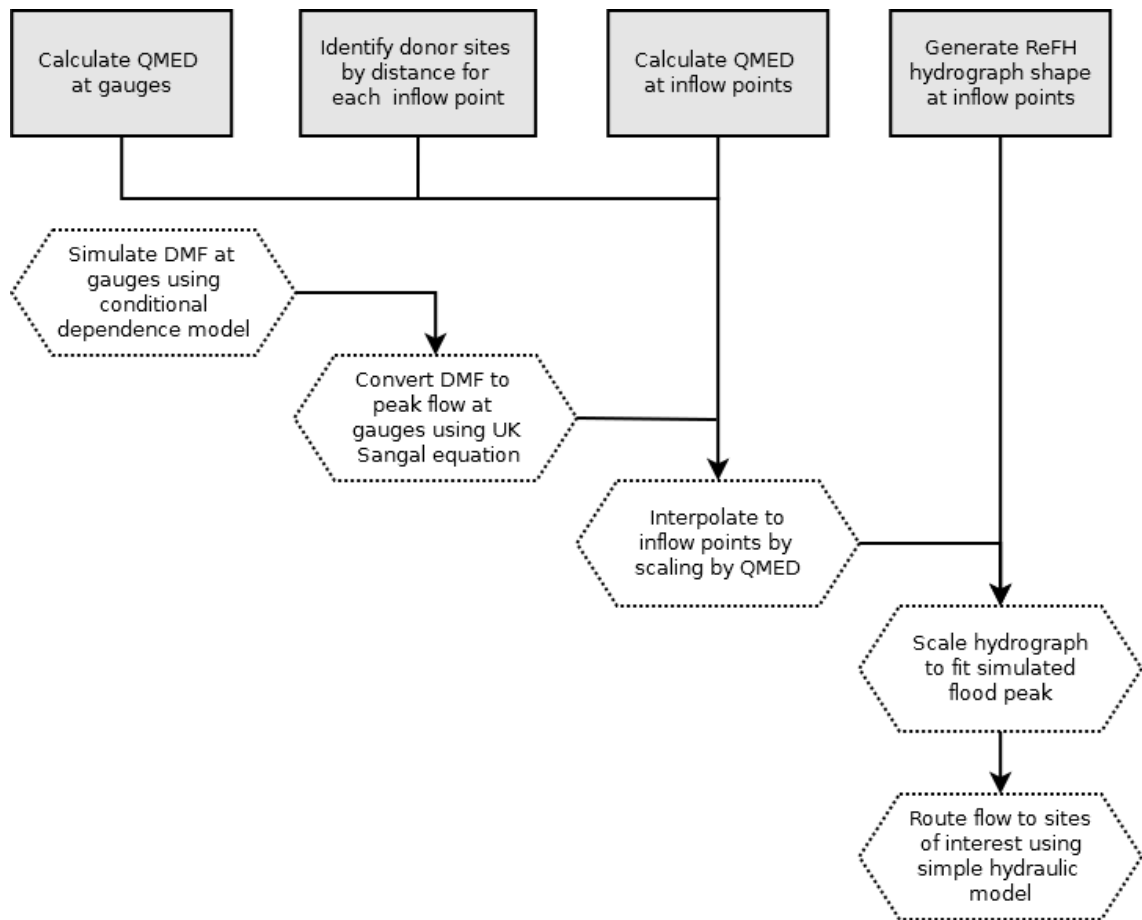
1. Estimate river width - Cross sections were extracted from the LiDAR data and the left and right banks identified as the point with the largest change in height between adjacent points. This was then checked by eye when reviewing the data.
2. Estimate bank full volume – at gauging stations this was available from the HiFlows-UK rating curves, at all other sections bankflow was assumed to be equivalent to QMED. QMED was estimated at the start and end point of each modelled reach and interpolated by distance for intermediary sections.
3. Estimate channel shape – assuming a trapezoidal shape with the top width set to the estimate river width, linear optimisation was used to establish the bed depth and channel width at the bed.

The process is illustrated in Appendix C.8 for the River Severn model. Long section plots were checked to ensure the river profile was realistic with no sudden changes in bed height. In the simple model bridges and other structures were not included. Floodplains were modelled using storage cells connected to the main channel by spill sections. Further details of the inundation modelling are given in Section 7.4.

7.2.5 Summary of fluvial flow simulation

A summary of the end to end water level simulation method is shown in Figure 7.8. Due to the pre-processing requirements to calculate QMED at each gauging station and model inflow point, and to generate representative hydrographs for each model location, this methodology is only suitable for a relatively small number of model inflow points. This illustrates the benefit of using a nested model structure which enables this detailed physical basis to be embedded within the systems model without compromising the representation of large scale events. An illustration of the end to end process for fluvial modelling in the River Severn cluster is given in Appendix C.8.

Given the uncertainty in interpolating to model inflow points due to the lack of suitable data to test the methodology, the simulated DMF are converted to peak flows at the gauging stations prior to interpolation. This prevents the propagation of additional uncertainties through the conversion method.



Grey boxes are calculated once for each site. Unshaded boxes are calculated for each event. Dotted lines have a temporal component.

Figure 7.8 Summary of physically based fluvial event simulation method

7.3 Coastal water levels

The total water level during a storm is made up of three components, the surge and tide components which together provide the still water level, and an additional wave component. The combination of all three is essential for modelling the impact of storm events on defences. Each component is considered individually below including discussion of its temporal and spatial variation. Section 7.3.5.2 describes how the various components are combined to provide a realisation of the total water level for each simulated event.

For ease of presentation most plots in this section refer to data on the Lincolnshire coast at Immingham (for tidal and surge data) and Dowsing (for wave data). Equivalent plots for other

gauges used in this project are provided in Appendix D.1. Where the data trends at other gauges are significantly different to Immingham and Dowsing they are discussed in the main text.

7.3.1 Surge component

The conditional dependence model is fitted to the skew surge at high tide and can be used to simulate a series of high tide skew surges (See Chapter 6).

Since the skew surge is only defined once per tidal cycle additional data is required to represent the growth and decay of the surge. This could involve using the surge residuals at each time step; however these are known to falsely represent the magnitude of the surge at mid-cycle due to temporal offsetting of the tide and observed water level (See Section 5.2.1.2). A more representative method is to calculate the low water skew surge and interpolate between the high and low water level skew surge to generate the full surge shape. This is the approach taken by the EA Coastal Flood Boundary Conditions project (SC060065, McMillian *et al.* 2011a), however unlike McMillian *et al* no attempt has been made in this thesis to interpolate between high and low tides as an increase in data resolution is not required for the purpose of this study.

McMillian *et al* (2011a, p126) reviewed surge profiles from around the UK and concluded that “skew surge profiles typically have one large surge peak lasting between 40 and 90 hours, and in some cases secondary peaks before and/or after the principle peak. In almost all cases and sites in the UK, the surge profiles also exhibit a fair amount of random, low magnitude (and less the 0.4mOD) noise before and after the primary peak.” The surge profiles at Immingham shown in Figure 7.9 and Figure 7.10 reflect this description although the largest surges at Immingham rarely last more than 24 hours. There are some occasions where the low water skew surge at Immingham is higher than the high water skew surge. Although this will not increase water levels at low tide to a dangerous level, it is important to consider as it means that the water level may not drop immediately with the tide and could lead to longer duration floods.

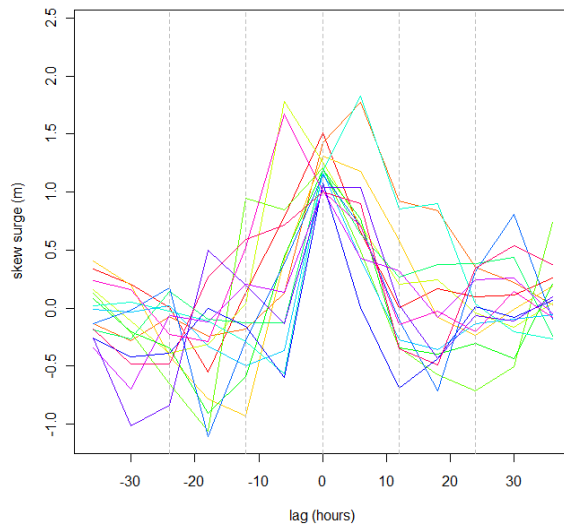


Figure 7.9 Fifteen largest surges at Immingham: 1960 - 2010

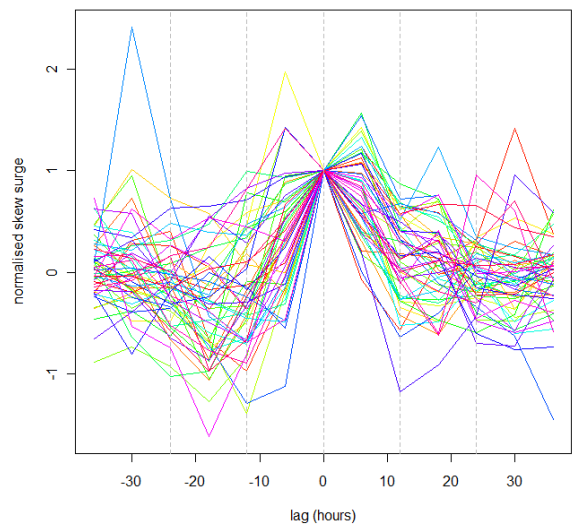


Figure 7.10 Normalised AMAX surges at Immingham: 1960 - 2010

The EA Coastal Flood Boundaries project (McMillian *et al.* 2011a) is aimed at providing a clear and concise methodology for practitioners for considering coastal water levels. For this purpose they have defined one standard surge shape using the 15 highest observed surges per region of the coast. In this thesis there is more flexibility and a variety of curve shapes can be included to maintain the natural variability in the risk model.

The approach used here is similar to the method used by Apel *et al.* (2004; 2006) and Vorogushyn (2009) for fluvial hydrographs. The attraction of this method is that a series of different surge shapes are produced which are then sampled based on their occurrence probability. The method works by normalising the AMAX surge shapes (as shown in Figure 7.10) then using Ward's algorithm (applied using code from Quick-R (2010) and the hclust hierarchical clustering method available from the R Stats package) to cluster the surge shapes based on minimising the distance between the centroids of each cluster and its member surge shapes.

The cluster dendrogram produced by the algorithm is shown in Figure 7.11, the coloured boxes represent the groups the surge shapes are assigned to (each colour illustrates a different total number of groups) and the numbers represent the AMAX event reference number. The number of groups required was tested for surge shapes at Immingham.

Figure 7.12 shows the average surge shapes produced by the method for different numbers of groups. Three distinct shapes can be identified;

1. A lagged skew surge event where the following low tide skew surge is higher than the high tide surge
2. A rapidly rising surge where the preceding high tide has a very low skew surge
3. A symmetrical surge shape with slightly increased high tide skew surge before and after the peak high tide skew surge

Therefore at least three groups are needed to fully represent the different surge shapes. Using more than three groups results in slight variations of the above three significant shapes and offers limited additional benefit. Three groups were also found to be adequate at the other tide gauges of interest (Cromer, Liverpool Bay, Llandudno and Holyhead) as illustrated in Appendix D.1. The probability of each surge shape is calculated based on the number of occurrences in the data set. For the three groups shown in Figure 7.12d the probabilities are given in Table 7.6, along with the surge shapes and associated probabilities for all gauges of interest.

There is some spatial variability evident in the surge shapes. Compared to Immingham, gauges in North Wales experience some surges with much longer durations where the normalised high tide skew surge remains above 0.2 up to 36 hours before and after the surge peak. There are also a few occasions at Liverpool, and to a lesser extent Llandudno, where a double peaked surge occurs. This could be due to the local bathymetry affecting the storm surge in the enclosed estuary around Liverpool however more detailed analysis would be required to support this explanation.

Comparison of the single averaged surge shape at Cromer from Wards algorithm, with the single averaged surge shape provided in McMillian *et al* (2011a) in Figure 7.13, shows close similarities in terms of the duration of the surge event and shape of the surge recession. These similarities give credibility to both methods.

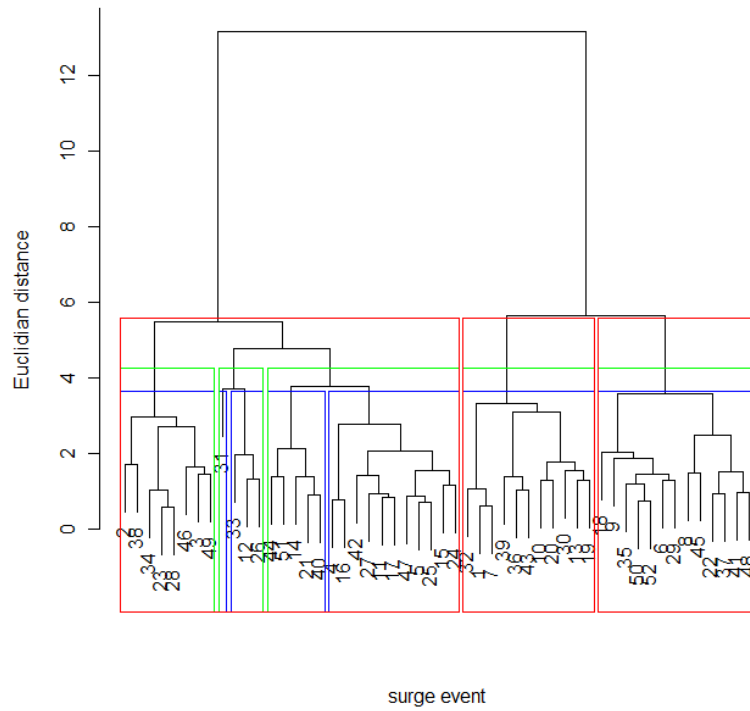


Figure 7.11 Immingham surge shape cluster dendrogram using Ward's clusters

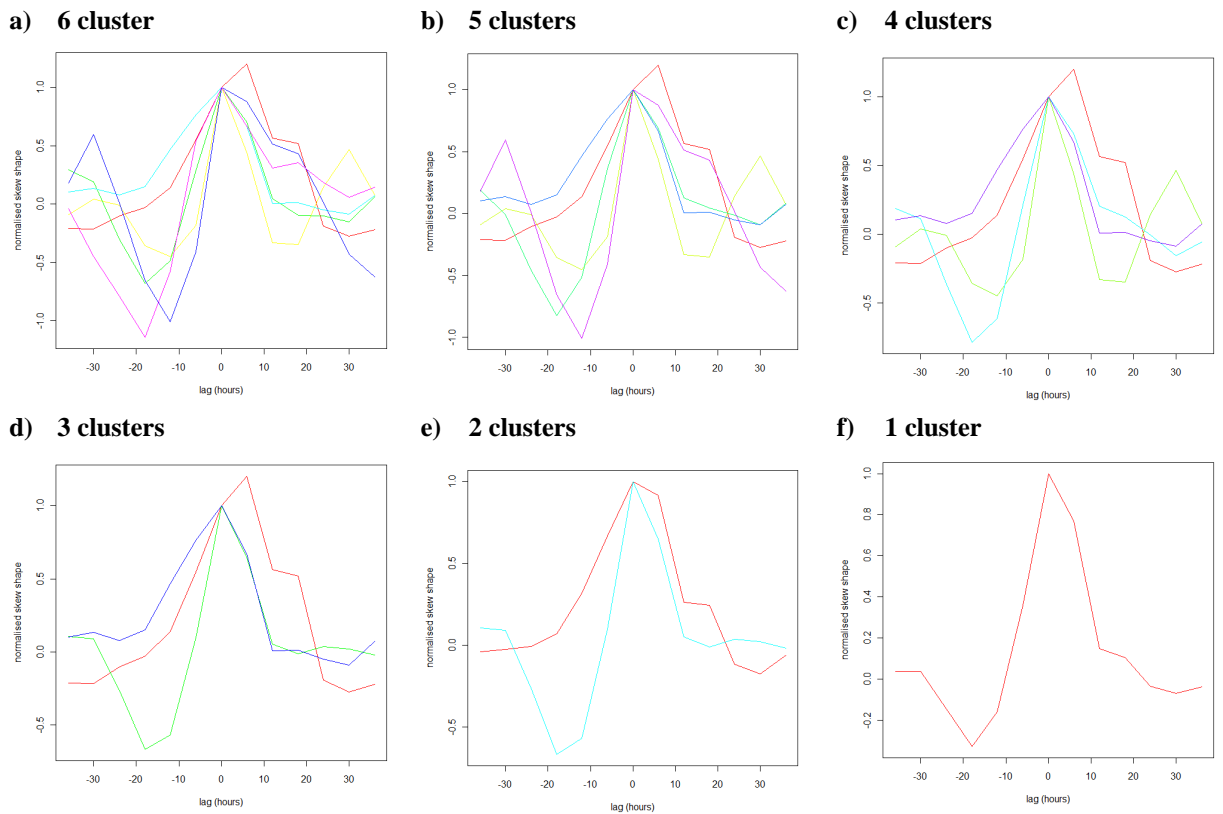
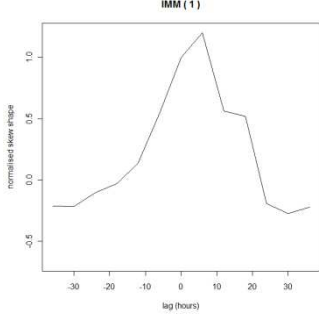
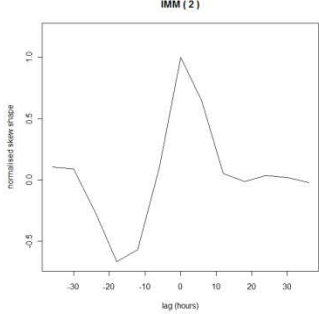
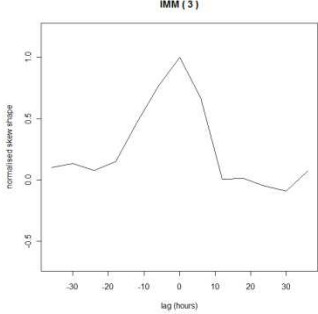
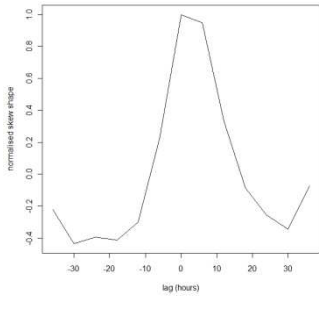
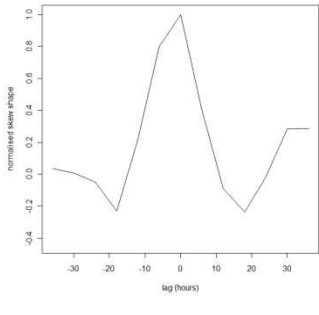
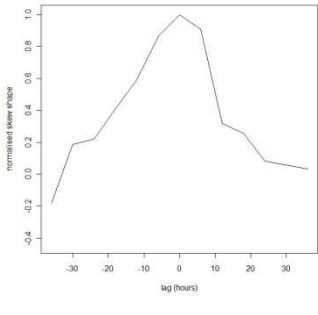
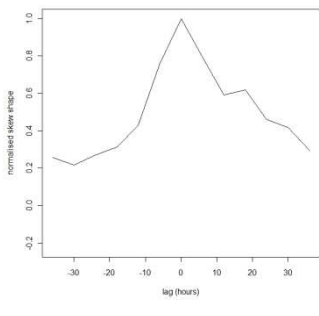
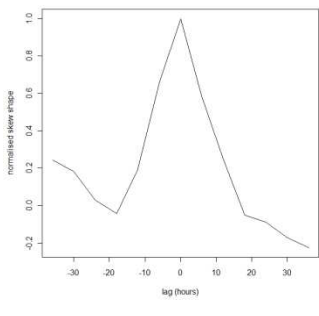
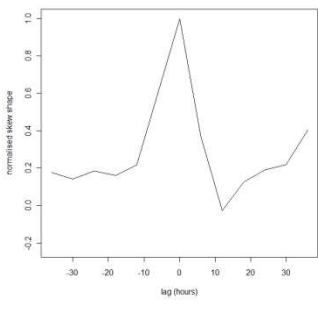
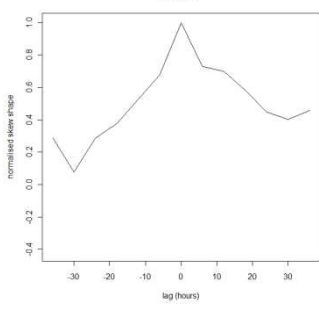
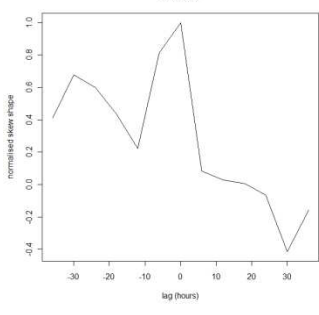
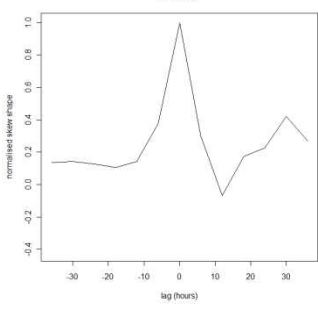
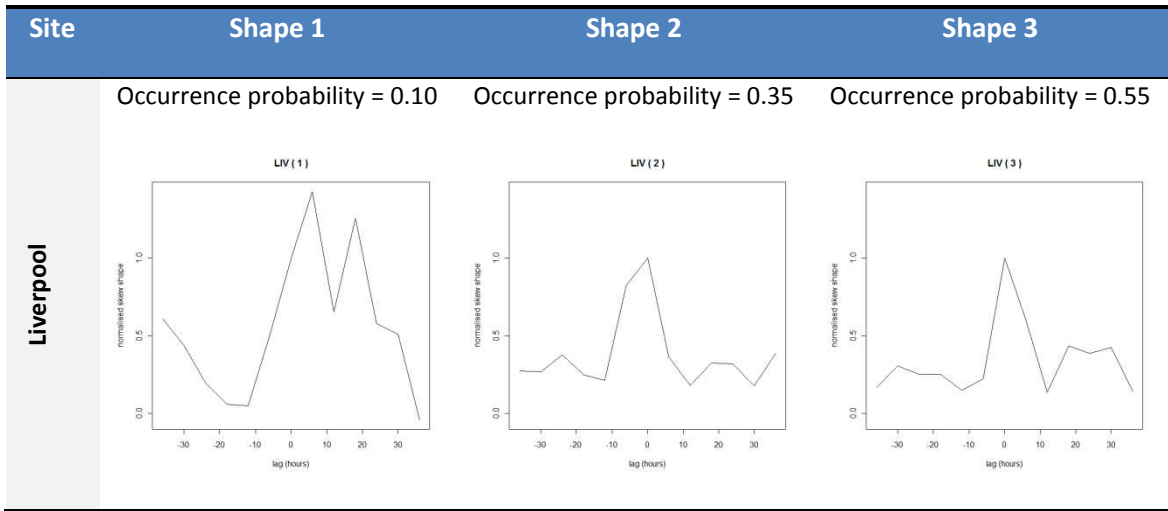


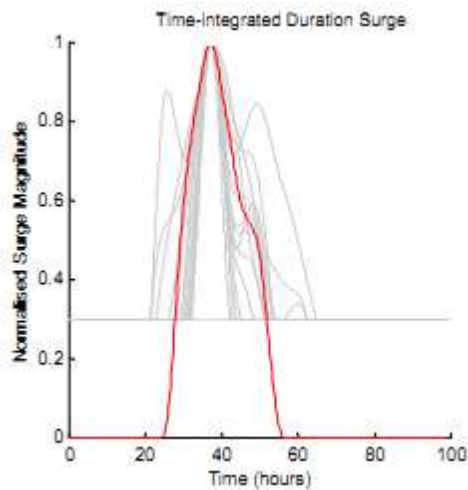
Figure 7.12 Averaged surge shapes produced using Ward's clusters with different numbers of cluster groups at Immingham

Table 7.6 Three representative surge shapes calculated used Ward’s clusters for core coastal sites and their occurrence probabilities

Site	Shape 1	Shape 2	Shape 3
Immingham	Occurrence probability = 0.21 	Occurrence probability = 0.54 	Occurrence probability = 0.25 
	Occurrence probability = 0.27 	Occurrence probability = 0.42 	Occurrence probability = 0.31 
	Occurrence probability = 0.38 	Occurrence probability = 0.25 	Occurrence probability = 0.37 
Llandudno	Occurrence probability = 0.33 	Occurrence probability = 0.17 	Occurrence probability = 0.50 

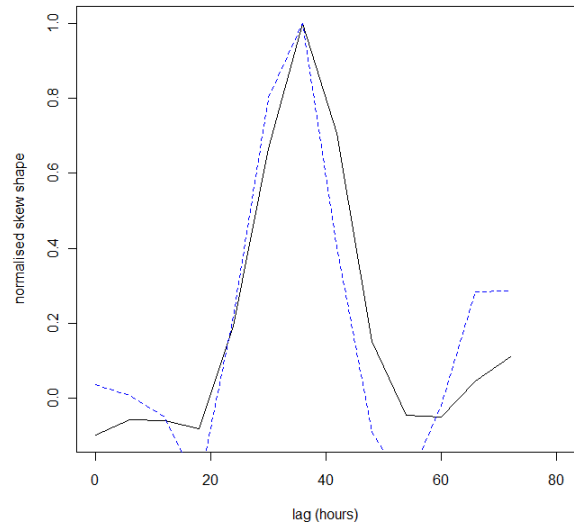


a) EA Time integrated surge shape



Source: McMillian *et al* (2011a, p129)
 Grey lines are the 15 sampled surge events
 Red line is the averaged surge

b) Wards algorithm averaged surge shape



Black solid line is the single averaged curve shape
 Blue dashed line is the most probably of the three averaged surge shapes in Table 7.6

Figure 7.13 Comparison of time-integrated duration surge shape with Wards algorithm surge shape at Cromer

7.3.1.1 Simulation of surge shape

Generating a sample surge shape for the full event duration requires four steps:

1. Simulate a peak event high water skew surge from the conditional dependence model.
2. Simulate skew surges at the previous and following high waters to maintain large scale dependencies and temporal dependencies for lags of up to 36 hours from the conditional dependence model.

3. Sample a surge shape from Table 7.6 and rescale it to fit the sampled peak event high water skew surge from step one.
4. Modify the surge shape to incorporate the simulated high water skew surges from step two.

Although step four will cause some deformation of the surge shape this is unlikely to be significant as the skew surges +/- 12 hours from the peak are relatively small and already incorporate a notable amount of noise (see Figure 7.10). This method therefore provides an acceptable compromise to maintain the larger scale dependence structures in the conditional dependence model while describing the surge shape between high tides.

Other options considered for this step were to use the conditional dependence model to simulate a series of high water skew surges and linearly interpolate between them at low water however since the surge is usually quite small by the previous or next high water level this will under estimate total water level over the full cycle and will not represent the slow decaying events identified in Figure 7.12. Alternatively, the conditional dependence model could have been used to simulate a series of high water skew surges then match these to the most representative surge shape from Table 7.6 to simulate the full surge profile at low water or to fit the model to both high and low water skew surge. The computational demands of this approach would be high.

7.3.2 Tide component

Unlike the surge component, the tide is deterministic and can be predicted well in advance. To incorporate the full nodal cycle (see Section 5.2.1.2), a sample period of 18.6 years of tide data is used for each gauge (extending back from the most recent record). For each event a tide curve is sampled and the tide level extracted for a lag of 36 hours before and after the peak at each gauging station. This means that every possible tidal cycle is given equal probability in the sample set. This data needs to be concurrent so the same tide day can be sampled at each site to maintain the spatial consistency. Where short gaps in the tidal record exist these can be infilled using linear interpolation from the observed values.

The advantage of using skew surge rather than the tidal residual is that skew surge is independent of the tide as shown in Figure 7.14. This means that a tide event can be sampled independently of the simulated skew surge.

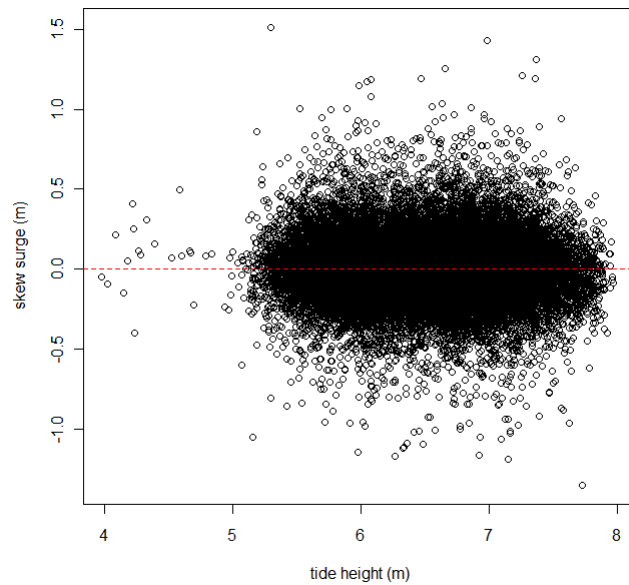


Figure 7.14 Evidence of independence of skew surge and tide height at Immingham

No consideration of sea level rise is made in this project. It is acknowledged that sea level rise in the UK has been around 1.5mm per year over the twentieth century (Pugh 2004), and will continue to rise in the future. Tides sampled from 18 years ago could therefore under predict the current total water level by up to 30mm, this is unlikely to be significant given the other uncertainties in this model but could be modified in the future if required or increased to incorporate possible climate change scenarios.

7.3.3 Wave component

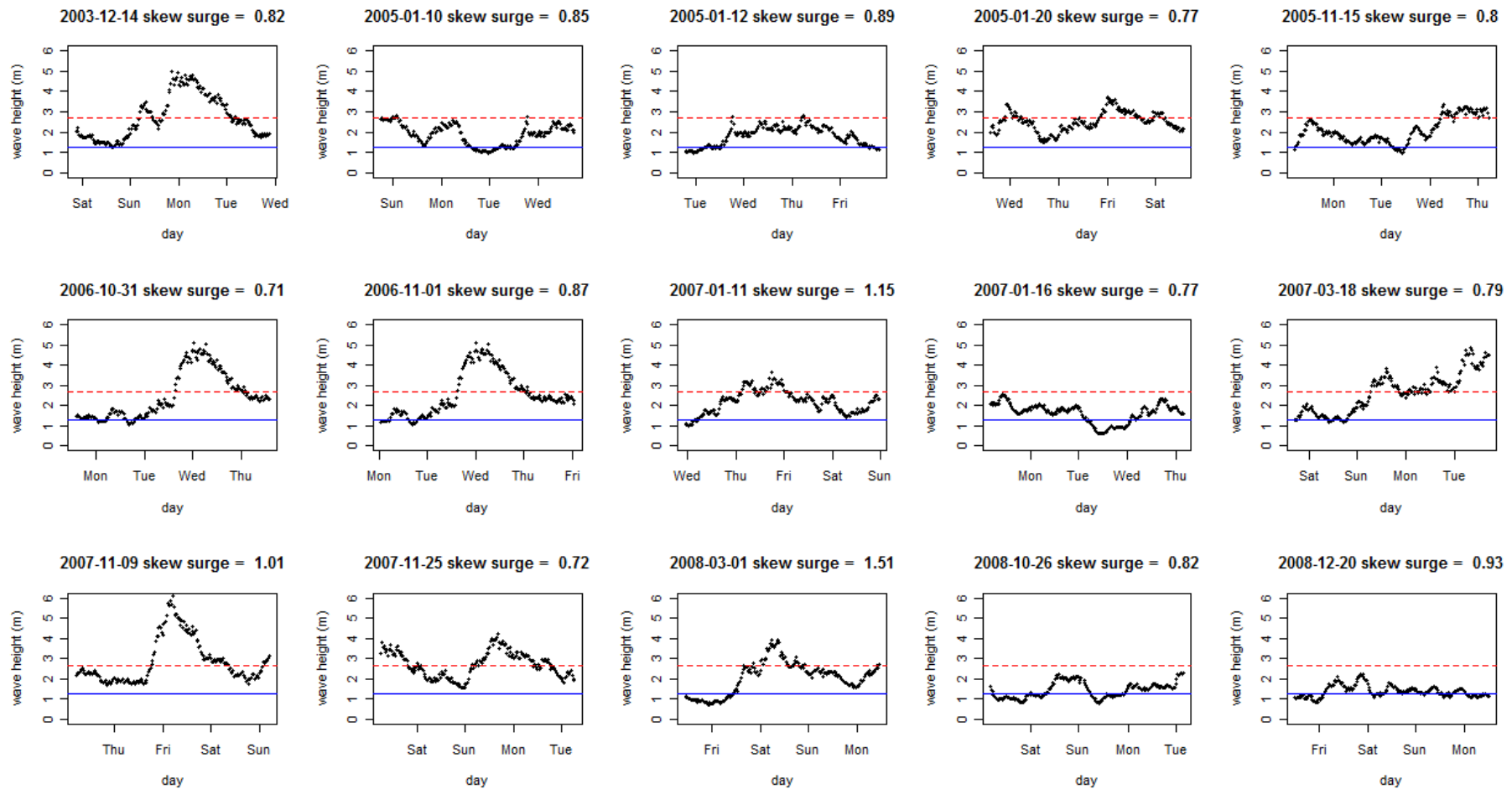
The final component of water level is the waves. Waves are normally defined by their height (H), period (T) and direction (α). The wave height usually refers to the significant wave height and period calculated from the average of the highest third of waves in a given wave record (Sorensen 2006).

In similar previous studies the wave component has been hindcast from wind data (for example Hawkes *et al.* 2002; McMillian *et al.* 2011b). This is because wave data are not as easily accessible as wind data and are often not available in useable locations or have a limited historical record. In this project wave data recorded from waveriders is used directly. Unlike hindcasting models, this data is freely available and provided a means of accessing the variable of interest directly hence minimising additional modelling uncertainties. The limited record length of observed data creates some issues when modelling extremes as discussed in Section 7.3.3.1. The waveriders that are used in this project are Dowsing and Liverpool Bay (see

Section 6.2). As the data record at these sites increases in the future this method will provide a robust means of representing the dependence between extreme waves and water level.

Due to the effect of shallow water process on waves, it is standard practice (Hawkes *et al.* 2002) to model the relationship between water level and wave height in deep water. The wave data are then transformed to the shoreline using the transformation methods discussed in Section 7.3.5.

The wave component is complex and depends on both the meteorological storm event and the tide. Wave data at Dowsing are only available from October 2003 therefore the following analysis is based on concurrent sea level and wave data from 2003 to 2010. As shown in Figure 7.15, for some peak surge events there is a clear rise in wave heights either at the same time as the peak surge or slightly after, however for others there is no notable deviation from the mean throughout the event. Sections 7.3.3.1 to 7.3.3.3 discuss how to deal with this variability.



Peak surge occurs at mid point of x axis. The blue solid line is the mean and the red dashed line in the Q95 threshold.

Figure 7.15 Fitted highest surge events with associated wave component at Dowsing

7.3.3.1 Wave height

Previous work has been carried out on the relationship between waves and water levels at Dowsing by Hawkes *et al* (2002). They found that there was a weak relationship between water level and wave height (Figure 7.16). They also observed that there is a time lag between the occurrences of peak surges and peak wave heights on the East Coast although they do not make explicit what this time lag is. The EA project (McMillian *et al*. 2011b) includes an alternative estimation procedure for wave heights but this is limited to the independent return periods and is not a full joint probability model.

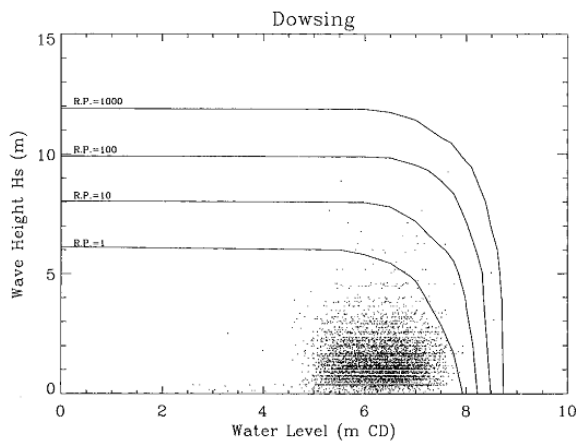
The data set used by Hawkes *et al* (2002) consisted of approximately 10 years of data, from recorded still water levels and wave data from a wave hindcast model from observed wind data, and 10 years of “synthetic” data simulated from the “observed” data. Hawkes *et al* (2002) assume that since peak surges and wave conditions last for less than half a day, observations at each high water can be considered as independent records.

The maximum wave height recorded by the waverider at Dowsing is 6m whereas the hindcast data used by Hawkes *et al* (2002) shows values of up to 10m. This could be due to the hindcast point being located in shallower water than the waverider buoy at Dowsing, a function of the hindcasting calculations, comparing peak wave height with significant wave height, or a data recording error. For the purpose of this application it is assumed here that the observed data at the Dowsing waverider is correct.

The joint return periods in Figure 7.17 were estimated by calculating the probability of the sea state exceeding a given still water level and wave height. For a large enough set of sampling points, this data can be plotted by joining the points with equal joint exceedance probabilities. The wave heights at each exceedance level are lower than Hawkes *et al* (2002) estimate. This is due to the observed wave heights being lower than the hindcast data. The analysis was repeated using wave data from various different time lags to identify the time lag between the occurrences of peak surges and peak wave heights however no clear differences were visible. Further analysis was therefore carried out, using the methodology presented by Keef *et al* (2009a; 2009b; 2009c) for investigating the temporal dependencies in river flows (see Section 5.3.3.3) to identify for a given extreme water level, X , for example the 90th quantile, what is the probability that wave height (Y) at lag r is also above a given level.

Using this method there is some indication in Figure 7.16 that the wave height may be higher in the 48 hours surrounding an extreme water level event however this relationship is largely masked by the impact of the tidal cycle. Repeating the analysis using skew surge rather than

combined water level to identify extremes Figure 7.19 shows that there is a temporal dependence between wave height and skew surge with the maximum wave heights most likely to occur 10 hours after the extreme skew surge event (just before the following high tide). One reasons for the clearer trend is that an extreme high water level may be caused by a high spring tide with only a moderate meteorological surge component therefore it is less likely that high waves will accompany all extreme water level events than extreme skew surge events. Although plots have been produced for water levels > 0.99 threshold, there are very few occurrences of extreme wave heights for these events therefore these results should be treated with caution.



Source: Hawkes *et al* (2002)

Figure 7.16 Joint probability of water level and wave height at Dowsing as calculated by Hawkes *et al* (2002)

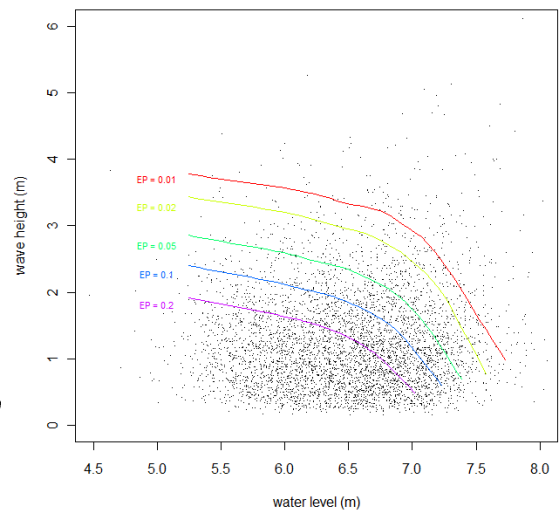


Figure 7.17 Joint observed probabilities of wave height and water level at Dowsing

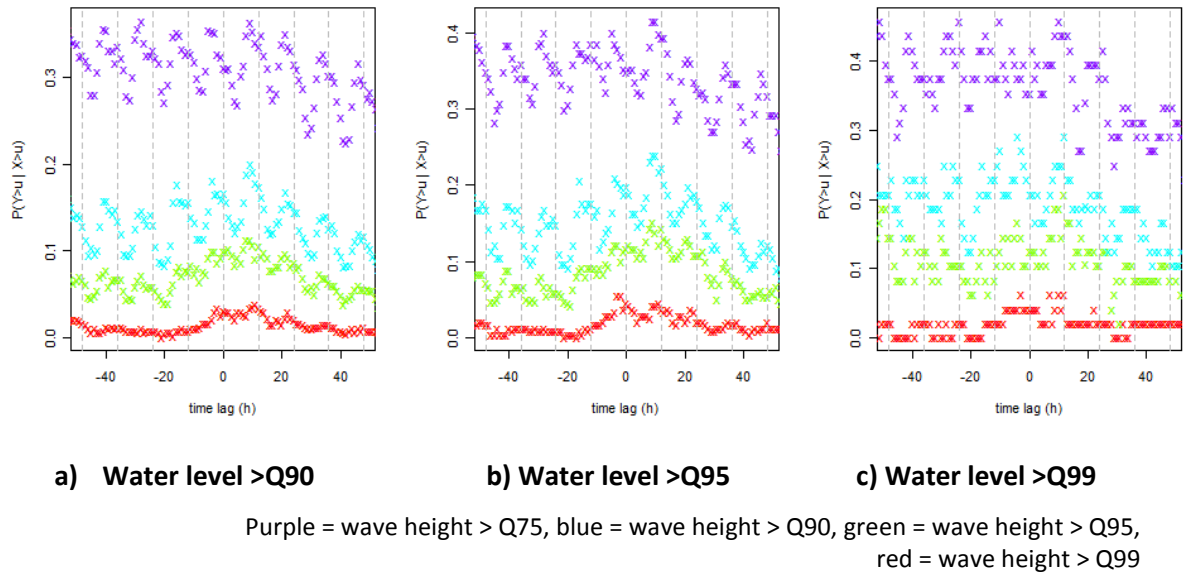


Figure 7.18 Temporal dependency of wave height with water level at Dowsing

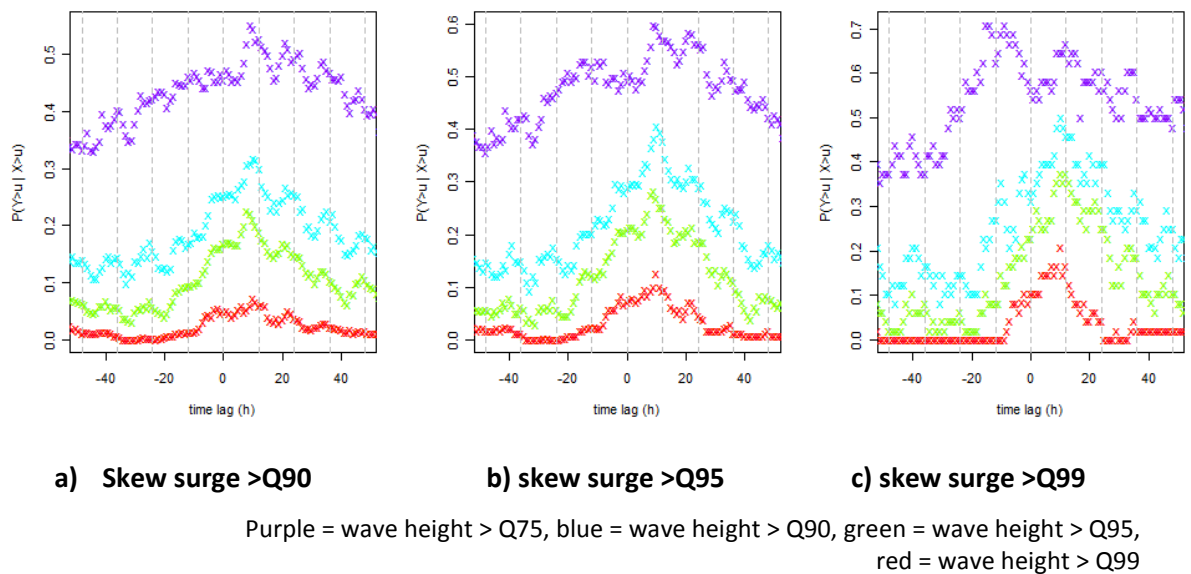


Figure 7.19 Temporal dependency of wave height with skew surge at Dowsing

The clearer temporal trend in Figure 7.19 compared to Figure 7.18 suggests that it may be beneficial to use skew surge as the conditioning variable rather than total still water level when simulating wave heights. This is possible when taking an event representation of the conditions, rather than concurrent conditions, since the tidal effects are implicitly included in the identification of maximum wave height over the full event tidal cycle. Although the link between surge and waves is acknowledged by Hawkes *et al* (2002) they do not use it when modelling wave height and comment that it is often masked by the relationship between wave height and water level.

Since extreme events in this thesis are defined by skew surge, which is independent of the tide, it is beneficial to use skew surge as the wave height predictor as this maintains the meteorological dependence between events without masking by the deterministic tidal component. An additional benefit of using skew surge as the predictor is that there is a direct link between the wave component and the dependence model for skew surge and fluvial water levels before the inclusion of the deterministic tidal component. The total water level is used in the onshore transformation method (Section 7.3.5) which ensures the tidal component is taken into account for the inshore waves which are more significantly depth limited.

Repeating the joint probability analysis for skew surge and wave height at Dowsing (Figure 7.20), and Liverpool (Figure 7.21) shows a stronger relationship than between water level and wave height. This is particularly evident at Liverpool. To incorporate the lag between peak surge and peak wave height identified in Figure 7.19, Figure 7.20 is based on the maximum wave height within -12 hours and +24 hours of the peak skew surge. The probability of extreme wave heights (>Q90) occurring after this period is less than 0.2. Due to the potential double counting of wave heights using this event definition, the skew surge data was de-clustered using the time based method explained in Section 6.3.3 with an r value of two, meaning the two tidal cycles before and after a peak skew surge event were removed from the analysis and therefore each maximum wave height from an event can only be assigned to one skew surge value. No threshold was specified to allow for consideration of the skew surge and wave height relationship across all possible event magnitudes.

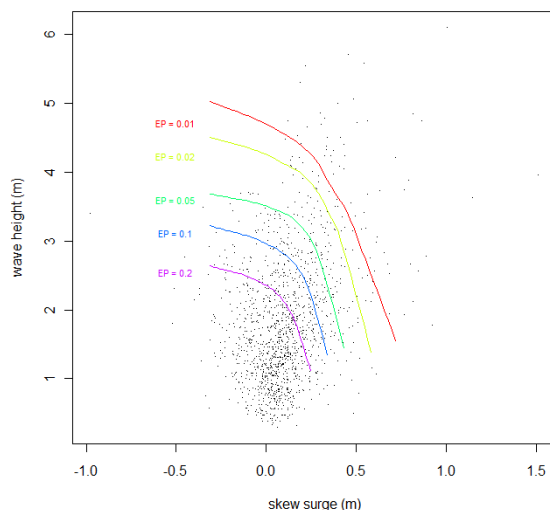


Figure 7.20 Joint probability of skew surge and wave height at Dowsing

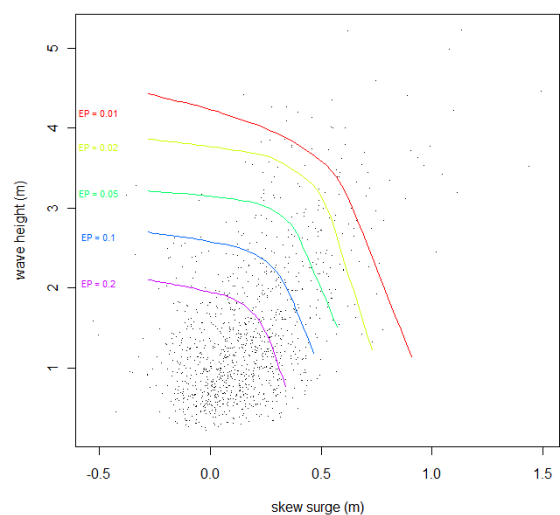
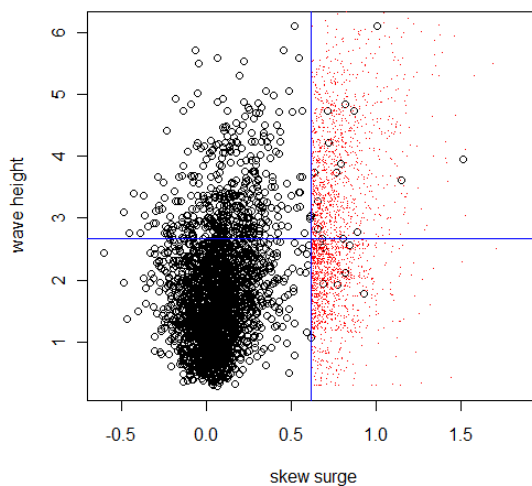


Figure 7.21 Joint probability of skew surge and wave height at Liverpool

Given the variability shown in Figure 7.15 for simplicity it is assumed that deep water wave heights remain constant over the full duration of the storm event. Developing a small number

of wave height profiles (similar to the surge shape profiles) is unlikely to adequately reflect the variable wave climate and is therefore not appropriate unless further details of the storm type are used for example the wind component to identify wind driven waves and swell. As the highest wave heights generally occur after the peak skew surge (Figure 7.18) the proposed method may overestimate the water level at the peak giving a conservative estimate of risk.

By processing the waverider data to include one value per high tide skew surge, the maximum wave height within -12 and +24 hours of the skew surge peak, it is possible to add wave height as an additional component to the conditional dependence model. As the relationship between skew surge and wave height is relatively weak, and the dominant cause of coastal flooding is the surge component (see Section 5.2.1.2), the model is fitted pairwise with skew surge as the conditioning variable. Keef *et al* (2009a) recommend a minimum of 20 years of concurrent data for fitting the conditional dependence model. There is only a maximum of eight years of waverider data so some relaxation of the conditions for fitting the dependence model is required. Details of the model fit are provided in Appendix D.2. An example of the data simulated from the model is shown in Figure 7.22, this shows a reasonable fit between the observed and simulated wave heights for extreme skew surges. The conditional dependence model was chosen in preference to other pairwise extreme models to provide consistency across the modelling framework.



Black circles are observations, red dots are simulated values, blue lines are the wave height and skew surge thresholds

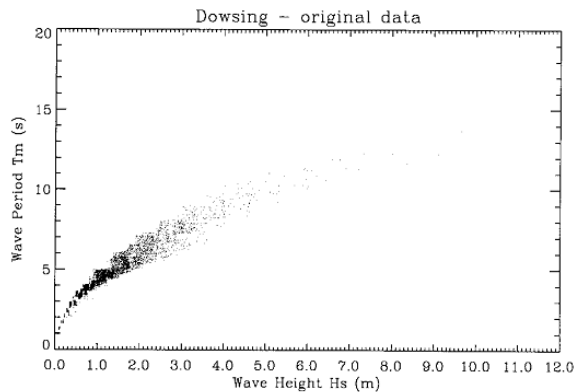
Figure 7.22 Simulated wave heights using pairwise relationship with skew surge at Dowsing

7.3.3.2 Wave period

Hawkes *et al* (2002) also investigated the relationship between wave height and mean wave period at high water (Figure 7.23), finding a strong, approximately linear relationship.

Repeating these plots with the seven years of observed waverider data shows a similar relationship between wave height and wave period for the maximum wave heights observed

from each period (Figure 7.24) but there is more scatter within each period and lower observed wave heights as previously discussed.



Source: Hawkes *et al* (2002)

Figure 7.23 Relationship between wave height and wave period at Dowsing from Hawkes *et al* (2002)

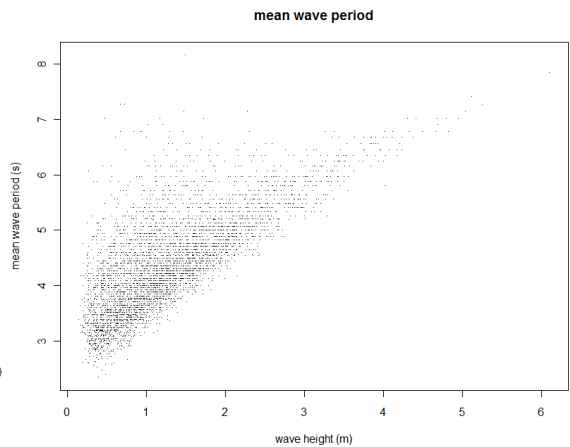


Figure 7.24 Relationship between wave height and wave period at Dowsing from observed data

Since the relationship between wave height and wave period is approximately linear (Figure 7.23 and Figure 7.24), wave period, which is required for the inshore transformation method, can be sampled dependent on the wave height as given in Equation 7.16, where m is the slope of the linear model and c is the intercept including some random variation sampled from a normal distribution of the residuals.

$$T_m = mH_0 + c \quad 7.16$$

7.3.3.3 Wave direction

Wave direction is also required for the inshore transformation method. The wave direction is closely related to the wave height, for example at Dowsing the largest waves only occur from the north or northwest. Therefore the wave direction is sampled based on the conditional probability of wave direction given wave height, the dominant components of which are given in Table 7.7 and Table 7.8. For computational reasons the conditional probabilities are calculated for each 30° band.

wave height (m)

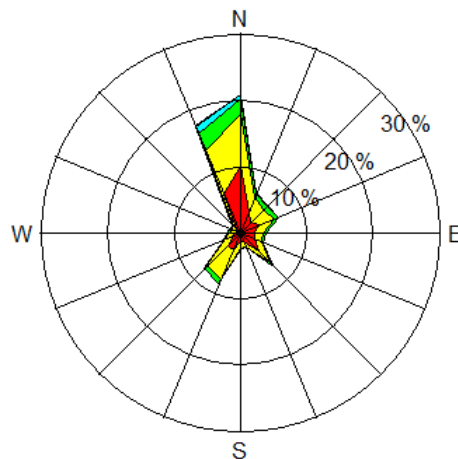
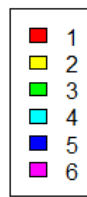


Figure 7.25 Wave rose showing wave height and direction at Dowsing

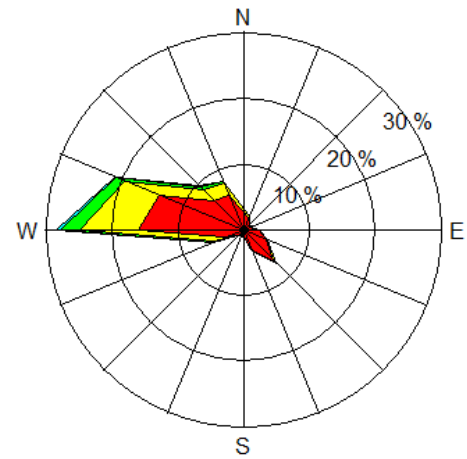


Figure 7.26 Wave rose showing wave height and direction at Liverpool Bay

Table 7.7 Conditional probability of wave direction at Dowsing

Wave height (m)	Probability of wave direction		
	300-330	330-360	0-30
0.0 – 0.5	0.02	0.22	0.21
0.5 – 1.0	0.02	0.23	0.18
1.0 – 1.5	0.02	0.25	0.15
1.5 – 2.0	0.02	0.27	0.13
2.0 – 2.5	0.02	0.35	0.12
2.5 – 3.0	0.02	0.42	0.13
3.0 – 3.5	0.02	0.53	0.15
3.5 – 4.0	0.01	0.69	0.15
4.0 – 4.5	0.01	0.78	0.11
4.5 – 5.0	0	0.81	0.11
5.0 – 5.5	0	0.93	0.02
5.5 – 6.0	0	0.86	0.13
6.0 – 6.5	0	1	0.0

Table 7.8 Conditional probability of wave direction at Liverpool Bay

Wave height (m)	Probability of wave direction		
	270-300	300-330	330-360
0.0 – 0.5	0.28	0.15	0.08
0.5 – 1.0	0.31	0.11	0.10
1.0 – 1.5	0.45	0.13	0.11
1.5 – 2.0	0.57	0.15	0.07
2.0 – 2.5	0.64	0.15	0.05
2.5 – 3.0	0.75	0.13	0.03
3.0 – 3.5	0.78	0.16	0.02
3.5 – 4.0	0.80	0.17	0.00
4.0 – 4.5	0.81	0.16	0.00
4.5 – 5.0	0.97	0.03	0.00
5.0 – 5.5	1.00	0.00	0.00

7.3.4 Simulation of total water level

The peak total water level at an individual site requires simulation of;

1. A high tide skew surge from the conditional dependence model
2. A maximum wave height from the conditional dependence model
3. A deterministic high tide from the historic tidal record.

These three components are added together to give the peak total water level. Since skew surge is defined once per tidal cycle there is no need to take account of the relative timing of peak surge and the tidal cycle.

The total water level at an individual site for a full event requires the above plus;

4. A skew surge shape sampled from the average profiles at the site
5. Extraction of a time series of historic tide record.

The wave height is assumed to remain constant throughout the event. The length of an event is based on the duration of the surge event. The profiles in Table 7.6 have a total duration of 72 hours. Beyond the 72 hour surge shapes, the surge is assumed to be zero. To ensure the full event is considered and to fit with the temporal resolution of the fluvial data, the total event duration is taken to be 24 hours.

The total water level at all sites throughout the full event is simulated using the conditional dependence model to ensure the correct spatial and temporal dependencies between sites are maintained. The model provides an event peak value for skew surge and wave height. The tide component is sampled by extracting the same historic tide event from the observed data at each site. It is unlikely that the shape of the surge profile will change significantly as it travels down the coastline, therefore similar surge shapes are sampled at nearby sites by grouping the surge profiles as shown in Table 7.6. The surge profile group selected is based on the probability of each surge shape defined at the conditioning gauge. The surge shape is modified to ensure that the spatial and temporal dependencies between high tide skew surge at multiple sites are maintained throughout the event. It should be noted that there will be a lag between the occurrence of the peak water level at each site due to the timing of the tidal cycles and travel time of the surge event between sites. A summary of each stage of the process is given in Table 7.9. A graphical outline of the process, including the onshore wave transformation, is given at the end of this section in Figure 7.29.

Table 7.9 Summary of offshore coastal water level simulation

Component	Depends on:	Method	Output	Contributes to:
Peak skew surge	Independent - can be modelled concurrently with fluvial event if required	Simulated concurrently at all gauges in the network using conditional dependence model	Vector of high tide skew surge at each gauge	<ul style="list-style-type: none"> • Wave height
Event skew surges	Peak skew surge	Conditional dependence model used in temporal form to simulate skew surge for pre/proceeding tidal cycles	Matrix of high tide skew surges for each time lag at each gauge	<ul style="list-style-type: none"> • Surge shape

Component	Depends on:	Method	Output	Contributes to:
Surge shape	Peak skew surge Event skew surges	Event surge shape sampled from averaged shapes at each gauge and scaled to fit simulated skew surges at each time lag	Matrix of high and low tide skew surge for each time lag at each gauge	<ul style="list-style-type: none"> • Still water level
Maximum wave height	High tide skew surge	Simulated independently for each tide and wave gauge pair using pairwise conditional dependence model	Vector of maximum wave height at each wave gauge	<ul style="list-style-type: none"> • Wave period • Wave direction • Inshore wave height
Tide component	Independent	Resampled (with replacement) from 18.6 years of observed data. The same tide event is used at all gauges	Matrix of tide height for each time lag at each gauge	<ul style="list-style-type: none"> • Still water level
Still water level	Surge shape Tide component	Add components	Varying total water level throughout event at each site	<ul style="list-style-type: none"> • Inshore wave height • Inshore total water level
Wave period	Wave height	Simulated from wave height and wave period regression model at each gauge	Vector of wave period at each gauge	<ul style="list-style-type: none"> • Inshore wave height
Wave direction	Wave height	Simulated from conditional probability of wave direction given wave height	Vector of wave direction at each gauge	<ul style="list-style-type: none"> • Inshore wave height

7.3.5 Onshore wave transformation

The wave data used in this PhD are recorded around 20km off shore in water depths of up to 25m. The data needs to be transformed to reflect the wave conditions at the coastline. The overtopping calculations in Section 7.3.6 require the following information at the toe of the defence; still water level, wave height (H_s), wave steepness (s_m), wave period (T) and deep water depth (d). This section discusses how these variables are determined.

As waves travel inshore they are affected by three processes; refraction, diffraction and reflection. These processes result in changes to the wave height (H), wave length (L), wave velocity and wave angle (α). The wave period (T) does not change. Refraction is the transformation of wave characteristics due to changes in water depth. Diffraction is changes due to other factors such as obstacles (Kamphuis 2000) which cause variation in crest height

resulting in a flow of energy along the wave crest (Sorensen 2006). Reflection occurs when a wave rebounds off a barrier in the direction it came. In many cases the effect of diffraction and reflection is minor compared to refraction and can be omitted (Sorensen 2006). Only refraction is considered further here.

The calculation package, CRESS v10 (Netherlands Ministry of Public Works, IHE-Delft *et al.* 2010) is used to calculate the onshore transformation of waves. Details of the calculation steps performed by the software are provided in Appendix D.3.

7.3.5.1 Application of wave transformation calculations

The first stage of the simplified inshore propagation method used in this PhD is to identify a perpendicular transect from the coastline to the waverider and analyse the local bathymetry. If the bed depths are smooth and gradually varying then no consideration is needed of the local bathymetry in the wave transformation methods. For the Lincolnshire coastline this is broadly the case except for the Silver Pit channel illustrated in Figure 7.27. Since this is a natural feature, and has been largely ignored in previous studies no consideration of this deep water channel is made in the following calculations. For North Wales the coastal bathymetry (Figure 7.28) shows a smooth transition for deep to shallow water.

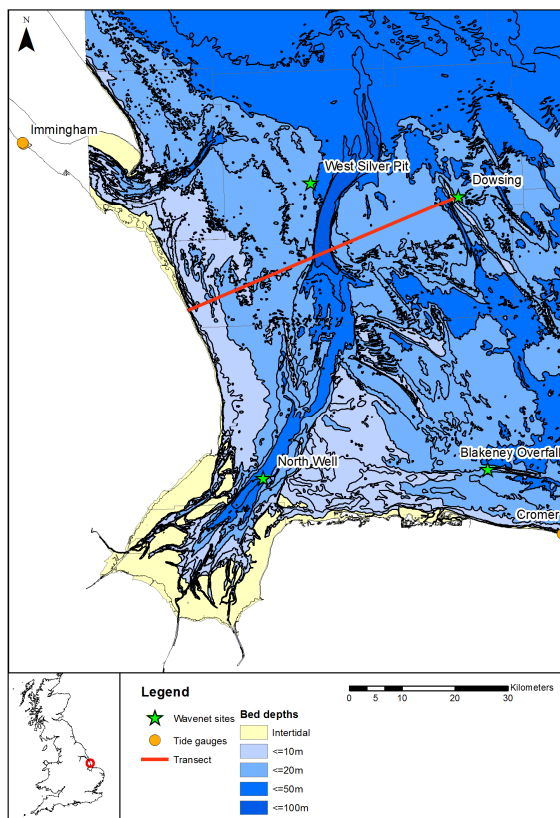


Figure 7.27 Lincolnshire coastal bathymetry

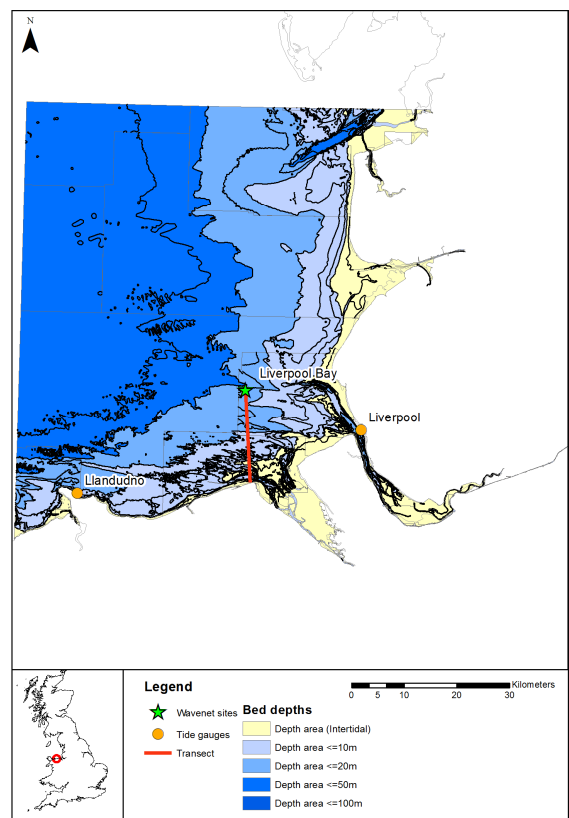
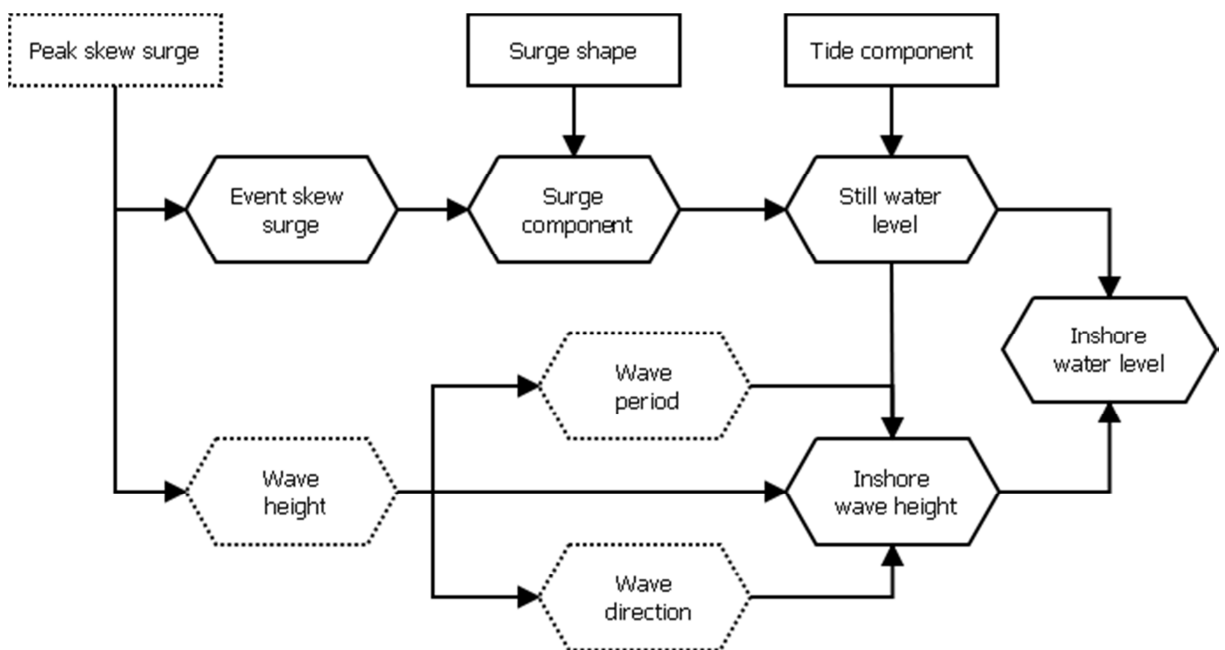


Figure 7.28 North Wales coastal bathymetry

A range of inshore wave heights were calculated from a range of wave conditions to create a look up table of results. Surface plots of the sampled wave conditions are shown in Appendix D.3. These results were then sampled from based on the wave conditions simulated as per Sections 7.3.3.1 to 7.3.3.3. Linear interpolation between results was used to provide greater variability in conditions.

7.3.5.2 Summary of water level and wave height calculation

A summary of the main components of total inshore water level is shown in Figure 7.29. For each conditional peak high tide skew surge a time varying inshore total water level is generated by adding the skew surge, tide and wave components.



Square boxes are simulated independently. Solid outlines have a temporal component. Dotted outlines are defined once per event

Figure 7.29 Summary of coastal simulation method

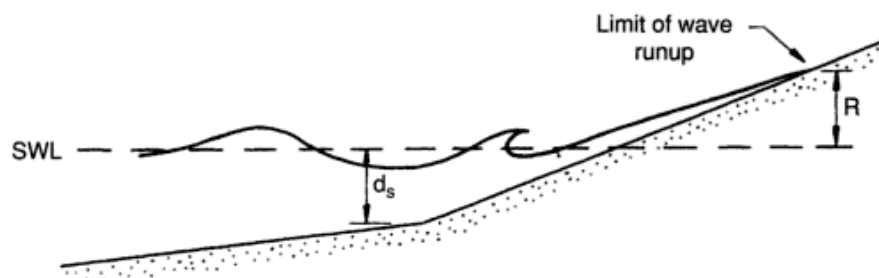
7.3.6 Overtopping of defences

Water may overtop a defence during a coastal flood event from several sources; wind driven spray, splash, and run up which is also known as green water overtopping (Die Küste 2007). It is usually only the green water overtopping that contributes a significant amount to the overtopping rate. British guidelines (Besley 1999) recommend the use of Owen’s equation (1980) to calculate the mean overtopping rate for sloping structures. There are a variety of other methods available (see Die Küste 2007) but Owen’s method is used here for its simplicity. The contribution of overtopping to defence failure is discussed in Chapter 7.

A limitation of the available overtopping methods is that they were generally designed for offshore breakwaters and sea walls where it is assumed that the water on the seaward side of the defence is relatively deep. Therefore to allow for use of these simplified versions of the overtopping methods, during a flood event it is assumed that the still water level reaches the base of the defence. This condition means no consideration needs to be taken of the beach conditions at the base of the defence. It is acknowledged that a major cause of defence failure is undercutting or erosion of the defence foundations, to include this failure mechanism in the future more detailed analysis of the wave conditions and defence structure would be required.

7.3.6.1 Wave runoff

Once a wave breaks its remaining energy causes water to run up the sloping face of a structure or beach (Sorensen 2006). The maximum runoff (R_u) is defined relative to the still water depth at the toe of the structure as shown in Figure 7.30. If the runoff level is high enough water will overtop the defence. Runup is calculated relative to the wave steepness, wave angle and slope roughness.



Source: Sorensen (2006, p44)

Figure 7.30 Graphical definition of maximum wave runup

7.3.6.2 Owen's equation for sloping structures

Overtopping occurs when the run up level exceeds the defence freeboard, R , the height between the crest and still water level. Owen (1980) considers this through the dimensionless freeboard, R_m^* (Equation 7.17) which includes the relative freeboard (R/H_s) where H_s is the wave height in front of the defence slope, and s_m the wave steepness.

$$R_m^* = \frac{R}{H_s} \left(\frac{s_m}{2\pi} \right)^{0.5} \quad 7.17$$

Using the dimensionless freeboard allows estimation of the mean overtopping discharge, \bar{Q} , as given in Equation 7.18, where a and b are empirical coefficients given in Table 7.10 depending

on defence slope, and r is a reduction coefficient for surface roughness, examples of which are given in

Table 7.11. The r coefficient allows Owen's equation to be extended from the smooth slopes it was designed for to rough and armoured slopes (Allsop *et al.* 2005). Further coefficients for a and b for bermed slopes are given in Burchart (1993), and in the Eurotop Manual (Die Küste 2007) which also includes further surface type roughness values. As limited data are known for the flood defences in this project, all defences are assumed to have no berms, wave walls or other design enhancements. This results in a worst case scenario for overtopping volumes. It should be noted that the mean overtopping discharge is unlikely to occur in reality as some waves will produce large amounts of overtopping while others may not overtop the defence crest at all. The mean overtopping discharge is assumed to occur over the full duration of the storm.

$$\bar{Q} = gH_s T_m \cdot a \exp\left(\frac{-bR_m^*}{r}\right) \quad 7.18$$

Table 7.10 Example a and b coefficients for Owen's equation

Slope	a	b
1:1	0.008	20
1:1.5	0.010	20
1:2	0.013	22
1:3	0.016	32
1:4	0.019	47

Table 7.11 Example r coefficients for Owen's equation

Surface type	r
Smooth impermeable (including smooth concrete and asphalt)	1.0
One layer of stone rubble on impermeable base	0.8
Gravel, gabion mattress	0.7
Rock rick-rap with thickness greater than $2D_{n50}$	0.5-0.6

7.3.7 Summary of assumptions

Linking statistical and physically based models of water levels requires a number of simplifications to be made. Physically based models are usually applied at small scales and with detailed input data. Using input data generated from statically models or over large scales restricts the detail available to input into the physically based model. The assumptions made during the coastal modelling process have been discussed in Sections 7.3.1 to 7.3.6. A summary of the assumptions is provided in Table 7.12.

Table 7.12 Summary of coastal modelling assumptions

Component	Summary of assumption	Justification
Surge	Skew surge is independent of the tide and can be sampled separately	See Figure 7.14
Surge	The surge shape can be represented by the high and low tide skew surge	No finer detail is required in this instance
Surge	Three surge shapes adequately reflects the variability of the surge shapes at each site	Using more surge shapes offers no significant improvement in accuracy (Section 7.3.1)
Surge	Surges last for less than 24 hours	Beyond 12 hours before or after peak skew surge is low and noisy (Figure 7.10)
Wave	A single waverider gauge can provide data for a long stretch of coastline	No alternative data is available of a sufficient record length
Wave	Wave height is consistent throughout the event	To adequately model the variability of wave height would require additional meteorological data so no further refinement is thought justifiable with the existing data
Wave	The maximum wave height occurs within 24 hours of the peak skew surge	The probability of extreme waves occurring outside this period is less than 25% (Figure 7.18 and Figure 7.19)
Tide	All tide cycles are equally likely to occur and the observed data record contains the full range of tidal conditions	The nodal tidal cycle lasts 18.6 years therefore 18.6 years of record should reflect the full range
Still Water level	The peak skew surge occurs at the same time as high tide at the conditioning site. There may be a lag at other sites.	The timing of skew surge is relatively unimportant as it has no effect on the peak water level
Wave height	Bottom contours can be assumed to be smooth and gradually varying	Silver Pit is the possible exception to this however to simplify onshore transformation this is ignored.
Wave height	There is a linear relationship between wave height and wave period	See Figure 7.24
Wave height	Skew surge can be used as a predictor for wave height	Stronger relationship identified between skew surge and wave height than still water level and wave height (Figure 7.20 and Figure 7.21)
Total water level	The full multisite event lasts less than 24 hours	Peak wave heights most likely to occur 10 hours after the peak skew surge (Figure 7.19). Surge profiles are low with considerable noise 12 hours before and after the peak (Figure 7.10)
Overtopping	Water levels during events are assumed to be above the defence toe therefore no consideration of beach conditions on defence foundations is needed	During extreme events that lead to overtopping this condition is likely to be met

7.4 Floodplain inundation modelling

Routing of flow across the floodplain was based on established inundation models. For fluvial sites the ISIS software was used as described in Section 7.4.1 and for coastal sites a 2D shallow water flow model was used (Liang 2010). This section outlines the setup of each of these models.

The modular structure of the methodology means that any type of inundation model can be used within the modelling framework. Here two methods are tested with varying degrees of detail illustrating the ability to model in more detail where required or data are available.

The coastal model includes flood defences which may overtop or breach as described in Chapter 7.

7.4.1 1D inland inundation model

Inland floodplain inundation was modelled using a 1D hydraulic model constructed using the ISIS software (See Section 7.2.4) with storage cells to represent the floodplain. Inundated area and flood depths were calculated using standard GIS processing in ArcMap v10 to;

1. Create a water level raster using triangular interpolation of the peak water level at modelled cross sections
2. Subtract the ground elevation from the LiDAR data from the water level raster to create a depth raster
3. Delete any areas of the depth raster with values less than zero and remove any areas not connected to the watercourse to produce a flood outline for the event.

7.4.2 2D coastal inundation model

For flooding in coastal areas a 2D shallow water flow model (Liang 2010) developed at Newcastle University was used. The model solves the full 2D shallow water equations using a finite volume Godunov-type numerical scheme. The model is particularly suited to an application of this type as it is able to calculate different types of flood wave from slow-varying inundations to extreme and violent floods and therefore copes well with defence breach scenarios as detailed in Chapter 8. For full details of the calculations readers are directed to Liang (2010), this section will outline how the model has been set up for use in this application. Details of the application of the inundation model are given in Chapter 8.

7.4.2.1 Data

The available data for construction of the hydraulic models are listed in Table 7.13. The output is the water level and velocity at each grid cell in the model domain.

Table 7.13 Available data for coastal inundation modelling

Item	Comments
Topographic data	2m LiDAR supplied by the Environment Agency
Defence locations	GIS polyline files identifying defence sections and locations supplied by the Environment Agency
Map data	OS 1:50,000 obtained from DigiMap
Any other data sources	Environment Agency flood outlines used to inform model domain

7.4.2.2 Model set up

The inundation model used requires input data as listed in Table 7.14. The model domain was specified with reference to the location of the flood defence system, the caravan sites of interest and the extent of the Environment Agency extreme flood outline. The influence of cell size on model runtime was tested (See Appendix D.4) and a 10m cell size was adopted.

The DEM is specified on a 2m grid from the Environment Agency LiDAR data. The DEM was aggregated to a 10m grid using the median value for each cell. The coastal boundary of the DEM was set at the defence locations, these cells were given a value of 1 in the mask file. The DEM was modified so that the raster cells relating to each defence were assigned the mean defence height for each defence section.

Where defence breaches occur (See Chapter 8) each individual breach location was assigned a reference value and an inflow_x file. The inflow_x file requires specification of the flow direction, in all cases it was assumed that the flow direction through the breach was perpendicular to the coastline.

Table 7.14 2D Coastal inundation model input files

File name	Description
dem.txt	ASCII file of digital elevation model
mask.txt	Mask file with values 0 for normal grid cells, 1 for boundary cells, 2 for cells outside of the domain and -1 for breached cells
u.txt, v.txt, h.txt	Initial water depth and velocity for each cell in the domain
Manning.txt	Roughness value for each cell in the domain
Inflow_x.dat	Inflow hydrographs at breach. X may take any integer from 1 to 9999 depending on the number of breaches in the scenario
set_up.ste	Summary file of scenario conditions including specification of time step, numerical calculation scheme, boundary types, number of breaches and point sources (e.g. river inflow) and output details

7.5 Water level and floodplain inundation in the system model

Chapter 7 has illustrated the process of converting the statistically simulated extreme DMF and skew surge values to physically representative events at the receptors.

For fluvial flows a methodology was presented to convert between DMF data and peak flows. Although this is well documented in other countries there has traditionally been little requirement for this in the UK due to the availability of peak flow data, however it is not practical to use concurrent peak flow data in a conditional dependence model of this type due to the data volumes. The proposed method provides a means of using advanced statistical methods for correctly specifying extreme events over large spatial or temporal scales while maintaining a physical basis for considering the impacts on the receptors.

For coastal events an integrated methodology has been derived which considers all aspects of a coastal flood event including surge, tide and wave height. A novel approach to modelling wave height conditional on skew surge has been illustrated as well as the first application of the conditional dependence model to wave height data.

It is accepted that many of the methodologies used in this chapter are simplified versions and more detailed methods are available. In the case of an integrated systems risk model such as this it is not appropriate to use more complicated methods as the additional data and computation involved preclude their use. The systems model outlined in Chapter 4 is modular, and as illustrated in Section 7.4 it is possible to use different methodologies within the systems model to represent different levels of available data or specific detail required in different areas.

8 Spatial and temporal flood defence reliability

8.1 Importance of flood defences to flood risk

A flood defence is a manmade or natural structure which provides protection for people, property and land from flooding during extreme events. Flood defences play an important role in flood risk management in the UK. The Environment Agency maintains 24,000 miles of defences in England and Wales (Environment Agency 2012) which range from hard sea walls to softer defences such as salt marshes. There are also numerous private defences. The provision of insurance cover in many flood risk areas is only possible due to the protection from flood defences (Association of British Insurers 2008).

Despite their importance, the degree to which the potential failure of flood defences is considered in flood risk studies varies considerably. Largely because the complexities involved in modelling flood defence failure are much greater than for other aspects of flood risk analysis. It is often difficult to combine into existing analysis frameworks, for example flood risk maps are often produced on a return period scale, however the simplest means of considering defence failure is scenario based, making it difficult to combine the results. Although accessible, a scenario based approach to defence reliability is also limited in that it does not fully address the various spatial and temporal dependencies embodied in flood defence reliability. Several research groups have proposed methods of overcoming these difficulties, most notably the RASP project in the UK which recommends different methodologies based on the detail required and data available (Hall *et al.* 2003; Dawson *et al.* 2005; Gouldby *et al.* 2008), and researchers at Postdam university working on large river systems in mainland Europe (Apel *et al.* 2006; Apel *et al.* 2009; Vorogushyn *et al.* 2010). These, and other available methodologies, are reviewed in Section 8.3.

At this point it is useful to define what is meant by defence failure. There is some ambiguity in the literature regarding this as some authors consider a defence to be failed if it has overtopped (Hall *et al.* 2003; Apel *et al.* 2006) while others consider failure to imply structural failure of the defence through breach, collapse, piping or other failure mode. This PhD takes the position that overtopping of the defence is not in itself a failure as the defence is still standing and hence the amount of water flowing into the floodplain is comparatively low. In most cases however overtopping increases the probability of failure due to the additional erosion forces acting on the defence structure. Overtopping is therefore treated separately however it is directly linked to the probability of failure. The probability of breaching alone is not sufficient to describe defence failure and analysis must also consider the physical development of breaches. The consideration of breaching is argued by Muir-Wood and

Bateman (2005) to be the most critical source of uncertainty for risk quantification and mitigation for storm surge flooding.

The first part of this chapter discusses the three main types of flood defences considered in this thesis, walls, embankments and sand dunes. The construction and potential failure mechanisms for each defence type are considered along with a review of the factors known to influence defence failure. Section 8.3 moves on to review existing methodologies for modelling flood defence failure. In keeping with the theme of spatial and temporal dependencies in flood risk which is central to this thesis, Section 8.4 considers the spatial variation in flood defence crest height and proposes a sampling methodology to incorporate this variability into a flood risk model. Section 8.5 outlines the simulation of flood defence reliability used in this thesis including initiation of breach points and breach growth. There are no flood defences in the vicinity of the caravan sites located on inland rivers, therefore the consideration of flood defence reliability has focused on coastal defences.

8.2 Flood defence types and failure models

Flood defences take a variety of different forms and serve different purposes. As such there are a number of different modes of failure. A flood defence is a unique structure in that most of the time it is subject to very little pressure however when required it must be able to withstand considerable external forces. An extensive list of failure models for different types of defence is given in FLOODsite Report T04-06-01 (Allsop *et al.* 2007). The summary provided below considers the most likely forms of failure of each of the defence types considered in this thesis; walls, embankments and dunes.

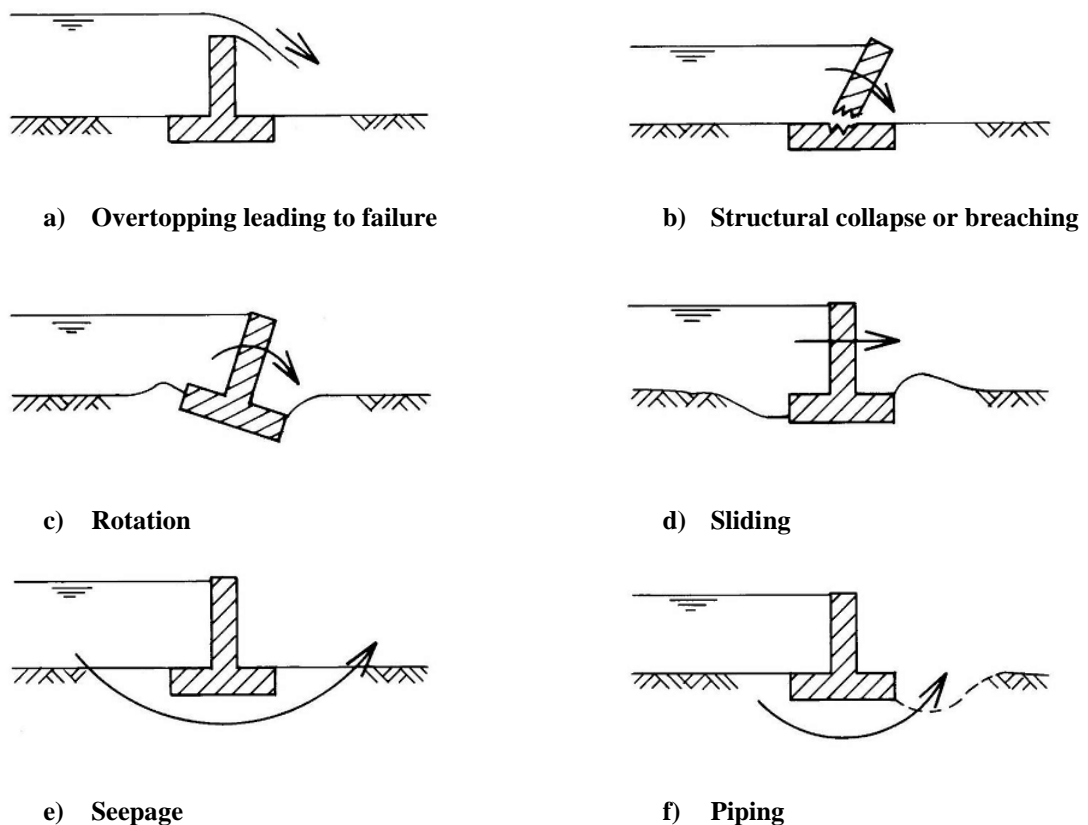
8.2.1 Failure modes

Overtopping of flood walls can lead to failure as water cascading over the wall can destabilise the foundations leading to collapse. Seepage occurs when small quantities of water travel underneath the defence. In extreme cases piping develops whereby the flow of water under the defence causes soil on the landward side to become buoyant, creating a void near the defence foundations. This can lead to rotation or sliding of the defence wall structure which can in turn lead to structural collapse (Rickard 2009). These common failure modes are illustrated in Figure 8.1. The height of vertical walls, particularly those in historic urban areas, may have been incrementally increased over time. This presents particular difficulties when assessing the reliability of the defence as different sections may perform differently and weak points may exist along the joins between different sections. An additional complication with vertical walls is that there are often discontinuities in the wall to allow for access. These are

usually filled with gates or demountable defences during flood events however this relies on the resources being in place to perform the necessary installation when required.

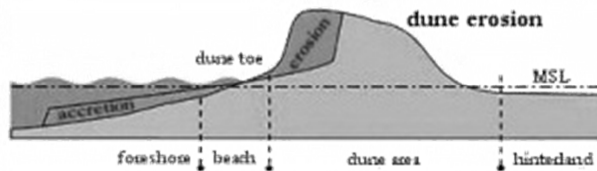
Embankments also suffer from overtopping and structural failure which manifests as breaching, this is most likely to occur in a concentrated section rather than along the full length of the defence. As identified in Section 8.4 low spots occur frequently along defence crests and therefore it is reasonable to assume that overtopping is likely to initiate in these locations leaving the defence susceptible to failure. Seepage is a particular problem for embankments and can occur through the embankment as well as under it. This is most likely to occur at weak points along the defence length for example at animal burrows or drainage culverts (Allsop *et al.* 2007; Rickard 2009).

The failure of sand dunes occurs when erosion of the seaward face due to wave attack weakens the dune profile and leads to breaching (Allsop *et al.* 2007) as shown in Figure 8.2.



Source: Rickard (2009)

Figure 8.1 Failure modes for flood defence walls and embankments



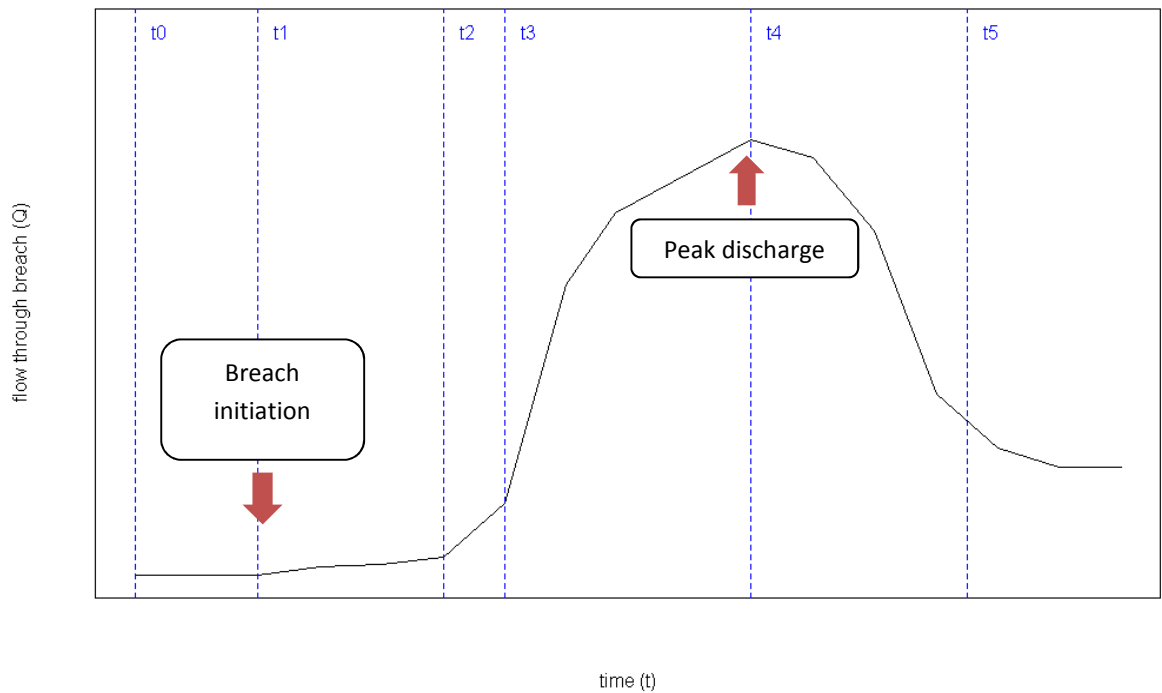
Source: Safecoast (2012)

Figure 8.2 Failure mode for dunes

8.2.2 Breaching process

There are two key factors to understanding breaching, firstly the defence and loading conditions required to initiate a breach and secondly how that breach develops over time.

Figure 8.3 shows a schematic diagram adapted from Morris *et al* (2008) of the various stages in the breaching process. The time it takes for this process to complete varies from seconds to years based on the defence type and loading conditions. In tidal scenarios it may take several tidal cycles to complete. A simplification made in many existing models of flood defence breaching is to assume that breaches instantaneously grow to their maximum size. In some cases however, the breaching process may not complete, for example if there is not enough water to complete breach formation (Morris *et al.* 2008) or due to human intervention resulting in repair of the breach before it is fully formed.



$t_0 - t_1$	$t_1 - t_2$	$t_2 - t_3$	$t_3 - t_5$	$> t_5$
Stable, no flow through or over defence	Progression of breach initiation, rate of change is slow and can be stopped.	Transition to breach formation, steady flow cuts through to face of defence initiates rapid and unstoppable erosion	Completion of breach formation including rapid vertical erosion and continued lateral erosion	Continued breach growth if supply of flood water continues

Adapted from Morris *et al* (2008)

Figure 8.3 Key features of the breaching process over time

8.2.3 Factors known to affect failure

Defence failure is not easy to predict and, even within defences of the same type, spatial variations in the defence structure and local conditions can result in different failure responses.

8.2.3.1 Defence structure

Extensive laboratory and field testing work as part of the EU FLOODsite project (FLOODsite 2009a) by Morris *et al* (2007; 2008; 2009a; 2009b) has identified a number of factors affecting the erodeability of flood defences. Their research forms the basis of the discussion in this section.

Firstly the type of material the defence is constructed from determines the erosion process; large blocky materials for example as used in the construction of Rip Rap erodes due to the

breakdown of interlocking mechanisms between the blocks, cohesive material, such as clay, is affected by head cut erosion, and non-cohesive material such as sand is eroded by continuous surface erosion. Both cohesive and non-cohesive materials were found to lead to breaches with straight sides due to the influence of pore water providing some cohesion even within non cohesive materials. This is a significant deviation from existing methodologies which often assume a trapezoidal or v shaped breach. Morris *et al* (2008) also found the erodability of different materials was influenced by the material texture, compaction moisture content, compaction energy and soil strength with complex interactions occurring between these different factors.

The defence structure should also be considered, for example embankments may be built with a sand core overlaid by a cohesive outer material, or defences may have been raised over time may consist of different materials in different layers. These composite defences do not react in the same way as their uniform counterparts and can exhibit very fast growth rates up to several metres per minute (Muir-Wood and Bateman 2005).

Defence construction is rarely uniform along the whole section. Variation occurs due to changing soil conditions, foundation type, animal burrowing, poor drainage and varying construction materials and methods during the defence's lifetime. As well as within section variation, the flooding in New Orleans following Hurricane Katrina highlighted the transition point between structures as a common cause of failure (Morris *et al*. 2009b).

8.2.3.2 Event and local conditions

Even assuming that all defence structures are constructed equally, they are not subject to identical conditions during a flood event. While developing RMS's CAT model, Muir-Wood and Bateman (2005) identified the hydraulic gradient across the breach as critical in determining the breach size and depth. Where rapid ponding occurs behind the breach hydraulic gradients are reduced leading to less erosion, however for wide flat floodplains where flood water quickly travels away from the breach location larger breaches are expected. In the same way they found neighbouring breaches are in competition with each other. Since water from the initial breach reduces the hydraulic gradient across the defence erosion rates for subsequent breaches will be lower, therefore, all things being equal, the first breach will be the largest.

Traditionally research has focussed on developing universal breach models however Morris *et al* (2009b) highlight that fluvial, tidal and reservoir breaching processes are different and therefore should be modelled individually. To date there is no suggestion in the literature about what form these separate models should take.

As well as the local scale geometry of the defences system, micro scale variations can also be critical in determining failure. The presence of vegetation is a good example of this. One of the major breaches during the 1953 storm surge was attributed to exposed roots from a bush growing on the embankment (Institution of Civil Engineers 1953; Muir-Wood and Bateman 2005). Predicting the effect of vegetation is difficult as vegetation results in complex interactions for example the vegetation both protects the surface of the defence but also provides preferential flow route for water into the defence core.

8.3 Methods of modelling of flood defence failure

Morris *et al* (2009) identify three methods of modelling flood defence breaches; non physically based empirical models, semi-physically based models and physically based models. Non physically based models were found to be the most commonly used as they are simple and fast, however there is little consideration of the breach development process and high levels of uncertainty surrounding the model parameters. Increasingly commercially available hydraulic modelling packages now include a semi-physically based breach model however the user still has to supply the breach growth rate and final breach width. Fully physically based models, such as HR-BREACH (FLOODsite 2012) are mainly produced in research settings (Morris *et al.* 2009a). The disadvantage of these models are long run times and the requirement for considerable preliminary data about the defence structure which requires field surveys. However Morris *et al* (2008) argue that even when used with design parameters, physically based models are likely to produce better results than empirical models. This is a particular problem for risk based frameworks as the model run times and preliminary data requirements effectively exclude their use in risk based frameworks. Therefore a compromise needs to be found between model run times and the usefulness of the results. This requires developments in both the field of breach modelling, to produce efficient breach models that can be used in a risk based framework, and within risk based defences modelling to incorporate breach development, as most existing models only consider a snap shot in time. At present risk based models use a simplified approach to modelling defence failure by using fragility curves. This is discussed further in Section 8.3.1. One of the major problems preventing the development of defence reliability models both in risk based and physically based frameworks is the lack of data available to calibrate models with (Morris *et al.* 2008).

Modelling flood defence breaches is of international significance and work is ongoing around the world. Care should be taken when 'borrowing' methodologies and software from different countries due to the location specific processes for example Buijss *et al* (2003) found that Dutch methods (used in the PC RING software) were not easy to apply in UK due to difference

in data type and availability. The scale of applicability is also important. Due to the lack of available case study data, models developed in the lab have been shown to be unrepresentative with different conditions in the field, and field tests are in turn based on small embankments and it is unknown if the methods will transfer to large embankments in a real breach event (Morris *et al.* 2008).

8.3.1 Risk based modelling of defence failure

Incorporating defence failure models into a risk based framework requires consideration of the factors known to cause and influence breaching (see Sections 8.2.1 to 8.2.3) and modification of available detailed failure models to allow for fast run times and limited data. Although risk based approaches are becoming more commonplace, the consideration of flood defence failure is often not truly risk based due to the practice of using scenarios based failure analysis for which the probability of each scenario cannot be fully determined (Apel *et al.* 2006; Vorogushyn 2009). This section reviews how defence failure has been included in three different modelling frameworks, RASP, work from the Postdam research group and CAT models. An overview of the general modelling framework used by these approaches was provided in Section 2.4, this section reviews how defence failure is incorporated into each approach through the use of fragility curves.

8.3.1.1 Fragility curves

Most risk based methods of representing flood defence failure use the concept of fragility curves. Fragility curves, according to Simms *et al.* (2009, p621), "quantify the relationship between the loading of an asset and the conditional probability of failure of the asset given that loading." An example fragility curve was shown in Figure 2.4. The curves are usually established by probability reliability analysis.

The concept of fragility curves was first used in the UK as part of the RASP project (Hall *et al.* 2005; Gouldby *et al.* 2008) which developed curves based on one failure mode, breaching following overtopping. Since then fragility curves have been extended to consider more failure modes (Dawson *et al.* 2005; FLOODsite 2009a) and more dimensions (Apel *et al.* 2009). The generalised fragility curves used in RASP are the only nationally available consistent dataset on defence fragility in the UK (Simms *et al.* 2009).

The benefits of fragility curves are that they allow failure to be considered with limited access to local data. However this does mean that they provide a simplified representation of conditions which can lead to uncertainties in the results. Following the 2007 floods Simms *et al.* (2009) reviewed the suitability of the established fragility curves in the UK. During the event

1000km of defence were tested by the floods, of this 525km overtopped and 4 embankments breached (a total length of 50m). This was a very low proportion of breaching compared to what would have been predicted using the established curves and illustrated that grassed embankments are able to withstand more overtopping than previously expected. Of the four breaches that occurred, three of them initiated when the water level was significantly below the crest level. This was found to be caused by local irregularities such as foxholes and vegetation rather than general poor defence quality which the established fragility curves were not able to consider. Based on this event Simms *et al* (2009, p626) conclude that "uncertainty about the presence of internal irregularities is probably a significant factor driving the small probabilities of failure in the fragility curves in the part where water levels are below crest level." In light of this they suggest that uncertainty in fragility curves could be reduced by local and historic insight and careful engineering investigation. In some instances this may be justifiable for example in the TE2100 project where the high levels of risk and uniqueness of the defence structures considered require careful consideration and the RELIABLE tool (FLOODsite 2009b) developed as part of this project enables this to be achieved. The general aim of the RASP project however was to provide a methodology that could be used over large scales with varying levels of data availability. Therefore rather than suggesting more detailed local data are required, there is also a need to modify the existing methodologies to incorporate the increased probability of failure due to local irregularities in defence structures. This is discussed further in Section 8.4.

8.3.1.2 RASP

The RASP method (Hall *et al.* 2003; Dawson *et al.* 2005; Gouldby *et al.* 2008) was previously outlined in Section 2.4.2. The original paper only covered breaching following overtopping however later work considered sliding and piping failure models. The key assumptions are repeated here (Hall *et al.* 2003):

1. Loading of all defences in the system is fully dependent, meaning all defences are subjected to the same load at the same time.
2. The strength of each defence section is assessed independently therefore although the load is the same, the probability of failure is unique for each defence section.
3. The resistance within each defence section is fully dependent meaning the whole section responds in the same way.

A central part of the RASP research was to establish a generic database of 600 fragility curves for specified defence types based on based on defence type, crest width, front, crest and rear

protection, construction, and defence condition. This database enables risk based consideration of defence failure in projects where detailed data on defence condition is not available. A criticism of the high level RASP methodology is that it does not take account on underlying geology which can affect seepage processes (Gouldby *et al.* 2009). For a high level study this type of detail is often not available, however the discussion in Section 8.2 highlights that there is a need for a high level methodology that is able to incorporate this spatial variability. The spatially varying crest height methodology developed in Section 8.4 could provide the foundations for this.

8.3.1.3 Inundation Hazard Assessment Model

Researchers at the University of Postdam have been working on a risk based modelling strategy for fluvial flood risk referred to as the Inundation Hazard Assessment Model (IHAM). There are various papers covering parallel developments and applications of the IHAM (Apel *et al.* 2004; Apel *et al.* 2006; Apel *et al.* 2009; Vorogushyn 2009; Vorogushyn *et al.* 2009; Vorogushyn *et al.* 2010). Much of the research was motivated from the observation that there has been a lack of comprehensive review of influence of dike failure for hazard and risk assessment (Vorogushyn 2009) both in terms of the consideration of the breaching process itself and the potential uncertainties in existing methods which are often overlooked. Like other established risk models, the IHAM has three modules representing a 1D hydrodynamic model of river routing, a probabilistic model of dike breach and a 2D inundation model. Dynamic coupling between modules and a Monte Carlo framework is used to address uncertainty (Vorogushyn *et al.* 2010). Only the failure module is discussed in this section.

To date the failure modes considered include overtopping, piping and slope micro-instability. Although multiple failure mechanisms are covered, no consideration is made of the potential interactions between them (Vorogushyn 2009). There are two main differences between the IHAM methodology and RASP, firstly the fragility curves are extended to fragility surfaces that also consider the duration as well as high water level, and secondly, the restriction of identical loading is removed to allow consideration of sequential defence failure. The dynamic consideration of the influence of upstream breaches on downstream water levels was found to show significant retention of floodwater behind upstream breaches therefore changing the shape of the flood peak (Apel *et al.* 2009). This is particularly significant on the large river systems of the Elbe and Rhine which the methodology has been applied to. The author is not aware of any attempts to repeat this analysis on UK rivers where the floodplain storage volumes may be significantly lower. It was however not possible to test the methodology as

part of this PhD due to the selected fluvial sites not being protected by flood defences (see chapter 3).

Some of the restrictions of the RASP methodology remain, for example defence sections are artificially split into lengths of less than 500m (Vorogushyn *et al.* 2010) with defence properties assumed homogeneous over this length, and breaches are assumed to grow to their maximum size within one hour. Fragility functions were generated for each defence type with the geotechnical properties of each defence section assumed to be random variables, In the absence of available data this offers a means of incorporating varying defence properties.

8.3.1.4 CAT models

Cat models provide a good example of the concept of fragility curves being applied in a large scale model with limited available data. As identified in Chapter 2, details of Cat models are restricted however a useful overview of the methodology used is available from AIR (Qu 2009) for fluvial defences and in two papers by Muir-Wood *et al.* (Muir-Wood and Bateman 2005; Muir-Wood *et al.* 2005) covering the consideration of coastal defences by RMS.

AIR include four defence types in their fluvial model; embankments, flood walls, storage areas and point structures. Data are inputted from the EA NFCDD database on defence characteristics and from detailed topographic maps on the physical properties such a crest height and attenuation area. Defences which are evident in the digital terrain model are included physically in the AIR Inland Flood Model as they can be included in the cross section geometry of modelled reaches. The failure of defences is modelled probabilistically in a standard way using fragility curves. Fragility curves are established for every stream link based on type and condition of the defence.

RMS also employ fragility curves as the central component of their defence reliability model using data from the 1996 EA Sea Defence Survey and calibrating against observations from the 1953 storm surge. Breaching occurs in the model due to overtopping and infiltration. The conceptual model states that all things being equal the probability of a breach in one or more places along a sea defence breaching a surge tide increases as:

- The length of defence increases
- The duration of high water increases
- The level of water increases
- The strength of the defence decreases

Similar simplifications were made to the RASP method including restricting the defence length, in this instance to 2km. Rather than constructing fragility curves for all construction types, defences were classified into four groups:

- Level 1 - purpose built reinforced concrete defences with strong foundations and foreshore protection.
- Level 2 - armoured defences but without full foreshore protection.
- Level 3 - unreinforced, purpose-built embankments.
- Level 4 - natural defences, such as sand dunes

Fragility curves were established based on reliability theory considering defence length and event duration. Since in reality the water raises slowly, peaks and then decays, the duration used was an integrated value representing the equivalent time at maximum water level.

8.3.2 Breach sizes and growth rate

As discussed in Section 8.2, once a breach has initiated the growth rate and maximum dimensions can vary due to the defence properties and event conditions. Incorporating this variability in failure models is difficult and leads to uncertainties, largely because of the limited observed events and, as observed by Muir-Wood and Bateman (2005), when breaching does occur it is ephemeral with repairs beginning within hours. For this reason there are limited data to validate methodologies. However observation from the Safe Coast project (2008) suggest that the uncertainties involved in estimating breach growth are small compared to the uncertainty in establishing the number of breaches in any given defence section.

There have been various proposed methods for dealing with breach growth. In most cases the breach growth rate is assumed to be negligible and to complete within one time step (for example see Vorogushyn *et al.* 2010). The variability between approaches is in the assumed breach dimensions. A table of breach sizes showing both observed and assumed values used in previous studies is provided in Appendix E.2.

The simplest means of estimating breach width is to use historic data or hypothetical scenarios to establish a standard breach width for each defence section. This is the approach taken in the Conwy Tidal Flood Risk Assessment (CTFRA, HR Wallingford 2002) however as identified by Vorogushyn *et al.* (2010) it is problematic for risk based analysis as the probability of each scenario is not known. An extension to the simplistic approach is to include a range of plausible breach dimensions for each section based on the erodibility of the defence material and sample from within this as part of a risk based framework. This is the approach taken by the IHAM project team (see Vorogushyn 2009 for details). The RASP method (Hall *et al.* 2003) takes an alternative approach and estimates the breach width (b_B) as a function of the event

magnitude (x) and the defence length (s_d) (Equation 8.1), rather than considering the defence material. Vorogushyn (2009) suggest that this approach may be problematic as the event magnitude may not always be known in a dynamic world. Although it offers potential advantages when the defence material and construction is not fully known, Hahn *et al* (2000, cite Vorogushyn 2009) identified that breach growth rates can vary up to 60 fold depending on dike material.

$$b_B = 0.05xS_d, b_B \leq S_d \tag{8.1}$$

Once a breach has initiated and its dimensions established the standard practice used in both research applications (for example see Hall *et al.* 2003; Vorogushyn 2009) and Cat models (Muir-Wood and Bateman 2005) is to use the broad crested weir equation (Equations 8.2 and 8.3) to calculate flow through the breach.

$$v = \sqrt{gh} \tag{8.2}$$

$$Q = v \times h \times width \tag{8.3}$$

Where v is the velocity of the water in m/s, g is the acceleration due to gravity, h is the height of the water above the base of the breach and w is the breach width. Q is the flux of water passing through the breach in m³/s.

8.3.3 Proposed methodology for flood defence failure

It is beyond the scope of this project to develop a detailed flood defence failure methodology. Instead attention is paid to the most significant limitations of existing models which is deemed to be the lack of consideration of spatial variation in the defence properties. In keeping with the spatial-temporal approach introduced in the analysis of extreme water levels, a spatial analysis of dike breaching is employed. In doing so, the proposed methodology avoids the arbitrary sub-division of dikes into discrete sections that has been adopted in previous approaches (e.g. Hall *et al.* 2003; Gouldby *et al.* 2008; Apel *et al.* 2006; 2009), which has been imposed in an attempt to deal with the so-called 'length effect'. These previous methods were based on the assumption that for any given dike section the whole section would respond to loading in the same way. For long dike sections this assumption is untenable as dependence in dike response to loading decays with distance. In the proposed methodology the assumption of fully dependent resistance is lifted, therefore there is no requirement to restrict defence section length.

Considering a system with g dike sections, $m = 1, \dots, g$. The event in which section m fails is written as D_m , whereas the event in which it does not fail is written $\overline{D_m}$. In recognition of the

fact that the most common failure mechanism is breaching caused by overtopping (Nagy and Tóth 2005; FLOODsite 2009a) only this failure method is considered here. It is acknowledged that other failure methods are possible and may in some cases be more significant. The methodology could be extended to include other mechanisms in the future.

The most critical variable in determining overtopping is the crest height. Analysis of surveyed crest height information and that contained in the EA NFCDD, which is used extensively in flood risk studies by the Environment Agency, research groups and Cat modellers (see Section 8.3.1), showed large variation between the record mean section crest height and surveyed crest height (as detailed in Section 8.4.1). As such the spatially varying crest height (c) of each defence section m , separated into sections based on defence type (t_m), is assumed to be spatially variable around the recorded mean crest height (\bar{c}_m). Realisations are sampled every 50m at sampling points k .

$$c_{m,k} = f(\bar{c}_m, t_m) \quad 8.4$$

Realisations of the spatially varying crest height are made within the risk based framework for each event scenario as detailed in Section 8.4.2. Overtopping (OT) is calculated at each sampling point using the water levels and wave heights as described in Chapter 7 such that;

$$OT_{m,k} = f(c_{m,k}, peak\ swl, peak\ wave\ height, defence\ slope) \quad 8.5$$

Failure is estimated using a standard fragility curve approach (Function 8.6), this is common to all risk based applications discussed in Section 8.3.1.1 and reflects the accepted method for risk based studies.

$$p(fail)_{m,k} = f(OT_{m,k}, t_m) \quad 8.6$$

Breach size is sampled using a scenario approach from a range of expert opinions as described in Section 8.5.2.3. This provides physically plausible breach widths but could be improved with more detailed knowledge of the local area. Multiple failure points are allowed within each defence section, where the distance between the failure points is less than the breach width the smaller breach merges into the large breach based on the assumption that the first breach is likely to be the largest and grow the fastest.

A summary of the process is given in Figure 8.4. Section 8.6 illustrates an end to end example of the consideration of flood defence reliability.

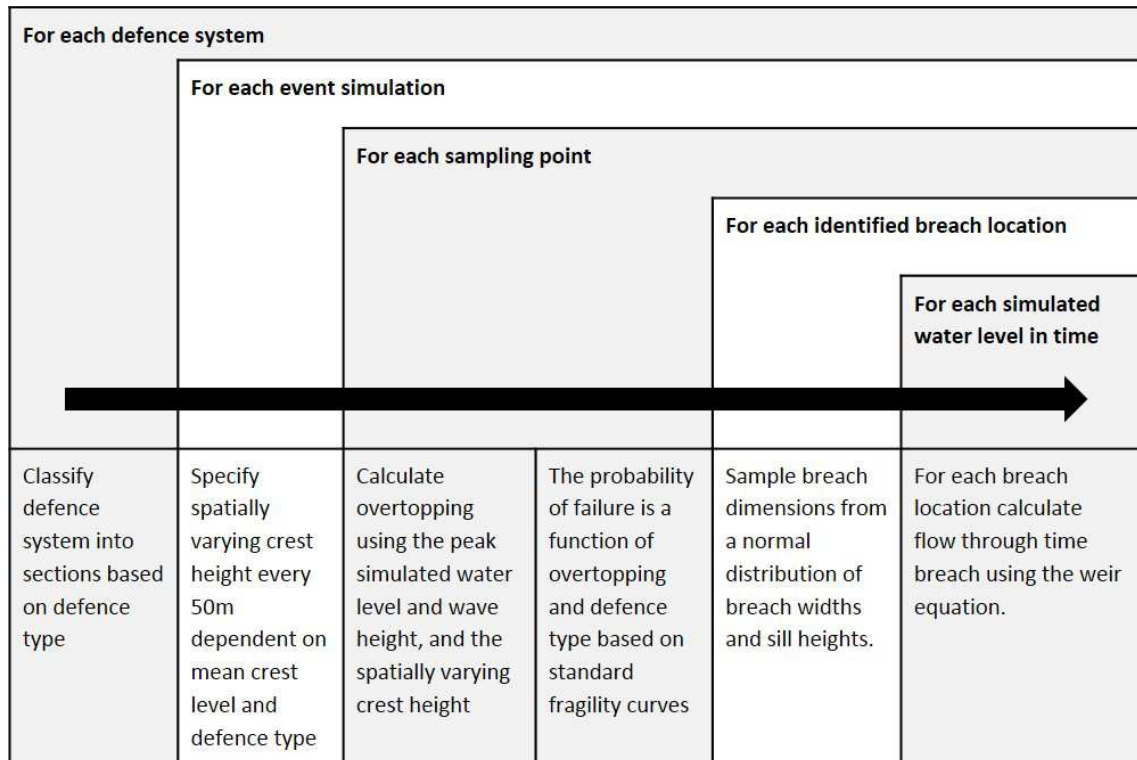


Figure 8.4 Summary of consideration of defence reliability

8.3.3.1 Summary of assumptions

It is recognised that the estimation of breach dimensions and flow into the floodplain are simplifications of a complex process. The methods proposed for use in this thesis represent the standard current practice and are suitable given the acknowledgment that the uncertainty in estimating breach dimensions is small in comparison to the uncertainty in establishing if breaching will occur (Safe Coast 2008). The key assumptions embodied in the process are that:

- Defence crests vary along their crest relative to the mean section elevation
- Defence material, construction and other properties (except crest height) are identical within each defence section
- Conditions at the foot of the defence are insignificant during flood events
- Overtopping alone will not cause damage to caravans unless breaching occurs
- Breaching caused by overtopping is the most critical failure mechanism
- The probability of failure can be represented by the peak overtopping rate and the defence type
- If breaches occur, initiation begins when the total water level is greater than 90% of the crest height
- If multiple breaches occur within one section, breaches will merge if the distance between the two breach locations is less than the widest breach width

- Breaches grow to their full size within one time step

8.4 Development of methodology for variable flood defence crest height

Flood defences in the UK have been developed in a piecemeal fashion (Muir-Wood and Bateman 2005) and are in varying states of repair. Similarly it is unlikely that their crest heights have been maintained to design standards, for example an earth embankment may have eroded in certain areas or been compressed by people walking along it. To some extent fragility curves can take account of these processes by incorporating probabilities of failure at water levels below the crest height. However in practice the probability of a defence overtopping is heavily dependent on the crest height which may vary along the length of the defence. The degree of variation is influenced by the defence type, its condition and the maintenance regime. The availability of defence crest height data varies across the UK, this data is mainly held by the Environment Agency and usually comprises of a mean crest height for each defence section.

In light of these difficulties a methodology was developed as part of this thesis to allow for plausible spatial variation in long section crest heights in the absence of detailed survey data. It was originally proposed to use an autocorrelation process to simulate the spatially variable crest level but as discussed in Section 8.4.1 this was shown to be inappropriate. Instead a Markov chain process is used whereby at each simulation point there is a strong probability of the simulated crest height being the same as the previous crest height and a lower probability that it will move to a new state. The properties of the Markov chain process were identified by review of flood defence survey data obtained from the Environment Agency for flood defences in Lincolnshire.

8.4.1 Review of surveyed crest height

Survey data for 59km of coastal flood defence between Cleethorpes on the Humber Estuary to Gibraltar Point at the edge of the Wash, were obtained from the Environment Agency as well as a GIS file of the defence locations. The survey data were separated into sections as detailed in Table 8.1. For each flood defence section data were available in printed summary sheets containing;

- The section location
- The defence type
- A typical survey cross section
- Physical parameters including the crest height, toe elevation, crest width and section length

- A long section plot showing the survey crest height, the crest height taken from DEM data and the mean crest height.

An example of the data available is shown in Appendix E.1. The survey resolution for the crest height is not known.

Survey data of this quality is not readily available in the UK, for most flood defences it is usually only possible to obtain the mean long section crest height. The survey data were therefore compared to the mean crest height to identify the potential uncertainty in using mean crest height to model flood defences rather than varying crest height along the defence section. The mean crest heights in the dataset were derived from various sources including as identified in Table 8.2.

Table 8.1 Summary of Environment Agency flood defences survey data by defence type for the Lincolnshire coast

Defence type	Number of sections	Total length (m)	Average crest height (m)	Minimum section length (m)	Maximum section length (m)	Median section length (m)
Walls	25	14545	7.02	96	1640	424
Embankments	29	19614	6.31	82	2208	495
Dunes	54	24831	7.62	58	1351	427

Table 8.2 Source of long section mean crest height by defence type for the Lincolnshire coast

Defence type	Number of section sources:					
	Typical SDS section	SDS sections mean	DTM long section mean	DTM cross sections mean	EA expert knowledge	Spot heights mean
Walls	17	1	7	0	0	0
Embankments	12	1	0	10	5	1
Dunes	20	9	14	5	0	6
Combination	49	11	21	15	5	7

SDS - Sea Defence Survey

A visual assessment of the variation between the mean crest height and the survey data was made using the classification schemes in Table 8.3 and Table 8.4. An assessment of the magnitude and direction of variation was also made based on visual interpretation of the long section profiles. The defence sections were separated into three groups for walls, embankments and dunes. The walls group consisted of vertical walls, wave return walls and stepped concrete aprons. As listed in Table 8.1 there were 25, 29 and 54 sections of each type.

Table 8.3 Classification of fit of long section mean crest height compared to survey data


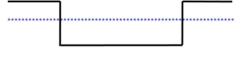
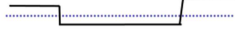




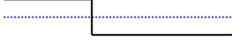


Fit of long section mean to survey	Description	Example
Very poor	Significant differences for most of defence length and / or including major low points that could lead to flooding	
Poor	Moderate differences for >50% of defence length	
Reasonable	Average is a reasonable representation of crest height except for some small areas	
Good	Close match for >50% of defence length	
Very good	Close to perfect match for most of defence length	

Table 8.4 Classification of type of variation between long section mean crest height and survey data

Type of misalignment	Description	Example
Consistent	Consistent crest height along long section (for DTM data this is also applied to consistent small variations)	
Variable	Varying defence crest along long section	
Block	Large block sections with consistent differences	
Low points	Main problem is low points not picked up by average crest height	
High points	Main problem is high points not picked up by average crest height	

8.4.1.1 Observations on fit of long section mean to survey data

A summary of the assessment results are shown in Figure 8.5 to Figure 8.8. The dunes survey showed most sections have notable variation in crest heights along the section length. This is poorly represented by the mean crest height with more dune sections classified as very poor than other defence types. In most cases the mean height was higher than the survey height, therefore flood risk could be underestimated if using the mean crest heights. Surprisingly the walls were poorly represented by the long section means. This was largely due to block variations in the crest height where part of the wall was higher or lower than the mean height. The long section means for the walls also tended to be lower therefore using the mean values would produce a conservative estimate of risk.

For all defence types the qualitative review of the degree of variation identified in most cases the difference between the long section mean and the surveyed data was between 0.1m and 0.5m. This is a maximum error of 8% in crest height which present a significant uncertainty for flood risk modelling.

Only the dunes obviously show a variable variation between long section mean elevation and survey elevation that could be characterised by an autocorrelation process. In most cases a block variation pattern was seen with part of the defence consistently above or below the mean height. The embankment surveys show consistent crest heights along the defence therefore in more cases the mean long section crest height provides a reasonable representation of the actual defence height.

A cross check was also made against defence length and construction type. There appeared to be no difference in degree of variation different section lengths or materials.

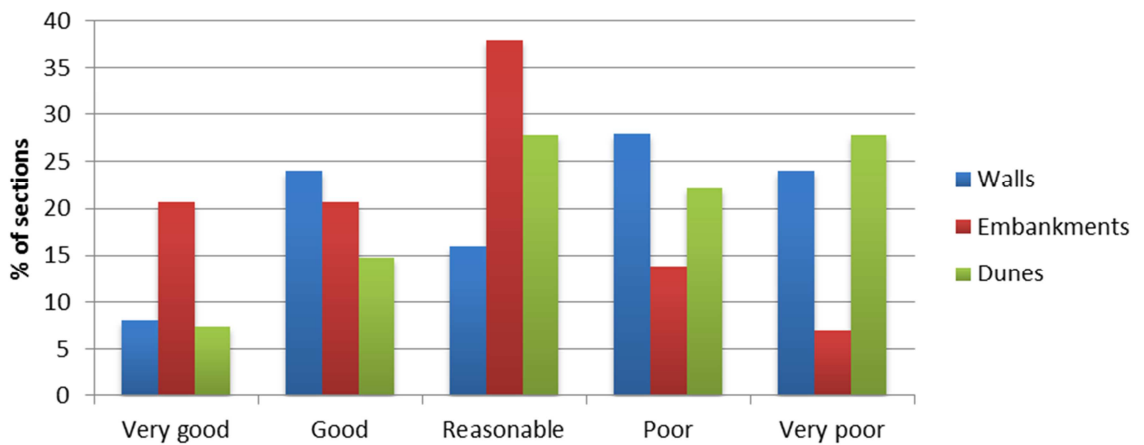


Figure 8.5 Fit of long section mean crest height to surveyed crest elevation

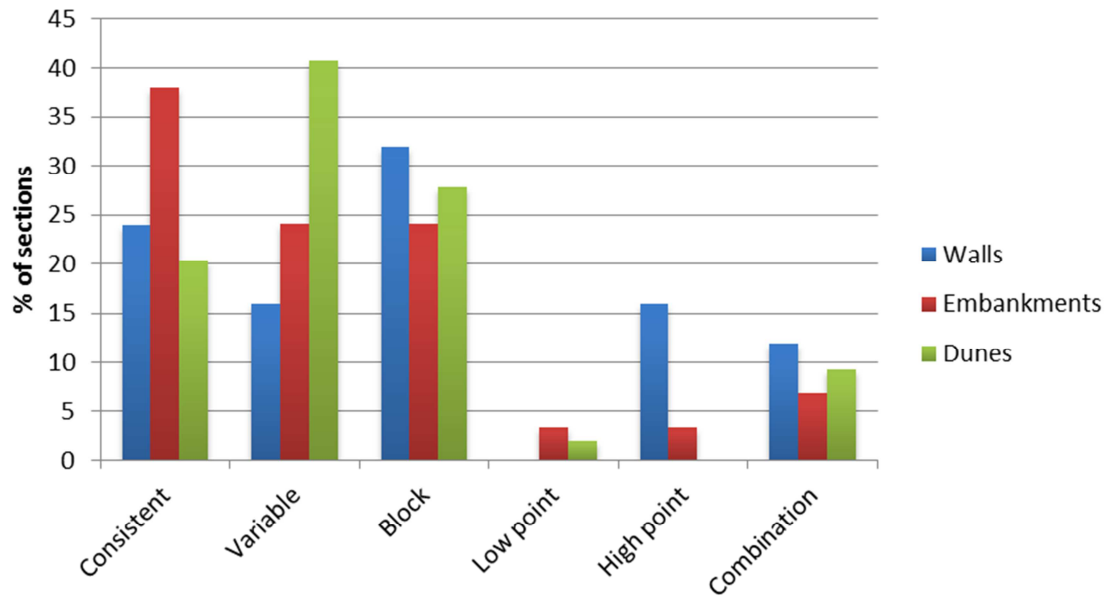


Figure 8.6 Type of variation between long section mean crest height and surveyed crest elevation

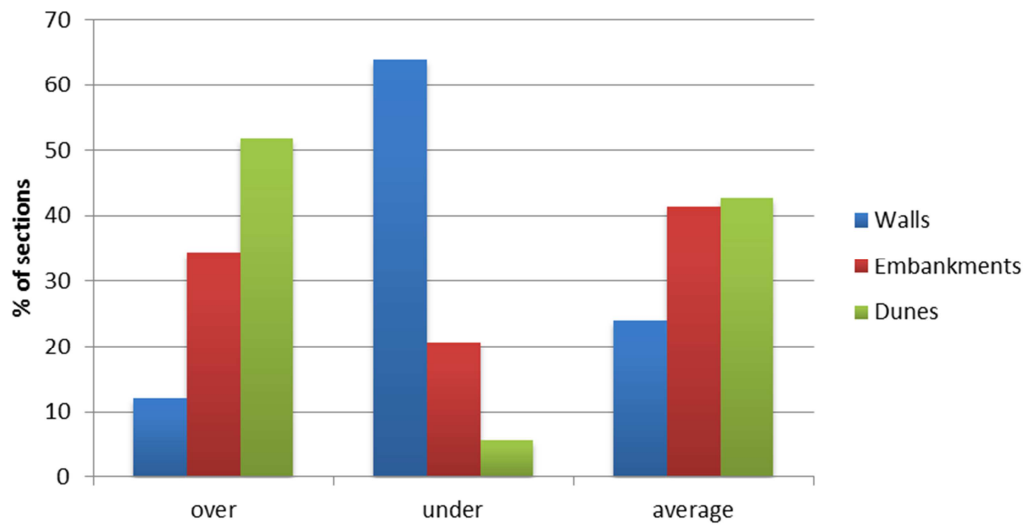


Figure 8.7 Direction of variation between long section mean crest height and surveyed crest elevation

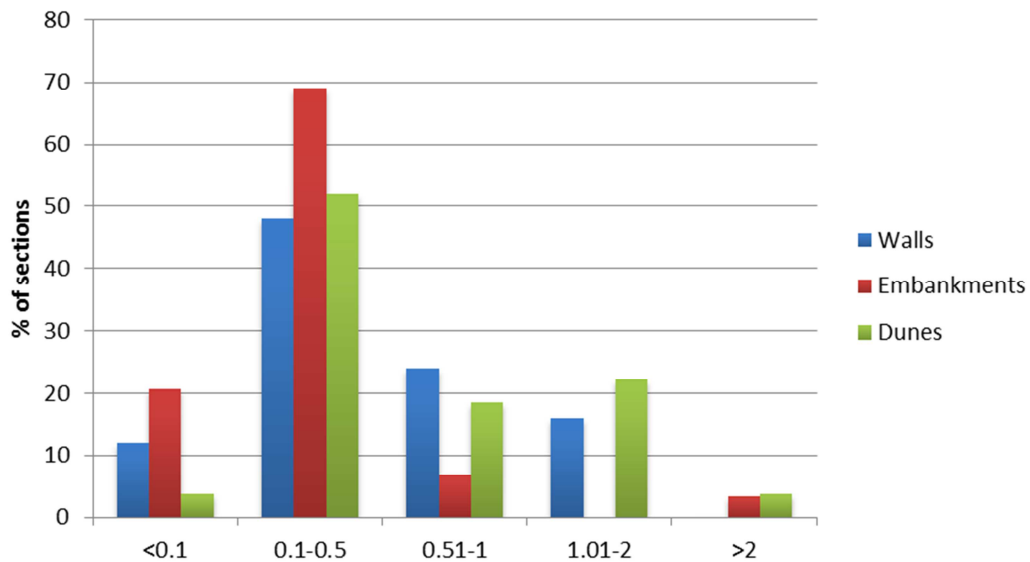


Figure 8.8 Magnitude of variation between long section mean crest height and surveyed crest elevation

8.4.1.2 Observations on data quality with reference to data source

Theoretically different data sources may provide a more accurate representation of crest height however as shown in Table 8.2, for some data sources there are less than 10 sections, therefore it is difficult to draw conclusions from the limited data. General observations suggest that crest heights taken from typical SDS survey sections provide the best representation of surveyed crest height while crest heights taken from the DTM long section are often very poor however this can be improved by taking the mean of DTM cross sections rather than using the long section directly.

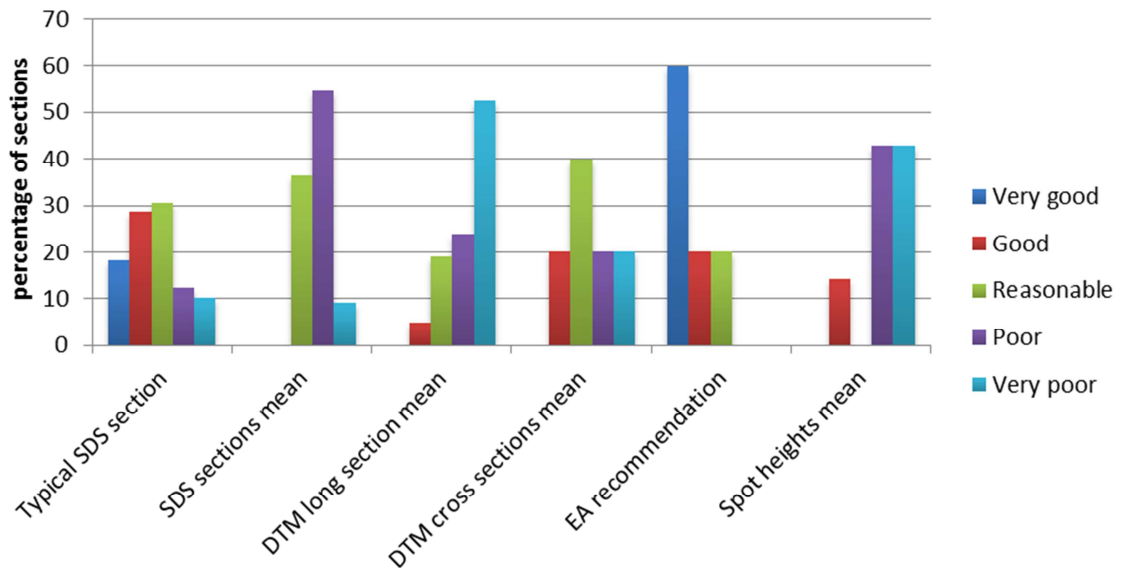


Figure 8.9 Representativeness of long section mean crest height compared to surveyed crest elevation from different data sources

8.4.1.3 Observations on data quality of DTM long sections

The above analysis was repeated comparing the survey data to the long section crest heights as taken from the DTM. Cat models (see Section 8.3.1.4) use the DTM data to provide crest heights therefore this could be a useful indication of the suitability of their defence crest representation. The difficulty with this approach is that in most cases the DTM data shows considerable variability which is not present in the survey data. However without knowing the resolution of the survey it is difficult to know which is correct.

The same plots as for the long section mean are shown below. The DTM data very rarely provides a good or very good representation of the crest. Most often it is rated as poor. The type of variation is variable. The DTM data usually shows frequent small variations of +/- 0.5m although sometimes much larger variations are seen. The direction of variation changes and magnitude may be several metres above or below the surveyed crest. In cases where the defence crest height changes along its length the DTM data may provide a better representation of the surveyed crest as than the long section mean as it picks up the trends in crest height and low points, even if the exact value is inaccurate. For dunes the DTM data over estimates the crest height. For walls and embankments there is a small trend towards under estimation. A possible reason for this is the difficulty in picking up wall and embankment features with a relatively small horizontal resolution in the DTM.

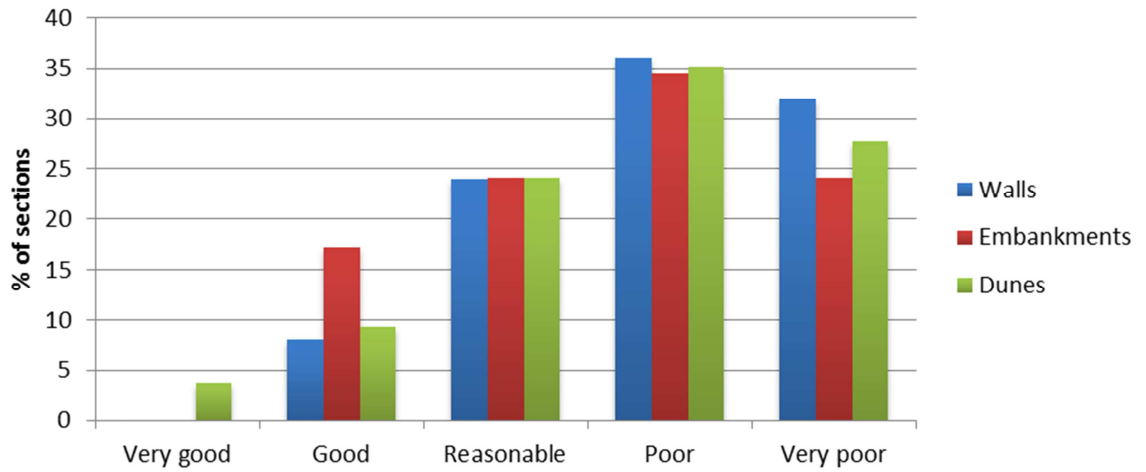


Figure 8.10 Fit of long section mean crest height to DTM crest height

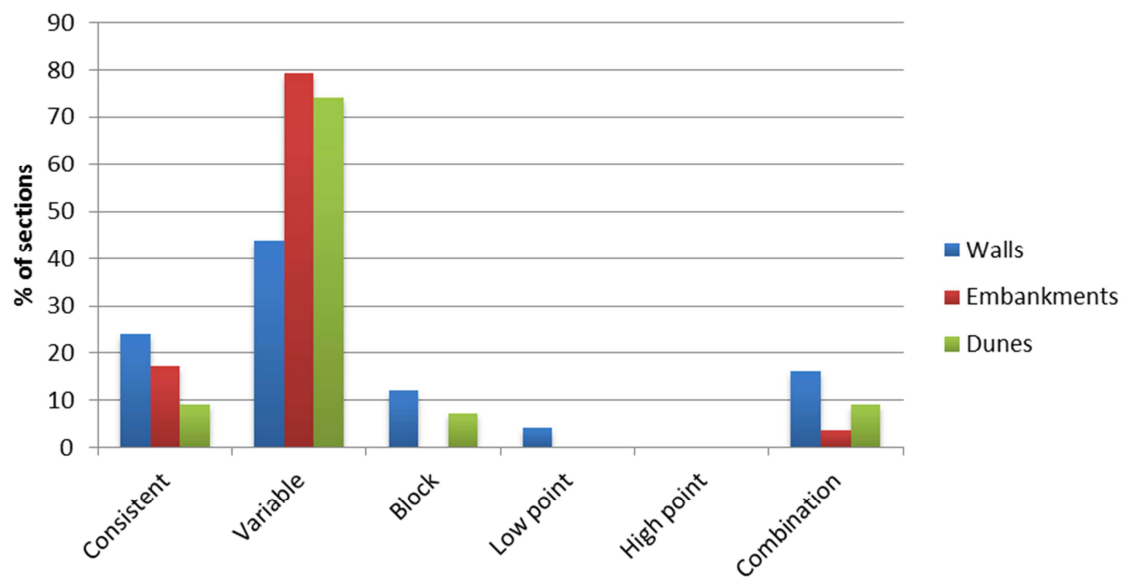


Figure 8.11 Type of variation between long section mean crest height and DTM crest height

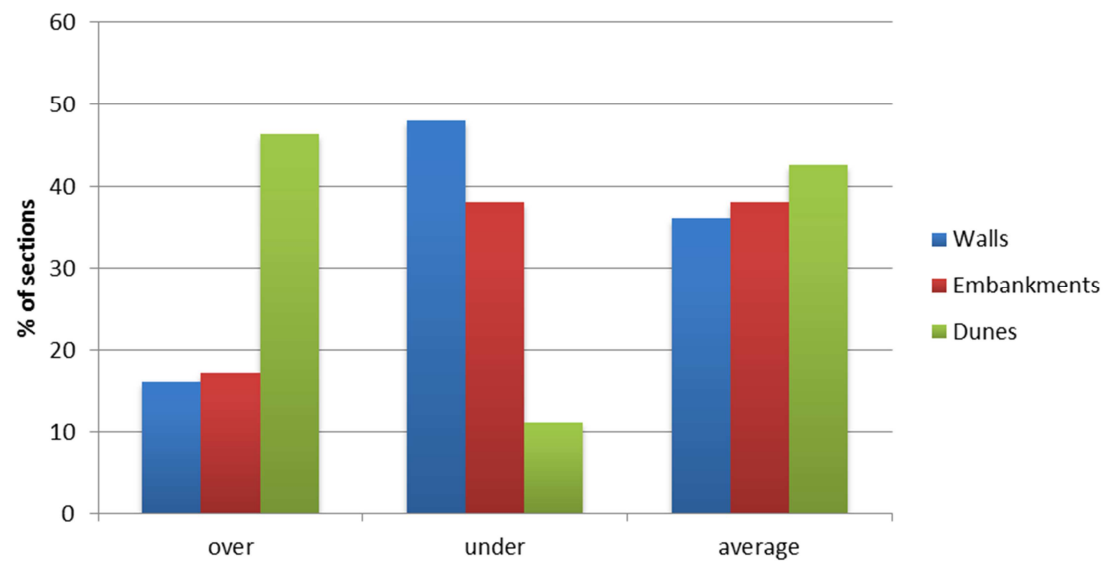


Figure 8.12 Direction of variation between long section mean crest height and DTM crest height

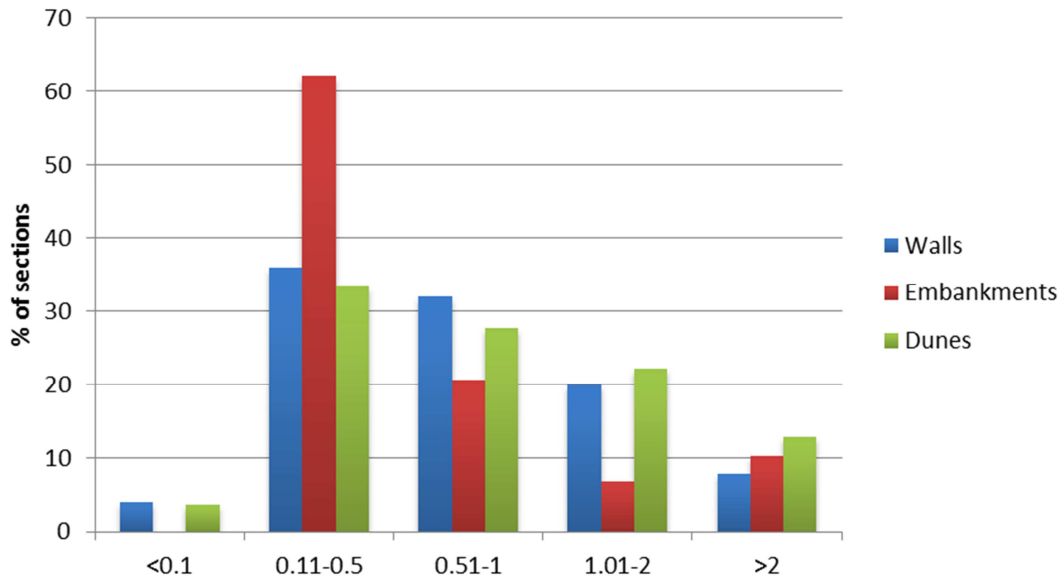


Figure 8.13 Magnitude of variation between long section mean crest height and DTM crest height

8.4.2 Simulation of plausible variation in long section crest height

Based on the data properties observed from the East Coast flood defence data it is possible to simulate a realisation of the plausible variation in crest height for any given defence type and mean long section crest height.

For each known defence type, a misalignment type is sampled based on the observed occurrences for each defence type. Then for each simulation a realisation of the crest height is generated based on a Markov chain process, whereby at each simulation point (taken as every 20m) there is a strong probability of the simulated crest height being the same as the previous crest height and a lower probability that it will move to a new state. The probabilities are based on the distribution properties of the observed data and are different for each misalignment type. The advantage of using a Markov chain process is that the same process structure can be used with all the misalignment types and the probabilities varied accordingly.

As well as the continuous variation, realisations of low and high points in the defence crest are superimposed onto the simulated crest height. The stages of this process are outlined in Figure 8.14 and detailed below.

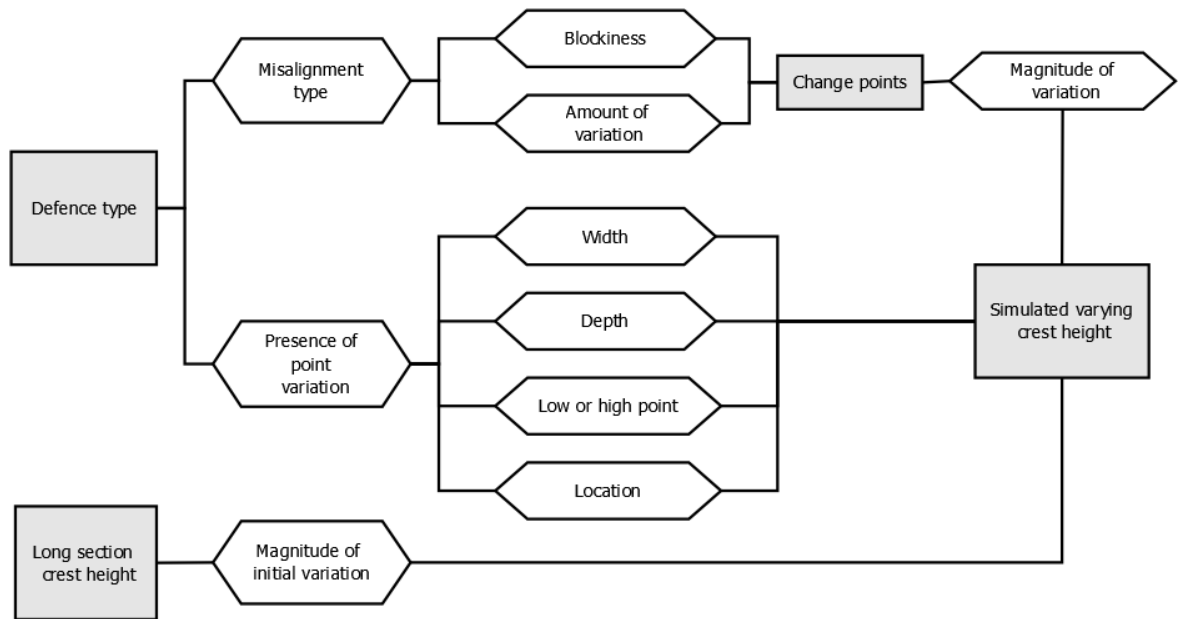


Figure 8.14 Plausible variation in long section crest height simulation

8.4.2.1 Misalignment

Type

For each defence type, wall, embankment or dune, the probability of the variation being constant, variable or block has been identified (Table 8.5). Given the defence type, a misalignment type is sampled using a random number generator based on these probabilities.

Table 8.5 Probability of type of variation between long section mean crest height and survey data as calculated from the Lincolnshire defence survey data by defence type

Defence type	Misalignment type		
	Consistent	Variable	Block
Wall	33	22	44
Embankment	44	28	28
Dune	23	46	31

Degree of variation

The amount that the crest height varies along its length is largely based on the variation type, however there are different degrees of variation observed within each class. The degree of variation can be characterised using two variables, the blockiness and the probability of variation.

The blockiness refers to the minimum number of simulation points between each change in crest height. This is sampled from a uniform distribution with the minimum and maximum range set based on comparison with the observed data. The sampling resolution is set at 20m

as it is unlikely that the defence survey was taken at a finer resolution than this so there are no data to support changes at smaller spatial scales.

The probability of variation refers to the probability that there will be no change in crest height at any sampling point from the previous sampling point. For consistent misalignment this value is set at 100%. For the variable and block misalignment the value is sampled from a normal distribution with the mean and standard deviation estimated by comparison to the observed data as detailed in Table 8.6.

Table 8.6 Distribution parameters characterising the degree of crest height variation

Variation variable	Misalignment type		
	Consistent	Variable	Block
Blockiness (no. simulation points)	NA	$u(4,10)$	$u(10,30)$
Probability (%)	100	$N(70,4)$	$N(90,2)$

Presence of low or high points

The presence of low or high points within the crest length occurs with all types of misalignments types. Therefore a point simulator is applied with all misalignment types. The point variation is superimposed on top of any previous variation due to misalignment.

The probability of point variation in crest level is specified based on the observed data for each defence type (Table 8.7). The presence of a high or low point is sampled from a random number generator based on these probabilities.

Table 8.7 Probability of low or height points within the defence section crest

Defence type	Probability of point variation
Wall	28
Embankment	10
Dune	9

If a point variation occurs the width and depth (as a proportion of the total crest height) of the variation are simulated using a normal distribution with mean and standard deviation specified from the observed data (Table 8.8). Due to the limited number of observed low and high points, the observed data are lumped together with no differentiation made for defence type.

Next it is specified whether the point variation is a low point or high point in the crest elevation. Again the probability of as low point occurring is based on the observed data for each crest height. However since all of the observed point changes in the dunes were low

points, a small probability (5%) of a high point has been introduced since it is not completely unlikely that a high point will occur.

Table 8.8 Distribution parameters characterising the shape of high or low points within the defence section crest

Defence type	Width (m)	Depth (proportion of crest height)	Probability low point
Wall			15
Embankment	N(33,24)	N(0.2,0.2)	75
Dune			95

Finally the location of the low or high point is specified randomly along the length of the defence crest, assuming that there is only one possible low or high point in the defence section. Given that the probabilities of a low or high point occurring are low, this is a valid assumption to make. If several point variations occurred in one defence section this would be classified as varying crest height rather than point variation. It should also be noted that the simulation method for point variations will sometimes produce shallow points which may not be significant when superimposed onto the existing simulated varying crest height.

8.4.2.2 Magnitude of variation

Initial variation

The degree to which the defence crest height varies from the mean long section value is given by:

$$z_x = z_m + \epsilon_x z_m \tag{8.7}$$

where z is the crest elevation, x is the sampling point, z_m is the mean long section elevation and ϵ is the simulated proportional error term from a normal distribution as specified in Table 8.9 for each defence type. A normal distribution is shown to be suitable for this purpose (Figure 8.15). The slightly blocky nature of the data plots in Figure 8.15 is due to the visual interpretation of error resulting in “round” error values such as 0.5m or 1m being recorded more often.

Table 8.9 Distribution parameters characterising the magnitude of variation from the long section mean crest height

Defence type	Magnitude of variation (proportion of crest height)
Wall	N(0.04,0.10)
Embankment	N(0.00,0.09)
Dune	N(-0.05,0.11)

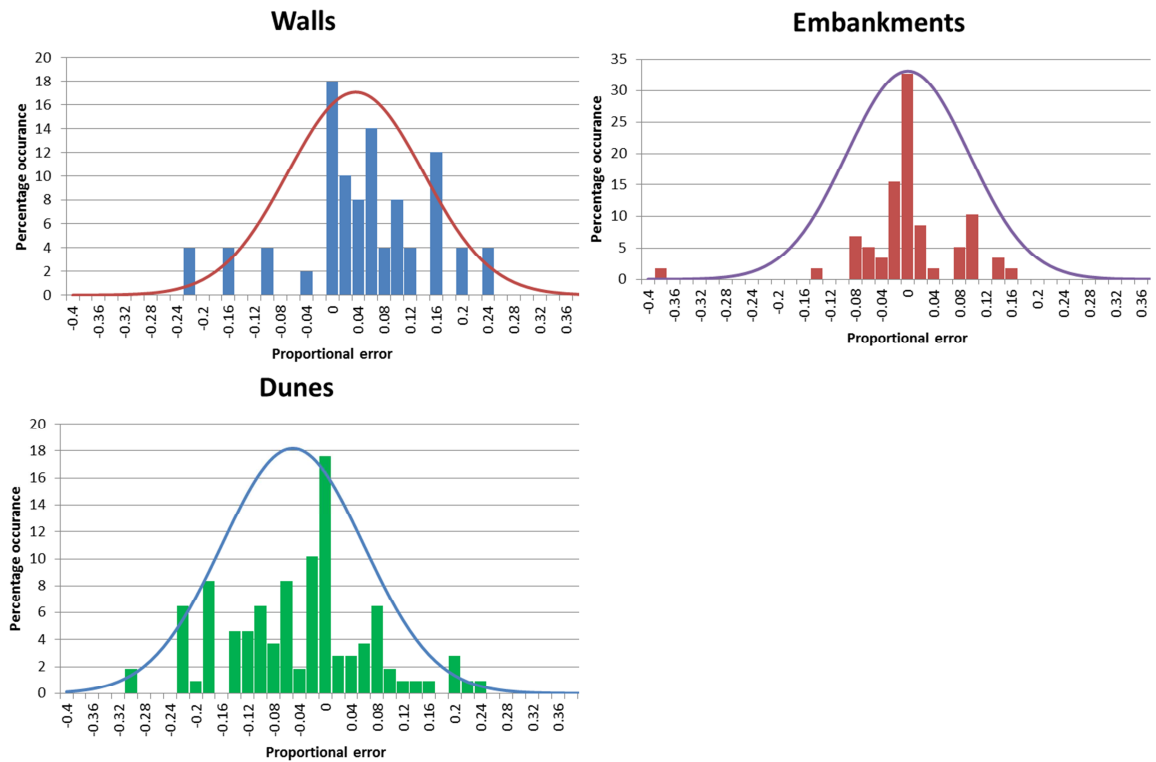


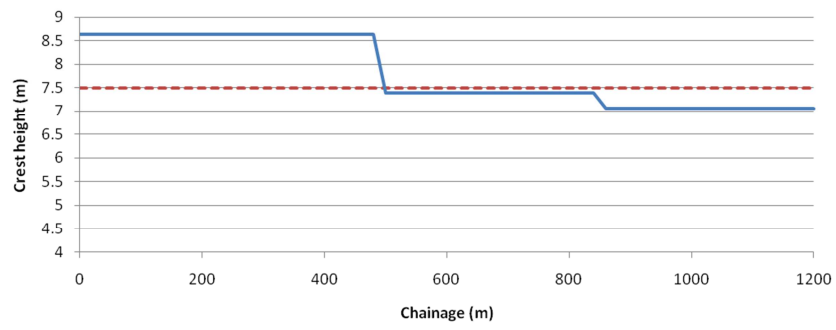
Figure 8.15 Fit of normal distribution for variation magnitude compared to observed proportional error between long section mean crest height and surveyed crest elevation

There is a physical limit to the amount of variation in crest height. Any major discrepancies are likely to be noticed during defence inspections and infilled as appropriate. For this reason a winsorising process was applied to the simulated variation magnitude with the limits set at a maximum variation of 25% of the mean long section height. This corresponds to the largest observed variation for dunes and walls.

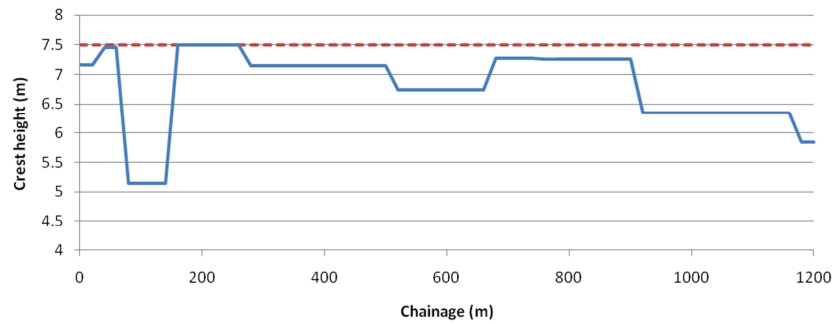
Variation at each change point

The above procedure is repeated at each point where a change in crest height is simulated. In each case the crest height changes relative to the mean long section crest height rather than the previous value.

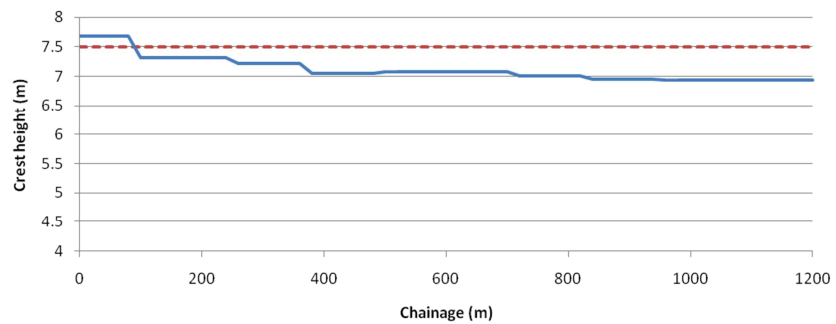
8.4.2.3 Example simulations



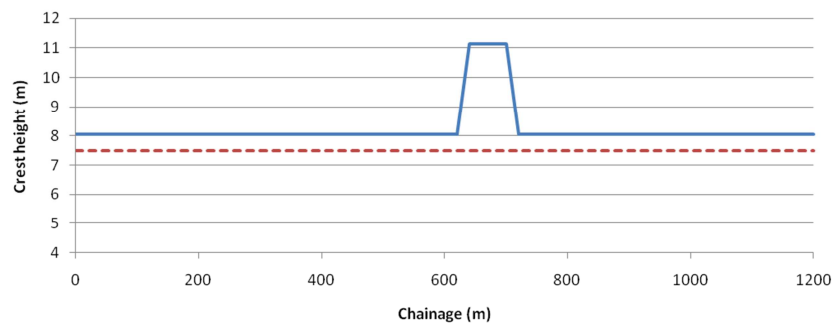
Defence Type	Misalignment	Blockiness	Probability	High/low points	Mean variation
Dune	Block	15	90	No	-0.3m



Defence Type	Misalignment	Blockiness	Probability	High/low points	Mean variation
Dune	Variable	3	74	Yes	0.68m



Defence Type	Misalignment	Blockiness	Probability	High/low points	Mean variation
Embankment	Variable	3	70	5	0.38m



Defence Type	Misalignment	Blockiness	Probability	High/low points	Mean variation
Wall	Constant	NA	100	Yes	-0.76m

Figure 8.16 Example simulations of plausible variations in crests heights for different defence types

8.4.2.4 Consistency

In most cases the separation of defences into sections is largely artificial and it is unlikely that there would be a large change in variation of the actual crest height and mean long section height between adjacent defence sections. To account for this the degree of variation at the end of one section is used as the initial variation for the next section.

Although no separate validation dataset was available, to check the suitability of the methodology 1000 simulations of the 59km of Lincolnshire crest height were made (the first 500 of which are shown in Figure 8.17). The simulated mean and standard deviation for each defence type are given in Table 8.10 which show a reasonable fit to the observed values given in Table 8.9 with only the mean variation of simulated dune and embankment crests showing a difference of 5% compared to the observed data.

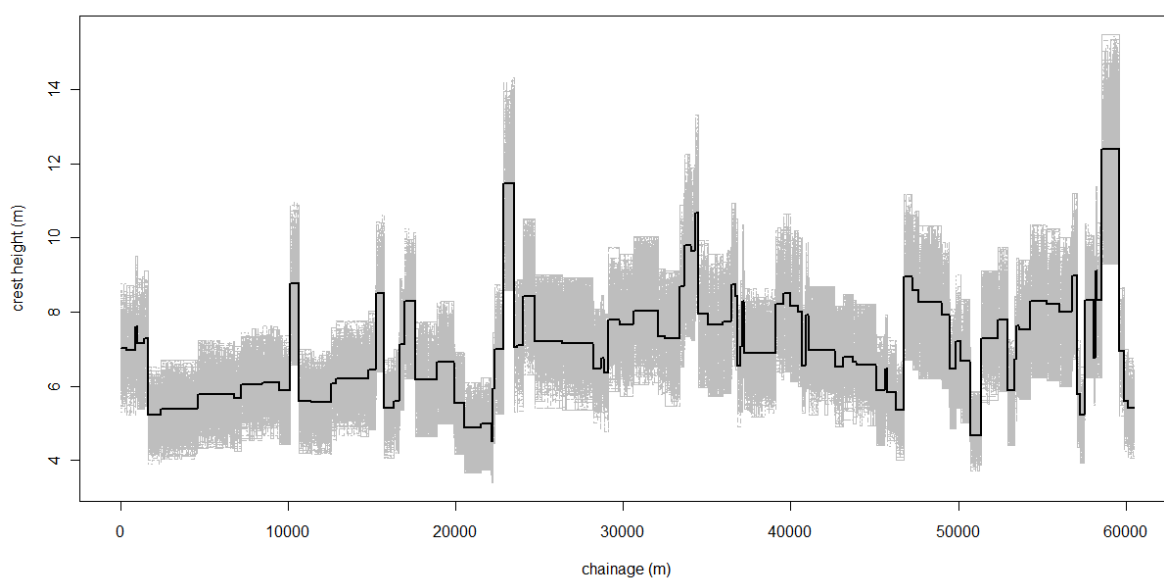


Figure 8.17 500 plausible simulations of varying crest height for the Lincolnshire coast compared to the long section mean

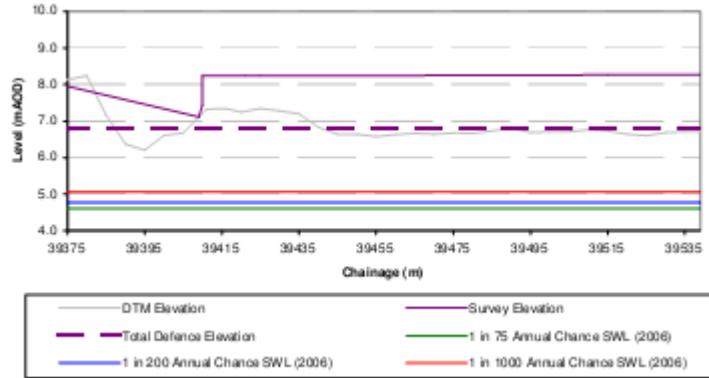
Table 8.10 Distribution parameters of 1000 plausible simulations of magnitude of crest height variation compared to the long section mean

Defence type	Simulated variation (proportion of crest height)	
Wall	Mean: 0.04	Std Dev: 0.09
Embankment	Mean: -0.05	Std Dev: 0.09
Dune	Mean: -0.00	Std Dev: 0.08

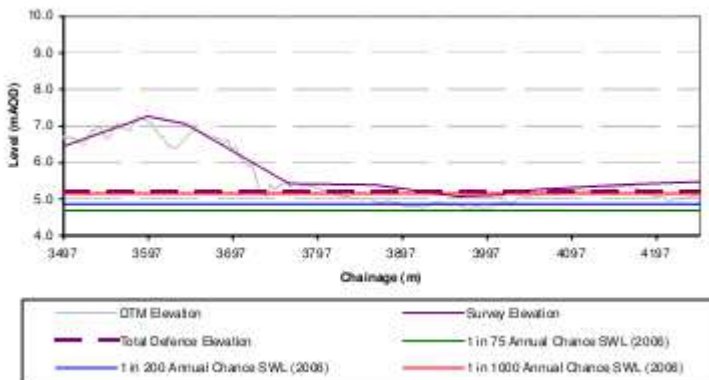
Visually the difference between the observed and simulated crest heights in Figure 8.17 appears large, however this is representative of the observed data, three examples of which

are shown in Figure 8.18 and illustrate the importance of taking account of this discrepancy in flood risk studies.

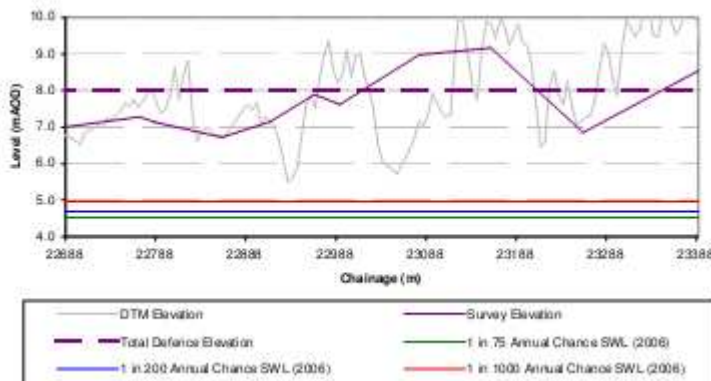
a) Wall



b) Embankment



c) Dunes



Data source: Environment Agency

Figure 8.18 Example observed variation in crest height from the Environment Agency survey data for different defence types

The methodology presented in this section provides a means of incorporating plausible variation in crest height for coastal flood defences. It is particularly useful where only limited crest height data are available, the data quality is known to be poor for example if taken from LiDAR data, or the data is of a large spatial resolution. A limitation of the proposed

methodology is that it cannot represent gentle sloping changes to crest height although this could be included if required by including an additional parameter characterising the number of steps (distance) between subsequent crest heights.

8.5 Simulation of flood defence reliability state

8.5.1 Available data

The consideration of flood defence reliability is dependent on the data sources available. For the case study areas used in this PhD the following data was available:

East Coast:

Detailed information on defence type, location, crest height and typical cross section was provided by the Environment Agency. Although detailed long section crest heights were available (see Section 8.4) they were not used directly in the flood defence reliability model due to the requirements to develop a generically applicable methodology.

North Wales:

NFCDD data for North Wales was provided by the Environment Agency. Previous work by Richard Dawson at Newcastle University as part of the Conwy Tidal Flood Risk Assessment (CTFRA, HR Wallingford 2002) was used as a data source. Data were available on defence type, location, crest height and typical cross section, including photographs of typical sections. In addition the CTFRA identified the most likely failure mechanism for each defence section.

8.5.2 Probabilistic consideration of breaching

To demonstrate the methodology only breaching following overtopping is considered in the case study applications in this thesis. It is however acknowledged that other failure methods are possible and may in some cases be more significant. The fragility curves used were specified as part of the CTFRA. Using established curves provides stability between this method and previous studies.

8.5.2.1 Overtopping

The calculation of overtopping takes place at every sampling point (every 20m) using Owen's equation (Section 7.3.6.2) and requires the simulated crest height at each point and the water level which comprises of:

- The simulated offshore wave height transformed to onshore
- The simulated skew surge
- The simulated tide curve

8.5.2.2 Failure probabilities

For embankments and revetments the failure probability is specified from the overtopping rate which is used as a proxy to damage caused to the rear of the structure (Table 8.11). The maximum overtopping rate is calculated using the highest water level (combined still water level and wave height). It is acknowledged that the probability of breaching increases with the duration of high water however this is not considered in this application. For dunes, failure is assumed to occur when wave runup lowers the dune crest and eventually leads to breaching. The failure rates from runup over dunes are given in Table 8.12.

Table 8.11 Defence failure probabilities from overtopping

Embankment		Revetment	
Overtopping rate (m ³ /s)	P(fail)	Overtopping rate (m ³ /s)	P(fail)
$Q \leq 0.002$	0	$Q \leq 0.05$	0
$0.002 < Q \leq 0.05$	0.1	$0.05 < Q \leq 0.2$	0.1
$0.05 < Q \leq 0.5$	0.2	$0.2 < Q \leq 2$	0.2
$0.5 < Q \leq 5$	0.3	$2 < Q \leq 20$	0.3
$Q > 5$	0.3	$Q > 20$	0.3

Source: CTFRA (HR Wallingford 2002)

Table 8.12 Defence failure probabilities from wave run-up

Dunes	
Wave runup (mAOD)	P(fail)
$R_u \leq 7$	0
$7 < R_u \leq 8$	0.05
$R_u > 8$	0.2

Source: CTFRA (HR Wallingford 2002)

Since the fragility curve depends on water depth relative to the crest height the probability of failure changes along the defence length, this allows for incorporation of low points in the defence but also allows for potential breaches in other areas. Previous methods only allow for one breach point per defence section, usually assumed to occur at the lowest point.

In a similar way to the crest height the strength of the defence is not uniform along its entire length. This is partly addressed through the probabilistic construction of the fragility curve and its associated uncertainty bounds. However to fully address this variability detailed survey information of the variation in defence construction would be required. At present the survey resolution is coarser than the known structure properties variation. Further work in this area in

the future could provide a useful means of incorporating the local scale weaknesses identified by Simms *et al* (2009) into generic fragility curves.

8.5.2.3 Assigning breach size

Breaches are generated based on the probability of failure at each of the sampling points along the defence crest. Breaches are assumed to initiate when the water level is above 90% of the crest height. Given the wide variation in observed and assumed breach dimensions (See Section 8.3.2 and Table A8.1) the breach sizes used in this study were based on the best available data set from the CTFRA. The same values were assumed to apply for the Lincolnshire coast.

The CTFRA specified expected breach sizes based on expert judgement, and historic records, these are given in Table 8.13. However these breach sizes were based on the critical failure model identified for each defence section, some of which are not included in this study. In light of this, and as taking a risk based approach allows more variation to be considered in the model, the breach invert and breach width were sampled from a normal distribution with the mean values as specified in Table 8.13. It was not possible to specify specific values for different defence types as most of the defences included in the Conwy study were sea walls. Allowing variation in the breach dimensions also allows for indirect incorporation of the observation that some breaches do not grow to their maximum potential size due to a lack of energy in the later stages of the flood event or human intervention (See Section 8.2). Consideration of contribution of breach size to the resulting damage from an event is made in Section 9.1.4.4.

The breach growth rate is assumed negligible. All breaches are assumed to grow to their full dimensions within one time step. If the breach occurs in the same defence section and the distance between them is less than the sampled breach width the breach points are assumed to belong to the same breach, with the smaller breach merging into the larger one.

Flow through the breach is calculated on an hourly time step using the Broad Crested Weir equation (8.2) on an hourly timestep and input to the 2D inundation model.

Table 8.13 CTFRA assumed breach dimensions for North Wales defence sections

Ref.	Type	Length (m)	Breach invert (proportion of crest height)	Breach width (m)
4A	Return sea wall	1241	0.19	248
4B	Return sea wall	970	0.21	194
4C	Vertical wall with mound	760	0.30	152
4D	Sloped masonry revetment with	725	0.15	145

Ref.	Type	Length (m)	Breach invert (proportion of crest height)	Breach width (m)
	crest wall behind			
4E	Vertical sea wall	300	0.28	60
4F	Sloped masonry revetment with crest wall behind	1200	0.15	240
4G	wave return wall	330	0.00	66
4H	wave return wall	380	0.10	17
4I	wave return wall	718	0.09	144
4J	wave return wall	593	0.00	66
4K	Dunes	150	0.44	60
4L	Dunes	40	0.44	16
4M	Saltmarsh / Dunes	141	0.33	56
4N	Vertical quay wall	280	NA	NA
Mean			0.21	112.6

Defence reference refers to the map in Figure 8.19

Source: CTFRA (HR Wallingford 2002)

8.6 Example application

To demonstrate the process lined in Sections 8.4 and 8.5 the application of the methodology is detailed for the North Wales site.

8.6.1 Model domain

The modelled domain considers the coastline from Hen Wrych in the West to the Clywd estuary in the East and includes a number of caravan sites in Abergele and Towyn as shown in Figure 8.19. This corresponds to an area of 11km by 6km. 7.8km of coastal flood defence is included in the model. The data for these defence sections were taken from the CTFRA. The reference labels (4A – 4N) correspond to the references used in the CTFRA. In addition, defences also exist along the Clywd estuary as shown in grey in Figure 8.19. These defences have not been included as the crest height data are unavailable, the defences are complex to model as they consist of embankments behind extensive saltmarsh and, as concluded in the CTFRA, failure of these sections is unlikely.

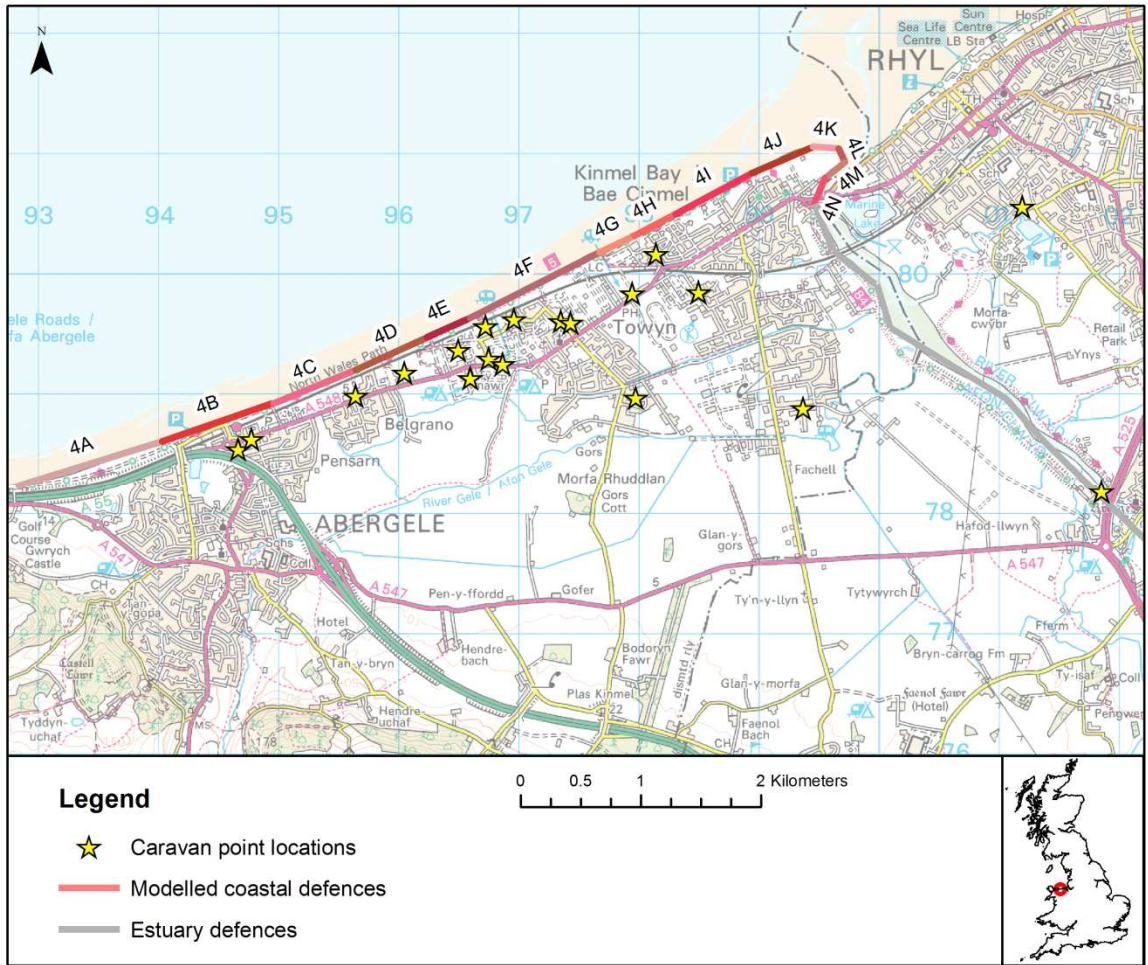
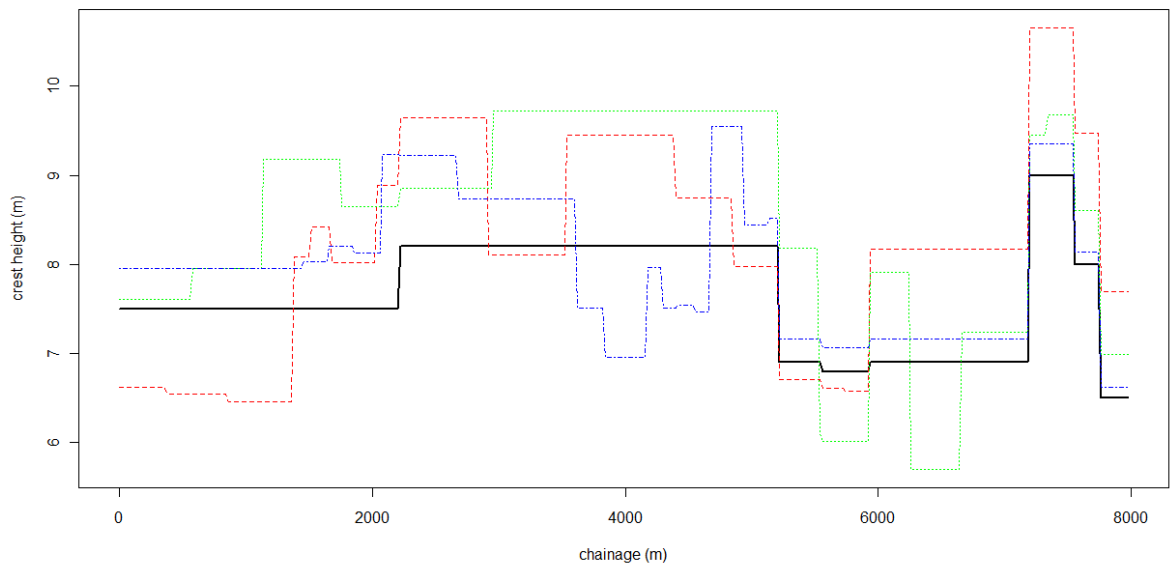


Figure 8.19 North Wales coastal model domain showing coastal defence sections and caravan site locations

8.6.2 Crest height

Crest heights were simulated using the Markov chain process outlined in Section 8.4 at each defence simulation point. Three example simulations are shown in Figure 8.20.



Black solid line is the mean crest height, coloured dotted lines are the simulated varying crest height.
Chainage = 0 at the western end of defence 4A.

Figure 8.20 Three example simulations of plausible variations in long section crest height for North Wales defences

8.6.3 Overtopping

Overtopping was calculated using Owen's equation at each defence simulation point. Defence slopes are taken from the composite defence slope calculated in the Towyn assessment (no slope is provided for defence 4M however as this is a vertical sea wall, a value of 1:0.5 has been used to maintain consistency with the sloped methodology). Values for the coefficients, a and b , were identified from Table 7.10. Where the slope is beyond the range of the table, a and b parameters are assigned using the values provided in the CTFRA. No account is taken of berms. A roughness value, r , is provided in the CTFRA, these values were crossed check against the pictures and descriptions of each defence section and the coefficients provided for use in Owen's equation and were found to be suitable.

8.6.4 Breach initiation

The failure probabilities for event loading were given in Table 8.11 and Table 8.12. Defences 4N and 4M are located within the Clywd estuary and as such are not affected by waves and not expected to fail (as stated in Conwy tidal risk assessment). In light of this, the wave height at these defences is set to 0 and a failure probability of 0.5 is specified if the still water level is greater than crest height, otherwise the failure probability was set to 0. An example scenario is shown in Figure 8.21.

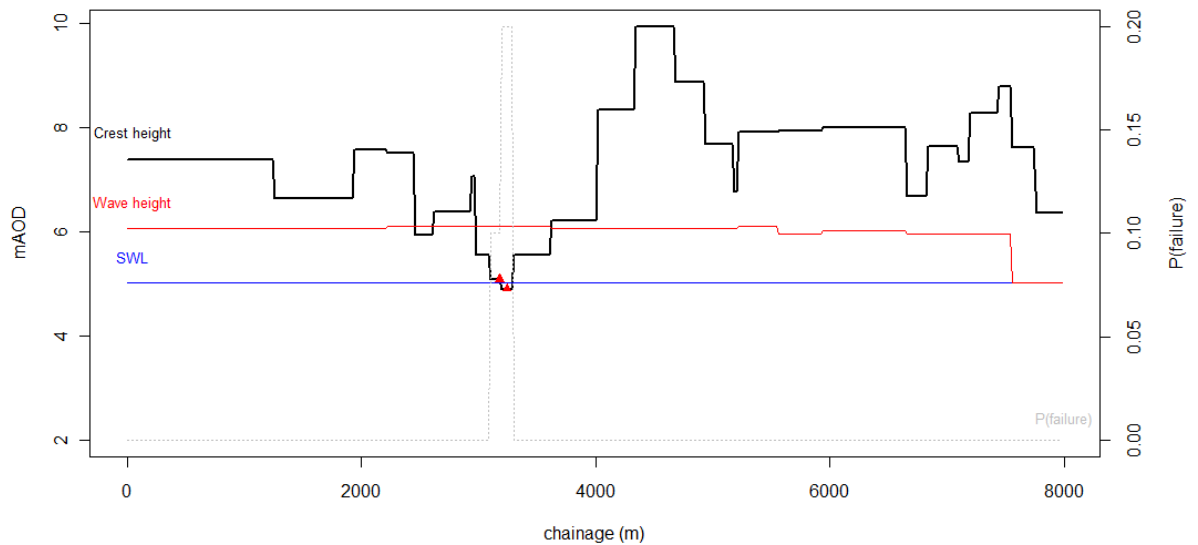


Figure 8.21 Identification of defence breach locations for a North Wales example overtopping scenario using simulated water level and defence crest height

8.6.5 Breach size

Breach dimensions for each of the breach initiation points are sampled from the normal distribution of breach scenarios as discussed in Section 8.5.2.3. Since the distance between the breaches is less than the width of the largest breach, the breaches are assumed to merge and only the largest breach is included in the inundation model.

Table 8.14 Simulated breach dimensions for a North Wales example overtopping scenario

Breach chainage (m)	Breach width (m)	Breach invert (proportion of crest height)
3150	30.84	0.19
3250	213.51	0.29

8.7 Using defence reliability in the system model

The consideration of defence reliability detailed in the chapter is fully integrated with the systems model outlined in Chapter 4. A risk based approach is maintained throughout accepting that the degree of information known about defence condition is limited and allowing the defence state to vary for each event simulation. The ability to include the spatially varying defence crest into the defence methodology reflects the importance of the spatial and temporal dependence between extreme events incorporated in the conditional dependence model. This is a useful extension of existing risk based methodologies which assume defence properties to be consistent within each defence section. The review of the spatially varying crest height of defences in Lincolnshire identified that this assumption could lead to large errors when calculating overtopping. A useful further extension of the method

would be to include spatially varying defence properties although this would require detailed survey data which was not available for this thesis.

The literature review in Section 8.2 identified a number of processes which are known to affect the breach growth rate and final breach dimensions. Existing risk based failure methodologies are limited in their consideration of these mechanisms due to the complexities and data requirements. There is a clear need for developing a methodology that is able to incorporate physical driving factors such as timing of initiation and floodplain type into a risk based framework for defence fragility, especially given the observations by Simms *et al* (2009) of the potential limitations of the standard fragility curve approach to address local scale weaknesses. The approach used in this thesis is based on the standard best practice available at present and as such provides a robust framework for considering defence reliability whilst accepting that the approach makes some necessary simplifications. The contribution of defence failure to risk is discussed further in Chapter 9 including an assessment of the sensitivity of the results to the breach size.

9 Calculating damage, loss and risk

9.1 Calculation of damage

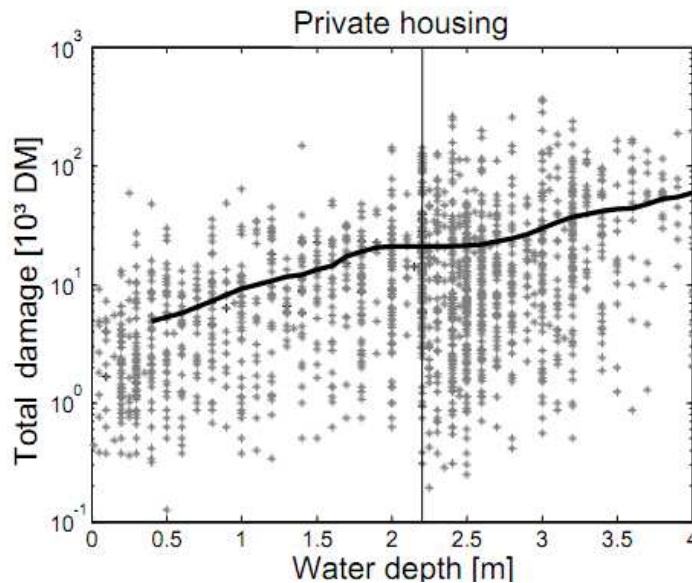
Damage during a flood event is caused by floodwater entering buildings and damaging the building structure, content and service infrastructure (e.g. sewerage). Indirect costs such as business interruption or relocation costs are also sometimes included. A review of the current practice in determining the economic impact of floods is provided by Merz *et al* (2010).

Within risk models, damage is usually estimated using a depth-damage curve whereby for a given structure type a relationship is established between damage caused for floodwaters at various depths. Depth damage curves are usually based on observed data, and / or expert judgement.

The consideration of damage is an integral part of the risk model however it often receives less detailed analysis than the source and pathway components (Merz *et al.* 2010). Various data sets have been collected to investigate the depth damage relationships using both observed damages following major events such as the Dundee tables in the UK (Black *et al.* 2006), HOWAS 21 (Deutsches GeoForschungsZentrum GFZ 2010) in Germany, and commercial research by Cat modelling companies, and using synthetic “what if” analysis including the database behind the Multi-coloured Manual (MCM) in the UK (Penning-Rowse *et al.* 2005). Other data sets have been collated around the world however due to the localised nature of building practices it is not usually sensible to transfer vulnerability data between different countries. It is widely acknowledged that depth-damage functions contribute a source of uncertainty to risk models due to the lack of understanding and wide variation in damage processes (Merz *et al.* 2004). There is some evidence to suggest that this uncertainty may be relatively small compared to uncertainties in the hazard calculation (Merz and Thieken 2009), although this is an under researched area (Merz *et al.* 2010) and is likely to depend on many site specific factors. Further details of the uncertainty contribution within this risk model are discussed in Section 9.4. Catlin believe the depth-damage curves are a significant contributor to uncertainty although this may be more due to the specification of floor level than the curves themselves

Merz *et al* (2004) identify that one of the biggest problems is that a depth-damage relationship alone cannot represent the wide variation in observed flood damages as shown for residential properties in Figure 9.1. Therefore additional data are required on individual building type, value, construction and occupation. This data is unlikely to be available for individual building types but as demonstrated by Penning-Roswell (2005) some assumptions can be made by

breaking down property types into smaller homogeneous damage units such as detached, semi-detached, terrace, flats or bungalows. Although the scatter shown in Figure 9.1 is concerning and indicates a restriction on our ability to estimate damages for an individual property, due to the law of large numbers, the uncertainty in total flood damage is reduced as the number of flooded properties increases (Merz *et al.* 2004).



Source: Merz *et al.* (2004, data from HOWAS 21) Thick blank line represents nonparametric depth-damage function. The line at 2.2m identified the point at which flood waters affected properties above cellar level.

Figure 9.1 Variation in residential flood damages in Germany

The simplistic depth-damage relationship could be extended to include other contributing factors such as salt water intrusion (Penning-Rowell *et al.* 2005), varying velocity (Kreibich, *et al.* 2009) or different durations of inundation (Penning-Rowell *et al.* 2005). A longer list of extensions is provided by Merz *et al.* (2010). The importance of these factors depends on the receptors being considered. No extensions to the basic depth-damage relationship are discussed here although a possible extension would be to investigate the impact of velocity as given the flimsy structure of caravans this could have a significant impact.

As outlined in Chapter 4, the modular nature of the methodological framework proposed in this thesis means that any spatially distributed receptor can be considered by using the relevant depth-damage information.

9.1.1 Flood damage to caravans

Although caravans are usually raised off the ground, site services such as electricity and water connected to a caravan suffer damage before water has entered the caravan itself. Static caravans are particularly vulnerable in floods as their light and flimsy structure makes them

prone to structural damage and to becoming unstable and dislodged from their bases (Hall *et al.* 2000). Because of these features depth-damage curve for caravans tend to be abrupt since once water and sediment enters a caravan it is normally a write off (Hall *et al.* 2000; McEwen *et al.* 2000).

Much of the existing work on depth-damage relationships has focussed on residential and commercial properties. The data on caravans are sparse, therefore the uncertainties around caravan depth damage curves are large. A study of 1272 of the 1300 static caravans flooded in the Avon valley during the 1998 floods carried out by McEwan *et al.* (2000) provides perhaps the most comprehensive available data set for identifying key features of the relationship in the UK. As part of this study they visited 21 parks immediately after the flood. Their interviews with park owners and residents found that:

- Seven of the parks had more than 50 static caravans destroyed
- There were 10 cases with 67% to 100% of total stock lost
- 682 caravans were reported as written off and replaced while 137 were repaired
- Claims for damage ranged from £1500 to £57800 with a median value of £16095.
- Claims for contents insurance ranged from £375 to £7500 with median value £1400

This study highlights the vulnerability of caravans to flood damage with a large proportion of units written off in this event. Although the exact depths at each site is unknown, the River Avon at Evesham rose 3m above the bank according to Environment Agency gauging (Environment Agency 2010a) during the 1998 event and flooding extended a mile onto the floodplain (Saunders 1998).

The recent floods in Mid Wales in June 2012 illustrated the damage flood water can do to caravan parks. The during and after photographs shown in Figure 9.2 clearly show the potential of floods to damage the external fittings of caravans in this case including verandas, gas canisters and the site infrastructure.

Unfortunately since the flood depths for the events in Section 3.4 are unknown, it has not been possible to collate depth-damage data to increase the availability of caravan specific data as part of this PhD. Two exiting sources of caravan-specific depth-damage functions are outlined below.

a) During the event



b) Damage to site



Photo credit: Lestyn Hughes, BBC News (2012)

Photo credit: Shropshire Star (2012)

Figure 9.2 Photographs of damage caused by the June 2012 floods at Riverside Caravan Park Llandre

9.1.1.1 Multicoloured manual caravan depth damage curves

The MCM (Penning-Rowse, Johnson *et al.* 2005) was developed as an aid to decision making for cost benefit analysis. It is used as the basis for most government funded risk management in the UK. It includes component based depth damage curves for building structure, content and fixtures for a variety of property types for developed from observed data and expert judgment. The most recent update of the MCM is from 2005, although the Environment Agency are currently funding a further revision (Environment Agency 2010c).

The MCM damage curves are scenario based. The base scenario is for a river flood of less than 12 hours duration and no prior flood warning. For non-residential properties such as caravans, data are provided on the average value of property components per m² and the expected damage per m². The user can change the property value based on site data if available, and is then expected to scale up the damage curve based on this size of the property of interest. This

is a sensible approach for large industrial units but appears less useful for caravans which are approximately the same size.

For caravans the written description of the depth-damage curve is:

“For fixed caravans use zero (minor damage) from ground level to undercarriage and then £16 000 to represent an average for total write-off cost, as at this level and above vans fall off their plinths, crumble and collapse and are often washed away. For many caravans, once a flood depth has been reached which results in the caravan floating (which can start around 0.60m) write-off would be expected. Regardless of duration, write-off is assumed to occur at a flood depth of 0.75m.” (Penning-Rowse *et al.* 2005, p94)

This description does not seem to relate to the quantified depth-damage curves for caravans shown in Figure 9.3 which only show a steep rise for moveable caravans and not static ones between 0.6 and 0.75m, and, even at depths of 3m, do not represent total write off. The MCM states that most moveable caravans are also raised by 0.5m and as they have limited fixture and fittings compared to static caravans, no damage is sustained below this threshold resulting in rapid increase in damages once the threshold is met. The difference between the text description of total write off and the depth-damage curves is because the MCM curves do not model total write off, the text description is therefore better able to represent the high vulnerability of caravans than the standard curve structure which is also used for more solid buildings. The MCM curves are derived from component based curves as shown in Figure 9.4. Comparing Figure 9.4 with the total damage curve in Figure 9.3 shows that the shape of the depth-damage curve is dominated by the structural curve which accounts for 78% of the caravan value. The structural damage does not exceed 30%, which is low given the MCM text description above and the results of the McEwan *et al* study (2000). The loss value of 80% and above at depths of 3m for movables, fixtures and services appears reasonable.

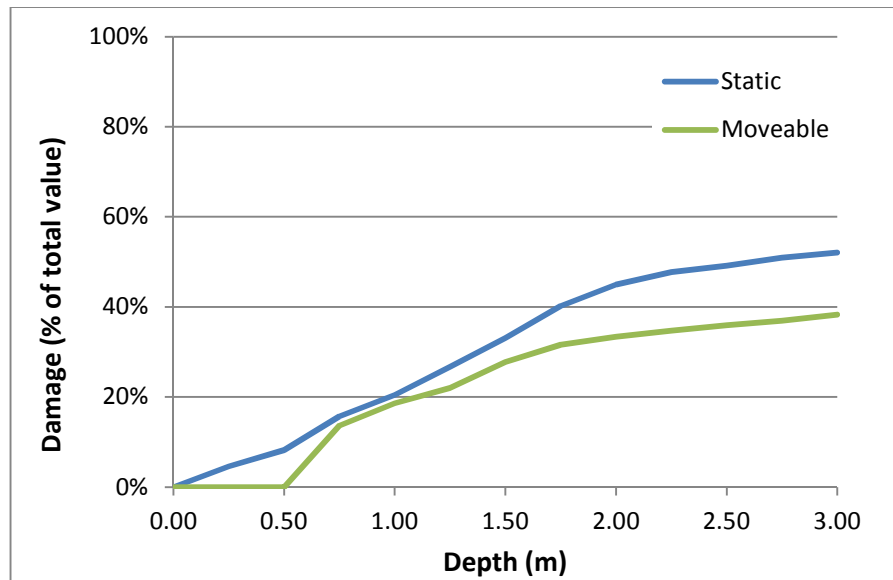


Figure 9.3 MCM depth-damage curves for caravans

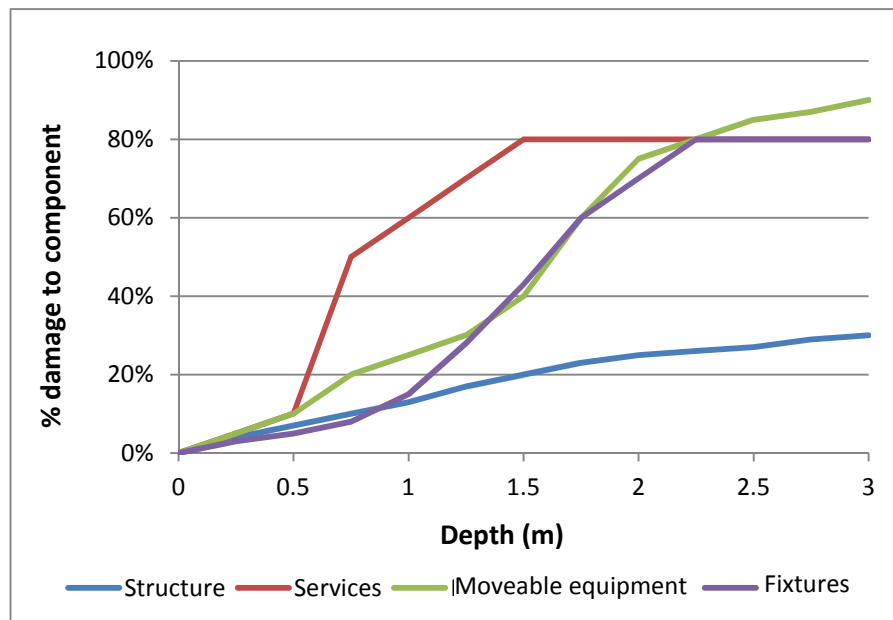


Figure 9.4 MCM depth-damage component curves for static caravans

9.1.1.2 Cat model damage curves

Damage curves are the main part of the vulnerability module of Cat models. Damage is quantified as a mean damage ratio, this is the ratio of loss compared to the replacement cost of the building (RMS 2008). Cat model damage functions are again developed from observed damage data collected after events. Although not explicit, it is likely that only limited data were used for caravan specific damage.

As discussed in Section 3.3.2 the damage curves in Cat models are built component wise with different curves available for structures of different type, age, use and construction material.

In addition the curves are enhanced to take account of modifiers such as awnings and external fittings or reduced if mitigation measures are present. The Cat model damage curves are more complex than those used in the MCM as they include additional factors such as business interruption and a multiplication factor for the scale and size of the event to account for the increasing cost of materials and labour for rebuilding following very large events.

It was not possible to gain access to the details of Cat model depth damage curves for caravans due to commercial sensitivity.

9.1.2 Development of depth-damage curve

Since the MCM damage curves appear unrealistic and the Cat model damage functions are unavailable, a new depth-damage curve for static caravans has been derived based on the MCM curve with some adjustment to better reflect the high vulnerability of caravans seen in the McEwan *et al* (2000) data, Catlin's existing assumptions, and observations from past claims.

The proposed depth-damage curve and component parts are shown in Figure 9.5 and Figure 9.6. The curve has been developed with reference to the following factors:

- Caravan assumed raised to 0.5m. Limited damage to the structure occurs below this level. Some low damages expected to services.
- The damage per m² is not necessary when Catlin only know an average value per unit. This is assumed to be £20,000 (see Chapter 3). This is equivalent to approximately 20m² using the MCM assumed values which seems reasonable (given some variation for changing component values since 2005). The proposed damage curve is given as expected damage based on average unit value. Since Catlin pay claims based on the current insured value, no account of depreciation is required.
- Catlin assume a structure to content ratio of 90:10 (see Chapter 3). This is approximately equal to the MCM ratio of 93:7 (when services and fixtures are included as structure) No change has been made to the MCM component distribution
- Catlin only insure new caravans (less than 5 years old) therefore it is assumed that modern water resilient products are used where possible therefore write off is not expected for very low water depths.
- The overall vulnerability of caravan structure is assumed higher than that represented by the MCM curves. A rapid increase in damage is expected for depths between 0.5 and 1m. Beyond this point the main structure of the caravan is assumed written off. Damage will continue to increase with depth for the moveable items and services.

- The shape of the damage curve for insurance purposes is less important above the point of significant damage. Although there may be some salvageable items below an internal flood depth of 0.5m, when a large proportion of value is destroyed it is normal for insurance companies to assume a complete write off.
- As no additional data are available, the shape of the damage curves for movables, fittings and services is retained from the MCM curves except for depths > 2.5m. At 3m it is assumed water is at top of caravans and all movables and fittings are written off.

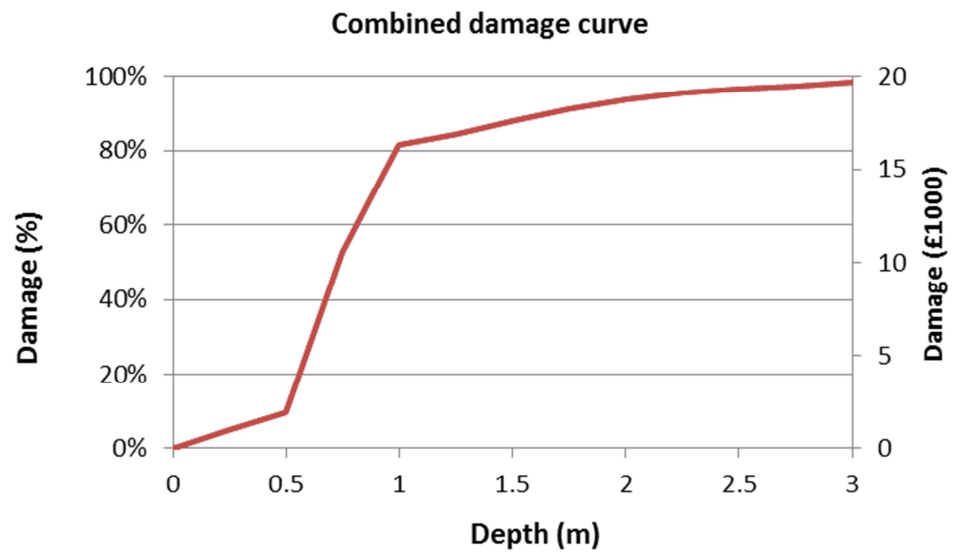


Figure 9.5 Proposed depth-damage curve for static caravans

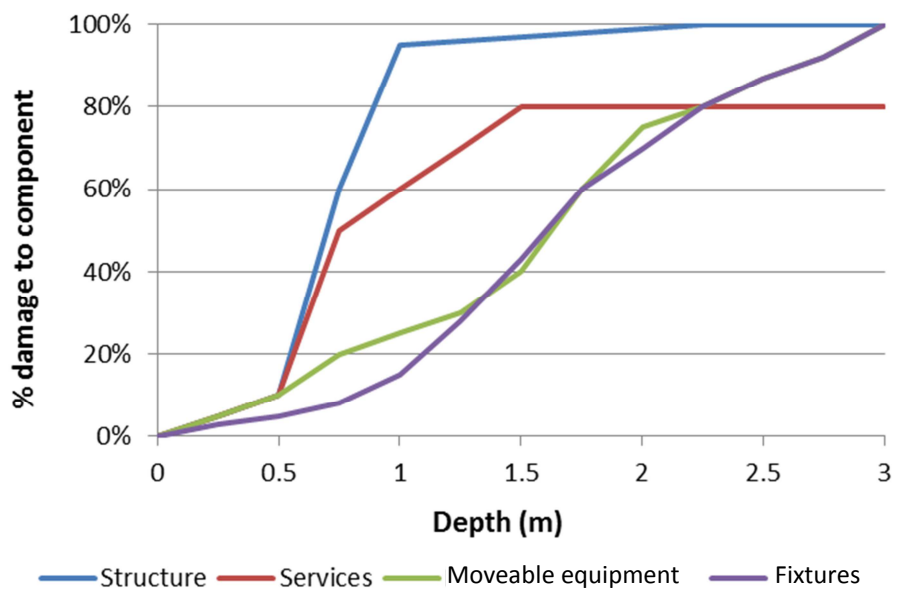


Figure 9.6 Proposed depth-damage component curves for static caravans

There are large uncertainties around the depth-damage curve due to the lack of data and the fact that not all caravans will respond equally to the same flood depths. The main point of uncertainty in the curve is the point at which serious damage starts to occur and where write off is expected. Here this is assumed to be between 0.5m and 1m. The importance of correctly specifying these points can be investigated by varying the values. In the absence of data to validate depth-damage curves, this approach of testing the most sensitive aspects of the curve is recommended as a feasible alternative (Merz *et al.* 2010). More details are provided in Section 9.1.4.3.

Ideally this proposed curve would be underpinned by observed data however it is not intended for general use beyond this PhD. It will allow the relative flood damages for different events to be calculated and, by having a greater understanding of the curve structure, will allow easier variation of the curve to account for uncertainty.

9.1.3 Calculation of loss

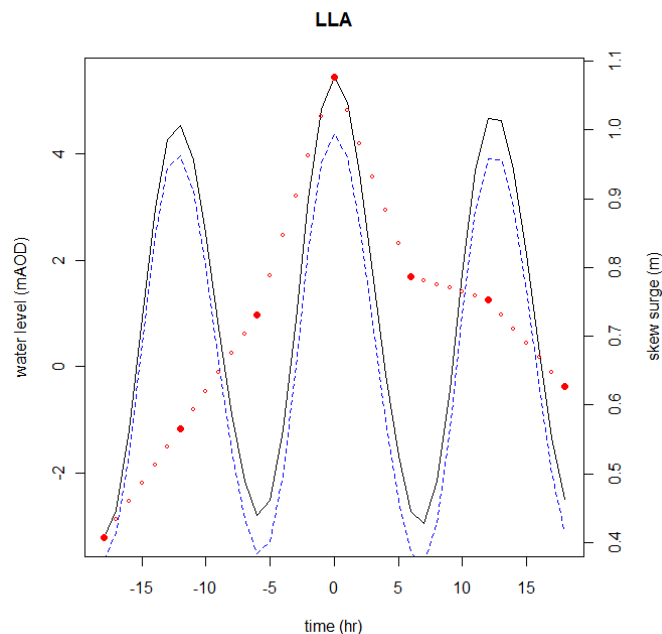
It should be noted that damage is not necessarily the same as insured loss. A property may suffer more damage than is paid out by the insurance company due to restrictions on the policy, whether new for old cover is included, and the amount of excess the property owner has to pay. To account for this insurance companies impose a losses model onto of the damage functions used. In some cases this can be quite complicated and involve several layers of calculation covering the various layers of re-insurance cover, however in the case of the caravan account used here the losses model simply comprises a reduction of damage based on an excess of £50 per caravan as specified by Catlin.

9.1.4 Factors affecting the calculation of damage and loss to caravans

9.1.4.1 Distribution of units on site

Cat models identify the location of assets at risk by postcodes. As discussed in Section 3.3.3 due to both the large spatial scale of sites and the size of postcode units in rural areas this approach may lead to errors in the estimation of risk. In light of these concerns the effect of using point locations for all caravan units on a site compared to distributing units evenly across the site was considered using the caravan sites in the North Wales cluster. Units were distributed across the site by dividing the number of units at each site by the number of grid cells within the site boundary. Only whole numbers of units were allowed within each grid cell. Where an even distribution was not possible, units were randomly assigned to grid cells within the site boundary.

A simplified example was set up where each defence section, 4A to 4M (see Section 8.6), was breached in turn at the midpoint. The water level and breach dimensions were kept consistent for each section. The breach width was 117m, the average of all breach dimensions specified in the Conwy Tidal Flood Risk Assessment. The breach sill was 5m, the lowest of the Conwy Tidal Flood Risk Assessment. The skew surge used was the 99th quantile of the simulated data whilst the tide height used was the 99th quantile of observed data. A surge shape was randomly sampled from the three representative surge shapes. The resulting components are shown in Figure 9.7. The still water level was scaled to account for long shore variation. The max still water level for this event is 5.64mAOD at Towyn. Comparison with the EA coastal flood boundaries project (McMillian *et al.* 2011a) indicates this is between a 0.33% AEP event and a 0.2% AEP event at Llandudno although the Conwy Tidal flood risk assessment only indicates this is a 1% AEP event at Kimmel Bay (HR Wallingford 2002). Whilst there is some inconsistency between these two reports, the simulated water level provides a realistic extreme event to test the location assumptions. No consideration of waves was made. The breach is assumed to occur one hour before high tide and inflow through the breach continues for three hours.



Blue dashed line is deterministic tide. Red dotted line is skew surge simulated at the bold points and interpolated in between. Black line is total still water level.

Figure 9.7 Still water level components used for location assumption testing

The damage and loss values sustained for each breach scenario are given in Table 9.1. Since the loss is a linear function of the damage, only the damage is discussed. In most cases the flood spreads along the lowland area behind the defence so there are not distinct flooded

regions for each breach scenario, however the flood depths are generally greatest close to the breach location. The spatial flood depths for a breach in section 4E and 4H are shown visually in Figure 9.8 and Figure 9.9. These two breach locations have been selected to demonstrate different sensitivities to caravan unit locations. For a breach at section 4H, the point location of caravans is located at the point of greatest flood depths. This location is at the boundary of the caravan site, the interior of which suffer much lower flood depths. In this case there may be some units on the site that are not flooded or suffer much lower flood depths than the point location represents. A breach at section 4E shows less disparity between point and distributed locations as the point locations affected are within the caravan site outlines and cover a range of flood depths which represent the depths experienced across the site.

Table 9.1 Damage and loss values for a breach in each North Wales defence section showing the difference between assumed point and distributed location of caravan units

Defence section	Max depth (m)	Area flooded (km ²)	For point locations			For distributed locations		
			N ^o . units flooded	Damage (£1000)	Loss (£1000)	N ^o . units flooded	Damage (£1000)	Loss (£1000)
4A	5.75	1.8	45	29.6	27.3	34	22.1	20.4
4B	3.23	2.2	45	440.6	438.4	61	281.1	278.0
4C	4.18	2.1	52	41.4	38.8	77	86.7	82.8
4D	4.86	2.4	662	637.1	604.0	591	995.4	965.8
4E	3.12	3.0	685	1729.0	1694.7	632	1358.8	1327.2
4F	2.64	2.8	438	449.9	428.0	466	668.3	645.0
4G	3.00	2.3	545	2278.8	2251.6	421	1290.2	1269.1
4H	3.31	2.0	452	2598.8	2576.2	296	450.6	435.8
4I	3.29	1.8	422	1309.9	1288.8	252	286.2	273.6
4J	3.55	1.8	408	582.6	562.2	197	173.3	163.4
4K	3.57	2.0	408	610.1	589.7	211	197.9	187.4
4L	3.42	0.6	0	0	0	0	0	0

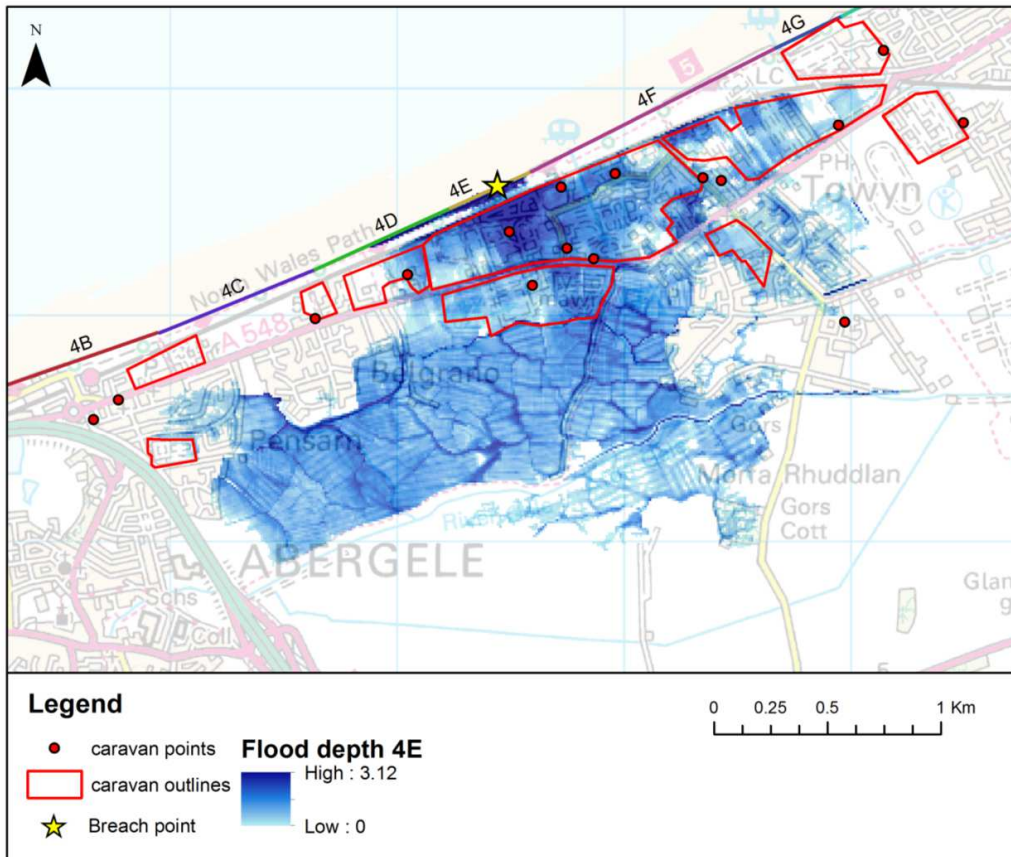


Figure 9.8 Simulated flood depths for a breach in North Wales defence section 4E

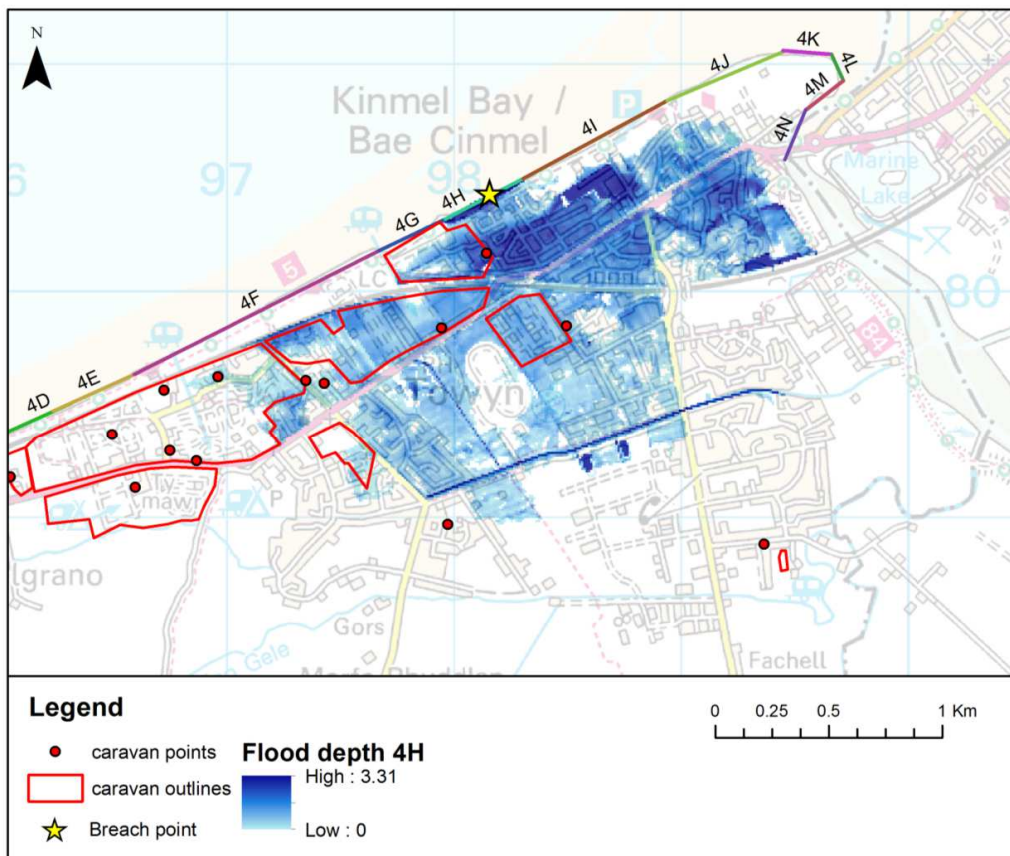


Figure 9.9 Simulated Flood depths for a breach in North Wales defence section 4H

Although this is a small example case study it is evident that the results are sensitive to the distribution of units. For the scenarios that caused flood damage there was an average difference of 19% between the point and distributed unit locations, this is equivalent to an absolute error of 58%. The degree of sensitivity to the location assumptions is likely to be affected by the scale of the flood event. As shown in Figure 9.10 the difference between the point and distributed locations is less for events affecting a larger area. This is because the point location is more likely to be within the flooded area. Therefore the results presented in this section could be considered as a conservative estimate of the sensitivity of damage to the unit location assumptions as the event used has a return period of greater than 1% AEP.

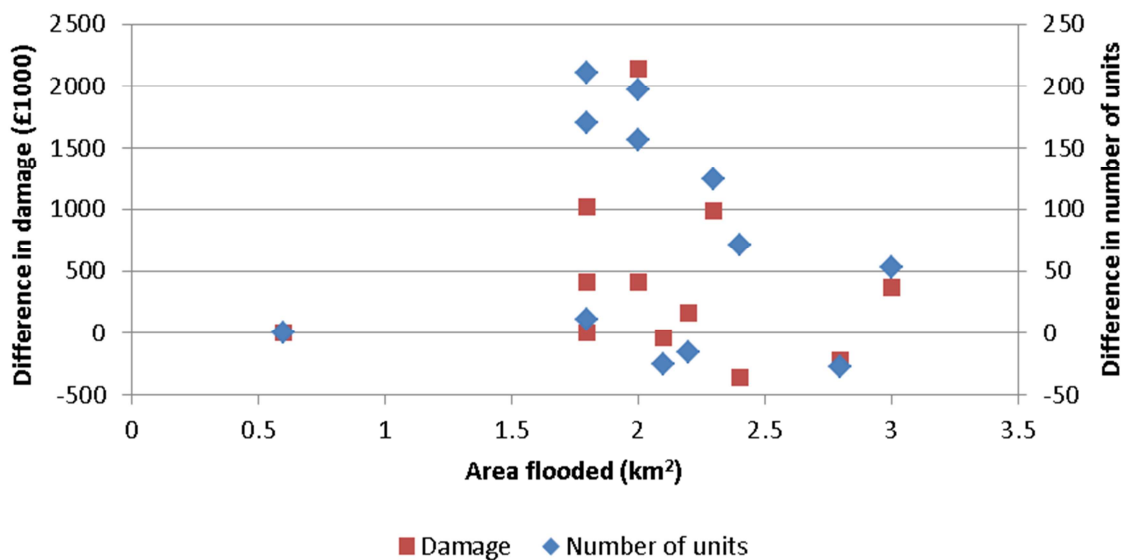


Figure 9.10 Difference in damage calculated using point and distributed caravan unit locations compared to the total area flooded

9.1.4.2 Unit value assumptions

In Section 3.3.1 Catlin’s assumption of an average unit value of £20000 was discussed. Here, using the same example application as in Section 9.1.4.1, the sensitivity of the event damage and loss to the assumed unit value was investigated. The results were summed over all defence section breaches and the percentage difference compared to a value of £20000 was calculated (Table 9.2). Although the number of units at each site decreases as the unit value increases due to the fact that the damage curve is specified based on percentage of total value there is no difference in the damage sustained for point locations. The differences in damage for distributed locations are due to the differing location of units across the site. There is a small difference in losses which is most evident in the point data as it is not affected by the unit locations. Raising the unit value increases the losses sustained as less deductibles are claimed. In general the sensitivity of the results to the unit value assumption is low compared to other areas of the methodology.

Table 9.2 Percentage variation in damage and loss values for different assumed unit values

Unit value (£)	For point locations			For distributed locations		
	N°. units flooded	Damage	Loss	N°. units flooded	Damage	Loss
5000	299.7%	0.0%	-5.9%	304.0%	0.8%	-7.9%
15 000	33.3%	0.0%	-0.7%	33.7%	4.2%	3.3%
25 000	0.0%	0.0%	0.0%	0.0%	0.0%	0.0%
35 000	-20.2%	0.0%	0.4%	-19.6%	-5.2%	-4.8%
45 000	-42.9%	0.0%	0.9%	-42.6%	-0.6%	0.6%
55 000	-55.6%	0.0%	1.1%	-54.9%	3.6%	5.3%

9.1.4.3 Sensitivity of depth-damage curves

The depth-damage curve was modified to investigate the sensitivity of the results to the shape of the damage curve in three areas; the floor height of the caravan, the vulnerability of the caravan to damage through the steepness of the rise of the main section of the curve and the point of write off. Plots of the different curve shapes are shown in Figure 9.11 to Figure 9.13. The floor height was tested from 0m to 1m at 0.25m intervals by changing the point at which damage to the caravan structure rather than just the external fitments was sustained. The curves are a slightly different shape from the original curve (shown in grey in Figure 9.11) to allow a standard shape to be used to represent most damage being sustained between floor height and 1m above floor height. Vulnerability of the caravan to damage was tested by multiplying the rate of change of the main section of the curve by 0% to 50%. The resulting curves are shown in Figure 9.12. The sensitivity to the point of write off was tested by changing this point from the original 3m to between 1m and 3.5m and 0.5m intervals. .

The flood depths from the sample breach event in each North Wales defence section (See Section 9.1.4.1) were used in the sensitivity calculations. The point damages were summed across all breach events to generate a large sample to test the damage curves. Area distributed damage values were not considered due to potential differences in the distribution of units across the site between runs. Flood depth for this event set ranged from 2.64m to 5.75m (Table 9.1).

As expected the damage was very sensitive to the floor level. If the caravans were situated at ground level rather than raised by 0.5m the damage would be over 300% greater. The

sensitivity is greatest for floor heights of less than 0.5m as at these depths a caravan may be flooded or not flooded by a change in floor height of a few cm. The sensitivity is less as the floor height increases, between 0.75m and 1m there is less than 1% difference in damage. Whilst this result is dependent on the flood depths sustained during an event, the levels are representative and the large areas affected means a range of flood depths would be sustained.

This high sensitivity is concerning as Catlin do not know site specific details about each caravan unit they insure and therefore do not know the floor level. The results in Figure 9.11 indicate that this could result in large errors in their risk calculation as small difference in floor level result in large differences in damage due to the steep rate of raise of the damage curve once the floor level is reached.

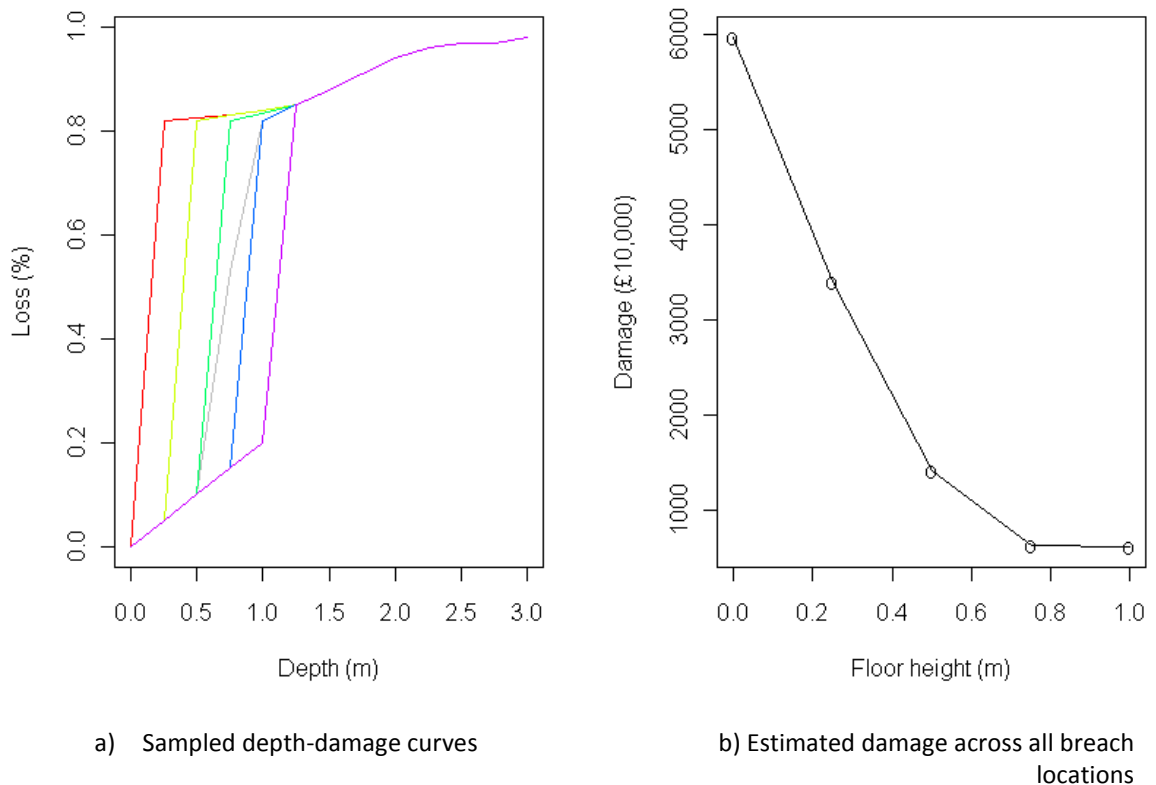
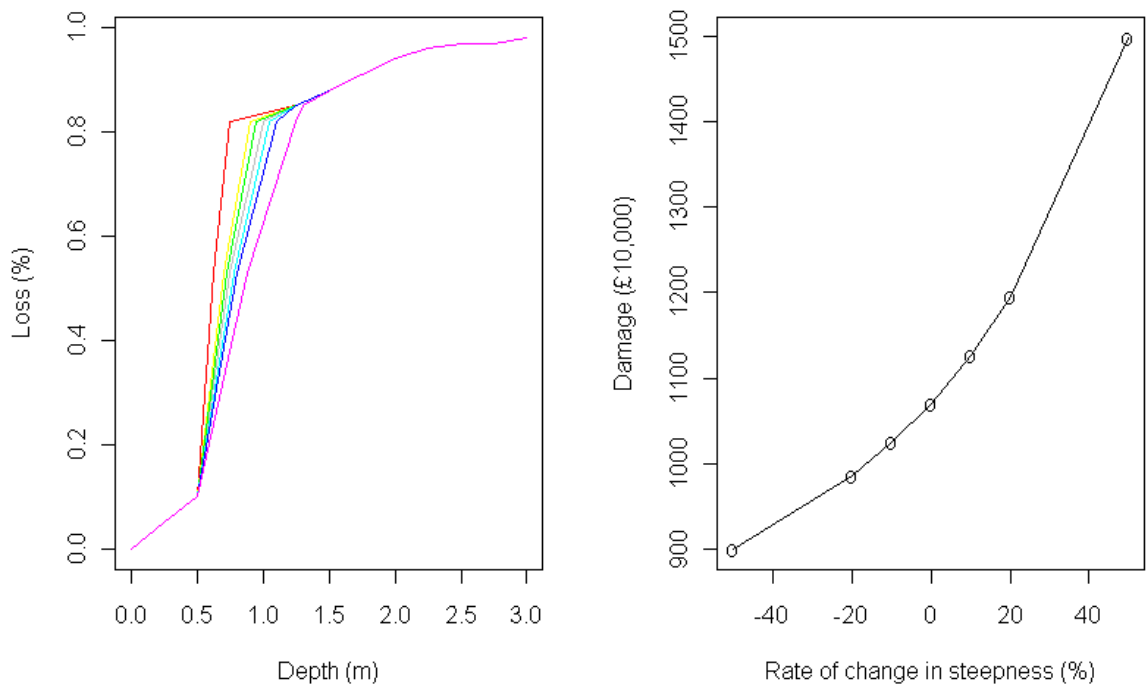


Figure 9.11 Testing of the sensitivity of simulated flood damage to floor height by varying the shape of the depth-damage curve

Little is known about the vulnerability of caravans to flood damage therefore by changing the rate of rise of the main section of the damage curve it is possible to investigate the effect this lack of knowledge has on risk estimates. The sensitivity of the results to the rate of rise of the curve is less sensitive than to the floor level. A 50% change in floor level resulted in difference in damage of 144% for a decrease and 56% for an increase. For a change in steepness of 50% the change in damage is 40% for a steeper curve and 16% for a shallower curve. Small changes in steepness of +/- 10% resulted in changes in damage of 4-5% and changes in steepness of +/-

20% in differences of 8-11% in damage. Given the other uncertainties involved in risk estimation, if the vulnerability of caravans is assumed to be within 20% of the best estimate of vulnerability used in this thesis with reference to existing depth-damage curves and expert knowledge the proposed damage curve shape between 0.5m and 1m gives a good approximation of damage.

The biggest increase in accuracy for damage estimation can therefore be achieved by accurate information on floor levels however if additional data on caravan vulnerability were collected this would be beneficial and help to pin down the damage curve shape.

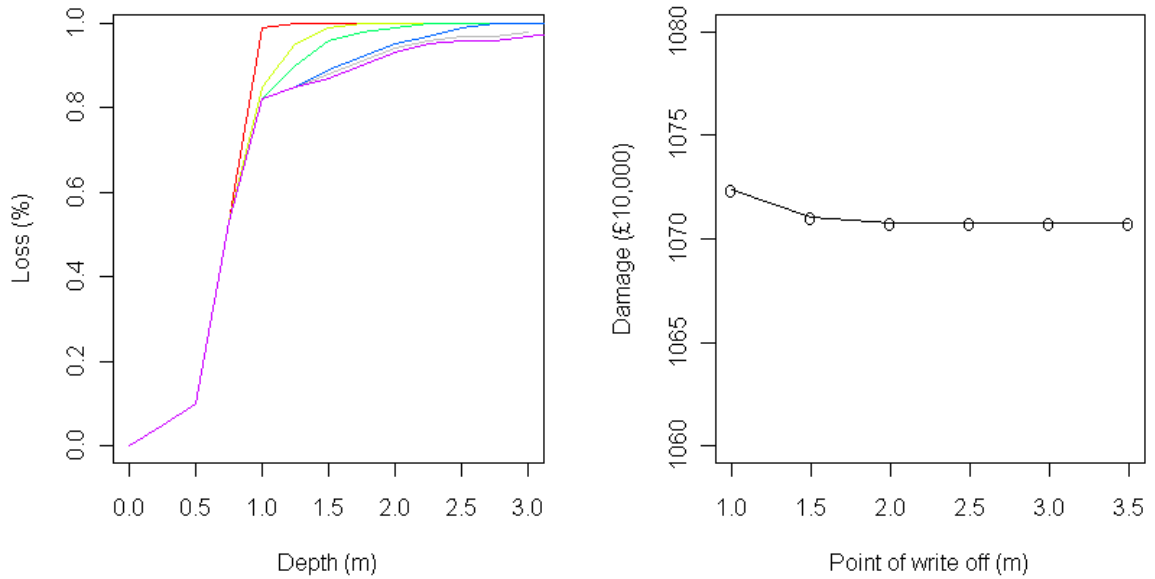


a) Sampled depth-damage curves

b) Estimated damage across all breach locations

Figure 9.12 Testing of the sensitivity of simulated flood damage to material vulnerability by varying the shape of the depth-damage curve

The damage curves were modified to investigate the effect of changing the point of write off however the flood depths in the sample scenarios only exceeded 3m at isolated locations therefore changing this upper section of the curve did not significantly change the damage. Reducing the point of write off to 1m only resulted in a 0.15% increase in damage compared to a 3m write off point. There was no change above 1.5m. Given the steepness of the curve between 0.5m and 1m and the high sensitivity to the flood level, the point of write off is not a significant feature of the damage curve.



a) Sampled depth-damage curves

b) Estimated damage across all breach locations

Figure 9.13 Testing of the sensitivity of flood damages to the point of total write off by varying the shape of the depth-damage curve

9.1.4.4 Specification of breach size

Previous research has identified the sensitivity of inundation models to breach dimensions. For breaches in one section of defence, 4E, using the event specified in Section 9.1.4.1 the effect of changing breach size was investigated. The dimensions were modified from the mean of the distribution for breach width and by up to two standard deviations. To provide a spread of breach areas, scenarios were also run for a wide breach, a deep breach and a narrow and deep breach as shown in Table 9.3.

Table 9.3 Range of dimensions used to investigate sensitivity of flood damage to breach size

Breach size scenario	Width (m)	Invert (mAOD)	Area (m ²)
Expert value	60	5.9	138
Mean of distribution	72	6.5	121
Plus 1 standard deviation	128	5.3	372.2
Plus 1.5 standard deviation	114	4.73	400
Plus 2 standard deviation	128	4.1	527
Minus 1 standard deviation	43	7.71	21
Minus 1.5 standard deviation	29	8.01	5
Very wide breach	200	5.9	460
Very deep breach	60	2.0	372
Narrow and deep breach	40	3.0	208

The results shown in Figure 9.14 show a trend of increasing damage with area. There is a suggestion that this trend is influenced more by the breach width than the invert although the invert level has a binary influence of whether significant amounts of water are able to reach the floodplain. More detailed investigation would be required with a larger sample size to quantify the impact of specifying breach dimensions on the uncertainty in damage calculations however the differences in damage for each breach size are large. A change in breach width and depth of one standard deviation compared with the mean of the distribution results in differences in damage of up to 100% for the same event. The smaller breach size caused no damage due to the high sill level and the larger breach size resulted in an increase of 91% in damages. The specification of breach size is therefore a critical component of the system model.

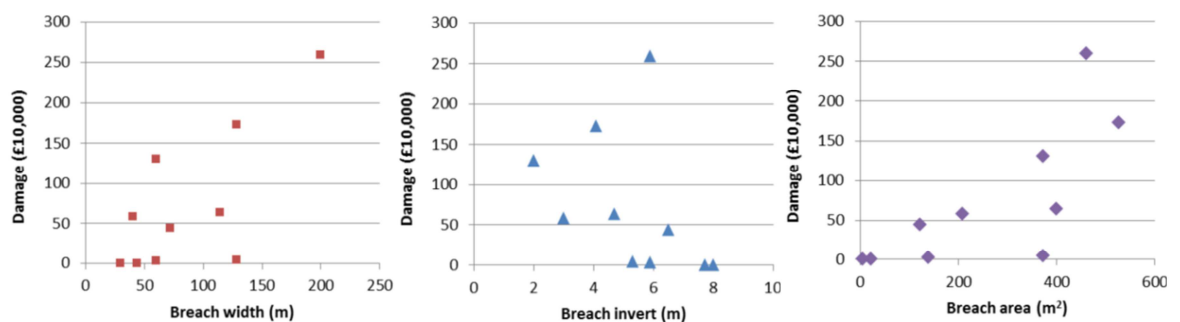


Figure 9.14 Variation of damage conditional on breach size

9.2 Calculation of risk

Risk is the probability of an event multiplied by the consequences (see Section 2.2). Risk is estimated using a Monte Carlo sample of events as defined in Section 4.2.7. This section outlines the final stages of converting the damage from the multi-site events simulated throughout this thesis into risk.

9.2.1 Multi-site calculation of risk using the systems model

With reference to the outline of the system model in Figure 4.1, a multi-site calculation of risk from fluvial and coastal events can be made for the selected risk clusters using the following steps (the section reference for each step is given in brackets)

1. Generate a large event set of dependent events across all core gauges (6.3.6), then for each simulated event,
2. Convert the simulated data to physical risk driving components.

For fluvial components this includes:

- i. Converting DMF to peak flow (7.2.1)

- ii. Interpolating peak flow to the sites of interest (7.2.2)
- iii. Generating an event hydrograph (7.2.3)
- iv. Calculating water level using hydraulic model (7.2.4)

For coastal components this includes:

- v. Simulating a peak wave height conditional on event skew surge (7.3.3)
 - vi. Calculating the total inshore water level and wave height (7.3.5)
3. Simulate defence crest realisation (8.4.2)
 4. Calculate potential overtopping and breaching conditional on the water level and defence crest (8.5)
 5. Run the relevant inundation model for each risk cluster to calculate flood depths (7.4)
 6. Calculate damage at each site (9.1.2)

This process results in the damage across all selected areas of interest conditional on each event. The probability of each multi-site event is defined based on the simulated values at the core gauges (Equation 4.14).

Computationally this requires generating a large event set from the conditional dependence model and running this through the systems model. The largest computational component is the inundation modelling which, due to the presence of flood defences, in most cases will not be required and the resulting flood damage will be zero. This means the computational burden is reduced and a large event set is achievable.

9.3 Informing decision making

The aim of this research was to develop a new methodology to help understand dependencies in risk exposure in the UK. This aim has been met through the consideration of individual components of the system leading to a review of the how each component should be taken account of in decision making for both insurance pricing and wider flood risk management. A summary of the main findings is provided below.

9.3.1 Sources

The statistical modelling of sources of fluvial and coastal risk identified that the dependencies in risk across large areas and different sources are weak, therefore by maintaining a good spatial distribution of assets insurance companies can manage their risk exposure. Exploration of the temporal dependence structure showed that the existing seven day window used by insurers will contain all dependent events however it was illustrated that in the UK the highest

large scale dependencies peak within three days, therefore this window may also incorporate other independent events.

9.3.2 Pathways

Consideration of the pathways illustrated the significance of flood defences to risk, particularly for the heavily defended coastal caravan sites. The representation of flood defences in risk models is poor due to lack of data and computation difficulties in incorporating details of defence failure into risk based approaches. The available details on defence failure in Cat models are simplistic however it is assumed that they are similar to those taken within academic models. In light of these concerns it is recommended that a precautionary approach is taken to risk pricing in defended areas. However defended locations may not necessarily be at higher risk than implied by existing models. Simms *et al* (2009) identified that flood defences during the 2007 event performed better than would be expected compared to the available fragility curves.

The link between correctly modelling the dependence between wave height and still water level is important as in most cases overtopping will not occur unless a high water level occurs with moderate to high wave heights. Similarly the use of skew surge to mitigate the need to consider the timing of high tide and storm surge is important as overtopping is most likely when the peak surge corresponds to a high tide.

9.3.3 Receptors

Limited data is known on the vulnerability of caravan structures to flood damage. The literature and expert opinion identified high vulnerability with steep depth-damage curves. The most important point in the depth-damage curve was found to be the floor height. Catlin already partly incorporate this in the insurance criteria by only insuring units above the historic maximum flood depth however given that RiskLink provides the functionality to include flood heights it is recommended that Catlin collect this data and use it routinely to improve their risk estimates.

The geocoding of unit locations was found to be significant, particularly for moderate events where only part of the site may flood. This is a particular issue for caravans which are located on large sites however it could also have implications for modelling other spatially distributed receptors with poor location data for example on industrial units or in large rural postcodes. The impact of the unit location will vary on a site by site basis and may average out across the whole portfolio. It is recommended that Catlin consider the effect of this particularly for high value sites where the point location could make a large contribution to the AAL.

9.3.4 Consequences and Risk

The consequence of interest is insured loss, in particular the potential for overexposure due to poor risk pricing. By reviewing the individual components of the S-P-R-C model it is possible to identify areas where improvements in modelling capabilities could lead to a more reliable estimate of AAL. The final stage of the process would be an integrated multi-site end to end calculation of risk from combined fluvial and coastal sources. Although this would provide a coherent demonstration of the strength of the system model across multiple sites this has not been attempted in this thesis. Due to the lack of available data, necessary simplifications in the process, and the cascade of uncertainty through the systems model (discussed in Section 9.4) it was not felt that the results of this large calculation would provide an improvement on the understanding gained from reviewing the individual components.

9.4 Contribution of uncertainty to the risk estimate from the system model components

The significant factor in the decision not to complete a multi-site calculation of risk as part of this thesis was concerns over the effect of cascading uncertainty through the system model. Although some stages of the process represent the best available science, others are compromised by a lack of data or knowledge.

Assessing the contribution of each system component to the overall uncertainty is difficult as the uncertainties and critical contributing components change as events get more extreme. The uncertainty in simulating the source components increases with event rarity (see Section 6.3.4) however due to the law of large numbers, the uncertainty in damage calculation reduces as floods become more extensive. A critical threshold for the industry is a 1.3 AEP event as this is the threshold at which they are obligated to provide insurance cover. An assessment of the system uncertainty at the 1.3 AEP event was attempted in this thesis however due to the dominance of the flood defences in controlling whether damage occurs this calculation was deemed largely irrelevant as the uncertainty at the 1.3 AEP event is approximately zero as coastal defences are very unlikely to breach below a 0.5 AEP event. Once the event magnitude increase above the design standard of the flood defences the increase in uncertainty is exponential due to the difference between zero damages if defences do not breach and very high damages if they do. The solution to this problem is to run a very large ensemble of events to explore this area of the domain in more detail. Although computationally wasteful across much of the domain this could provide a useful tool for insurance companies in helping to quantify the sensitivity of their results to the interface point between zero and very large damages.

In light of these difficulties a qualitative review of the contribution to uncertainty is discussed in the following sections. Figure 9.15 provides a graphical representation of the contribution of each individual component to the overall uncertainty in risk estimation based on three criteria; whether the uncertainty is explicitly included in the systems risk method, whether the contribution to the uncertainty in the individual component is significant and whether the contribution to the system uncertainty is significant. The reasoning behind this assessment is detailed in Table 9.4. Given the acknowledged difficulties in assessing uncertainty for the whole system due to interactions between the components (see Section 4.4) a visual summary such as this provides a clear means of communicating where the most significant uncertainties are and how these feed into later stages of the system.

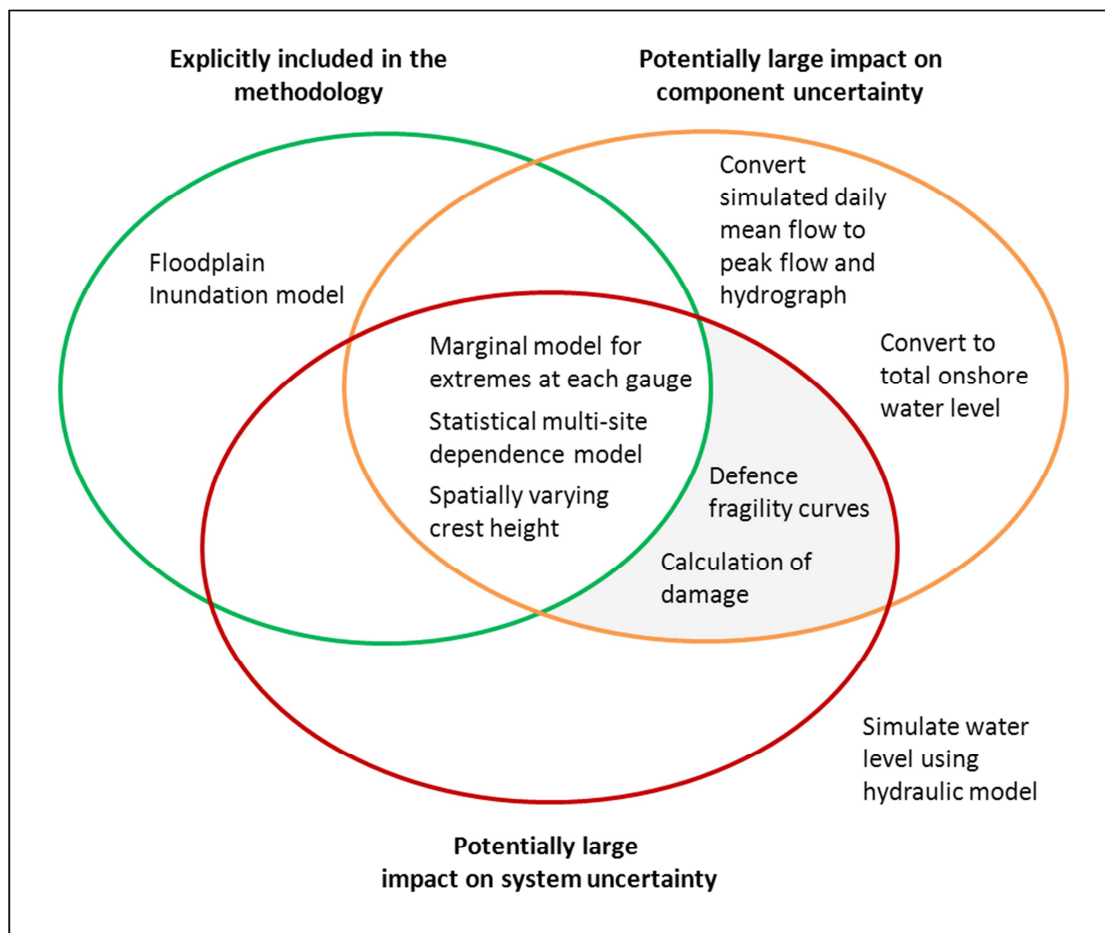


Figure 9.15 Assessment of uncertainty of systems model component

Table 9.4 Assessment of uncertainty in individual model components and contribution to overall uncertainty in system risk calculation

System Component	Source of uncertainty	How is this included in the system model?	What are the implications of the uncertainty?	Assessment of significance	Recommendation
Fit marginal model to extremes at each gauge	<ul style="list-style-type: none"> Limited data Suitability of marginal model 	<ul style="list-style-type: none"> Statistical testing of model fit 	Model may not be a correct representation of the extremes and hence simulated extremes may be unrepresentative. The shape of the marginal distribution in the upper tail could result in too many, or not enough, high values.	Although contribution to uncertainty is potentially high, limited data is acknowledged as a problem in all statistical modelling of extremes therefore it is accepted that the methods used in this thesis address this issue in the best available way.	Update model as data record increases. Priority: Low
Fit statistical dependence model to extremes	<ul style="list-style-type: none"> Limited data Suitability of dependence model 	<ul style="list-style-type: none"> Infilling methodology makes best use of all available data Dependence model shown to be suitable by Keef et al 	Model may not be a correct representation of the dependence in the extremes. Wave data record particularly short however contribution of waves to total water level is small compared to tide and surge.	As above	Update model as data records increase. Priority: Low
Simulate multi-variate extreme event set	<ul style="list-style-type: none"> If the fit of the marginal and dependence characteristics is incorrect the simulated extreme event set may be unrepresentative. 	<ul style="list-style-type: none"> Simulated event set shown to be a good match to observed events 	Simulated events may be unrepresentative of extreme dependence structure however using only observed data would exclude possible very extreme events therefore use of simulated events is required and reduces overall uncertainty.	As above	Update model as data records increase. Priority: Low

System Component	Source of uncertainty	How is this included in the system model?	What are the implications of the uncertainty?	Assessment of significance	Recommendation
Convert simulated daily mean flow to peak flow hydrograph	<ul style="list-style-type: none"> Daily mean flow data is known to not well represent flood peak for UK rivers. Lack of suitable gauged network to validate ungauged site transfer method External data sources such as FEH PCDs 	<ul style="list-style-type: none"> Daily mean flow to peak flow method tested using a variety of established methods and a large data set of UK gauges. Temporal event simulation using the conditional dependence model was used to maintain large scale temporal dependence structures. The selection of the gauged network ensured the closest suitable gauges to the sites of interest were used. Compromises between gauge location and data quality were well documented. 	Peak flow and hydrograph shape potentially poorly represented, however since the method used is the same at all fluvial sites this is unlikely to affect the large scale multi-site dependence structure and the relative magnitude of events will be preserved.	There are embodied simplifications in the method and the uncertainty is not fully quantified due to lack of suitable validation data. The daily mean flow to peak flow method is acceptable as the best available approach established from a large data set. The additional uncertainty in converting to ungauged sites is likely to be comparatively small due to the well selected gauge locations.	<p>Further work is required on ungauged site transfer method at the local scale between gauged locations and site of interests. This would require local data sets.</p> <p>Priority: Low unless very detailed local analysis is required</p>

System Component	Source of uncertainty	How is this included in the system model?	What are the implications of the uncertainty?	Assessment of significance	Recommendation
Simulate water level using hydraulic model	<ul style="list-style-type: none"> Simple hydraulic model constructed using only LiDAR data. 	<ul style="list-style-type: none"> No available data to improve this 	Likely to be small compared to simulation of extreme event. Only affects fluvial sites. No effect on relative magnitude of events.	The effect of this simplification is not fully quantified however the uncertainty is acceptable given the requirements for a multi-site model which can be applied using readily available data and larger uncertainties from simulation of extreme events.	<p>Could improve using more detailed hydraulic modelling for fluvial sites of interest if required.</p> <p>Priority: Low unless very detailed local analysis is required</p>
Convert simulated surge and wave to total inshore water level	<ul style="list-style-type: none"> Simplification of onshore transformation and no inclusion of beach processes. 	<ul style="list-style-type: none"> No available data to improve this. 	Likely to be small compared to simulation of extreme event. Only affects coastal sites. Impact of beach processes will be limited during extreme events when water level above beach elevation. No effect on relative magnitude of events.	The effect of this simplification is not fully quantified however the uncertainty is acceptable given the requirements for a multi-site model which can be applied using readily available data and larger uncertainties from simulation of extreme events. Well established methods are have been used.	<p>Could improve using more detailed onshore wave modelling for coastal sites of interest if required.</p> <p>Priority: Low unless very detailed local analysis is required</p>
Simulate spatially varying defence crest height	<ul style="list-style-type: none"> Mean crest heights do not reflect the spatial variation in crest height along defence sections meaning low points may not be included. 	<ul style="list-style-type: none"> Comparison of surveyed crest heights and mean crest heights used to establish spatially varying crest height simulation method 	Flood depths were shown to be greatest nearest to breach location. Breaching most likely at low points in defence crest, if these are not modelled then risk will appear low.	The correct representation of crest height is very significant as in most cases the damage will be zero if the defence does not breach so it is important to correctly incorporate low (potential failure) points.	<p>When detailed survey information is not available the spatially varying crest height simulation should be used to incorporate potential low points.</p> <p>Priority: High</p>

System Component	Source of uncertainty	How is this included in the system model?	What are the implications of the uncertainty?	Assessment of significance	Recommendation
Assign fragility curve to defence type	<ul style="list-style-type: none"> Fragility curves are simplistic and do not fully represent failure modes or potentially spatially variable defence reliability. Only breaching following overtopping considered. Breach is assumed to grow to full width in one time step. 	<ul style="list-style-type: none"> No available data to improve this. Sensitivity of damage to breach size and location investigated. 	Flood depths were shown to be greatest nearest to breach location. Breaching is most likely at weak points along the defence crest, if these are not modelled then risk will appear low.	The correct representation of failure probability is very significant as in most cases the damage will be zero if the defence does not breach so it is important to correctly incorporate weak (potential failure) points. This is particularly important for coastal caravan sites.	<p>There is a need to incorporate the available research into defence failure into system models. The spatially varying crest height methodology could be adapted for spatially varying defence reliability. The analysis should be extended to other failure modes where these are considered important to the sites of interest.</p> <p>Priority: High</p>
Model floodplain inundation	<ul style="list-style-type: none"> Limited data on floodplain elevation and obstructions affects inundation modelling. Compromise required between detailed floodplain modelling and computational time for system risk calculation. 	<ul style="list-style-type: none"> Two methods illustrated including simple 1D model for fluvial locations and more complex 2D model for coastal locations. 	The flood depth at any given location within floodplain could be incorrect which would lead to a false calculation of damage.	For large events that cause high damages minor differences in floodplain inundation are unlikely to significantly affect the results, particularly in this case study where the exact location of caravan units is unknown and the depth-damage data is limited.	<p>Suitable inundation models should be chosen based on the level of detail required at specific site locations and the computational time available.</p> <p>Priority: Medium</p>

System Component	Source of uncertainty	How is this included in the system model?	What are the implications of the uncertainty?	Assessment of significance	Recommendation
Calculate damage	<ul style="list-style-type: none"> Depth-damage curves are simplistic and the vulnerability data used for caravan specific curves is very limited. Distribution of units across sites affects damage however caravan units usually modelled at single postcode point. Floor height of units not known. 	<ul style="list-style-type: none"> Sensitivity of damage to individual facets of the depth-damage curve was investigated. Damage calculated at point and distributed unit locations. 	Over or underestimation of flood damages	The lack of data on caravan vulnerability is a significant uncertainty in the system risk model. Due to the high vulnerability of caravans to relatively low water depths their location on the site is important and could result in the different between zero damage and total write off.	<p>More data is required on flood receptors.</p> <p>Following an event data should be collected on flood damages to caravans and depth-damage curves re-assessed.</p> <p>Consideration should be given to the spatial distribution of caravan units across sites, particularly where sites are large.</p> <p>Priority: High</p>

9.4.1 Simulation of extreme events

The contribution to system uncertainty from the sources component of the methodology is generally acceptable. There is some inherent uncertainty due to the difficulty of modelling extremes with limited observed data however this is a feature of all extreme value models. Robust statistical techniques have been used to ensure good model fits for the marginal data at each gauge (see Section 6.3.4). The uncertainty in the conditional dependence model used for the multivariate simulation has been shown to be acceptable for this type of analysis by Keef *et al* (2009a; 2009b; 2009c) and the sensibility check of the results (Figure 6.13, Figure 6.18, Figure 6.19) illustrate a good fit between simulated and observed data for the gauges used in this thesis.

Some areas of the sources component are more uncertain than others. Most significantly the modelling of wave heights using the conditional dependence model which violates the best practice guidance set out by Keef *et al* due to the short record length. However the relative importance of this component is low compared to estimation of the tide and surge height. The effect of missing data across the gauged network was shown in Table 6.14 to contribute to uncertainty but the simple infilling methodology outlined in Section 6.3.5.1 was shown to offer significant improvements to the model fit when the infilled time series was used. The contribution of missing data to uncertainty in the sources component will depend on the amount of missing data and will vary across different network structures.

This assessment of uncertainty in the sources component may initially appear at odds with the acknowledged acceptance that the estimation of extreme events is severely compromised by the limited record lengths. While not denying this important problem, in the context of a flood risk system model, this component is well understood and the contribution to uncertainty well documented and possible to quantify through statistical techniques. Therefore although independently the uncertainty is high in statistical modelling of extremes, relatively this component is less concerning for the estimation of risk in a systems model compared to other areas. Unlike defence failure or floor level changes in the source events will result in a gradual change in risk rather than a step change.

9.4.2 Conversion of simulated DMF to events at the receptors

To ensure use of the best available data compromises were required in the selection of suitable gauges and data formats, therefore additional uncertainty stems from converting between the simulated extreme source events and physically useful event variables at the receptors

A major source of uncertainty at this stage in the framework is the lack of a suitable gauged network to validate the ungauged site methodology as the distance between gauges in the dataset used was much greater than between the gauges and model inflow points that the method is applied over. Therefore although it is assumed that the uncertainties at the application stage are smaller than those shown in Appendix C.7, especially for the River Severn example where the main river and tributaries are all gauged upstream of the points of interest, there are no data available to support this assumption.

External sources of uncertainty are added to the system model through the use of external data sources, such as the FEH PCDs, and methods, in this case the ReFH Rainfall Runoff method. These are not considered in detail here but still contribute to the overall system uncertainty.

9.4.3 Conversion of simulated skew surge to total inshore water level, wave height and overtopping

Similarly to the conversion of DMF to events at the receptors, the uncertainty stemming from the conversion of simulated skew surge to total inshore water level is largely derived from a lack of data to assess the uncertainty. In the case of the coastal components the uncertainty is less than for the fluvial components as well established methods have been used and therefore the uncertainties are better understood. The uncertainty could further be reduced by incorporating more information on the beach and defence profiles. In addition the use of more complex methods would enable simplifications to be removed, such as the assumption of deep water at the defence toe, would be beneficial however given the high uncertainty in defence reliability this is not considered an immediate priority.

9.4.4 Consideration of flood defence reliability

The available data on flood defence properties are poor. The review of data for the East Coast in Section 8.4 showed that the long section mean which is commonly provided in the Environment Agency NFCDD and used in Cat models and other inundation risk models is a poor representation of the actual crest height. In most cases the amount of variation is between 0.1 and 0.5m. The proposed methodology to simulate spatially plausible varying long section crest heights from the mean crest height outlined in Section 8.4 offers a means of explicitly incorporating the uncertainty from limited data on defence properties into the risk model.

The literature review in Section 8.3 identified that the risk based consideration of defence failure is limited and does not take full advantage of the recent scientific advances in understanding flood defence reliability. The accepted approach has been to use fragility curves which, due to the inclusions of small probability of failure below the defence design standard

allow some consideration of uncertainty to be included in the method. However Simms et al (2009) review of the performance of fragility curves following the 2007 flooding identified that the current implementation of fragility analysis across England and Wales failed to capture a number of key uncertainties, in particular variability along the flood defence length (see Section 8.3.1.1 for details). Fragility analysis is dependent on robust observations and field evidence, and to enable broad scale analysis, many of the fragility calculations assessed by Simms et al (2009) were reliant on generic assumptions. Approaches to model spatial variability along a flood defence length require a high sampling of data. The resolution and detail of such monitoring, and associated reduction in uncertainty, must be balanced against the cost and practicality involved in collecting this information. Other work, for example by Dawson and Hall (2002) has sought to incorporate uncertainty analysis explicitly within the fragility model. Although useful this poses interpretation challenges for decision makers.

The review of caravan sites in Section 3.2 showed that most sites in coastal locations are located behind flood defences and therefore do not suffer flooding from moderate events but are highly vulnerable to defence failure. Changes in the defence reliability assumptions or crest height result in large changes in damages as sites will flood or not flood depending on whether flood defences fail. For this reason the limited data on flood defence properties available in this thesis, and the lack of credible methods of representing flood defence failure in a systems risk model framework, are considered to be the biggest barriers preventing a believable estimation of risk. The varying crest height methodology makes steps towards a potential framework for including spatially varying defence reliability however considerably more research and data collection is required to extend this proposed framework to defence resistance properties as well as crest height.

9.4.5 Calculation of damage

Sections 9.1.4.1 to 9.1.4.3 illustrated the large uncertainties in the calculation of flood damages. Lack of knowledge about the vulnerability of caravans to floods and lack of data on individual unit locations and floor heights combine to produce high uncertainties that have a significant impact on results.

The impact of this lack of data can be the difference between zero damages and very high damage if a unit is taken out of the inundation area either by moving it to an unflooded area of the site or raising it above the maximum water level.

Unlike uncertainty from flood defence reliability this is not a problem caused by lack of scientific understanding or modelling capabilities but rather a problem caused by limited data collection and therefore can be addressed by simple measures such as promoting better data

collection both before and following an event and using this to validate existing depth-damage curves or produce more appropriate alternatives.

10 Conclusions

Motivated by the growing acceptance of the importance of considering spatial and temporal dependencies in flood risk and by changes in the insurance climate, this thesis has illustrated the development of an integrated systems risk model which enables detailed site based risk assessment to be carried out within a national context through the use of a nested model structure. The research has followed a SPRC concept throughout. Fluvial and coastal sources of flood risk have been considered, including the impact of waves in a complex statistical model. The reliability of coastal flood defences has been reviewed and a methodology established to incorporate the potential spatial variation in crest height compared to available summary data. The research has been based on a case study of flood risk to static caravans, and, as such a review of depth-damage curves relating to caravans was carried out. The methodological framework is however modular and adaptable to other receptors by modifying the depth-damage functions.

This final chapter will be structured around reviewing how the thesis has addressed the research objectives set out in Chapter 1 and identifying recommendations for both Catlin and further research.

10.1 Meeting the research aims and objectives

10.1.1 *Static caravans and flood damage*

"1. Review the geographical disposition of fixed caravan sites in the UK and their approximate financial values and investigate trends in historic flood damage to these sites"

Due to the large proportion of UK caravans Catlin Insure, the review of Catlin's caravan portfolio in Chapter 3 can be thought of as representative of the distribution of caravan sites more generally across the UK. The review identified that one third of caravan sites were located within 1km of the sea, many clustered in particular popular tourist areas such as the Lincolnshire coast. This is problematic for insurance companies as it leads to an over exposure of risk in particular areas and means that the principle of spreading risk across a portfolio to protect against major losses being sustained from a single event is compromised.

There are limited historic data available on flood damage to static caravans. This is potentially problematic, especially as this thesis has shown that modern static caravans are worth an

average of £20,000 each with the most expensive models costing over £100,000. Due to the lack of available data it was not possible to conduct a full review of damage from recent events compared to the observed flood depths.

The past event data available made no connection between flood damage claims to insurance companies and observed flood levels. This is due to differing priorities between those collecting the different data types. Even the academic papers reviewing past events at caravan sites do not include this type of information. Ideally it should not require large scale studies, such as the Dundee Tables UK in the UK (Black *et al.* 2006) to establish this link. It is recommended that claim adjusters make a record of the observed water level, even if this is a qualitative assessment such as "half way up the door" as this would provide insurance companies with a means of assessing the performance of their depth-damage curves which are a central component of their risk estimation methods and assessed in Section 9.4 to be a major source of uncertainty. Although more detail is known about the vulnerability of residential properties, the routine collection of depth data by claims adjusters would be good practice for all property types.

The historic review identified that Catlin did not sustain major losses during the large floods in 2007. This is due to the way their portfolio is managed in that Catlin will only insure new caravans, with floatation devices, which are located above the highest recorded water level. These broad brush assumptions and reactive review appear to have worked well for Catlin in the past but with a potentially changing climate resulting in an increase in flood risk and more intense storms leading to a different type of flooding, this approach may not provide a robust long term solution for managing the portfolio.

The review of caravan locations identified four clusters which were used as the detailed nested sites within the systems model. The sites were selected based on the number of caravans at risk and to provide a good coverage of spatial location and flood risk sources. These clusters were; the Lincolnshire coastline which was selected due to the high density of caravan sites in the area and the vulnerability to north sea storm surge, the North Wales coastline again selected for the number of sites at risk and to consider coastal issues in a different geographical location, the River Severn around Stourport-on-Severn which provided an example of the interaction between multiple tributaries, and the River Thames near Hurley which was selected because of the political sensitivity of flood risk in the Thames and to provide an example of the spatial dependencies between large scale river systems.

Transparent caravan specific depth-damage curves were established which utilised the understanding of historic damages from Catlin with data from external sources. The curves were modified to investigate the sensitivity of the risk estimate to the curve shape. The most critical point in the depth-damage curves was found to be the floor height.

10.1.2 Statistical modelling of multivariate spatial extremes

"2. Establish a multivariate spatial extreme value statistical model for river flow, surge and waves at selected sites"

The Heffernan and Tawn (2004) conditional dependence model was used to provide a robust statistical basis for the systems model. The conditional dependence model has previously been used to model spatial dependencies in flood risk in the UK by Keef *et al* (Keef 2006; Lamb *et al.* 2009; Keef *et al.* 2009a; Keef *et al.* 2009b; Keef *et al.* 2009c; Lamb *et al.* 2010) and has been shown to correctly represent the spatial and temporal dependencies between flood events. The use of Heffernan and Tawn's conditional dependence model in this thesis illustrates an example of a complex statistical model being used by a non-professional statistician. This is an important application as to date the model has mainly been used only by colleagues of Heffernan and Tawn or professional statisticians. This is a difficulty many research models face and illustrating that they can be used by specialists without a statistical background shows the potential for more wide scale uptake of this kind of models, resulting in an improvement in the representation of extreme events in a broad range of applications.

The conditional dependence model was fitted to extreme river flows using DMF data at six core flow gauges and sea states using skew surges at six core tide gauges. Rather than use a UK wide gauged network as per previous statistical models of UK extremes, a novel nested model structure was used with more gauges located close to the sites of interest whilst still representing the large scale spatial dependence of events on a national scale. In addition to the previous application by Keef *et al*, the model was also fitted to extreme wave heights using a pairwise dependence structure between skew surge and wave heights. The limited record length at wave gauges meant that only a pairwise version of the model could be used to represent the relationship between skew surge and wave height. Skew surge was shown to be a more suitable variable than the traditionally used still water level to model the relationship between surge events and waves as it is not overshadowed by the effect of the tide.

The results from the conditional dependence model show that all gauged pairs display positive

extremal dependence. The most extreme events at all sites are shown to be very localised, however the large catchments of the Severn and Thames display some dependence structure across large areas. Coastal events are shown to display weaker larger scale dependences than fluvial events, particularly across different coastlines. The dependence between gauges on the same coastline however is strong even across relatively large distances. The temporal dependence between coastal and fluvial events is generally weaker than between events of the same type, although fluvial events in North Wales and the River Severn can occur at the same time as large coastal events in North Wales. The converse however is not true as coastal events in North Wales do not necessarily result in fluvial extremes.

For the purposes of insurance pricing it was shown that the current seven day insurance window incorporates all dependent extreme weather events from both fluvial and coastal sources across large areas of the UK. The peak dependence was found to fall within three days, therefore the seven day window could potentially include additional independent localised events.

10.1.3 Linking a robust statistical model to a physically based model

“3. Develop a process-based method to connect these source terms with variables (e.g. flood depth) from which damage can be computed”

Aside from the difficulties in understanding and applying statistical models such as the conditional dependence model used in this thesis, linking statistical and physically based models is difficult due to differing data requirements and scales of analysis. This thesis has investigated a range of methods to integrate existing hydrological and hydraulic methodologies with the systems model.

The conditional dependence model required concurrent time series for a large network of gauges. Previous applications had used DMF data to fulfil this requirement however DMF is of limited use to assess flood depths. To overcome this problem, methodologies for transforming DMF to peak flow data were tested and a UK specific equation based on the work of Sangal (1983) was established which estimates peak flow using the concept of a triangular hydrograph. This method was particularly attractive for this application as it incorporates the temporal dependencies in DMF from the conditional dependence model.

Data are only available at gauging stations not at sites of interest therefore interpolation was

required between gauges and sites of interest. Unfortunately the gauging station network available was not dense enough to validate the ungauged site interpolation method. Instead a methodology was selected based on accepted practice in the field. At each ungauged location, donor sites were selected based on the distance between catchment centroids and the modelled flow scaled by the difference in QMED between donor and ungauged sites.

One of the strengths of the proposed methodology is its modular nature. This was illustrated through the inclusion of two different types of inundation model. For fluvial sites a simplified 1D hydraulic routing model was used which required minimum data to set up as it was based entirely on LiDAR data with channel cross sections assumed to contain the QMED flow. Flood depths were established by routing the modelled water level across the floodplain using simple GIS processing techniques. In contrast the coastal floodplain inundation model illustrates how a complex 2D flood routing model can be nested within the system model structure and used to expand the modelling capabilities. The more detailed 2D coastal routing model was required in this case to represent the rapid inundation for flood defence breaches.

10.1.4 Consideration of spatial variability in flood defence systems

“4. Consider the representation of flood defences and potential failure mechanisms in flood risk models and incorporate this into a systems based risk model”

The representation of flood defences is a critical component in flood risk models. This thesis has reviewed the existing modelling of defence reliability and has established that it is not fully risk based. Many existing models use scenario based failure models due to lack of data and the high computational requirements of modelling multiple failure scenarios.

A key theme throughout this thesis has been the representation of spatial and temporal dependencies in flood risk. Established methods of considering flood defence failure were shown in the literature to not fully account for this, for example by assuming simultaneous loading of all defences in a defence system and not fully considering the breach growth process which is linked to defence properties, duration of high water and the sequencing of breaches.

This thesis addressed the issue of the spatial variability in defence properties through analysis of the variation in crest height compared to the mean crest height which is commonly available in datasets such as the Environment Agency NFCDD which forms the basis of many

Cat Models flood defence modules. A review of the surveyed crest height data for the East Coast identified that the mean defence height is a poor representation of the actual crest height. A methodology was established to represent this variability within the risk model by simulating physically realistic defence crest heights using a Markov Chain process. The incorporation of spatially varying defence properties allows the artificial restriction on defence section length which is used in previous risk based failure models to be lifted.

A similar variability is expected to occur within the defence strength properties due to differing construction practices and materials along a defence section and variation in maintenance. Detailed geophysical data were not available to test these assumptions. A useful extension of the spatial variability in crest height method would be to establish similar models for the variability in defence properties and use these to construct a spatially varying reliability curve for flood defences in the future. Further work is also required on the dependencies in breach growth which are not considered fully in this thesis.

10.1.5 Contribute to integrated and informed decision making

“5. Review the importance of each component in the systems risk model and discuss how the improved knowledge about each component and the links between them can help improve insurance pricing decisions and wider flood risk management”

This thesis has shown how information can be cascaded from a high level methodology to a detailed site based assessment through the nested model structure. The nested structure is useful as it enables large scale and local dependencies to be modelled. Care must be taken in the design of the nested structure as the results from the conditional dependence model were shown to be influenced by the differences in network density between fluvial and coastal gauges.

For Catlin the results from the conditional dependence model are promising. Although they highlight the known vulnerability along the East Coast with long stretches of coastline affected by the same event, the dependence between different coastlines and between fluvial and coastal events is weak, especially on the East Coast. Therefore by ensuring that they continue to insure sites spread across the whole UK, Catlin will be able to spread their exposure risk and protect themselves from large losses from the same event.

The discussion in Section 9.4 highlighted that the greatest source of uncertainty in the system stems from limited data for all components. In particular this affects the ability to adequately model defence failure and calculate flood damages for caravans. In light of these concerns it was concluded that the cascade of uncertainty through the system model would significantly affect the usefulness of a final calculation of risk. In spite of this limitation, the process understanding gained from this research are beneficial and highlight where further research is required to improve flood risk modelling and can be used to justify risk based decision making.

The most critical area is concluded to be the representation of flood defence reliability both in terms of data available to adequately model flood defences and in the available risk based failure models. Existing methods were shown to be not fully risk based and to perform poorly when tested in real events. The review of crest height data also identified significant simplifications in the representation of spatial variability within the flood defence system which, given the importance of small scale weaknesses in controlling defence failure, is a significant limitation.

Regardless of the potentially large uncertainties in flood risk modelling it has been shown throughout this thesis that the most effective way to improve across all components is by increasing data availability. Insurance companies are in a prime position to be able to instigate this by improving their own data collecting protocols both before and after flood events. Even very simple measures such as recording a flood depth alongside the insurance claim would help validate depth-damage curves and reduce uncertainty in flood risk estimation. This is especially important for caravans where the steep depth-damage curves result in large jumps between zero damages and high damages for small changes in water level.

An end to end assessment of uncertainty in Cat models, even at the qualitative level given in Section 9.4, would be beneficial to insurance companies and would help end users identify where the greatest uncertainties lie and what this means for their individual portfolios. In this case the geographical review of caravans identified large concentrations of sites located behind flood defences hence the large uncertainties from defence reliability analysis are particularly concerning when pricing this portfolio and Catlin's current approach of adding a risk load of 30-40% to insurance premiums (Equation 1.1) is justifiable. Further assessment of the uncertainties in RMS' defence reliability modelling is required to better assess exactly what this percentage should be.

10.1.6 Development of a coherent modelling framework that meets essential modelling criteria

Although not specified as a research objective, the literature review in Chapter 2 resulted in the identification of five key criteria for models used to inform risk based decision making. Reviewing the systems based methodology developed as part of this thesis shows that the proposed method meets all of these criteria. It is transparent as it clearly states the modelling assumptions, it also explicitly considers the effect of the input data on the results and in some cases develops unique methodologies to deal with limited data availability for example the consideration of plausible variation in long section defence crest heights compared to the observed defence crest mean. The modular nature of the systems methodology was demonstrated through the use of two different inundation models providing differing levels of detail as required in different situations. The adaptability of the dependence model was also illustrated through the modification of the method to incorporate wave data with a comparably short record length. This adaptability ensures that the methodology is flexible and can be adapted to different applications as required for example by changing the depth-damage curves to look at alternative receptors. The nested model structure ensures that the methodology is efficient as detailed calculations can be made at a site level, for example in the consideration of how the distribution of units on a site affects the damage calculation, whilst maintaining an overview of the large scale dependencies in risk for example between sites on different coastlines.

The simplicity of a fully integrated systems risk model is hard to establish due to the interconnections between different components. This thesis has demonstrated a transparent model where each component is explicitly considered allowing the end user to identify how the modelling assumptions at each stage affect the output. The thesis has been structured in such a way as to lead the end user through the SPRC model and show how each stage of the methodology feeds into the next. The discussion in Section 9.4 identified the potential uncertainties as each stage of the process and how these feed into the subsequent calculations.

10.2 Recommendations

Two sets of recommendations are made in light of this research. Firstly for Catlin to improve their management of the caravan portfolio it is recommended that;

1. A broad spatial distribution of caravan sites is maintained across the UK. The current apparent over exposure on the East Coast is mitigated by the weak dependence between extreme events on the coastline and fluvial and coastal events elsewhere in the country.

2. Better pre and post event data collection procedures are put in place to develop a database of caravan unit locations, floor heights and explicitly to link flood depth with insurance claims.
3. Depth-damage curves are reviewed following an event using the improved database
4. In the short term Catlin should continue to add a risk load to their insurance pricing calculations for defended sites to account for the potential vulnerability to defence failure and limited modelling capabilities in this area.
5. In the long term Catlin should request more detailed information from Cat modelling companies on uncertainty in Cat models and consider funding, or contributing to, further research, particularly on flood defence reliability modelling.

Secondly for broader improvements in systems based risk modelling it is recommended that research is undertaken to:

6. Improve the availability of data on flood defence including crest height and construction.
7. Address the problem of limited data and knowledge on crest height and defence reliability properties by using the plausible crest height variation methodology presented in Chapter 8 in flood risk studies. Development of a similar methodology for variation in defence properties would also be beneficial to take account of potential weak points along the defence section length.
8. Consider how the recent improvements in the understanding of flood defence failure mechanisms can be included in systems risk models. Advances in computational ability mean more complex methods could be used in a risk based framework however questions still need to be answered about the suitable scale of application and the availability of detailed data to support increased complexity.
9. Review how uncertainty in systems risk models is assessed and develop means of communicating the impact of this to decision makers. Including making explicit assessments of component uncertainty and how this contributes to the and overall system uncertainty as discussed in Section 9.4.

10.3 Concluding comments

This thesis has illustrated the development of a full systems based model that is achievable at a national scale by focusing on particular areas of interest using a novel nested framework. The cross cutting analysis has drawn together state of the art methods to explicitly consider each risk component. Each component has been analysed in detail, an approach that is rare in similar studies with most emphasis often being placed on the researcher's main area of

expertise.

A core strength of the research has been the development of a transparent and flexible systems risk framework that incorporates the critical spatial and temporal dependencies in flood risk at a range of scales through a conditional dependence model. Although the Heffernan and Tawn (2004) model has been used previously for similar flood risk dependency analysis by Keef *et al*, several unique approaches were developed in this thesis including fitting the model to wave height and skew surge and using the model within the nested framework.

A key focus of this thesis was to demonstrate the use of a robust statistical model of extremes to provide a solid foundation for process based understanding and decision making. To facilitate this discussion of the challenges of stepping between the two fields is discussed throughout. These challenges can be split into three areas; data availability at required locations, data quality, and communication of assumptions and results. Making the best use of available data and state of the art methods whilst being explicit about the sources of uncertainty is essential for well informed decision making. This thesis has been explicit about the assumptions at each stage in the process and how these contribute to the overall uncertainty to provide a rare assessment of the relative importance of each component and to make clear recommendations of where further research would have the greatest impact to reduce overall uncertainty.

One of the biggest challenges for the future is to improve modelling capability and data availability so that systems based models such as this can be used with a consistent, and practical, level of uncertainty. The move towards increasing openness between Cat modellers, academia and end users offers a promising potential to develop useable systems risk models with realistic uncertainty bounds.

11 References

- AghaKouchak, A., Bardossy, A., and Habib, E. (2010). "Copula-based uncertainty modelling: application to multisensor precipitation estimates." *Hydrological Processes* 24(15): 2111-2124.
- AIR Worldwide. (2008). "The Air Inland Flood Model for Great Britain." Retrieved July 2009, from <http://www.air-worldwide.com/PublicationsItem.aspx?id=15766>.
- AIR Worldwide. (2009). "Company website." Retrieved March 2009, from <http://www.air-worldwide.com/Default.aspx>.
- Allsop, W., Bruce, T., Pearson, J., and Besley, P (2005). "Wave overtopping at vertical and steep seawalls." *Proceedings of the institution of civil engineers: maritime engineering* 158(MA3): 103-114.
- Allsop, W., Kortenhuis, A., and Morris, M. (2007). Failure mechanisms for flood defence structures, FLOODsite. Report Number: T04-06-01.
- Anderson, C. (2009). *Extreme rainfall. Spatial extremes, theory and applications*, Lisbon, Portugal.
- Apel, H., Merz, B., and Thieken, A.H (2009). "Influence of dike breaches on flood frequency estimation." *Computers and Geoscience* 35(5): 907-923.
- Apel, H., Thieken, A. H., Merz, B., and Bloschl, G. (2004). "Flood risk assessment and associated uncertainty." *Natural hazards and earth systems* 4: 295-308.
- Apel, H., Thieken, A. H., Merz, B., and Bloschl, G. (2006). "A probabilistic modelling system for assessing flood risks." *Natural Hazards* 38: 79-100.
- Association of British Insurers (2005a). *ABI Statement of principles on the provision of flood insurance: Updated Version November 2005*.
- Association of British Insurers (2005b). *Revisiting the partnership: five years on from autumn 2000*, Association of British Insurers: 8.
- Association of British Insurers (2007). *Summer Floods 2007: Learning the Lessons*, Association of British Insurers: 27.
- Association of British Insurers (2008). *Revised statement of principles on the provision of flood insurance*.
- Barrow, E. and Hulme, M. (1997). *Describing the surface climate of the British Isles. Climates of the British Isles: present, past and future*. E. Barrow and M. Hulme. London, Routledge.
- BBC News. (1998). "Body of third flood victim found." Retrieved January 2012, from <http://news.bbc.co.uk/1/hi/uk/77137.stm>.
- BBC News. (2006). "Village evacuated amid flooding." Retrieved May 2011, from http://news.bbc.co.uk/1/hi/scotland/tayside_and_central/6177937.stm.
- BBC News. (2007). "The summer floods: what happened." Retrieved January 2010, from <http://news.bbc.co.uk/1/hi/uk/7446721.stm>.
- BBC News. (2008). "UK storm causes 14 flood warnings." Retrieved May 2011, from <http://news.bbc.co.uk/1/hi/uk/7287662.stm>.

- BBC News. (2009). "Homes and roads hit by flooding." Retrieved May 2011, from http://news.bbc.co.uk/1/hi/wales/wales_politics/8359751.stm.
- Besley, P. (1999). Overtopping of seawalls: design and assessment manual. Technical Report No.W178. Bristol, Environment Agency.
- Beven, K., Leedal, D. and McCarthy, S. (2011). Framework for assessing uncertainty in fluvial flood risk mapping. FRMRC Research Report SWP1.7
- Black, A., Werritty, A., Paine, J. (2006). Financial costs of property damages due to flooding; the Halifax Dundee flood loss tables 2005. University of Dundee.
- BODC. (2009). "UK tide gauge network data" Retrieved June 2009, from http://www.bodc.ac.uk/data/online_delivery/ntsIf/.
- Bonazzi, A., Cusack, S., Hewson, S., and Mitas, C. (2011). European Wind Storms: an extreme value analysis of joint wind gust measured by anemometers across major cities. EGU2011, Session NH1.2/AS4.7/HS12.6. Vienna.
- Bowen. A. and Pallister, J. (2001) A2 Geography, Heinemann Educational Publishers, Oxford.
- Buijs, F. A., van Gelder, and Hall, J.W (2004). "Application of reliability-based flood defence design in the UK." *Heron* 49(1): 33-50.
- Buijs, F. A., van Gelder, P., Vrijling, J. K., Vrouwenvelder, A., Hall, J. W., Sayers, P. B., and Wehrung, M. J. (2003). Application of Dutch reliability-based flood defence design in the UK. *Safety and Reliability, Vols 1 and 2*. Bedford, T. and van Gelder, P.: 311-319.
- Burcharth, H. F. (1993). The design of breakwaters. Coastal, estuarial and harbour engineer's reference book. M.B. Abbot and W.A. Price. London, Chapman and Hall: 381-434.
- Calver, A., Lamb, R., and Morris, S.E. (1999). "River flood frequency estimation using continuous runoff modelling." *Proceedings of the Institution of Civil Engineers-Water and Maritime Engineering* 136(4): 225-234.
- Catlin Group Limited. (2009). "Catlin Group Limited Homepage." Retrieved January, 2009, from www.catlin.com.
- Catlin Group Limited (2010). Building a business for the future: annual report and accounts.
- Cefas. (2009). "Wave Net." Retrieved June 2009, from <http://www.cefas.co.uk/data/wavenet.aspx>.
- CEH (1999). Flood Estimation Handbook, Centre for Ecology and Hydrology, Wallingford.
- CEH. (2009a). "National River Flow Archive." Retrieved June 2009, from <http://www.ceh.ac.uk/data/nrfa/index.html>.
- CEH (2009b). The Flood Estimation Handbook CD-ROM 3, Centre for Ecology and Hydrology, Wallingford.
- CEH. (2011). "Improved access to the UK's river flow data." Retrieved December 5th 2011, from http://www.ceh.ac.uk/news/news_archive/NRFA-data-release_2011_63.html.
- Climatepredictions.net. "The UK Autumn 2000 floods." Retrieved January 2010, from <http://climateprediction.net/content/uk-autumn-2000-floods>.
- Coles, S. (2001). An introduction to statistical modelling of extreme values. London, Springer.

- Coles, S., Heffernan, J. E. and Tawn, J. (1999). "Dependence Measures for Extreme Value Analyses." *Extremes* 2(4): 339-365.
- Coles, S. and Stephenson, A. G. (2010). *ismev: An introduction to statistical modelling of extreme values*. R package version 1.35.
- Coles, S. and Tawn, J. (2005a). "Seasonal effects of extreme surges." *Stochastic Environmental Research and Risk Assessment* 19(6): 417-427.
- Coles, S. and Tawn, J. (2005b). "Bayesian modelling of extreme surges on the UK east coast." *Philosophical Transactions of the Royal Society A - Mathematical Physical and Engineering Sciences* 363(1831): 1387-1406.
- Coles, S. G. and Tawn, J. (1996). "A Bayesian analysis of extreme rainfall data." *Applied Statistics-Journal of the Royal Statistical Society Series C* 45(4): 463-478.
- Collier, C. G., Fox, N. I. and Hand, W.H. (2002). *Extreme rainfall and flood event recognition*. . R&D Technical Report: FD2201. London, DEFRA/Environment Agency.
- Collins, S. (2008a). "Cat modelling firm promises future developments." *Business Insurance Europe*, Retrieved February 2009, from <http://www.bieurope.com/cgi-bin/article.pl?articleId=25913>.
- Collins, S. (2008b). "Cat modelling to enter new era: NCAR." *Business Insurance*, Retrieved February 2009, 2009, from <http://www.businessinsurance.com/cgi-bin/news.pl?newsId=14728>.
- Communities and Local Government (2006). *Planning Policy Statement 25: Development and Flood Risk*. London, The Stationary Office: pp50.
- Coumou, D. and Rahmstorf, S. (2012). "A decade of weather extremes." *Nature Climate Change* advance online publication.
- Crichton, D. (2003). *Flood Risk & Insurance in England and Wales: Are there lessons to be learned from Scotland?* London, Benfield Greig Hazard Research Centre: 168.
- Davison, A. and Hinkley, D. V. (1997). *Bootstrap methods and their application*, Cambridge University Press.
- Dawson, R. and Hall, J. (2002) *Improved condition characterisation of defences*. Proc. Conf. Breakwaters, Coastal structures and coastlines 2001. London, Thomas Telford, 123-134.
- Dawson, R., Hall, J., Sayers, P., Bates, P. and Rosu, C. (2005). "Sampling-based flood risk analysis for fluvial dike systems." *Stochastic Environmental Research and Risk Assessment* 19(6): 388-402.
- Dawson R.J., Speight L., Hall, J.W., Djordjevic, .S, Savic, D. and Leandro, J. (2008) "Attribution of flood risk in urban areas." *Journal of Hydroinformatics*, 10(4): 275-288
- DEFRA (2004). "Risk Assessment for Flood and Coastal Defence for Strategic Planning, R&D Technical Report W5B-030/TR."
- Defra and HM Government (2012). *UK climate change risk assessment: government report*.
- Denuit, M., Dhaene J., Goovarrts, M. and Kaas, R. (2005). *Actuarial theory for dependent risks: measures, orders and models*. Chichester, Wiley.

- Deutsches GeoForschungsZentrum GFZ (2010). "HOWAS 21 - Online database for flood damage." September 2010, from <http://nadine-ws.gfz-potsdam.de:8080/howasPortal/client/start>.
- Die Küste (2007). EurOtop: wave overtopping of sea defences and related structures: assessmeny manual. Archive for research and technology on the North Sea and Baltic Coast.
- Dixon, M. J. and J. Tawn (1995). "Estimates of extreme sea conditions, Extreme sea levels at the UK A-class sites: Optimal site by site analyses and spatial analyses for the East coast." Proudman Oceanographic Laboratory, Internal Document 72.
- Dixon, M. J. and J. Tawn (1997). "Estimates of extreme sea conditions, Final Report: Spatial analyses for the UK Coast." Proudman Oceanographic Laboratory, Internal Document 112.
- Dixon, M. J. and J. A. Tawn (1994). "Estimates of extreme sea conditions, Extreme sea levels at the UK A-class sites: a site by site analysis." Proudman Oceanographic Laboratory, Internal Document 65.
- Dixon, M. J. and J. A. Tawn (1999). "The effect of non-stationarity on extreme sea-level estimation." *Journal of the Royal Statistical Society Series C-Applied Statistics* 48: 135-151.
- Dixon, M. J., Tawn, J. A. and Vassie, J.M. (1998). "Spatial modelling of extreme sea-levels." *Environmetrics* 9(3): 283-301.
- Donat, M. Pardowitz, T., Leckebusch, G. and Ulbrich, U. (2011). Estimating the risk of losses caused by winter storms in Germany. EGU General Assembly. Vienna.
- Draper, D. (1995). "Assessment and propagation of model uncertainty." *Journal of the Royal Statistical Society Series B-Statistical Methodology* 57(1): 45-97.
- Environment Agency. (2007). "2007 summer floods review." Retrieved May 2011, from <http://www.environment-agency.gov.uk/research/library/publications/33887.aspx>.
- Environment Agency. (2008). "2007 summer floods - A table showing the likelihood of the 2007 summer floods occurring at places where we measure river flows and levels." Retrieved 19th January 2011, from http://www.environment-agency.gov.uk/static/documents/Research/returnperiods_1918541.pdf.
- Environment Agency (2009a). *Flooding in England: a national assessment of flood risk*. Rio House, Bristol, Environment Agency.
- Environment Agency. (2009b). "Flood Map." Retrieved March 2009, from <http://maps.environment-agency.gov.uk/wiyby/wiybyController>
- Environment Agency. (2010a). "HiFlows-UK." Retrieved January 2010, from <http://www.environment-agency.gov.uk/hiflows/91727.aspx>.
- Environment Agency. (2010b). "SC080053 - Update of Multi-coloured Manual." Retrieved September 2010, from <http://evidence.environment-agency.gov.uk/fcerm/en/Default/HomeAndLeisure/Floods/WhatWereDoing/IntoTheFuture/ScienceProgramme/ResearchAndDevelopment/FCRM/Project.aspx?ProjectID=b979b5d3-98c2-477f-be33-0b4416572c3a&PageID=3679217f-8f79-4c83-b935-f277aaadbdf1>.
- Environment Agency. (2011a). "How is flood risk managed?" Retrieved June 2011, from <http://www.environment-agency.gov.uk/homeandleisure/floods/31666.aspx>.

- Environment Agency (2011b). Design swell waves. Coastal flood boundary conditions for UK mainland and islands. Project SC060064.
- Environment Agency. (2012a). "Environment Agency company website." Retrieved 1st April 2012, from www.environment-agency.gov.uk.
- Environment Agency (2012b). Improving probabilistic flood risk modelling through improved model validation and reuse of existing models. Science Report-SC090008.
- Environment Agency (unknown date). Understanding flood risk, Our National Flood Risk Assessment (NaFRA).
- European Parliament Council (2009). Directive 2009/138/EC on the taking-up and pursuit of the business of insurance and reinsurance (Solvency II).
- European Parliament Council (2012). "Amending Directive 2009/138/EC on the taking-up and pursuit of the business of Insurance and Reinsurance (Solvency II) as regards the dates of its transposition and application and the date of repeal of certain Directives."
- European Parliament and the Council of the European Union (2009). On the taking-up and pursuit of the business of insurance and reinsurance (Solvency II). DIRECTIVE 2009/138/EC.
- Fawcett, L. and D. Walshaw (2006). "A hierarchical model for extreme wind speeds." *Journal of the Royal Statistical Society: Series C-Applied Statistics* 155(5): 631-646.
- Fill, H. and Steiner A. (2003). "Estimating instantaneous peak flow from mean daily flow data." *Journal of Hydrologic Engineering ASCE* 8(6): 365-369.
- FLOODsite. (2009a). "Integrated flood risk analysis and management methodologies." Retrieved April 2010, from www.floodsite.net.
- FLOODsite (2009b). RELIABLE.
- FLOODsite. (2012). "HR Breach Model." Retrieved May 2012, from http://www.floodsite.net/html/HR_Breach_Model.htm.
- Fuller, W. (1914). "Flood flows." *Transactions of the American Society of Civil Engineers* 77: 564-617.
- Gilleland, E., Katz, R. and Young, G. (2010). *extRemes: extreme value toolkit*. R package version 1.62.
- Gouldby, B., Sayers, P., Mulet-Marti, J., Hassab, M. and Benwell, D. (2009). "Discussion: A methodology for regional-scale flood risk assessment." *Proceedings of the institution of civil engineers: water management* 162: 347-348.
- Gouldby, B., Sayers, P., Mulet-Marti, J., Hassab, M. and Benwell, D. (2008). "A methodology for regional-scale flood risk assessment." *Proceedings of the Institution of Civil Engineers-Water Management* 161(3): 169-182.
- Green, M. (2005). "Professor: Cat models lack a common ground." *Best's Review*, Retrieved February, 2009, from <http://www.thefreelibrary.com/Professor:+cat+models+lack+a+common+guide-a0139601723>.
- Grossi, P. and H. Kunreuther, Eds. (2005). *Catastrophe modelling: a new approach to managing risk*. Huebner International Series on Risk, Insurance, and Economic Security. New York, Springer Science Business Media, Inc.

- Grossi, P. and C. TeHennepe (2008). Catastrophe modelling fundamentals. The Review: A guide to catastrophe modelling. Available online
<http://www.rms.com/Publications/RMS%20Guide%202008.pdf>.
- Gusman, P. (2008). "Insurers overly focused on Cat models, says expert." NU Online News Series, Retrieved 26th February, 2009, from
<http://www.propertyandcasualtyinsurancenews.com/cms/nupc/Breaking%20News/2008/04/17-CATRELIANCE-pg>.
- Haigh, I., Eliot, M. and Pattiaratchi, C. (2011). "Global influences of the 18.61 year nodal cycle and 8.85 year cycle of lunar perigee on high tide levels (preview)." *Journal of Geophysical Research* 116.
- Hall, J. W., Dawson, R. Sayers, P., Rosc, C., Chatterton, J. and Deakin, R. (2003). "A methodology for national-scale flood risk assessment." *Proceedings of the Institution of Civil Engineers-Water and Maritime Engineering* 156: 235-247.
- Hall, J.W., Manning, L.J. and Hankin, R.K.S. (2011). "Bayesian calibration of a flood inundation model using spatial data." *Water Resources Research* 47(5).
- Hall, J. W., Sayers, P. B. and Dawson, R. (2005). "National-scale assessment of current and future flood risk in England and Wales." *Natural Hazards* 36(1-2): 147-164.
- Hall, T., Harrison, M., McEwen, C. and Dempsey, M.. (2000). "Danger - caravans afloat." *Town and Country Planning* 69: 226 - 227.
- Harvey, C., Dixon, H. and Hannaford, J. (2010). Developing best practice for infilling daily river flow data. BHS Third International Symposium: Managing consequences of a changing global environment. Newcastle upon Tyne, British Hydrological Society.
- Harvey, G., Evans, E., Thorne, C. and Cheng, X. (2009). Scenario analysis technology for river basin flood risk management in the Taihu basin: a China:UK scientific co-operation project. Discussion paper 44, University of Nottingham.
- Haslett, S., K. (2000). *Coastal systems*, Routledge.
- Hawkes, P. J., Gonzalez-Marco, D., Sanchez-Arcilla, A. and Prinos, P. (2008). "Best practice for the estimation of extremes: A review." *Journal of Hydraulic Research* 46(2): 324-332.
- Hawkes, P. J., Gouldby, B. R., Tawn, J.A. and Owen, M.W. (2002). "The joint probability of waves and water levels in coastal engineering design." *Journal of Hydraulic Research* 40(3): 241-251.
- Heffernan, J. E. and Tawn, J. A. (2004). "A conditional approach for multivariate extreme values." *Journal of the Royal Statistical Society Series B-Statistical Methodology* 66: 497-530.
- Holmes, M. G. R., Young, A. R., Gustard, A. and Grew, R. (2002). "A region of influence approach to predicting flow duration curves within ungauged catchments." *Hydrology and Earth System Sciences* 6(4): 721 - 731.
- Horner, M. W. and Walsh, P. D. (2000). "Easter 1998 Floods." *Water and Environment Journal* 14(6).
- Horsburg, K. J. and C. Wilson (2007). "Tide-surge interaction and its role in the distribution of surge residuals in the North Sea." *Journal of Geophysical Research* 112.

- HR Wallingford (2002). Conwy Tidal Flood Risk Assessment. Report EX 4667.
- HR Wallingford (2009a). Exploring the unknown - advanced application of RASP methods 2009. *Edge*. 16: 10-11.
- HR Wallingford (2009b). A new era for flood system risk analysis. *Edge*. 16: 9.
- Hudson, P. (2011). "The weather forecast and media hype." *Weather*
<http://www.bbc.co.uk/blogs/paulhudson/2011/10/the-winter-forecast-and-media.shtml>
Accessed 1st January 2012.
- Humber, M. (2004). *Reforming the UK Flood Insurance Regime: The Breakdown of a Gentlemen's Agreement*. London, London School of Economics and Political Science: 25.
- Institution of Civil Engineers (1953). *Conference on the North Sea Floods of 31 January / 1 February 1953: A collection of papers presented at the institution, London, The Institution of Civil Engineers*.
- JBA Consulting. (2007). "The November 2007 Storm Surge: A Near Miss." Retrieved February 2009, from http://www.jbaconsulting.ie/news/November_2007_Storm_Surge_Ireland.pdf.
- JLT Re (2008a). *Compass Caravan, General, Direct and Private Clients; UK windstorm, coastal flood and river flood Catlin's share catastrophe analysis*.
- JLT Re (2008b). *Compass Caravan, General, Direct and Private Clients; RMS version 7.0.2 and version 8 comparison*.
- Johnson, J. (2008). *Spatial Modelling of extreme wind and rain*. Royal Statistical Society North Eastern seminar series, University of Durham.
- Kamphuis, J. W. (2000). *Introduction to coastal engineering and management*. London, World Scientific.
- Katz, R., Parlange, M. and Naveau, P. (2002). "Statistics of extremes in hydrology." *Advances in Water Resources* 25: 1287-1304.
- Keef, C. (2006). "Spatial dependence of river flooding and extreme rainfall." *Doctoral Thesis, Lancaster University*
- Keef, C., Lamb, R. and Tawn, J. (2009a). *Spatial coherence of flood risk – Methodology report Environment Agency. Science Report – SC060088/SR*.
- Keef, C., Lamb, R., Tawn, J. and Laeger, S. (2010). *A multivariate model for the broad scale spatial assessment of flood risk. BHS Third International Symposium: managing consequences of a changing global environment. Newcastle upon Tyne, British Hydrological Society*.
- Keef, C., Svensson, C., and Tawn, J. (2009b). "Spatial dependence in extreme river flows and precipitation for Great Britain." *Journal of Hydrology* 378: 240-252.
- Keef, C., Tawn, J. and Svensson, C. (2009c). "Spatial risk assessment for extreme river flows." *Journal of the Royal Statistical Society Series C- Applied Statistics* 58(5): 601-618.
- Kelman, I. (2003). "Defining Risk." *FloodRiskNet Newsletter* 2: 6-8.
- Kenneth, P., Saye, S. and Blott, S. (2007). *Sand dune processes and management for flood and coastal defence: Part 1: Project overview and recommendations. R&D Technical Report FD 1302/TR, Defra and Environment Agency*.

- Kjeldsen, T. (2007). The revitalised FSR / FEH rainfall-runoff method. Flood Estimation Handbook: Supplementary report No.1. Wallingford, Centre for Ecology and Hydrology.
- Kjeldsen, T. R., Jones, D.A., Bayliss, A.C. (2008). Improving the FEH statistical procedure for flood frequency estimation, Environment Agency. Science Report: SC050050.
- Kilsby, C. G., Jones, P. D., Burton, A., Ford, A., Fowler, H., Harpman, C., James, P., Smith, A. and Wilby, R.L. (2007). "A daily weather generator for use in climate change studies." *Environmental Modelling & Software* 22(12): 1705-1719.
- Kreibich, H., Piroth, K., Seifert, I., Maiwald, H., Kunert, U., Schwarz, J., Merz, B. and Thieken, A.H. (2009). "Is flow velocity a significant parameter in flood damage modelling?" *Natural Hazards and Earth System Sciences* 9(5): 1679-1692.
- Lamb, R., Keef, C., Dunning, P., Tawn, J. and Batstone, C. (2009). Spatial coherences of flood risk - final proof of concept report, Environment Agency. Science Report: SC060088.
- Lamb, R., Keef, C., Tawn, T., Laeger, S., Meadowcroft, I., Surrendran, S., Dunning, P. and Batstone, C. (2010). "A new method to assess the risk of local and widespread flooding on rivers and coasts." *Journal of Flood Risk Management* 3(4): 323-336.
- Lane, S. (2008). "Climate change and the summer 2007 floods in the UK." *Geography* 93(2): 91-97.
- Lavakare, A. and Mawk, K. (2008). Exposure data quality. The Review: A guide to Catastrophe modelling. available online <http://www.rms.com/Publications/RMS%20Guide%202008.pdf>.
- Ledingham, J. (2011). The Estimation of flood frequency curves by mapping from rainfall flood frequency curves. PhD Thesis, Newcastle University.
- Liang, Q. H. (2010). "Flood Simulation Using a Well-Balanced Shallow Flow Model." *Journal of Hydraulic Engineering-ASCE* 136(9): 669-675.
- Lighthill Risk Network. (2011). "The Lighthill risk network." from <http://www.lighthillrisknetwork.org>.
- Lloyd's. (2006). "Cat models cannot replace common sense." Retrieved 17th June 2011, from http://www.lloyds.com/News-and-Insight/News-and-Features/Archive/2006/05/Cat_models_cannot_replace_common_sense.
- Lloyds. (2010). "Flood risk tool." Retrieved January 2010, from <http://www.lloyds.com/The-Market/Tools-and-Resources/Research/Exposure-Management/Flood-risk-tool>.
- Marsh, T. J. and Dale, M. (2002). "The UK floods of 2000-2001: a hydrometeorological appraisal." *Water and Environmental Journal* 16(6): 180-188.
- McEwen, C., Hall, T., Hunt, J., Dempsey, M., Harrison, M. (2000). "Flood warning, warning response and planning control issues associated with caravan parks in the April 1998 floods on the lower Avon floodplain, Midlands Region, UK." *Applied Geography* (22): 271-305.
- McMillian, A., Batstone, C., Worth, D., Tawn, J., Horsburgh, K. and Lawless, M. (2011a). Science Report SC060065/TR2: design sea levels. Coastal flood boundary conditions for UK mainland and islands. Bristol, Environment Agency.

- McMillian, A., Johnson, A., Worth, D., Tawn, J. and Hu, K. (2011b). Science Report SC060064/TR3: Design swell waves. Coastal flood boundary conditions for UK mainlands and islands. Bristol, Environment Agency.
- McSweeney, C. (2007). Daily rainfall variability at point and areal scales: Evaluating simulations of present and future climates. PhD Thesis, University of East Anglia.
- Mendes, B. V. D. and Pericchi, L. R. (2009). "Assessing conditional extremal risk of flooding in Puerto Rico." *Stochastic Environmental Research and Risk Assessment* 23(3): 399-410.
- Merz, B., Kreibich, H., Schwarze, R. and Thieken, A. (2010). "Review article 'Assessment of economic flood damage'." *Natural Hazards and Earth System Sciences* 10(8): 1697-1724.
- Merz, B., Kreibich, H., Thieken, and Schmidtke, R. (2004). "Estimation uncertainty of direct monetary flood damage to buildings." *Natural Hazards and Earth System Sciences* 4(1): 153-163.
- Merz, B. and Thieken, A. H. (2009). "Flood risk curves and uncertainty bounds." *Natural Hazards* 51(3): 437-458.
- Messner, F., Penning-Rowsell, E., Collin, G., Meyer, V., Turnstall, S. and van der Veen, A. (2007). Evaluating flood damage: guidance and recommendations on principles and methods, FLOODsite. Report number: T09-06-01
- Met Office. (1998). "Easter 1998 Floods." Retrieved January 2010, from <http://www.metoffice.gov.uk/climate/uk/interesting/easter1998/>
- Met Office. (2011a). "Case Study - Boscastle." November 2011, from <http://www.metoffice.gov.uk/education/teens/case-studies/boscastle>.
- Met Office. (2011b). "Floods and flooding." Retrieved July 2011, from http://www.metoffice.gov.uk/education/teens/casestudy_floods.html#p02.
- Met Office. (2011c). "Monday 26 February 1990 (Towyn Floods)." Retrieved July 2011, from http://www.metoffice.gov.uk/media/pdf/3/4/Towyn_Floods_-_26_February_1990.pdf.
- Milly, P. C. D., Betancourt, J., Falkenmark, M., Hirsch, R. M., Kundzewicz, Z. W., Lettenmaier, D. P. and Stouffer, R. J. (2008). "Climate change - Stationarity is dead: Whither water management?" *Science* 319(5863): 573-574.
- De Moel, H., Van Alphen, J. and Aerts, J. (2009). "Flood maps in Europe - methods availability and use." *Natural Hazards Earth Systems Sciences* 9: 289-301.
- Morris, M., Hanson, G. and Hassan, M. (2008). "Improving the accuracy of breach modelling: why are we not progressing faster?" *Journal of Flood Risk Management* 1(3): 150-161.
- Morris, M., Hassan, M., Kortenhaus, A. and Visser, P. (2009). Breaching processes: a state of the art review, FLOODsite. Report Number: T06-06-03.
- Morris, M., Kortenhaus, A. and Visser, P. (2009). Modelling breach initiation and growth, FLOODsite. Report Number: T06-08-02.
- Morris, M., Kortenhaus, A. and Visser, P. (2009). Modelling Breach Initiation and Growth: Executive Summary FLOODsite. Report Number. T06-08-01.
- Morris, M. W., Hassan, M. and Vaskinn, K.A. (2007). "Breach formation: Field test and laboratory experiments." *Journal of Hydraulic Research* 45: 9-17.

- Muir-Wood, R. (1999). "Employing catastrophe loss modelling to price and manage European flood risk." *Global Change and Catastrophe Risk Management: Flood Risks in Europe*. Retrieved 17th April, 2009, from <http://www.iiasa.ac.at/Research/RMS/june99/papers/muirwood.pdf>.
- Muir-Wood, R. and W. Bateman (2005). "Uncertainties and constraints on breaching and their implications for flood loss estimation." *Philosophical Transactions of the Royal Society A - Mathematical Physical and Engineering Sciences* 363: 1423-1430.
- Muir-Wood, R., Drayton, M., Berger, A., Burgess, P. (2005). "Catastrophe loss modelling of storm-surge flood risk in eastern England." *Philosophical Transactions of the Royal Society A - Mathematical Physical and Engineering Sciences* 363.
- Nadarajah, S. (2001). "Multivariate declustering techniques." *Environmetrics* 12: 357-365.
- Nagy, L. and Tóth, S. (2005). WP 6: Monitoring and Case Study. Detailed Technical Report on the collation and analysis of dike breach data with regards to formation process and location factors. IMPACT project. Available online http://www.impact-project.net/AnnexII_DetailedTechnicalReports/AnnexII_PartE2_WP6/IMPACT_DTReport_EURAQ_2005-01-15.pdf.
- Nature (2011). "Heavy weather." *Nature* 477(7363): 131-132.
- Nelsen, R. (2006). *An introduction to copulas*. New York, Springer.
- NERC (1975). *Flood Studies Report*, Natural Environment Research Council.
- Netherlands Ministry of Public Works, IHE-Delft, et al. (2010). *CRESS - Coastal and River Engineering Support System*.
- NGfL Cymru. (2011). "Coastal flooding at Towyn." Retrieved July 2011, from http://www.ngfl-cymru.org.uk/vtc/towyn_flood/eng/Learningobjecti/Default.htm.
- North West England and North Wales Coastal Group. (2008). "North West England and North Wales Shoreline Management Plan (DRAFT)." Retrieved 15th September 2009, from <http://mycoastline.org/documents/processesB.pdf>.
- OASIS. (2012). "OASIS loss modelling framework." Retrieved June 2012, from <https://connect.innovateuk.org/web/oasis-open-access-catastrophe-model/overview>.
- Owen, M. W. (1980). *Design of seawalls allowing for wave overtopping*. Report EX 924, HR Wallingford.
- Pappenberger, F. and K. J. Beven (2006). "Ignorance is bliss: or seven reasons not to use uncertainty analysis." *Water Resources Research* 42.
- Penning-Rowsell, E., Johnson, C., Tunstall, S., Tapsell, S., Morris, J. Chatterton, J. and Green, C. (2005). *The benefits of flood and coastal risk management: a handbook of assessment techniques*, Middlesex University Press.
- Pitt, M. (2008). *The Pitt Review - Learning Lessons from the 2007 floods*. London, Cabinet Office
- Pugh, D. (2004). *Changing sea levels: effect of tides, weather and climate*. Cambridge, Cambridge University Press.

- Qu, Y. (2009). "Modelling Great Britain's Flood Defences." Retrieved July 2009, from <http://www.air-worldwide.com/PublicationsItem.aspx?id=16230>.
- Quick-R. (2010). "Cluster Analysis." Retrieved June 2010, from <http://www.statmethods.net/advstats/cluster.html>.
- R Development Core Team (2009). R: A language and environment for statistical computing. R Foundation for Statistical Computing. Vienna, Austria.
- Rickard, C. E. (2009). Floodwalls and flood embankments. Fluvial design guide. J. C. Ackers, C. E. Rickard and D. S. Gill, Environment Agency.
- RMS (2008). A Guide to Catastrophe Modelling. The Review: Worldwide Reinsurance, RMS.
- RMS. (2009). "RMS company website." Retrieved March 2009, from <http://www.rms.com/>.
- RMS. (2010). "U.K. inland flood ", from http://www.rms.com/Publications/UK_Inland_Flood.pdf.
- Robson, A. and Reed, D. (1999). Flood Estimation Handbook, Vol 3: Statistical procedures for flood frequency estimation. Wallingford, Institute of Hydrology.
- Rougier, J., Sparks, S. and Hill, L. (In press). Risk and uncertainty assessment for natural hazards, Cambridge University Press.
- Rowland, K. (2012). Flooding is the United Kingdom's biggest climate threat. Nature: news and comment.
- Royal Meteorological Society (2010). Catastrophe modelling: Improving our understanding of the impact of extreme weather in the financial markets, London, UK.
- SafeCoast. (2008). "Comparison between different flood risk methodologies: action 3B report." Retrieved 17/3/2010, from http://www.safecoast.org/editor/databank/File/a3breport_finalversion%5B1%5D.pdf.
- SafeCoast. (2012). "Examples of flood defence failure mechanisms for both hard defences (dikes, dams) and soft defences (dunes)" Retrieved July 2012, from http://www.safecoast.org/cohesion/risk_assessment.php.
- Sanders, D., Anders, B., Duffy, P., Forster, W., Hartington, T., Jones, G., Levi, C., Paddam, P., Papachristou, D., Perry, G., Rix, S., Ross, F., Smith, A.J., Seth, A., Westcott, D., and Wilkinson, M. (2002). "The management of losses arising from extreme events." GIRO.
- Sangal, B. P. (1983). "Practical methods of estimating peak flow." Journal of Hydraulic Engineering-Asce 109(4): 549-563.
- Saunders, M. (1998). The UK floods of Easter 1998, Benfield Greig Hazard Research Centre.
- Sayers, P., Gouldby, B., Simms, J., Meadowcroft, I. and Hall, J. (2003). Risk, performance and uncertainty in flood and coastal defence - a review, Defra / Environment Agency. R&D Technical Report FD2302/TR1.
- Sayers, P. B., Hall, J. W. and Meadowcroft, I.C. (2002). "Towards risk-based flood hazard management in the UK." Proceedings of the Institution of Civil Engineers-Civil Engineering 150: 36-42.

- Shah, H. (2008). Learning lessons from the unexpected. The review: A Guide to Catastrophe Modelling. Available online
<http://www.rms.com/Publications/RMS%20Guide%202008.pdf>.
- Silva, E. and Tucci, M. (1998). "Relacao entre as vazoes maximas diarias e instantaneas." *Revista Brasileira de Recursos Hidricos* 3(1): 133-151. [in Portuguese]
- Simms, J., Gouldby, B., Sayers, P., Flikweert, J.-J., Wersching, S., Bramley, M. (2009). Representing fragility of flood and coastal defences: getting into the detail;. Flood risk management: research and practice, Oxford, Taylor and Francis Group.
- Sivapalan, M., Takeuchi, K., Franks, S. W., Gupta, V. K., Karambiri, H., Lakshmi, V., Liang, X., McDonnell, J. J., Mendiondo, E. M., O'Connell, P. E., Oki, T., Pomeroy, J. W., Schertzer, D., Uhlenbrook, S. and Zehe, E. (2003). "IAHS decade on Predictions in Ungauged Basins (PUB), 2003-2012: Shaping an exciting future for the hydrological sciences." *Hydrological Sciences Journal-Journal Des Sciences Hydrologiques* 48(6): 857-880.
- Smith, A. (2009). A national scale rainfall analysis and event-based model of extremes for the UK. PhD Thesis, University of Newcastle.
- Smith, R. (1984). Threshold methods for sample extremes. *Statistical extremes and applications*. J. Tiago de Oliveira. Dordrecht, Reidel: 621-638.
- Smith, R. (1989). "Extreme value analysis of environmental time series: an application to trend detection in ground-level ozone." *Statistical Science* 4(4): 367-393.
- Smith, R. (1990). "Max-stable processes and spatial extremes." Retrieved 8th June 2009, from <http://www.stat.unc.edu/postscript/rs/spatex.pdf>.
- Smith, R. L. and Weissman, I. (1994). "Estimating the extremal index" *Journal of the Royal Statistical Society Series B-Methodological* 56(3): 515-528.
- Snell, E. (1953). Damage to the Essex coastline and restoration works. Conference on the North Sea floods of 31 January / 1 February: A collection of papers presented at the Institution in December 1953. London, The Institution of Civil Engineers: 155 - 165.
- Society of Actuaries in Ireland. (2011). "Risk measurement - is VaR the right measure?" Retrieved August 2011, from <https://web.actuaries.ie/sites/default/files/event/2010/11/110124%20-%20Risk%20meaurment%20is%20VAR%20the%20right%20measure.pdf>.
- Sorensen, R. (2006). Basic coastal engineering, third edition. New York, Springer.
- Spalding, J. (1953). A general survey of the damage done and action taken. Conference in the North Sea floods of 31 January / 1 February, 1953: A collection of papers presented at the institution in December 1953. London, Institution of Civil Engineers: 5-13.
- Speight, L., Hall, J., Kilsby, C.G. and Kershaw, P. (2011). Understanding spatial and temporal dependencies in flood risk exposure in the UK. EGU General Assembly. Vienna, Geophysical Research Abstracts. Vol. 13.
- Steenbergen, H. M. G. M., Lassing, B. L., Vrowenvelder, A.C.W.M. and Waarts, P.H. (2004). "Reliability analysis of flood defence systems." *Heron* 49(1): 51-73.
- Stephenson, A. G. (2001). "evd: Extreme Value Distributions." *R News* 2(2): 31-32.

- Svensson, C. and Jones, D. A. (2002). "Dependence between extreme sea surge, river flow and precipitation in eastern Britain." *International Journal of Climatology* 22(10): 1149-1168.
- Svensson, C. and Jones, D. A. (2004). "Dependence between sea surge, river flow and precipitation in south and west Britain." *Hydrology and Earth System Sciences* 8(5): 973-992.
- Swiss-Re (2002). *An introduction to re-insurance*. Technical Publishing. Zurich, Swiss Reinsurance Company.
- Tawn, J. A. (1988). "An extreme value theory model for dependent observations." *Journal of Hydrology* 101(1-4): 227-250.
- Thomas, R.S. and B. Hall (1992). *Seawall design*. London, Ciria.
- UK Climate Projections. (2009). "UKCP09." Retrieved 21st January 2010, from <http://ukclimateprojections.defra.gov.uk/content/view/12/689/>.
- Vorogushyn, S. (2009). *Analysis of flood hazards under consideration of dike breaches*. PhD, University of Potsdam.
- Vorogushyn, S., Merz, B. and Apel, H. (2009). "Development of dike fragility curves for piping and micro-instability breach mechanisms." *Natural Hazards and Earth System Sciences* 9(4): 1383-1401.
- Vorogushyn, S., Merz, B., Lindenschmidt, K-E. and Apel, H. (2010). "A new methodology for flood hazard assessment considering dike breaches." *Water Resources Research* 46.
- Walshaw, D. (1994). "Getting the most from your extreme wind data: a step-by-step guide." *Journal of Research of the National Institute of Standards and Technology* 99(4): 399-411.
- Wilkinson, K. (2004). *Fantasy Island*, Flickr, <http://www.flickr.com/photos/karent/2152314881/>.
- Williams, M. (2010). *Towyn floods remembered: 20 years on*. North Wales News.
- Willis Research Network. (2011). "The science of managing extremes." from <http://www.willisresearchnetwork.com>.
- Wolf, J. and R. A. Flather (2005). "Modelling waves and surges during the 1953 storm." *Philosophical Transactions of the Royal Society A-Mathematical Physical and Engineering Sciences* 363(1831): 1359-1375.
- Wood, R. M., Drayton, M., Berger, A., Burgess, P. and Wright, T. (2005). "Catastrophe loss modelling of storm-surge flood risk in eastern England." *Philosophical Transactions of the Royal Society A - Mathematical Physical and Engineering Sciences* 363(1831): 1407-1422.
- World Meteorological Organisation (2008). *Manual on low flow estimation and prediction*. Operational Hydrology Report No.50
- Wyre Forest District Council. (2008). *Strategic Flood Risk Assessment: Level 1 Report*, Wyre Forest District Council.
- Zeileis, A and Grothendieck, G (2005). "zoo: S3 Infrastructure for Regular and Irregular Time Series." *Journal of Statistical Software* 14(6): 1-27.